

**MULTIPLE DAMAGE IDENTIFICATION OF
BEAM STRUCTURE USING VIBRATION
ANALYSIS AND ARTIFICIAL INTELLIGENCE
TECHNIQUES**



Amiya Kumar Dash

Multiple Damage Identification of Beam Structure using Vibration Analysis and Artificial Intelligence Techniques

Thesis Submitted to the

*Department of Mechanical Engineering
National Institute of Technology, Rourkela*

for award of the degree

of

Doctor of Philosophy

by

Amiya Kumar Dash

under the guidance of

Prof. Dayal R. Parhi

&

Prof. H.C. Das



**Department of Mechanical Engineering
National Institute of Technology Rourkela
Orissa (India)-769008**

May 2012

Declaration

I hereby declare that this submission is my own work and that, to the best of my knowledge and belief, it contains no material previously published or written by another person nor material which to a substantial extent has been accepted for the award of any other degree or diploma of the university or other institute of higher learning, except where due acknowledgement has been made in the text.

(Amiya Kumar Dash)

Date:

Certificate

*This is to certify that the thesis entitled, “**Multiple Damage Identification of Beam Structure Using Vibration Analysis and Artificial Intelligence Techniques**”, being submitted by Mr. Amiya Kumar Dash to the Department of Mechanical Engineering, National Institute of Technology, Rourkela, for the partial fulfillment of award of the degree Doctor of Philosophy, is a record of bona fide research work carried out by him under our supervision and guidance.*

This thesis in our opinion, is worthy of consideration for award of the degree of Doctor of Philosophy in accordance with the regulation of the institute. To the best of our knowledge, the results embodied in this thesis have not been submitted to any other University or Institute for the award of any degree or diploma.

Prof. D.R. Parhi
(Supervisor)

Prof. H.C. Das
(Co-Supervisor)

Acknowledgements

In this thesis, I have received very valuable support of many people who motivated me to do my best effort.

First of all, I would like to thank my principal supervisor Prof. Dayal R. Parhi for guiding me to do my thesis at N.I.T. Rourkela and for his enormous support to develop this work. His patience, stimulating suggestions and encouragement helped me in all the time of research for and writing of this thesis.

I would like to thank my co-supervisor Prof. H.C. Das for his guidance and for directing the PhD on to the right track. His comments and suggestions throughout this time have helped me in my training as a researcher.

I am thankful to Prof. Sunil Kumar Sarangi, Director of National Institute of Technology, for giving me an opportunity to work under the supervision of Prof. Dayal R. Parhi. I am thankful to Prof. K.P. Maiti, Head of the Department, Department of Mechanical Engineering, for his moral support and valuable suggestions regarding the research work.

I express my deepest gratitude to Prof. Manojranjan Nayak, President, Siksha O Anusandhan University, Bhubaneswar, Orissa, who gave me the opportunity of pursuing this research work. His constant inspiration, encouragement and valuable advice have profoundly contributed to the completion of the present thesis.

I would like to thank Mr. P.K. Mohanty, PhD research scholar for his help during my stay at N.I.T. Rourkela.

Finally I would like to thank my wife, Mrs. Rosalin Dash, for all her support and encouragement. I would like to mention a special thanks to my Parents, brothers and all family members for their constant support. I thank my daughter, Ms. Aditi Dash, for her patient and moral support during my research.

Synopsis

This thesis investigates the problem of multiple damage detection in vibrating structural members using the dynamic response of the system. Changes in the loading patterns, weakening/degeneration of structures with time and influence of environment may cause cracks in the structure, especially in engineering structures which are developed for prolonged life. Hence, early detection of presence of damage can prevent the catastrophic failure of the structures by appropriately monitoring the response of the system. In recent times, condition monitoring of structural systems have attracted scientists and researchers to develop on line damage diagnostic tool. Primarily, the structural health monitoring technique utilizes the methodology for damage assessment using the monitored vibration parameters. In the current analysis, special attention has been focused on those methods capable of detecting multiple cracks present in system by comparing the information for damaged and undamaged state of the structure. In the current research, methodologies have been developed for damage detection of a cracked cantilever beam with multiple cracks using analytical, Finite Element Analysis (FEA), fuzzy logic, neural network, fuzzy neuro, MANFIS, Genetic Algorithm and hybrid techniques such as GA-fuzzy, GA-neural, GA-neuro- fuzzy. Analytical study has been performed on the cantilever beam with multiple cracks to obtain the vibration characteristics of the beam member by using the expressions of strain energy release rate and stress intensity factor. The presence of cracks in a structural member introduces local flexibility that affects its dynamic response. The local stiffness matrices have been measured using the inverse of local dimensionless compliance matrix for finding out the deviation in the vibrating signatures of the cracked cantilever beam from that of the intact beam. Finite Element Analysis has been carried out to derive the vibration indices of the cracked structure using the overall flexibility matrix, total flexibility matrix, flexibility matrix of the intact beam. From the research done here, it is concluded that the performance of the damage assessment methods depends on several factors for example, the number of cracks, the number of sensors used for acquiring the dynamic response, location and severity of damages. Different artificial intelligent model based on fuzzy logic, neural network, genetic algorithm, MANFIS and hybrid techniques have been designed using the computed vibration signatures for multiple crack diagnosis in cantilever beam structures with higher accuracy and considerably low computational time.

Table of Contents

Declaration.....	iii
Certificate	iv
Acknowledgements	v
Synopsis.....	vi
Contents	vii
List of Tables	xii
List of Figures.....	xiv
Nomenclature	xix
1 INTRODUCTION	1
1.1 Motivation for damage detection	1
1.2 Focus of the thesis	2
1.3 Organization of the thesis	4
2 LITERATURE REVIEW	7
2.1 Introduction	7
2.2 Methodologies for fault detection	7
2.3 Analysis of different methodologies for crack detection	10
2.3.1 Crack detection using classical methods	11
2.3.2 Crack detection using finite element method	18
2.3.3 Crack detection using AI techniques	21
2.3.3.1 Fuzzy inference method	21
2.3.3.2 Neural network method	23
2.3.3.3 Genetic algorithm method	26
2.3.3.4 Multiple adaptive neuro fuzzy inference system	29
2.3.3.5 Hybrid method	31
2.3.3.5.1 Neuro-fuzzy technique	32
2.3.3.5.2 Genetic fuzzy technique	34

2.3.3.5.3	<i>Genetic neural technique</i>	35
2.3.3.5.4	<i>Genetic neural fuzzy technique</i>	36
2.3.4	<i>Miscellaneous methods and tools used for crack detection</i>	37
2.4	Findings of literature review	41
3	EVALUATION OF DYNAMIC CHARACTERISTICS OF BEAM STRUCTURE WITH MULTIPLE TRANSVERSE CRACKS	42
3.1	Introduction	42
3.2	Vibration characteristics of multi cracked cantilever beam	43
3.2.1	<i>Theoretical analysis</i>	43
3.2.1.1	<i>Evaluation of local flexibility of the damaged beam under axial and bending loading</i>	43
3.2.1.2	<i>Vibration analysis of multi cracked cantilever beam</i>	47
3.2.2	<i>Numerical analysis</i>	51
3.2.2.1	<i>Results of theoretical analysis</i>	51
3.3	Analysis of experimental results	57
3.3.1	<i>Experimental results</i>	57
3.3.2	<i>Comparison between the results of experimental and numerical analysis</i>	62
3.4	Discussions	64
3.5	Summary	64
4	ANALYSIS OF FINITE ELEMENT FOR MULTIPLE CRACK DETECTION	65
4.1	Introduction	65
4.2	Finite element analysis	66
4.2.1	<i>Analysis of the cracked beam using finite element analysis (FEA)</i>	67
4.3	Results and discussions of finite element analysis	73
4.4	Summary	75
5	ANALYSIS OF FUZZY INFERENCE SYSTEM FOR MULTIPLE CRACK DETECTION	76
5.1	Introduction	76
5.2	Fuzzy inference system	77
5.2.1	<i>Modeling of fuzzy membership functions</i>	78
5.2.2	<i>Modeling of fuzzy inference system using fuzzy rules</i>	80
5.2.3	<i>Modeling of defuzzifier</i>	81

5.3	Analysis of the fuzzy model used for crack detection	82
5.3.1	<i>Fuzzy mechanism for crack detection</i>	83
5.3.2	<i>Results of fuzzy model</i>	93
5.4	Discussions	93
5.5	Summary	96
6	ANALYSIS OF ARTIFICIAL NEURAL NETWORK FOR MULTIPLE CRACK DETECTION	97
6.1	Introduction	97
6.2	Neural network technique	100
6.2.1	<i>Model of a neural network</i>	100
6.2.2	<i>Use of back propagation neural network</i>	102
6.3	Analysis of neural network model used for crack detection	103
6.3.1	<i>Neural model mechanism for crack detection</i>	105
6.3.2	<i>Neural model for finding out crack depth and crack location</i>	108
6.4	Results and discussions of neural model	109
6.5	Summary	112
7	ANALYSIS OF GENETIC ALGORITHM FOR MULTIPLE CRACK DETECTION	113
7.1	Introduction	113
7.2	Analysis of crack diagnostic tool using GA	114
7.2.1	<i>Approach of GA for crack identification</i>	114
7.3	Results and discussion	124
7.4	Summary	124
8	ANALYSIS OF HYBRID FUZZY-NEURO SYSTEM FOR MULTIPLE CRACK DETECTION	125
8.1	Introduction	125
8.2	Analysis of the fuzzy-neuro model	127
8.2.1	<i>Analysis of the fuzzy segment of fuzzy-neuro model</i>	131
8.2.2	<i>Analysis of the neural segment of fuzzy-neuro model</i>	131
8.3	Results and discussions of fuzzy-neuro model	132
8.4	Summary	135

9 ANALYSIS OF MANFIS FOR MULTIPLE CRACK DETECTION	136
9.1 Introduction	137
9.2 Analysis of multiple adaptive neuro-fuzzy inference system for crack detection	138
9.3 Results and discussions of MANFIS model	145
9.4 Summary	148
10 ANALYSIS OF GENETIC FUZZY MODEL FOR MULTIPLE CRACK DETECTION	149
10.1 Introduction	149
10.2 Analysis of Genetic- fuzzy system for crack detection	150
10.2.1 <i>Analysis of the GA segment of GA-fuzzy model</i>	151
10.2.2 <i>Analysis of the fuzzy segment of GA-fuzzy model</i>	152
10.3 Results and discussions of GA-fuzzy model	159
10.4 Summary	160
11 ANALYSIS OF GENETIC-NEURO-FUZZY MODEL FOR MULTIPLE CRACK DETECTION	161
11.1 Introduction	162
11.2 Analysis of GA-neural and Genetic-neuro-fuzzy system for crack detection	162
11.2.1 <i>Analysis of the GA segment of GA-neural model</i>	170
11.2.2 <i>Analysis of the GA segment of GA-neuro-fuzzy model</i>	170
11.2.3 <i>Analysis of the neural segment of GA-neural model</i>	170
11.2.4 <i>Analysis of the neural segment of GA-neuro-fuzzy model</i>	171
11.2.5 <i>Analysis of the fuzzy segment of GA-neuro-fuzzy model</i>	171
11.3 Results and discussions of GA-neural and GA-neuro-fuzzy models	172
11.4 Summary	174
12 ANALYSIS AND DESCRIPTION OF EXPERIMENTAL SETUP	176
12.1 Detail specifications of the vibration measuring instruments	176
12.2 Experimental procedure and its architecture	179
12.3 Results and discussions of experimental analysis	182
13 RESULTS & DISCUSSIONS	184
13.1 Introduction	184
13.2 Analysis of results	184

14 CONCLUSIONS AND FUTURE WORK	191
14.1 Contributions	191
14.2 Conclusions	192
14.3 Future work	196
REFERENCES	196
PUBLISHED PAPERS	218
APPENDIX	228

List of Tables

Table 2.1	Examples of Activation Functions used in ANN	26
Table 3.1	Comparison of results between Numerical analysis and experimental setup	63
Table 4.1	Comparison of results between FEA, numerical analysis and experimental setup	74
Table 5.1	Description of fuzzy Linguistic terms.	88
Table 5.2	Examples of twenty fuzzy rules used in fuzzy model	89
Table 5.3 (a)	Comparison of results between fuzzy Gaussian model, fuzzy triangular model, fuzzy trapezoidal model and experimental setup.	94
Table 5.3 (b)	Comparison of results between fuzzy Gaussian model, numerical and FEM analysis	95
Table 6.1	Test patterns for NN model other than training data	108
Table 6.2 (a)	Comparison of results between neural model, fuzzy Gaussian model and experimental analysis.	110
Table 6.2 (b)	Comparison of results between neural model, FEA analysis and Numerical analysis.	111
Table 7.1	Examples of initial data pool for the genetic algorithm	116
Table 7.2 (a)	Comparison of results between GA model, neural model, fuzzy Gaussian model and experimental analysis.	122
Table 7.2 (b)	Comparison of results between GA model, FEA and numerical analysis.	123
Table 8.1 (a)	Comparison of results between trapezoidal fuzzy neural model, triangular fuzzy neural model, Gaussian fuzzy neural model and experimental analysis.	133
Table 8.1 (b)	Comparison of results between Gaussian fuzzy neural model, GA model, Neural model and fuzzy Gaussian model	134
Table 9.1 (a)	Comparison of results between MANFIS model, Gaussian fuzzy neural model, GA model and experimental analysis.	146

Table 9.1 (b)	Comparison of results between MANFIS model, FEA and numerical analysis.	147
Table 10.1	Description of fuzzy Linguistic terms for input parameters of fuzzy segment for GA-fuzzy Model	155
Table 10.2	Description of fuzzy Linguistic terms for output parameters of fuzzy segment for GA-fuzzy Model	156
Table 10.3	Examples of ten fuzzy rules used in fuzzy segment of GA-fuzzy Model	156
Table 10.4 (a)	Comparison of results between GA-fuzzy model, MANFIS model, Gaussian fuzzy neural model, and experimental analysis.	157
Table 10.4 (b)	Comparison of results between GA-fuzzy model, FEA and numerical analysis.	158
Table 11.1 (a)	Comparison of results between GA-neuro-fuzzy model, GA-neural model, GA-fuzzy model, and experimental analysis.	166
Table 11.1 (b)	Comparison of results between GA-neuro-fuzzy model, FEA and numerical analysis.	167
Table 11.1 (c)	Comparison of results between GA-neural model, GA-fuzzy model, MANFIS model and experimental analysis.	168
Table 11.1 (d)	Comparison of results between GA-neural model, FEA and numerical analysis.	169
Table 12.1	Specifications of the instruments used in the experimental set up	177

List of Figures

Fig. 3.1	Geometry of beam, (a) Cantilever beam, (b) Cross-sectional view of the beam	44
Fig. 3.2	Relative Crack Depth (a_1/W) vs. Dimensionless Compliance ($(\ln(C_{i=1,2,j=1,2}))$)	46
Fig. 3.3	Front view of the cracked cantilever beam	47
Fig. 3.4a	Relative amplitude vs. relative distance from the fixed end (1 st mode of vibration), $a_1/W=0.083$, $a_2/W=0.333$, $L_1/L=0.1875$, $L_2/L=0.5625$	52
Fig. 3.4a1	Magnified view of fig. 3.2.4a at the vicinity of the crack location $L_1/L=0.1875$	52
Fig. 3.4a2	Magnified view of fig. 3.2.4a at the vicinity of the crack location $L_2/L=0.5625$	53
Fig. 3.4b	Relative amplitude vs. relative distance from the fixed end (2 nd mode of vibration), $a_1/W=0.083$, $a_2/W=0.333$, $L_1/L=0.1875$, $L_2/L=0.5625$	53
Fig. 3.4b1	Magnified view of fig. 3.2.4b at the vicinity of the crack location $L_1/L=0.1875$	54
Fig. 3.4b2	Magnified view of fig. 3.2.4b at the vicinity of the crack location $L_2/L=0.5625$	54
Fig. 3.4c	Relative amplitude vs. relative distance from the fixed end (3 rd mode of vibration), $a_1/W=0.083$, $a_2/W=0.333$, $L_1/L=0.1875$, $L_2/L=0.5625$	55
Fig. 3.4c1	Magnified view of fig. 3.2.4c at the vicinity of the crack location $L_1/L=0.1875$.	55
Fig. 3.4c2	Magnified view of fig. 3.2.4c at the vicinity of the crack location $L_2/L=0.5625$	56
Fig. 3.5	Schematic block diagram of experimental set-up	57
Fig.3.6 (a)	Relative amplitude vs. relative distance from the fixed end (1 st mode of vibration), $a_1/W=0.166$, $L_1/L=0.0625$, $a_2/W=0.25$, $L_2/L=0.3125$	58
Fig.3.6 (b)	Relative amplitude vs. relative distance from the fixed end (2 nd mode of vibration), $a_1/W=0.166$, $L_1/L=0.0625$, $a_2/W=0.25$, $L_2/L=0.3125$	58
Fig.3.6 (c)	Relative amplitude vs. relative distance from the fixed end (3 rd mode of vibration), $a_1/W=0.166$, $L_1/L=0.0625$, $a_2/W=0.25$, $L_2/L=0.3125$	59
Fig.3.7 (a)	Relative amplitude vs. relative distance from the fixed end (1 st mode of vibration), $a_1/W=0.083$, $L_1/L=0.25$, $a_2/W=0.333$, $L_2/L=0.5625$	59
Fig.3.7 (b)	Relative amplitude vs. relative distance from the fixed end (2nd mode of vibration), $a_1/W=0.083$, $L_1/L=0.25$, $a_2/W=0.333$, $L_2/L=0.5625$	60

Fig.3.7 (c)	Relative amplitude vs. relative distance from the fixed end (3 rd mode of vibration), $a_1/W=0.083$, $L_1/L=0.25$, $a_2/W=0.333$, $L_2/L=0.5625$	60
Fig.3.8 (a)	Relative amplitude vs. relative distance from the fixed end (1 st mode of vibration), $a_1/W=0.166$, $L_1/L=0.1875$, $a_2/W=0.083$, $L_2/L=0.5$	61
Fig.3.8 (b)	Relative amplitude vs. relative distance from the fixed end (2 nd mode of vibration), $a_1/W=0.166$, $L_1/L=0.1875$, $a_2/W=0.083$, $L_2/L=0.5$	61
Fig.3.8 (c)	Relative amplitude vs. relative distance from the fixed end (3 rd mode of vibration), $a_1/W=0.166$, $L_1/L=0.1875$, $a_2/W=0.083$, $L_2/L=0.5$	62
Fig. 4.1	View of a crack beam element subjected to axial and bending forces	67
Fig.4.2 (a)	Relative amplitude vs. relative distance from the fixed end (1 st mode of vibration), $a_1/W=0.166$, $L_1/L=0.3125$, $a_2/W=0.083$, $L_2/L=0.625$	69
Fig. 4.2 (b)	Relative amplitude vs. relative distance from the fixed end (2 nd mode of vibration), $a_1/W=0.166$, $L_1/L=0.3125$, $a_2/W=0.083$, $L_2/L=0.625$	69
Fig. 4.2 (c)	Relative amplitude vs. relative distance from the fixed end (3 rd mode of vibration), $a_1/W=0.166$, $L_1/L=0.3125$, $a_2/W=0.083$, $L_2/L=0.625$	70
Fig. 4.3 (a)	Relative amplitude vs. relative distance from the fixed end (1 st mode of vibration), $a_1/W=0.25$, $L_1/L=0.4375$, $a_2/W=0.166$, $L_2/L=0.625$	70
Fig.4.3 (b)	Relative amplitude vs. relative distance from the fixed end (2 nd mode of vibration), $a_1/W=0.25$, $L_1/L=0.4375$, $a_2/W=0.166$, $L_2/L=0.625$	71
Fig. 4.3 (c)	Relative amplitude vs. relative distance from the fixed end (3 rd mode of vibration), $a_1/W=0.25$, $L_1/L=0.4375$, $a_2/W=0.166$, $L_2/L=0.625$	71
Fig.4.4 (a)	Relative amplitude vs. relative distance from the fixed end (1 st mode of vibration), $a_1/W=0.166$, $L_1/L=0.3125$, $a_2/W=0.083$, $L_2/L=0.625$	72
Fig. 4.4 (b)	Relative amplitude vs. relative distance from the fixed end (2 nd mode of vibration), $a_1/W=0.166$, $L_1/L=0.3125$, $a_2/W=0.083$, $L_2/L=0.625$	72
Fig.4.4 (c)	Relative amplitude vs. relative distance from the fixed end (3 rd mode of vibration), $a_1/W=0.166$, $L_1/L=0.3125$, $a_2/W=0.083$, $L_2/L=0.625$	73
Fig. 5.1(a)	Triangular membership function	79
Fig. 5.1(b)	Gaussian membership function	79
Fig.5.1(c)	Trapezoidal membership function	80
Fig. 5.2	Fuzzy inference system	81
Fig. 5.3(a)	Triangular fuzzy model	83

Fig. 5.3(b)	Gaussian fuzzy model	83
Fig. 5.3(c)	Trapezoidal fuzzy model	83
Fig. 5.4(a1)	Membership functions for relative natural frequency for first mode of vibration	85
Fig. 5.4(a2)	Membership functions for relative natural frequency for second mode of vibration	85
Fig. 5.4(a3)	Membership functions for relative natural frequency for third mode of vibration	85
Fig. 5.4(a4)	Membership functions for relative mode shape difference for first mode of vibration	85
Fig. 5.4(a5)	Membership functions for relative mode shape difference for second mode of vibration	85
Fig. 5.4(a6)	Membership functions for relative mode shape difference for third mode of vibration	85
Fig. 5.4(a7) (a)	Membership functions for relative crack depth1	85
Fig. 5.4(a7) (b)	Membership functions for relative crack depth2	85
Fig. 5.4(a8) (a)	Membership functions for relative crack location1	85
Fig. 5.4(a8) (b)	Membership functions for relative crack location2	85
Fig. 5.5(b1)	Membership functions for relative natural frequency for first mode of vibration	86
Fig. 5.5(b2)	Membership functions for relative natural frequency for second mode of vibration	86
Fig. 5.5(b3)	Membership functions for relative natural frequency for third mode of vibration	86
Fig. 5.5(b4)	Membership functions for relative mode shape difference for first mode of vibration	86
Fig. 5.5(b5)	Membership functions for relative mode shape difference for second mode of vibration	86
Fig. 5.5(b6)	Membership functions for relative mode shape difference for third mode of vibration	86
Fig. 5.5(b7) (a)	Membership functions for relative crack depth1	86
Fig. 5.5(b7) (b)	Membership functions for relative crack depth2	86
Fig. 5.5(b8) (a)	Membership functions for relative crack location1	86
Fig. 5.5(b8) (b)	Membership functions for relative crack location2	86
Fig. 5.6(c1)	Membership functions for relative natural frequency for first mode of vibration	87
Fig. 5.6(c2)	Membership functions for relative natural frequency for second mode of vibration	87
Fig. 5.6(c3)	Membership functions for relative natural frequency for third mode of vibration	87
Fig. 5.6(c4)	Membership functions for relative mode shape difference for first mode of vibration	87
Fig. 5.6(c5)	Membership functions for relative mode shape difference for second mode of vibration	87
Fig. 5.6(c6)	Membership functions for relative mode shape difference for third mode of vibration	87

Fig. 5.6(c7) (a)	Membership functions for relative crack depth1	87
Fig. 5.6(c7) (b)	Membership functions for relative crack depth2	87
Fig. 5.6(c8) (a)	Membership functions for relative crack location1	87
Fig. 5.6(c8) (b)	Membership functions for relative crack location2	87
Fig. 5.7	Resultant values of relative crack depths and relative crack locations when Rules 3 and 17 of Table 5.3.2 are activated	90
Fig. 5.8	Resultant values of relative crack depth and relative crack location when Rules 3 and 17 of Table 5.3.2 are activated	91
Fig. 5.9	Resultant values of relative crack depth and relative crack location from trapezoidal fuzzy model when Rules 3 and 17 of Table 5.3.2 are activated	92
Fig. 6.1	Neuron model	100
Fig. 6.2	Back propagation technique	102
Fig. 6.3	Neural model	104
Fig. 6.4	Multi Layer feed forward back propagation Neural model for damage detection	104
Fig.7.1	Single cross point, value encoding crossover for fnf, snf, tnf, fmd, smd, tmd, rcl1,rcd1,rcl2,rcd2	119
Fig.7.2	Mutation of genes for fnf, snf, tnf, fmd, smd, tmd	120
Fig.7.3	Flow chart for the proposed Genetic Algorithm	121
Fig. 8.1	Triangular fuzzy-neural system for damage detection	128
Fig. 8.2	Gaussian fuzzy-neural system for damage detection	129
Fig. 8.3	Trapezoidal fuzzy-neural system for damage detection	130
Fig. 9.1	Bell-shaped membership function	140
Fig. 9.2 (a)	Multiple ANFIS (MANFIS) Model for crack detection	143
Fig. 9.2 (b)	Adaptive-Neuro-Fuzzy-Inference System (ANFIS) for crack detection	144
Fig. 10.1	Fuzzy model for crack detection	151
Fig. 10.2(a1)	Membership functions for relative natural frequency for first mode of vibration	153
Fig. 10.2(a2)	Membership functions for relative natural frequency for second mode of vibration	153
Fig. 10.2(a3)	Membership functions for relative natural frequency for third mode of vibration	153
Fig. 10.2(a4)	Membership functions for relative mode shape difference for first mode of vibration	153
Fig. 10.2(a5)	Membership functions for relative mode shape difference for second mode of vibration	153
Fig. 10.2(a6)	Membership functions for relative mode shape difference for third mode of vibration	153
Fig. 10.2a7 (a)	Membership functions for interim relative crack depth1	153
Fig. 10.2a7 (b)	Membership functions for interim relative crack depth2	153
Fig. 10.2a8 (a)	Membership functions for interim relative crack location1	153

Fig. 10.2a8 (b)	Membership functions for interim relative crack location2	153
Fig. 10.2a9 (a)	Membership functions for final relative crack depth1	154
Fig. 10.2.a9 (b)	Membership functions for final relative crack depth2	154
Fig. 10.2.a10 (a)	Membership functions for final relative crack location1	154
Fig. 10.2.a10 (b)	Membership functions for final relative crack location2	154
Fig. 10.3	Genetic-Fuzzy system for fault detection	154
Fig. 11.1	GA-neural system for fault detection	164
Fig. 11.2	GA-neuro-fuzzy system for fault detection	165
Fig. 12.1	View of the experimental set-up	178
Fig.12.2 (a)	Vibration analyzer	179
Fig.12.2 (b)	Data acquisition (accelerometer)	180
Fig.12.2 (c)	Concrete foundation with beam specimen	180
Fig.12.2 (d)	Function generator	180
Fig.12.2 (e)	Power amplifier	181
Fig.12.2 (f)	Modal Vibration exciter	181
Fig.12.2 (g)	Vibration indicator (PULSE labShop software)	181
Fig.12.2 (h)	PCMCIA card	182
Fig. A1	FEA model of the cantilever beam model	228
Fig. A2	ALGOR generated 2 nd mode vibration of the cantilever beam model	228
Fig. A3	Plot of graph for epochs vs mean squared error from NN	229
Fig. A4	Plot of graph for actual value vs predicted value	230
Fig. A5	Plot of graph for Estimation Error vs Number of Generations	230

Nomenclature

a_1, a_2	= depth of crack
A	= cross-sectional area of the beam
A_i (i = 1 to 18)	= unknown coefficients of matrix A
B	= width of the beam
C_{11}	= Axial compliance
$C_{12} = C_{21}$	= Coupled axial and bending compliance
C_{22}	= Bending compliance
\bar{C}_{11}	= Dimensionless form of C_{11}
$\bar{C}_{12} = \bar{C}_{21}$	= Dimensionless form of $C_{12} = C_{21}$
\bar{C}_{22}	= Dimensionless form of C_{22}
C'_{12}	= Axial compliance for first crack position
$C'_{12} = C'_{21}$	= Coupled axial and bending compliance for first crack position
C'_{22}	= Bending compliance for first crack position
C''_{12}	= Axial compliance for second crack position
$C''_{12} = C''_{21}$	= Coupled axial and bending compliance for second crack position
C''_{22}	= Bending compliance for second crack position
E	= young's modulus of elasticity of the beam material
F_i (i = 1, 2)	= experimentally determined function
i, j	= variables

J	= strain-energy release rate
$K_{1,i} \text{ (} i = 1, 2 \text{)}$	= stress intensity factors for P_i loads
K_{ij}	= local flexibility matrix elements
K'	= Stiffness matrix for first crack position
K''	= Stiffness matrix for second crack position
L	= length of the beam
L_1	= location (length) of the first crack from fixed end
L_2	= location (length) of the second crack from fixed end
L_e	= Length of the crack from one end of the beam
L_c	= Length of crack element
$M_i \text{ (} i=1,4 \text{)}$	= compliance constant
$P_i \text{ (} i=1,2 \text{)}$	= axial force ($i=1$), bending moment ($i=2$)
Q	= stiffness matrix for free vibration.
$u_i \text{ (} i=1,2 \text{)}$	= normal functions (longitudinal) $u_i(x)$
x	= co-ordinate of the beam
y	= co-ordinate of the beam
$y_i \text{ (} i=1,2 \text{)}$	= normal functions (transverse) $y_i(x)$
W	= depth of the beam
ω	= natural circular frequency

β_1	= relative first crack location (L_1/L)
β_2	= relative second crack location (L_2/L)
ρ	= mass-density of the beam
Λ	= aggregate (union)
\wedge	= minimum (min) operation
\forall	= for every

Chapter 1

INTRODUCTION

Crack diagnosis in vibrating structures has drawn a lot of attention from the science and engineering community in the last three decades. The presence of cracks in a structure, if undetected for longer period of time will lead to the failure of the system and may cause loss of life and loss of resources. Utilization of the dynamic response of the member is one of the technique, which has been widely accepted for crack diagnosis in different engineering systems. The present chapter emphasizes the various techniques that are being used for fault diagnosis. The background and motivation in the field of analysis of dynamically vibrating damaged structures has been depicted in the first section. The second part of this chapter describes the aims and objective of the research. The last part of the current chapter gives a brief description of each chapter of the thesis for the current research.

1.1 Motivation for damage identification

Engineering structures play a vital role in the lives of a modern community. They are normally designed to have longer life period. The failure or poor performance of engineering structures may lead to disruption of transportation system or may result in loss of lives and property. It is therefore, very important to ensure that the structural members perform safely and efficiently at all times by monitoring their structural integrity and undertaking appropriate remedial measures.

Many techniques have been employed in the past for fault diagnosis. Some of these are visual (e.g. dye penetrant method) and other use sensors to detect local faults (e.g. acoustic emission, magnetic field, eddy current, radiographs and thermal fields). These methods are time consuming and cannot indicate that a structure is fault free without testing the entire structure in minute details. Furthermore, if a crack is buried deep within the structure it may not be detectable by these localized methods. Based on the changes in the modal parameters researchers have developed Artificial Intelligence (AI) based techniques for fault identification for single crack scenario. The AI techniques have been designed with an aim for faster and accurate estimation of fault present in the structures.

Motivated by the above reasons, this thesis aims at exploring the use of AI techniques such as fuzzy, neural network, genetic algorithm and hybrid methods such as fuzzy-neuro,

genetic-fuzzy, genetic-neural and genetic-neural-fuzzy for multiple crack diagnosis in engineering structures at an early stage by capturing the vibration parameters.

1.2 Focus of the thesis

The process of monitoring and identifying faults is of great importance in aerospace, civil and mechanical engineering. The structures associated with aerospace, civil or mechanical engineering must be free from cracks to ensure safe operation. Cracks in machine or any engineering systems may lead to catastrophic failure of the machine and must be detected early.

In different engineering systems (e.g. steel structures, industrial machinery) beams are commonly used as structural members and are subjected to static and dynamic loads. Due to the loading and environment effect they may experience cracks, which drastically reduce the life cycle of the structural system. The cracks present in the system may be considered to develop the analytical model to study the effect of cracks on the modal response of the system. The damage in the beam member introduces the stiffness, which can be used along with the prevailing boundary conditions to formulate the vibration characteristic equation to obtain the mode shape, natural frequency of vibration, crack parameters such as relative crack severities and relative crack positions. The current analysis aims at development of a multi crack identification tool for intelligent condition monitoring of structures using the change in modal parameters of the structural member due to presence of cracks.

For this purpose, a cantilever beam with uniform cross section has been considered, which act as a structural member in various engineering applications. The dynamic responses of the cantilever beam have been measured in the undamaged state, which act as references. Afterwards, multiple damages have been induced and sequential modal identification analysis has been performed at each damaged stage, aiming at finding adequate correspondence between the dynamic behavior and the presence of cracks in the structure. Comparison between different techniques based on the performance to identify the various cracks level have been carried out to find out the most suitable method, to identify multiple cracks in damaged structures. The aim is to use the dynamic response parameters to develop AI methods for structural health monitoring in multiple crack scenario.

In the present study, literature review has been carried out related to the domain of fault diagnosis in engineering applications. From the previous analysis, it is observed that the results obtained by the researchers have not been systematically used to develop tools for real applications such as multiple crack diagnosis. In the current investigation, an attempt has been made to design and develop a multiple crack diagnostic tool using the dynamic behavior of cracked and undamaged cantilever beam structure using theoretical analysis, finite element analysis, experimental analysis and artificial intelligence techniques.

The different phases for the present study are listed below:

1. Theoretical analysis for the cantilever structure with two transverse cracks has been performed to evaluate the modal parameters.
2. Finite Element Analysis (FEA) has been carried out to measure the vibration parameters of the cracked and undamaged cantilever beam with different multiple crack configurations.
3. Experimental set up has been developed and is being used to obtain the values of first three relative natural frequencies and average relative mode shape differences of the cracked cantilever member.
4. The modal parameters such as natural frequencies and mode shapes obtained from theoretical, finite element and experimental analysis have been used to design and train the artificial intelligence techniques. The developed AI based methodologies utilizes the first three relative natural frequencies and first three average relative mode shape differences as the input parameters and relative crack locations and relative crack depths are the outputs from the AI model.

The theoretical study has been developed for a cantilever beam with two transverse cracks to obtain the dynamic characteristics by utilizing the expressions of strain energy release rate and stress intensity factors. The presence of cracks produces the local flexibility at the vicinity of the crack locations and reduces the stiffness of the structure. With different boundary conditions the stiffness matrix has been derived to find out the effect of relative crack depths on the dimensionless compliances of the structure. The derived vibration signatures from theoretical, finite element and experimental analysis of the beam member have been used to design and train the AI model (fuzzy, neural network, genetic algorithm,

fuzzy-neuro, MANFIS, genetic-neuro, genetic-neuro-fuzzy model). Finally, relative crack locations and relative crack depths are the outputs from the model.

The results obtained from the various methodologies such as theoretical, finite element, experimental, fuzzy, neural network, genetic algorithm and hybrid techniques like fuzzy-neuro, MANFIS, genetic-neuro, genetic-neuro-fuzzy devised in the present research have been compared and a close agreement has been found. Concrete conclusions have been drawn from the results of respective sections. Experimental analysis has been carried out to validate the results from the different techniques cited above.

1.3 Organization of the thesis

The content of the thesis is organized as follows:

The analyses carried out in the current research for fault identification in damaged structures are presented in fourteen chapters.

Chapter 1 is the introductory one; it states about the effect of crack on the functionality of different engineering applications and also discusses about the methodologies being adopted by the scientific community to diagnose faults in different industrial applications. The motivation to carry out the research along with the focus of the current investigation is also explained in this chapter.

Chapter 2 is the literature review section representing the state of the art in relation to published work from the field of damage detection using vibration analysis and fault detection using AI techniques. This section also expresses the classification of methodologies in the domain of fault detection and also explains the reasons behind the direction of the current research.

Chapter 3 introduces the theoretical model to measure the vibration indicators (natural frequencies, mode shapes) by using SIF, strain energy release rate and laying down different boundary conditions. The crack developed in the structure generates flexibility at the vicinity of the crack which in turn, gives rise to a reduction in natural frequencies and the change in the mode shapes. This basis has been applied in the numerical analysis to identify the

presence of cracks in the cantilever structure and also to evaluate the crack locations and their severities.

Chapter 4 of the thesis describes the finite element analysis being applied on the cracked beam element to measure the dynamic response of the multiple cracked cantilever beams, subsequently the measured values are used to identify the presence of cracks and crack parameters. The results from finite element method are compared with the results from experimental method and numerical analysis for validation.

Chapter 5 shows the applicability of fuzzy inference system for fault diagnosis in cracked structure. The procedures required for developments of the fuzzy models are outlined in this chapter. The gaussian, triangular and trapezoidal membership function based intelligent model with their detail architecture are briefly discussed. The results from the fuzzy models are compared with the experimental results and discussions regarding the same have been presented.

Chapter 6 introduces an inverse analysis based on the artificial neural network technique for effective identification of crack damage in a cracked cantilever structure containing multiple transverse cracks. The multi layer perceptron with the input and output parameters are presented and explained in detail. The results from artificial neural network are presented and discussed to demonstrate the applicability of the AI model.

Chapter 7 analyses the application of genetic algorithm method to design a damage diagnostic tool. Different evolutionary techniques form GA methodology are presented and discussed in length. Results for relative crack locations and relative crack depths from GA model are compared with experimental results for validation. Finally, the summary of the analysis of GA for crack prediction is presented.

Chapter 8 discusses about the hybrid fuzzy-neuro model for estimation of crack parameters present in a structural system. The steps adopted to design the fuzzy layer and neural layer of the fuzzy-neuro system are presented. A discussion about the comparison of results from the Gaussian fuzzy-neuro, Trapezoidal fuzzy-neuro, Triangular fuzzy-neuro, numerical, finite element and experimental analysis is presented.

Chapter 9 outlines the working principles of multiple adaptive neuro fuzzy inference system (MANFIS) to identify the presence of cracks and predict the location of cracks and their depths. The adaptive system utilizes the modal parameters as inputs and finally, gives the output as relative crack locations and relative crack depths. The predicted results from the MANFIS are compared with the results from theoretical, Gaussian fuzzy-neuro, GA, FEA, experimental analysis and a discussion about the comparison is presented.

Chapter 10 describes a novel hybrid GA-fuzzy model designed for multiple crack diagnosis of beam structures. The design procedures of the first layer (GA model) and the second layer (fuzzy model) of the hybrid system are systematically explained with the detailed architecture of the proposed system. The discussions about the results from GA-fuzzy model and evaluation of the accuracy of its performance have been stated.

Chapter 11 presents two intelligent inverse models i.e. two layer (GA-neural) and three layer (GA-neuro-fuzzy) hybrid intelligent system to identify both locations and severities of the damages in structural systems based on genetic algorithm, neural network, and fuzzy logic. Methods for development of the GA, neural and fuzzy segments of the hybrid intelligent models are outlined. The predicted values for relative crack locations and relative crack depths from GA-neuro-fuzzy, GA-neural, GA-fuzzy, MANFIS, FEA, theoretical, experimental analysis are compared and the conclusions regarding its performance are depicted.

Chapter 12 presents the experimental procedure along with the instruments used for validating the results from methodologies being adopted in the present analysis for multiple crack identification. The results from the developed experimental set-up have been obtained and presented for discussion.

Chapter 13 provides a comprehensive review of the results obtained from all the techniques adopted in the current research.

Chapter 14 discusses the conclusions drawn from the research carried out on the current topic and gives the recommendations for scope of future work in the same domain.

Chapter 2

LITERATURE REVIEW

This chapter presents a state of the art about dynamic model based damage identification in structural systems. The main goal is to review the developments made by researchers during the past few decades. Issues addressed are historical context of the applicability of damage methods, general methods of classification, and a review of a selected group of methods. Finally, the applications of artificial intelligence techniques for crack diagnosis are discussed from the past and recent developments.

2.1 Introduction

The literature review section presents the analysis of the published work confined to the areas of structural health monitoring, damage detection algorithm, fault diagnostic methodologies and modal testing. The review begins with the description of different vibration analysis methods used for damage identification. Next, dynamics of cracked structures, fault identification methodologies to develop crack diagnostic tool using Finite Element Analysis (FEA) and wavelet technique are discussed. Following the artificial intelligence techniques (fuzzy logic, neural network, genetic algorithm, MANFIS and hybrid techniques) intelligent models for crack identification can be designed. The aim of the present investigation is to propose an artificial intelligent technique, which can be capable to predict the presence of multiple cracks in vibrating structures. The possible directions for research can be obtained from the analysis of the literature cited in this section.

From the published works it is seen that the idea regarding fault finding in different systems varies widely. In spite of the fact that, there is a wide variation in development of fault diagnostic methodology next section presents the review of the literature pertaining to damage detection and fault identification.

2.2 Methodologies for fault detection

Researchers to date have focused on many methodologies for detection of fault in various segments of engineering structures. Vibration based methods are found to be effectively used

for health monitoring in faulty systems. The recent methods adapted for fault diagnosis are outlined below.

Moore et al. [1] have proposed a new method to identify the size, location, and orientation of a single crack in a simply supported plate subjected to free vibration by employing finite element method and Markov-chain Monte-Carlo implementation of Bayes' Rule. They have claimed that their approach can be effectively used to identify the crack present in real engineering system. Lang et al. [2] have applied the concept of transmissibility to the non-linear case by introducing the transmissibility of Non-linear Output Frequency Response Functions. They have developed a NOFRF transmissibility-based technique for the detection and location of both linear and non-linear damage in MDOF structural systems. The results from their proposed technique have been verified by the numerical simulation and experimental analysis on a three storey building. Hein et al. [3] have presented a new method for identification of delamination in homogeneous and composite beams. They have used Haar wavelets and neural networks to establish the mapping relationship between frequencies, Haar series expansion of fundamental mode shapes of vibrating beam and delamination status. They have revealed that the simulations show the proposed complex method can detect the location of delaminations and identify the delamination extent with high precision. Huh et al. [4] have proposed a new local damage detection method for damaged structures using the vibratory power estimated from accelerations measured on the beam structure. A damage index is newly defined by them based on the proposed local damage detection method and is applied to the identification of structural damage. Numerical simulation and experiment are conducted for a uniform beam to confirm the validity of the proposed method. In the experiments, they have considered the damage as an open crack such as slit inflicted on the top surface of the beam. Salam et al. [5] have proposed a simplified formula for the stress correction factor in terms of the crack depth to the beam height ratio. They have used the proposed formula to examine the lateral vibration of an Euler-Bernoulli beam with a single edge open crack and compared the mode shapes for the cracked and undamaged beam to identify the crack parameters. Douka et al. [6] have presented a method for crack identification based on the sudden change in spatial variation of the transformed response of the beam structures using wavelet analysis. They have

established an intensity factor law for accurate prediction of crack size and the results from the proposed method has been validated experimentally. Nahvi et al. [7] have developed a technique for identification of crack in cantilever beam using analytical, finite element method based on measured natural frequencies and mode shapes of the beam structure. The results from the proposed method have been authenticated using the results obtained from experimental analysis. Tahaa et al. [8] have introduced a method to improve pattern recognition and damage detection by supplementing intelligent health monitoring with used fuzzy inference system. The Bayesian methodology is used to demarcate the levels of damage for developing the fuzzy system and is examined to provide damage identification using data obtained from finite element analysis for a pre-stressed concrete bridge. Mahamad et al. [9] have proposed an artificial neural network (ANN) based methodology to predict accurate remaining useful life (RUL) for a bearing system. The ANN model has been designed using measurements of hazard rates of root mean square and kurtosis from its present and previous state. Kong et al. [10] have proposed a fault diagnosis methodology using wavelet transformer fuzzy logic and neural network technique to identify the faults. They have found a good agreement between analytical and experimental results. Liu et al. [11] have taken the help of genetic algorithm (GA) for optimal sensor placement on a spatial lattice structure. They have taken the model strain energy (MSE) and modal assurance criterion (MAC) as the fitness function. A computational simulation of 12-bay plain truss model has been used as modified GA and the data were compared against the existing GA using the binary coding method and found better results through the modified GA. Sanza et al. [12] have presented a new technique for health monitoring of rotating machinery by integrating the capabilities of wavelet transform and auto associative neural network for analyzing the vibration signature. The proposed technique effectiveness has been evaluated using the numerical and experimental vibration data and the developed technique has demonstrated accurate results. Hoffman et al. [13] have employed a diagnostic technique based on neural network. As described in the paper, it is impossible to determine the degree of imbalance in a bearing system using single vibration feature and to overcome this problem they have used the neural network technique for processing of multiple features. For the purpose of fault detection of different bearing conditions they have employed different neural network technique and compared their performances. They have found that the developed

algorithm can be suitably used for identifying the presence of defects. Murigendrappa et al. [14] have proposed a technique based on measurement of change of natural frequency to detect cracks in long pipes containing fluid at different pressure. In their experimental analysis they have used aluminium & mild steel Pipes with water as the fluid and used pressure gauges to obtain the change in natural frequency which are subsequently used to locate the crack present on the pipes carrying fluids. Darpe et al. [15] have studied the unbalanced response of a cracked rotor with a single centrally situated crack subjected to periodic axial impulses using an electrodynamics exciter for both rotating & non rotating condition. They have found that the spectral response of the crack rotor with and without axial excitation is found to be distinctly different. They have concluded that the response of the rotor to axial impulse excitation can be used as a reliable diagnosis tool for rotor crack. Curry et al. [16] have proposed a closed loop system with the help of sensors to formulate a fault detection and isolation methodology based on fixed threshold. They have observed that the proposed technique has been capable of detecting and isolating failures for each of the particular sensors.

The various techniques employed by the researchers in the domain of fault detection varies with their approach to identify the faults present in a system. The next section depicts the categorization of the different methods used for fault diagnosis in engineering systems.

2.3 Analysis of different methodologies for crack detection

In this current investigation, the various methods applied for crack identification in damaged dynamic structures have been described briefly. The different methods that have been proposed by various authors for damage identification are sectioned into four different categories such as:

- 1 Classical method
- 2 Finite Element Method
- 3 AI method
- 4 Miscellaneous methods.

2.3.1 Crack detection using classical methods

In the current section, spatial variation of the transferred response, modal response methods, energy based method, analytical methods, algorithms based on vibration etc. used for locating the crack location and its intensity in dynamically vibrating damaged structures have been discussed. The research papers connected to the above techniques are discussed below.

Muller et al. [17] have proposed a method for crack detection in dynamic system. They have established a relation between shaft cracks in turbo rotors by applying a model-based method using the theory of Lyapunov exponents. In their research, they have studied chaotic motions and strange attractors in turbo rotors. Owolabi et al. [18] have carried out experimental investigations of crack location and crack intensity for fixed beams and simply supported beams made of Aluminum. They have measured the changes in the first three natural frequencies and the corresponding amplitudes to forecast the crack in a structure. Chinchalkar [19] has developed a generalized numerical method for fault finding using finite element approach. His approach is based on the measurement of first three natural frequencies of the cracked beam. The developed method of fault detection accommodates different boundary conditions and having wide variations in crack depth. Tada et al. [20] have established a platform to formulate compliance matrix in damaged structural members for estimating the crack location and crack depth. Loutridis et al. [21] have proposed a new technique for crack detection in beam based on instantaneous frequency and empirical mode decomposition. The dynamic behaviors of the structure have been investigated both theoretically and experimentally. They concluded that the variation of the instantaneous frequencies increases with increase in crack depth and this variation have been used for estimation of crack size.

Song et al. [22] have described an exact solution methodology based on Laplace transform to analyze the bending free vibration of a cantilever laminated composite beam having surface cracks. They have used the Hamilton's variational principle in conjunction with Timoshenko beam model to develop the technique for damage detection in crack structure. Ravi et al. [23] have carried out the modal analysis of an aluminium sheet having micro cracks. They have used compression loading to generate the micro cracks on the surface of the sheet and

monitored the deformation using the acoustic emission technique. Using the lines scans around the area of deformation; they have detected the effect of micro cracks and the modal parameters of the aluminium sheet specimen. Law et al. [24] have proposed a time domain method for crack identification in structural member using strain or displacement measurement. They have modeled the open crack using Dirac delta function and evaluated the dynamic response based on modal superposition. They have validated the proposed identification algorithm by comparing the results from impact hammer tests on a beam with a single crack. Dado [25] has formulated a mathematical model to predict the crack location and their severities for beams with various end conditions such as pinned-pinned, clamped free, clamped-pin and clamped-clamped. They have developed the mathematical model, assuming the beam to be a rectangular Euler-Bernoulli beam. They have concluded that, though the assumption of the beam does not meet the requirements for real time application but the results obtained for the model developed can be used as a initial step to formulate crack identification methodology which can be used in general practice. Douka et al. [26] have studied the non-linear dynamic behavior of a cantilever beam both theoretically and experimentally. They have analyzed both the simulated and experimental response data by applying empirical mode decomposition and Hilbert transform method. They have concluded that the developed methodology can accurately analyze the nonlinearities caused by the presence of a breathing crack. Benfratello et al. [27] have presented both numerical and experimental investigations in order to assess the capability of non-Gaussianity measures to detect crack presence and position. They have used the skewness coefficient of the rotational degrees of freedom for the identification purpose of the crack in a damaged structure. Fledman [28] has introduced the application of Hilbert transform to non-stationary and nonlinear vibration system. He has demonstrated concepts of actual mechanical signals and utilizes the Hilbert transform for machine diagnostics and identification of mechanical systems. Routolo et al. [29] have analyzed the vibrational response of cracked beam due to harmonic forcing to evaluate the non linear characteristics. They have used the frequency response function to identify the location and depth of crack to set a basis for development of an experimental structural damaged identification algorithm.

Behzad et al. [30] have devised a continuous model for flexural vibration of beams containing edge crack perpendicular to neutral plane of the beam. They have taken the

displacement field as a superposition of the Euler Bernoulli displacement and displacement due to the presence of crack. They have taken the crack displacement as the product of time function and exponential space function. The results obtained are in good agreement with the results obtained from finite element analysis. They have used the beam with horizontal and vertical edge crack. Prasad et al. [31] have investigated the effect of location of crack from free end to fixed end in a vibrating cantilever beam. They compared and analyzed crack growth rate at different frequencies using the experimental setup. Rezaee et al. [32] have used perturbation method for analysis of vibration of a simply supported beam with breathing crack. From the analysis it is observed that for a given crack location on the beam structure with the increase in the relative crack depth the stiffness of the beam decreases with time. Dimarogonas et al. [33] have proposed a technique for crack identification in cracked rotating shafts using the dynamic response of the system. They have stated that the change in the modal response is due to the local flexibility introduced due to the presence of crack and dissimilar moments of inertia. He has found that the system behaves non-linearly because of the crack present in the rotating shaft. The results obtained from the developed analytical method for the closing crack condition is based on the assumption of large static deflections commonly found in turbo machinery. Faverjon et al. [34] have used constitutive relation error updating method to develop a crack diagnosis tool in damaged beam structures. Mazanoglu et al. [35] have carried out vibration analysis of non-uniform Euler – Bernoulli beams with cracks using energy based method and Rayleigh – Ritz approximation method. They have measured the change in strain in the cracked beam due to bending. They have also analyzed the beam using finite element program and compared the obtained results with that of the analytical method and found the results to be in good agreement. Wang et al. [36] have studied a composite cantilever having a surface crack and found that the variation in the modal response depends on two parameters i.e. crack location and material properties. They have concluded that the change in frequency can be effectively used to locate the crack position and measure its severities. Al-said [37] has presented a crack diagnostic method using the change in natural frequencies for a stepped cantilever beam carrying concentrated masses. He has also applied finite element analysis to validate the results obtained from the proposed method. He has successfully used the developed algorithm to identify cracks present in overhead gantry and girder cranes. Lee [38] has proposed a damage detection

methodology in beam structures using Newton-Rapson method and assuming the cracks present in the system as rotational springs. Yumin et al. [39] have analyzed cracked pipes to measure local flexibility matrix and stress intensity factor to develop an algorithm for damage identification. They have developed the method by dividing the cracked pipe into series of thin annuli. As described them, experimentally they have calculated the local flexibility matrix of the damaged pipes without calculating the Stress intensity factor. A modified version of the local flexibility has been proposed by Zou et al. [40] have studied the vibrational behavior of cracked rotor to design crack diagnostic model. They have described that, their developed method is suitable for the theoretical model. Cerri et al. [41] have investigated the vibrational characteristics of a circular arch both in damaged and undamaged state obtained from the theoretical model and compared the results with that of the experimental analysis to present a crack identification method. They have used the natural frequencies and vibration modes to develop the crack identification methodology by assuming the arch as a torsion spring at the cracked section. Nobile et al. [42] have presented a technique to find out the crack initiation and direction for circumferentially cracked pipes and cracked beams by adapting strain energy density factor. As stated by them, the strain energy density theory can be effectively used to analyze the different features of material damage in mixed mode crack propagation problem. Humar et al. [43] have investigated different vibration based crack identification techniques and find out the draw backs in them. The modal response parameters, stiffness, damping are directly affected by the presence of crack in the structure. According to them, most of the vibration based crack diagnosis techniques fail to perform when applied to real structures because of the inherent difficulties. They have presented computer simulation studies for some of the commonly used methodologies and suggested the conditions under which they may or may not perform. They have concluded that, all the practical challenges present in a real system cannot be simulated through computer applications entirely making the vibration based crack estimation methods a challenging field. Viola et al. [44] have studied the dynamic behavior of multi-stepped and multi-damaged circular arches. They have analyzed the arches both in damaged and undamaged condition to find out the numerical solutions by using Euler characteristics exponent procedure, generalized differential quadrature method. Shin et al. [45] have analyzed of the vibration characteristics of circular arches having variable cross section.

They have presented the equation for deriving the natural frequencies of the system at different boundary conditions with the help of generalized differential quadrature method, differential transformation method and the results obtained from their proposed method have been compared with the previously published work. Cerri et al. [46] have investigated a hinged plane circular arch for development of a structural damage detection technique by studying the changes in the natural frequencies of the system. They have discussed two different approaches for crack detection. One of the approaches is based on comparison of the variation of natural frequencies obtained from the experimental and theoretical method and the other is based on search of an intersection joint of curves obtained by the modern equations. Labuschagne et al. [47] have studied Euler – Bernoulli, Timo Shenko and two dimensional elasticity theories for three models of cantilever beams. From the analysis of the vibration parameters, they have concluded that the Timo Shenko theory is close to the two dimensional theory for practical purpose and the application of Euler – Bernoulli theory is limited. Babu et al. [48] have presented a technique i.e. amplitude deviation curve, which is a modification of the operational deflection shape for crack identification in rotors. They have described that for the damage diagnosis in rotors the parameters used to characterize the cracks are very complicated. Xia et al. [49] have proposed a technique for damage detection by selecting subset of measurement points and corresponding modes. In their study, two factors have been used for detecting the cracks, the sensitivity of a residual vector to the structural damage and the sensitivity of the damage to the measured noise. They have claimed that, the developed method is independent of damage status and is capable of detecting damage using the undamaged state of structure. Douka et al. [50] have derived the affect of cracks on the anti resonances of a cracked cantilever beam using analytical and experimental methods. They have used the shift in the anti resonances to locate cracks in the structure. The results obtained from their theoretical model have been validated using the results obtained from experimentation of Plexiglas beams for crack diagnosis. Sinha [51] has analyzed the non linear dynamic behavior in a mechanical system using higher order spectra tools for the identification of presence of harmonics in signals obtained from the system. They have found that, misaligned rotating shaft and cracked shaft, exhibits non linear behavior due to the presence of higher harmonics present in the signal. According to them, the higher order spectra tools can be effectively used for condition monitoring of mechanical

systems. Patil et al. [52] have derived an algorithm for damage assesment in a slender Euler-Bernoulli beam using variation in natural frequencies and transfer matrix method. They have assumed the cracks as rotational spring for development of the proposed technique for crack detection. Kim et al. [53] have presented a methodology for crack diagnosis in structures using the dynamic response of a two span continuous beam. During the development of the technique, they have reviewed two algorithms and eliminated the some of the assumptions and limitations in those methods. They have stated that, their methodology shows an improved accuracy in crack detection. Ebersbach et al. [54] have proposed a vibration based expert system for health monitoring of plant machinery, laboratory equipment to perform routine analysis. They have concluded that, their system can be used for high accuracy fault detection using the dynamic response of the system. Gounaris et al. [55] have presented a crack identification method in beam structures assuming the crack to be open and using eigenmodes of the structure. During the investigation, they have found out the relationship between the crack parameters and modal response. Finally, they have checked the authenticity of their method by comparing the eigenmodes for the damaged and undamaged beam in pre-plotted graphs. Shen et al. [56] have proposed a crack diagnostic procedure by measuring the natural frequencies and mode shapes. They have checked the robustness of their proposed method from the simulation results of a simply supported Bernoulli-Euler beam with one-side or symmetric crack. Ebrahimi et al. [57] have presented a new continuous model for bending analysis of a beam with a vertical edge crack which can be used for load-deflection and stress-strain assessment of the crack beam subject to pure bending. According to them, their proposed model assumes that the displacement field is a superposition of the classical Euler-Bernoulli beam's displacement and of a displacement due to the crack. Their developed bending differential equation of the cracked beam has been calculated using static equilibrium equations. They have found a good agreement between the analytical results and finite element method. Jasinski et al. [58] have developed a method for analyzing higher order spectra for forecasting and identification of the degree of degradation of a sample's dynamic properties. They have proposed residual bi-spectrum as a basis enabling to determine the initiation of a beam's fatigue-related crack. They have developed an experimental set up for checking the robustness of their proposed technique for fatigue crack identification present in a system. Hasheminejad et al [59] have studied the free

vibration of cracked nano wires considering the effects of surface elasticity and residual surface stress. The Euler–Bernoulli beam theory has been used by them and the crack is modeled by a rotational spring representing the discontinuity in the slope and proportional to the crack severity. They have demonstrated examples to evaluate the influence of beam length, and crack position and severity on the calculated values of natural frequencies of an anodic alumina nano wire in the presence of surface effects. They have stated that, their proposed study may be of interest for the design, performance improvement, and health monitoring of nano wire-based components. Rubio et al. [60] have presented a flexibility expression for cracked shafts having elliptical cracks based on the polynomial fitting of the stress intensity factors, taking into account the size and shape of the elliptical cracks. They have calculated the static displacements in bending of the shaft for different boundary conditions. From the analysis of the results obtained from experimental set up and finite element analysis they have concluded that their methodology can be suitably used for analyzing the behavior of the cracked shaft. Argatov et al. [61] have considered a problem of detecting localized large-scale internal damage in structures with imperfect bolted joints. During their analysis, they have utilized the structural damping and an equivalent linearization of the bolted lap joint response to separate the combined boundary damage from localized large-scale internal damage. In their approach, they have illustrated the longitudinal vibrations in a slender elastic bar with both ends clamped by bolted lap joints with different levels of damage. They have concluded that their proposed strategy can be utilized for estimation of internal damage severity in structures. Farshidi et al. [62] have investigated the non-contact EMA for evaluating the structural dynamics of a beam structure by exciting a cantilever beam using a collimated air impulse controlled by a solenoid valve. They have measured the reflected airwave from the beam surface by a microphone array. They have stated that the experimental tests demonstrate the effectiveness of their proposed methodology to both accurately and cost-effectively measure structural dynamics in translational and rotational degrees using a non-contact excitation and sensor mechanism. Casini et al. [63] have investigated the non-linear modal properties of a vibrating 2-degree of freedom system. They have found that, its non-linear frequencies are independent of the energy level and uniquely depend on the damage parameter. An analysis of the nonlinear normal modes has been performed by them for a wide range of damage parameter by

employing numerical procedures and Poincare maps. The influence of damage on the non-linear frequencies has been investigated and modes in internal resonance, with a significantly different shape than that of modes on fundamental branch, have been proposed. Carr et al. [64] have studied the influence of a surface fatigue crack on vibration behavior of tee-welded plates and results are compared to the influence of machined through-thickness cuts on the dynamic response of cantilever beams. They have analyzed the influence of naturally grown fatigue cracks on the oscillation frequencies and compared to two and three-dimensional numerical modeling results. The results obtained from their analysis showed the ability of the experimental technique to detect fatigue cracks from relatively earlier than the other method studied. Ribeiro and Fontul [65] have studied the dynamic response of structure excited at a given set of coordinates using transmissibility concept to identify fault present in the structure.

The finite element methods and wavelet analysis have been used for locating the size and severity of cracks and those are being discussed in the next section.

2.3.2 Crack detection using finite element method

Other than the classical methods the finite element methods is also applied by various researchers for crack detection in damaged structures, those have been described in this section.

Saavedra et al. [66] have presented a theoretical and experimental vibration analysis of a multibeams structure containing transverse crack. They have derived a new cracked finite element stiffness matrix to analyse the vibrational behavior of crack systems with different boundary conditions. Qian et al. [67] have developed a finite element model for crack detection in a damaged beam using stress intensity factors. They have also validated their model with the experimental results obtained for a cantilever beam. According to them their method is also applicable to complex structures with crack. Andrausa et al. [68] have investigated the features of non-linear response of a crack beam using two dimensional finite element model (FEM). They have considered the behavior of the breathing crack as a frictionless contact problem. They have compared the linear dynamic response with the non-linear dynamic response of the cantilever beam and presented a non-linear technique for

crack identification. Viola et al. [69] have developed a finite element model for a cracked Timoshenko beam for crack identification based on the changes in the dynamic behavior of the structure. They have derived the stiffness matrix and consistent mass matrix for developing the crack identification technique. Chondros et al. [70] have studied the torsional vibrational behavior of a circumferentially cracked cylindrical shaft using analytical and numerical finite element analysis; they have used HU-WASHIZU-BARR variational formulation to develop the analytical method for the cracked shaft. Ariaei et al. [71] have presented an analytical approach for determining the dynamic response of the undamped Euler-Bernoulli beams with breathing crack and subjected to the moving mass using discrete element technique and finite element method. They have observed that the presence of cracks alters the beam response patterns. Potirniche et al. [72] have developed a two dimensional finite element method to study the influence of local flexibility on the dynamic response of a structure. Narkis [73] has detected the crack by using inverse technique, that is, through the measurement of frequency of first two natural frequencies of a simply supported uniform beam. He has validated the developed method by comparing the results with the results from numerical finite element calculations. Ostachowicz et al. [74] have analyzed the forced vibrations of the beam and find out the impact of crack parameters such as crack position and its severity on the vibrational characteristics and discussed a basis for crack diagnosis. They have modeled the beam with triangular disk finite elements and assumed the crack to be a breathing crack. Zheng et al. [75] have analyzed the natural frequencies and mode shapes of a cracked and undamaged beam by developing an overall additional flexibility matrix using finite element method. They have also developed a shape function to compute the vibrational characteristics of the cracked beam. The gauss quadrature and least square method has been used by them to compute the overall additional flexibility matrix. The authors have constructed the shape function which can very well satisfy the local flexibility conditions of the crack locations. Kisa et al. [76] have used finite element and component mode synthesis methods to analyze the free vibration of uniform and stepped cracked beam of circular cross section. They have used stress intensity factor and strain energy release rate functions to calculate the flexibility matrix and inverse of the compliance matrix taking into account inertia forces. According to them, crack depth and crack location have considerable affect on the natural frequencies and mode shapes of the cracked beam with non propagating open

cracks. Karthikeyan et al. [77] have proposed a technique for estimation of crack location and size in beam structure from the free and forced response of the beam. They have used finite element method to analyze the modal response for the beam structure with transverse open crack.. In this work they have included the effect of proportionate damping and used an external unit to harmonically excite the beam. They have used an iterative algorithm and regularization technique for locating the crack positions and size on the cracked beam and the results are in good agreement with other methods even in presence of error and noise. Hearndon et al. [78] have formulated a methodology using Euler-Bernoulli and Timoshenko theories to analyze the affect of crack on dynamic properties of a cantilever beam subjected to bending. To evaluate the influence of crack location and size on the structural stiffness and calculation of transfer function a finite element model has been proposed by them. According to them the reduction in global component stiffness due to the crack is used to determine its dynamic response by a modal analysis computational model. In this work they have revealed that the natural frequencies decreases with increasing crack length. Al-Said [79] has proposed an algorithm based on a mathematical model to identify crack location and depth in an Euler-Bernoulli beam carrying a rigid disk. He has applied Lagrange's equation to develop the mathematical model for analyzing the lateral vibration of the beam model. The proposed method utilizes mode shapes of two uniform beams connected by mass less torsional spring to establish the trial function. The presented method utilizes the first three natural frequencies to estimate the crack parameters. Results from the presented technique have been authenticated using the finite element software. Shekhar et al. [80] has derived a method to calculate the vibration characteristics using model based on finite element analysis. Panigrahi [81] have performed a three dimensional non-linear finite element analysis to evaluate the normal and shear stress along the overlap zone in a fiber reinforced composite material.

Excepting the classical, wavelet analysis and finite element methods, Artificial Intelligence Techniques are also being adapted by authors for damage identification.

2.3.3 Crack detection using AI technique

In this section different types of Artificial Intelligence Techniques are analyzed in the field of crack detection in damaged structures. The methods are being sub grouped into five categories.

- a) Fuzzy Inference method
- b) Neural Network method
- c) Genetic Algorithm method
- d) MANFIS method
- e) Hybrid method
 - i) Neuro-Fuzzy Technique
 - ii) Genetic-fuzzy Technique
 - iii) Genetic-neural Technique
 - iv) Genetic-neural-fuzzy Technique

2.3.3.1 Fuzzy inference method

In this section various fuzzy inference methods used for crack identification are outlined.

Hasanzadeh et al. [82] have introduced a non-phenomenological method to solve the inverse problems, especially for the case of AC field measurement (ACFM) technique to identify surface cracks in metals. Their method is based on a formal framework of aligning electromagnetic probe responses by using the concept of similarity measures created by a fuzzy recursive least square algorithm as a learning methodology. They have claimed that, the proposed technique provides a means to compensate for the lack of sufficient samples in available crack databases for prediction of crack in structures. They have shown that the combination of this fuzzy inference method and the method of the adaptation for different crack shapes provides sufficient means as a priori empirical knowledge for the training system. Chandrashekhhar et al. [83] have shown that the geometric and measurement uncertainty cause considerable problem in the damage assessment. They have used Monte Carlo simulation to study the changes in the damage indicator due to uncertainty in the geometric properties of the beam. The results obtained from the simulation are used for

developing and testing the fuzzy logic system. In this paper they have addressed the uncertainty associated with the fuzzy logic system for structural damage detection. Kim et al. [84] have presented a computer based crack diagnosis system for concrete structures using Fuzzy set theory. They have used the crack symptoms and characteristics to build the rooms for the proposed fuzzy inference system. When they have applied the developed methodology to diagnose the crack the proposed system provided results similar to those obtained by experts system. Saravanan et al. [85] have proposed a technique based on the vibration signals acquired from the operating machines to effectively diagnose the conditions of inaccessible moving components inside the machine. The proposed technique has been designed using fuzzy classifier and decision tree to generate the rules automatically from the feature set. The developed fuzzy classifier has been tested with representative data and the results are found to be encouraging. Boutros et al. [86] have developed four condition monitoring indicators for detection of transient and gradual abnormalities using fuzzy logic approach. They have successfully tested and validated the fuzzy based technique in two different applications. Wu [87] has proposed a novel fuzzy robust wavelet support vector classifier (FRWSVC) based on a wavelet function and developed an adaptive Gaussian particle swarm optimization (AGPSO) algorithm to seek the optimal unknown parameter of the FRWSVC. The results obtained from experimentation are compared with that of the hybrid diagnosis model and are found to be closer. Sugumaran et al. [88] have presented the use of decision tree of a fuzzy classifier for selecting best few feature that will discriminate the fault condition of the bearing from given trained samples. The vibration signal from a piezoelectric transducer is captured for different types of fault condition of bearing and is used to build the fuzzy rules. The results drawn from the fuzzy classifier when compared with results from the experimental analysis, they are found to be close proximity. Miguel et al. [89] have developed a decision making module based on fuzzy logic for model based fault diagnosis applications. A fault detection and isolation system based on the input and output parameters have been successfully applied in laboratory equipments to reduce the uncertainties for the output parameter. Wada et al. [90] have proposed a fuzzy control method with triangular type membership functions using an image processing unit to control the level of granules inside a hopper. They stated that the image processing unit can be used as a detecting element and with the use of fuzzy reasoning methods good process responses

were obtained. Parhi [91] has developed a fuzzy inference based navigational control system for multiple robots working in a clumsy environment. They have been designed to navigate in an environment without hitting any obstacles along with other robots. Fox [92] has studied the use of fuzzy logic in medical diagnosis and raised a broad range of issues in connection to the role of information-processing techniques in the development of medical computing. Zimmermann [93] has applied fuzzy linear programming approach for solving linear vector maximum problem. The solutions are obtained by fuzzy linear programming. These are found to be efficient solutions then the numerous models suggested solving the vector maximum problem. Angelov et al. [94] have presented two new approaches for improving the performance of on line fuzzy classifier. They have used the developed fuzzy system for image classification in on line mode. Mohanta et al. [95] have developed a fuzzy Markov model to address the maintenance scheduling of a captive power plant by considering the various parameters affecting the failure repair cycle.

2.3.3.2 Neural network method


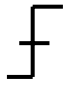
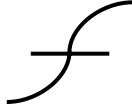
In this section different types of Neural network methods applied for crack identification are described. The Artificial Neural Networks (ANN) has been used as promising technique in the domain of inverse problem for fault identification.

Schlechtingen et al. [96] have presented a comparison of results among the regression based model and two artificial neural network based approaches, which are a full signal reconstruction and an autoregressive normal behavior model used for condition monitoring of bearings in a wind turbine. From the comparison of results they have revealed all three models were capable of detecting incipient faults. They have concluded that the neural network model provides the best result with a faster computational time with comparison to regression based model. Ghate et al. [97] have proposed a multi layer perceptron neural network based classifier for fault detection in induction motors which is inexpensive, reliable by employing more readily available information such as stator current. They have used simple statistical parameters as input feature space and principal component analysis has been used for reduction of input dimensionality. They have also verified their methodology to noise and found the performance of the proposed technique encouraging. Eski et al. [98] have presented a fault detection based on neural network for an experimental industrial

welding robot. Joint accelerations of robot have been considered by them as evaluation criteria. For this purpose, an experimental setup has been used to collect the related values and the accelerations of welding robot, which has six degrees of freedom, are analyzed. The results obtained show that the proposed RBNN has a robust stability to analyze the accelerations of manipulator joints during a prescribed trajectory. Fan et al. [99] have presented a fault detection and diagnosis (FDD) strategy for local system of air handling unit. Their strategy consists of two stages which are the fault detection stage and the fault diagnosis stage, respectively. In the first stage, the neural network fault detection model has been used by them for generating estimates of sensor values and they are compared to actual values to produce residuals. The proposed neural network fault detection model has been trained using an abundance of characteristic information from the historical data in the HVAC system. They have claimed that the trained neural model can detect the abnormal condition in the system. Paviglianiti et al. [100] have devised a scheme for detecting and isolating sensor faults in industrial robot manipulators. They have adopted a procedure for decoupling of the disturbance effect from the effect of the fault generated in the system. The dynamics of the proposed scheme has been improved by using radial basis functions neural network. Wang et al. [101] have proposed a new fault diagnosis method by using the difference of AR coefficients with back propagation neural network. The diagnosis results obtained by them are compared with the three methods, which include the difference of AR coefficients with BPNN, the AR coefficients with BPNN and the distance of AR coefficients method for various samples. They have found that the difference of AR coefficients with BPNN were superior to AR coefficients with BPNN and distance of AR coefficients methods. Suresh et al. [102] have presented a method considering the flexural vibration in a cantilever beam having transverse crack. They have computed modal frequency parameters analytically for various crack locations and depths and these parameters are used to train the neural network to identify the damage location and size. In this paper They have made a comparative study of the performance of two widely used neural network i.e. multi layer perception (MLP) network, radial basis function (RBF) network and shown the variation of actual output with the network output. Finally, they have concluded that the radial basis function network performance is better than multi layer perception network. Little et al. [103] have solved exactly a linearized version of the model and explicitly show that the capacity of

the memory is related to the number of synapses rather than the number of neurons. In addition, he has shown that in order to utilize this large capacity, the network must store the major part of the information in memory to generate patterns which evolve with time. Mehrjoo et al. [104] have presented a fault detection inverse algorithm to estimate the damage intensities of joints in truss bridge structure using back propagation neural network method. Agosto et al. [105] have applied neural network method with a combination of vibration and thermal damage detection signatures to develop a damage defection tool. They have applied the developed technique on sandwich composite for the purpose of crack detection. Saravanan et al. [106] have dealt with the robustness of an artificial neural network, wave let and proximal support vector machine based on fault diagnostic methodology for a gear box. They have used the proposed methodology for fault diagnosis in bevel gear box. Oberholster et al. [107] have presented a methodology for online structure health monitoring of axially flow for blades with the use of neural network. The developed neural network has been trained with the extracted vibration features from the experimental test structures. They have used frequency response function and finite element models for designing the neural network based technique. According to them the proposed technique can handle the online damage classification using sensor for the test structures. Wu et al. [108] have described a condition monitoring and fault identification techniques for rotating machineries using wavelet transform and neural network method. The sound emission from the gear set have been used along with continuous wavelet transform technique and feature selection of energy spectrum to design the neural network based fault diagnostic tool. The experimental results from their methodology pointed out that the sound emission from the system can be used for effective fault diagnosis for condition monitoring. Wu et al. [109] have investigated a fault diagnosis technique for internal combustion engine using discrete wavelet transform (DWT) and neural network. The DWT technique has been combined with feature selection of energy spectrum for the development of the purposed fault detection algorithm. Some of the activation functions used by researchers in designing of artificial neural network are presented in Table 2.1 given below.

Table 2.1 Examples of Activation Functions used in ANN

Name	Input/output Relation	Symbol
Hard Limit	$a=0 \quad n<0$ $a=1 \quad n\geq 0$	
Symmetrical Hard Limit	$a= -1 \quad n<0$ $a= +1 \quad n\geq 0$	
Hyperbolic tangent sigmoid	$a = \frac{e^n - e^{-n}}{e^n + e^{-n}}$	

2.3.3.3 Genetic algorithm method

In the process of development of various methods for crack identification genetic algorithm is also used efficiently for accurate measurement of the damage location and depth and also fault detection in engineering systems. The genetic algorithm based methodologies are discussed in this section.

Meruane et al. [110] have implemented an hybrid real-coded Genetic Algorithm with damage penalization to locate and quantify structural damage. The performance of five fundamental functions based on modal data is studied by them. In addition, the authors have proposed the use of a damage penalization that satisfactorily avoids false damage detection due to experimental noise or numerical errors. They have tested the effectiveness of the proposed technique on a tridimensional space frame structure with single and multiple damages scenarios and stated that this approach reaches a much more precise solution than conventional optimization methods. Nobahari et al. [111] have proposed an efficient optimization procedure using genetic algorithm to detect multiple damage in structural systems based on the changes in the natural frequency. They have applied finite element analysis to evaluate the required natural frequencies. Two numbers of bench mark tests have been utilized to demonstrate the computational advantages of the proposed method by them. Li et al. [112] have presented a novel feature extraction and selection scheme for hybrid fault diagnosis of gearbox based on transform function, non-negative matrix factorization (NMF) and multi-objective evolutionary genetic algorithms. The transform function has been adapted to acquire the vibration signals for various fault condition of the gear system and the

non-negative matrix factorization (NMF) was employed to extract features from the time–frequency representations. The genetic algorithm has been used for accurate classification of hybrid faults of gearbox. Results from the experiments as described by them revealed that the proposed feature extraction and selection scheme demonstrate to be an effective and efficient tool for hybrid fault diagnosis of gearbox. Fernando et al. [113] have dealt with the crack detection in structural elements by means of a genetic algorithm optimization method taking into account the existence of contact between the interfaces of the crack. They have addressed bi- and three-dimensional models to handle the dynamics of a structural element with a transverse breathing crack. Physical experiments have been performed by them with a cantilever damaged beam and the resulting data are used as input in the fault diagnostic genetic algorithm. The benefits of applying automated fault detection and diagnosis to chillers include less expensive repairs, timely maintenance, and shorter downtimes. Han et al. [114] have employed feature selection (FS) techniques, such as mutual-information-based filter and genetic algorithm to help search for the important sensors in data driven chiller fault detection and diagnosis applications, to enhance the performance of fault identification technique. The results shows that the eight features/sensors, centered around the core refrigeration cycle and selected by the proposed method, outperform the other three feature subsets by the linear discriminant analysis. Hussain et al. [115] have described a novel method for real time fault detection in gearboxes using adaptive features extraction algorithm to deal with non-stationary faulty signals. They have claimed that their proposed method is based on combination of conventional one-dimensional and multi-dimensional search methods, which showed high performance and accurate fault detection results compared with evolutionary algorithms like genetic algorithms. Singh et al. [116] have developed a two stage identification methodology, which identifies a number of cracks, their locations on a cracked shaft and its sizes. In the methodology they have utilized transverse forced responses of the shaft system at different frequencies of a harmonic excitation. A multi-objective genetic algorithm technique has been designed using the frequency response of the dynamic structure for crack detection in shaft like structures. Lei et al. [117] have proposed a new multidimensional hybrid intelligent diagnosis method to identify different categories and levels of gear damage automatically using Hilbert transform, wavelet packet transform (WPT) and empirical mode decomposition (EMD) methods to extract additional fault

characteristic information. They have used the extracted features of the system to develop the multidimensional features based genetic algorithm technique to identify gear faults. Sette et al. [118] have presented a method to simulate a complex production process using a neural network and the optimization by genetic algorithm for quality control of the end product in a manufacturing environment. He has applied this method to a spinning production process where input parameters are machine settings and fiber quality, and the yarn strength, elongation are output parameters for the neural network model. He has used the genetic algorithm with a sharing function and a Pareto optimization to optimize the input parameters for obtaining the best yarns. According to him the results from this method are considerably better than current manual machine intervention. Xiang et al. [119] have proposed a new method for crack location and depth in a shaft by following rotating Rayleigh-Euler and Rayleigh-Timoshenko beam elements of B-spline wavelet on the interval. He has described that the cracked shaft is modeled by using wavelet-based elements to gain precise frequencies. According to him the 1st three frequencies are measured to locate the crack and the depths are detected by genetic algorithm. The robustness of the proposed method has been validated by some numerical examples and experimental cases and he has concluded that the method is capable of the detecting the crack in a shaft. He et al. [120] have studied the crack detection in a rotating machine shaft by using finite element method to optimize the problem and subsequently used genetic algorithm to search the solution. Their proposed method has been found to solve a wide range of inverse identification problem. Zhang et al. [121] have used genetic programming (GP) in finding faults in rotating machinery. They compared the solution through GP with other techniques like artificial neural network (ANN) and support vector machines (SVMs). They have found that GP demonstrates performance equal or better compared to ANN and SVMs. Zhang et al. [122] have studied the fault in rolling element bearing by the combination of genetic algorithm (GA) and fast kurtogram. For the initial analysis of the vibration signals of the bearing they have used fast kurtogram and subsequently for final optimization they have used GA. The results of their combined applications of GA and kurtogram have been found to give better results over the other optimal resonance demodulation techniques. Baghmisheh et al. [123] have used genetic algorithm (GA) to monitor the changes in natural frequencies of a cantilever beam having crack. They have used an analytical model to formulate the crack beam structure and

numerical methods to obtain the natural frequencies. The depths and crack locations have been solved by using binary and continuous genetic algorithms (BGA, CGA). Perera et al. [124] have used genetic algorithm for solving multi objective optimization to detect damage. They have compared GA optimizations based on aggregating functions with pareto optimality. Friswell et al. [125] have combined genetic algorithm (GA) and eigen sensitivity method for determination of location of damage in structures. The GA has been used by them to optimize the discrete damage location variables. They have used eigen sensitivity method to optimize the damage extent.

2.3.3.4 Multiple adaptive neuro fuzzy inference system (MANFIS)

This section depicts, the literature review of published paper from the domain of applications of MANFIS technique in various fields and fault diagnosis.

A neuro-fuzzy inference system, or equivalently, a neuro-fuzzy system is a fuzzy inference system which employs neural network learning techniques. Multiple adaptive neuro-fuzzy inference system (MANFIS) [127, 128, 129] is an extension of a single-output neuro-fuzzy system, ANFIS, so that multiple outputs can be handled. A neuro-fuzzy system is a nonparametric regression tool, which models the regression relationship non-parametrically without reference to any pre-specified functional form, and it is capable of modeling highly nonlinear and approximately known systems.

Cheng et al. [130] have optimize a multiple output system using the MANFIS neuro-fuzzy network for modeling the system and genetic algorithm has been used to optimize the multiple objective function. The validity of the technique has been performed using a practical problem. Buyukozkan et al. [131] have studied the performance of a new product development process (NPD) under uncertain conditions and given their effort to improve the quality of decision-making in NPD by following new iterative methodology. They have used fuzzy logic, neural networks and MANFIS technique for improvising the methodology for new product idea selection. Hengjie et al. [132] have presented a probabilistic fuzzy neural network (ProFNN) approach for handling randomness in the system by introducing the probability of input linguistic terms and providing linguistic meaning into the connectionist

architecture. The results from the proposed technique have been compared with that of multi-input–multi-output-ANFIS (MANFIS), self-organizing adaptive fuzzy neural control and Extreme Learning Machine for validation of the probabilistic fuzzy neural network. Vairappan et al. [133] have illustrated an improved adaptive neuro-fuzzy inference system (ANFIS) for the application of time-series prediction. The proposed improved version of ANFIS has introduced the application of self-feedback connections for modeling the temporal dependence. The effectiveness of the proposed methodology has been validated by using three benchmark time-series tests. Gholamian et al. [134] have presented a systematic design for multi objective problems using hybrid intelligent system to solve ill-structured situations. Fuzzy rules and neural networks are used in this systematic design and the developed hybrid system is established with the ability of mapping between objective space and solution space. The results obtained are authenticated on three test problems. Ellithy et al. [135] presented a methodology based on ANFIS to improve the damping of power systems in the presence of load model parameters uncertainty. The proposed ANFIS is trained over a wide range of typical load parameters to adapt the gains of the SVC stabilizer. They have claimed that the simulation results are showing encouraging trends in comparison to SVC stabilizer operating on other techniques. Güneri et al. [136] have developed a new approach to address the supplier selection problem. The proposed ANFIS model has been trained with parameters relating to supplier selection criteria. They have tested the results from their technique by comparing with the results of the multiple regression method, demonstrating that the ANFIS method performed well. Nagarajan et al. [137] in their study have proposed the design of Adaptive Neuro-Fuzzy Observer based sensor fault detection in a three-tank interacting level process. They have designed the fault detection algorithm with Multiple Adaptive Neuro-Fuzzy Inference System (MANFIS) that uses a neural network to fix optimal shape and parameters for the membership functions and effective rule base for the fuzzy system. Fault detection is being performed by them estimating the states of the level process and comparing them with measured values. Jassar et al. [138] have established a technique to find out the temperature in heating space utilizing an adaptive neuro-fuzzy inference system. The proposed system has been developed by combining the fuzzy inference systems and artificial neural networks. The results from the developed method have been cross verified by experimentation. Asensi et al. [139] have formulated a system

based on multiple adaptive neuro-fuzzy inference systems (MANFIS) to analyze the performance characteristics of analog circuit. Zhang et al. [140] have studied a dynamic system and developed an algorithm to identify the chaotic signals present in a system by adopting adaptive-neuro-fuzzy-inference system (ANFIS) and MANFIS methodology.

Nguyen et al. [141] have used vibration analysis and fuzzy logic technique to develop a fault detection method in bearings. The parameters representing the condition of the system have been used to design the proposed technique based on Adaptive Network based Fuzzy Inference System (ANFIS) and Genetic Algorithm (GA). The results obtained from the developed model have been tested with other set of bearing data to exhibit the reliability of the chosen model. Lei et al. [142,143] have proposed a method for fault diagnosis of rolling element bearing system using multiple adaptive neuro-fuzzy inference systems (MANFIS) and empirical mode decomposition (EMD). The robustness of the developed mechanism has been checked by employing the same on different bearing systems.

So in the subsequent section algorithm have been discussed used for fault diagnosis using hybrid AI techniques such as Neuro-Fuzzy, Genetic-fuzzy Technique, Genetic-neural Technique and Genetic-neural-fuzzy Technique.

2.3.3.5 Hybrid method

Scientists have developed hybrid techniques by fusing the capabilities of various artificial intelligence methodologies such as fuzzy logic, neural network and genetic algorithm for condition monitoring of damaged structures. The hybrid methods can be sub grouped into four sections.

- i) Neuro- fuzzy Technique
- ii) Genetic-fuzzy Technique
- iii) Genetic-neural Technique
- iv) Genetic-neural-fuzzy Technique

2.3.3.5.1 Neuro-fuzzy technique

This section analyzes the application of Neuro-fuzzy technique in the domain of fault diagnosis.

Salahshoor et al. [144] have devised an innovative data-driven fault detection and diagnosis methodology on the basis of a distributed configuration of three adaptive neuro-fuzzy inference system for an industrial power plant steam turbine. Each neuro-fuzzy classifier has been developed for a dedicated category of four steam turbine faults. A proper selection of four measured variables has been configured to feed each classifier with the most influential diagnostic information. A diverse set of test scenarios has been carried out to illustrate the successful diagnostic performances of the proposed fault detection system. Sadeghian et al. [145] have used nonlinear system identification method to predict and detect process fault of a cement rotary kiln. To identify the various operation points in the kiln, locally linear neuro-fuzzy model trained by LOLIMOT algorithm has been adapted by the authors. Then, using this method, they have obtained three distinct models for the normal and faulty situations. At the end, they have checked the proposed technique with the validation data. Eslamloueyan et al. [146] have proposed a hierarchical artificial neural network (HANN) for isolating the faults of the Tennessee–Eastman process which is the simulation of a chemical plant created by the Eastman Chemical Company to provide a realistic industrial process for evaluating process control and monitoring methods. Fuzzy clustering algorithm has been used by them to divide the fault patterns space into a few sub-spaces. They have developed supervisor network along with the special neural networks to diagnose the fault present in the system. Simon et al. [147] have describes the pattern recognition based data analysis of an existing industrial batch dryer, and the comparison of three artificial intelligence techniques suited to perform classification tasks: neural networks, neuro-fuzzy and Takagi–Sugeno fuzzy models. They have found that the neural networks trained with the Bayesian regularization have shown the most robust classification performance with respect to other two methods. They have claimed that since the proposed method for pattern recognition is not case specific it can be directly used for the monitoring of a large variety of drying processes. Quteishat et al. [148] have proposed a modified fuzzy min-max network for improved performance when large hyper boxes are formed in the network. This methodology is used to facilitate the extraction of rule set from FMM to justify the predictions. The results from the developed

FMM have been authenticated with the sensor measurements collected from a power generation plant for fault diagnosis. Topcu et al. [149] have studied the optimum uses of pozzolans as supplementary cementing material for blended cement production. They have developed a system based on artificial neural network and fuzzy logic for predicting the strength parameters for different types of cement motors. Tran et al. [150] presented a fault diagnosis technique based on adaptive neuro-fuzzy inference system in combination with classification and regression tree. The ANFIS model has been trained with the results obtained from the least square algorithm. They have observed that the developed ANFIS model has the potential for fault diagnosis of induction motors. Fang et al. [151] have explored performance of a structural damage detection technique based on frequency response and neural network. In this paper they have investigated a tunable steepest descent algorithm using heuristics approach for improving the converging speed. From the analysis of the result of the proposed method for a cantilever beam they have concluded that the neural network technique can estimate the damage condition with high accuracy. Beena et al. [152] have proposed a new approach for fault detection in structural system using fuzzy logic technique and neural network based on hebbian-learning. They have used the continuum mechanics and finite element method to measure the vibration parameters because of structure damage. The developed technique works quite well for structural damage even in the presence of noise. Kuo et al. [153] have presented a symbiotic evolution based fuzzy neural diagnostic system for fault detection of a propeller shaft used in the marine propulsion system. The system auto-generates its own optimal fuzzy neural architecture for fault diagnosis. They have stated that the results from the hybrid fuzzy neural system have been found to be more closure with the real conditions than the other traditional methods. Ye et al. [154] have developed a new online diagnostic algorithm to find out the mechanical fault of electrical machine using wavelet packet decomposition method and adaptive neuro fuzzy inference system. According to them the new integrated fault diagnostic system significantly reduces the system complexity, and computational time of the system. They have validated results from the diagnostic technique for a 3-phase induction motor drive system. Kuo [155] has proposed a fault detection system using data acquisition, feature extraction and pattern recognition for detecting faults of blades by applying multiple vibration sensors. The feature extraction algorithm has been developed based on back propagation artificial neural network. The fuzzy

logic technique has been employed to speed up the training speed. According to him the results from the system are very close to the results obtained from the experimental analysis. Zio et al. [156] have presented a fault diagnostic problem using neuro fuzzy approach. They have used this approach for the purpose of high rate of correct classification and to obtain an easily interpretable classification model. The efficiency of the approach has been verified by applying to a motor bearing system and the results obtained are quite encouraging. Wang et al. [157] have presented the comparison of the performance for two fault diagnosis systems that is recurrent neural networks and neuro fuzzy systems using two benchmark data sets. As described by them, it is found that the neuro fuzzy prognostic system is more reliable for machine health condition monitoring than the neural network fault diagnostic system. Zhang et al. [158] have proposed a bearing fault detection technique based on multi scale entropy and adaptive neuro fuzzy inference system (ANFIS) to measure the nonlinearity existing in a bearing system. They have conducted experiments on electrical motor bearing with three different fault categories and the results obtained from the experimentation have been used to design and train the ANFIS system for fault diagnosis.

2.3.3.5.2 Genetic-fuzzy technique

The research papers reviewed from the domain of application of Genetic-fuzzy technique for crack and fault detection in structural and mechanical systems are presented in this section.

Wu et al. [159] have presented a new version of fuzzy support vector machine to diagnose faults in automatic car assembly. The input and output variables have been described by them as fuzzy numbers in the fuzzy based system. They have shown that the modified GA helps the fuzzy support vector classifier machine to seek optimized parameters. The results from their methodology in car assembly for fault diagnosis confirm the feasibility and the validity of the diagnosis method. Pan et al. [160] have analyzed the effect of random delays in network controlled system by using fuzzy PID models. They have tuned the models by minimizing the time multiplied absolute error and squared model output with stochastic algorithms viz. the GA and particle swarm optimization. After analyzing the performance of the algorithm they have shown that random variation in network delay can be handled efficiently with fuzzy logic based PID models over other techniques as mentioned in the

paper. Pawar et al. [161] have devised a structural health monitoring methodology using genetic fuzzy system for online damage detection. They have used displacement and force based measurement deviations between damage and undamaged condition for building the rules and data pool for the fuzzy and genetic system respectively. The developed methodology has been applied for composite rotor blades and the results are found to be encouraging. Yuan et al. [162] have proposed an artificial immunization algorithm (AIA) to optimize the parameters obtained from support vector machines (SVM) generally used as machine learning tool for fault-diagnosis. They have used the proposed fault diagnosis model for a turbo pump rotor and found that the SVM optimized by AIA gives higher accuracy than the normal SVM.

2.3.3.5.3 Genetic-neural technique

The Genetic-neural techniques used by various authors for development of crack diagnostic tools are depicted in this section.

Hajnayeb et al. [164] have designed a system based on artificial neural networks (ANNs) to diagnose different types of fault in a gear box. They have used experimental set of data to verify the effectiveness and accuracy of the proposed method. Their developed system has been optimized by eliminating unimportant features using a feature selection method. This method of feature selection has been compared with Genetic Algorithm (GA) results and is found to be in close agreement. Chen et al. [165] have proposed a robust fault diagnosis system of rotating machine adapting machine learning technology by employing a set of individual neural networks based on structured genetic algorithm. The frequency signals and the corresponding faults have been used to train the developed technique. They have stated that the advantage of using their approach is to obtain the optimal parameters automatically and improved performance in diagnosis accuracy. Firpi et al. [166] have used genetically programmed artificial feature (GPAF) for fault detection of a rotating machine part. They have extracted artificial features using GPAF algorithm while taking vibration data as a source of information. Samanta [167] has compared the performance of gear fault detection using artificial neural network (ANN) and support vector machines (SVMs) and has found that the classification accuracy of SVMs is better than ANN without genetic algorithm (GA) optimization while with GA optimization performance of both classifiers are comparable.

Jack et al. [168] have used support vector machines (SVMs) and artificial neural network (ANN) with genetic algorithm (GA) optimization technique to detect faults in rotating machinery. They have compared the performance of this classification and improve the overall performance by using GA based features selection process.

2.3.3.5.4 Genetic-neural-fuzzy technique

The literature reviewed from the published papers using Genetic-neural-fuzzy Technique for crack and fault detection in various systems are discussed in this section.

Li et al. [169] have presented a novel enhanced genetic algorithm (EGA) technique to overcome the problems present in classical GA like slow convergence and time consumption and to provide a more efficient technique for system training and optimization. The developed method has been used to train a neural-fuzzy predictor for real-time gear system monitoring and found that their technique outperforms the classical GA in terms of convergence speed. Zheng et al. [170] have presented a method which combines the genetic algorithm and fuzzy logic to optimize the centers and widths of the radial basis function neural network (RBFNN) for structural health monitoring of a glass epoxy composite laminates. They have used the linear least-squared method to adjust the neural network connection weights. From the analysis of results they have concluded that the simulation demonstrates that the neural network based on genetic algorithm and fuzzy logic is robust and promising. Saridakis et al. [171] have studied the dynamic behavior of a shaft with two transverse cracks considered to the along arbitrary angular positions at some distance from the clamped end. They have developed a fuzzy logic based crack diagnosis model by using the effect of bending vibrations of the cracked shaft. Genetic algorithm and neural network have been used for the developed technique to reduce the computational time without any significant loss in accuracy. Kolodziejczyk et al. [172] have investigated the potential of various artificial intelligence techniques to predict the damage parameters mainly arising due to wearing out of the contact surfaces. The proposed technique has been designed using fuzzy logic, neural network and genetic algorithm. The results from the developed methodology are found to be closer to the experimental data. They have also optimized the proposed crack diagnose model to reach high robustness.

2.3.4 Miscellaneous methods and tools used for crack detection

Excepting the various methods cited above miscellaneous methods and tools are also used for crack detection and some of them are briefly discussed in this section.

Gordis et al. [173] have developed two global–local algorithms for the analysis of quasi-static crack propagation in a structure based on frequency domain structural synthesis. The crack propagation problem has been based on a simple two-layer finite element where the two layers are connected by inter-layer springs. At the end they have found that the synthesis-based algorithms significantly outperform the traditional finite element solution. Bachschmid et al. [174] have used the model of a turbo-generator unit to perform a numerical sensitivity analysis, in which the vibrations of the shaft-line, and more in detail the vibrations of the shaft in correspondence to the bearings, have been calculated for all possible positions of the crack along the shaft-line, and for several different values of the depth of the crack. They have established a relation between the dynamic response and the position of crack location and depth present in the system. Jun has [175] proposed a diagnosis system using dynamic time warping (DTW) and discriminant analysis with oxidation–reduction potential (ORP) and dissolved oxygen (DO) values for fault detection in a swine wastewater treatment plant. Finally he has concluded that the ORP method outperforms the other two methods which have been employed for fault identification in the system. Yiakopoulos et al. [176] have designed a K-means clustering approach for the automated diagnosis of defective rolling element bearings. They have stated as K-means clustering is an unsupervised learning procedure, the method can be directly implemented to measured vibration data. Thus, the need for training the method with data measured on the specific machine under defective bearing conditions is eliminated. They have concluded that, the proposed system is an effective tool to detect faults in bearing systems. Cusido et al. [177] have paper proposed a different signal processing method, which combines wavelet and power spectral density techniques giving the power detail density as a fault factor. The method shows good theoretical and experimental results. Cao et al. [178] have developed a novel Laplacian scheme to form an improved damage identification algorithm. They have measured the modal curvature to develop the diagnostic method. The results from the proposed Laplacian scheme have been validated with experimental results. Fagerholt et al. [179] have described

an investigation on the fracture behavior of a cast aluminium alloy. They have used classical flow theory for modeling the fracture. They have also used Digital Image Correlation (DIC) to obtain information of the displacement and strain field in the specimen. The results from the numerical investigation are found to be in agreement with the experimental data. Karaagac et al. [180] have studied the effect of crack ratios and positions on the natural frequencies and buckling loads of a slender cantilever Euler beam with a single edge crack using the local flexibility concept. Experiments have been conducted by them to validate the numerical results. Rus et al. [181] have presented a work based on hyper singular shape sensitivity boundary integral equation for solution of the inverse problem for crack estimation. The accuracy and convergence of the sensitivity for the proposed method has been verified with the simulated/experimental results. Kyricazoglou et al. [182] have presented method to detect the damage in composite laminates by measuring and analyzing the slope deflection curve of composite beams in flexure. They have provided the damage mechanism and location of damage from comparison of dynamic results with the dynamic response from the damaged laminates. He suggested that slope deflection curve is a promising technique for detection initial damage in composites. Peng et al. [183] have introduced a new concept of non linear output frequency response functions (NOFRFS) to detect cracks in beams using frequency domain information. As stated by him the NOFRFS are a sensitive indicator of presence of cracks. He has suggested that this method establishes a basis for the application of NOFRF concept in fault diagnosis of structures. Friswell [184] has given an overview of the use of inverse method in the detection of crack location and size by using vibration data. He has suggested that in this method the uncertain parameters associated with the model have to be identified. In this work he has discussed a number of problems with this method for health monitoring, including modeling error, environmental efforts, damage localization and regularization. Zheng et al. [185] have presented a tool for vibrational stability analysis of cracked hollow beams. According to him each crack is assigned with a local flexibility coefficient which is a function of depth of crack. He has used least squared method to device the formulae for shallow cracks and deep cracks. In this work he has adapted Hamilton's principle to formulate the governing equation by employing the flexibility coefficient of the cracks which serves as that of the rotational spring. Leontios et al. [186] have presented a new method of crack detection in beams based on Kurtosis. As

stated by him the location of the crack has been determined by the abrupt changes in spatial variation of the analyzed response and the size of the crack is calculated by the estimation of Kurtosis. In this work the proposed method has been validated by experiments on crack Plexiglas beams. According to him the proposed Kurtosis-based prediction method is more attractive than the existing methods for crack detection due to low computational complexity. Bayissa et al. [187] have presented a new method for damage identification based on the statistical moments of the energy density function of the vibration responses in time-frequency domain. According to this article the major advantage of this method is that the time-frequency analysis conducted using the wavelet transform provides a tool to characterize deterministic as well as random responses and can be used to detect slight changes in the response of local vibration. Finally he has suggested that the proposed method is more sensitive to damage than the other methods. Dilella et al. [188] have shown that the natural frequency and anti resonant frequency contains certain generalized Fourier coefficients of the stiffness variation due to damage. According to him the results of numerical simulations on rods with localized or diffused cracks are in good agreement with theory. He has concluded that the experimental results show that the inverse problem solution, noise and modeling errors on anti resonances amplified strongly than the natural frequency data used. Kim et al. [189] have developed a technique to address the problem of condition-based maintenance scheme in industrial machines by correctly measuring the remaining life of the machine component utilizing the support vector machine tool. As claimed by them, the results from their method have been very encouraging and can be used as a potential tool for prediction of remaining life of machineries. Jafari et al. [190] have discussed an approach for fracture density estimation in an oil well structure using an adaptive neuro-fuzzy inference system. They have stated that, the proposed method have produced results in close proximity with measured values. Bacha et al. [190] have presented a novel technique for fault classification in a power transformer using dissolved gas analysis and multi-layer support vector machine classifier. When the developed technique is compared with other methods; the proposed methodology performance in detecting the faults in the power transformer has been superior. Mandal et al. [192] have proposed a new leak detection technique to address the problem of false leak detection in pipelines carrying fluids by applying rough set theory and support vector machine (SVM). They have designed the

SVM using artificial bee colony algorithm and particle swarm optimization technique. They have found from the experimental analysis that, their method is capable of detecting leaks with higher accuracy. Rao et al. [193] have presented a method for crack identification in a cracked cantilever beam. They have identified the crack by analyzing the vibration signatures using continuous wavelet transform technique. The results obtained using this method has been validated both by analytical and experimental methods over a cantilever beam containing transverse surface crack. Quek et al. [194] have investigated and presented the sensitivity of wavelet technique in the detection of cracks in beam structures considering the effects of different crack characteristics, boundary conditions, and wavelet functions. From the analysis, they have concluded that the wavelet transform is a useful tool in detection of cracks in beam structures. Wang et al. [195] have studied the damage detection in structural systems using spatial wavelets technique. According to them, their technique is neither dependent on the complete analysis of the structure nor on the material properties nor prior stress states of the structure. They have also checked the authenticity of this new technique by numerical and analytical analysis. Loutridis et al. [196] have presented a method based on wavelet analysis using the sudden changes in the spatial variations of the dynamic response of the cracked structures. The proposed technique has been validated by analytically and experimentally. Gentile et al. [197] have investigated to develop a technique based on continuous wavelet transform for detecting the location of open crack in damaged beams by minimizing the measurement data and baseline information of the structure. Pieper [198] has suggested a control design for a flexible manipulator for position control using soft computing. Torres-Torriti [199] has proposed a novel approach using Kalman filter for localization of mobile robots in clumsy environment by minimizing Hausdorff distance. Rout et al. [200] have discussed about a methodology to simulate the real condition for optimized design of a manipulator. The design has been carried out using differential evolution optimization and orthogonal array technique. Samantaray et al. [201] have presented a bond graph model to simulate systems to validate the steady-state results obtained from the theoretical study. Panigrahi et al. [202] have proposed a new evolutionary algorithm method adopting Adaptive Particle Swarm Optimization to measure the parameters such as amplitude, phase and frequency of a power quality signal. Casanova et al. [203] have presented a new technique for 2D localisation of moving objects. They have used laser and

radio frequency in the system to find out the robot position and orientation. Packianather et al. [204] have investigated the effect of processing and geometric factor on the injection molding performance for polymer material using computational technique.

2.4 Findings of the literature review

By analyzing the reviewed literature as discussed in the above section, it is observed that analytical methods and artificial intelligence (AI) techniques exist for identification of single crack in structural members, but extension to multiple numbers of cracks to the author knowledge, are unsolved problems. Various types of AI methods such as fuzzy inference, neural network, genetic algorithm can be potentially used as the basis for development fault detection algorithms. But it is seen that, the capabilities of artificial intelligence techniques are not completely explored to design and develop intelligent model for multiple crack diagnosis.

In the current research, a systematic effort has been made to develop AI based intelligent system for structural health monitoring of cantilever beam model using fuzzy inference, neural network, genetic algorithm, MANFIS and hybrid techniques. The parameters required to design and train the AI model have been obtained by using the theoretical, finite element and experimental analysis of the cantilever beam structure.

Publication

- D. R. K. Parhi and Dash Amiya Kumar, Analysis of methodologies applied for diagnosis of fault in vibrating structures, Int. J. Vehicle Noise and Vibration, Vol. 5, No. 4, 2009, 271-286.

Chapter 3

EVALUATION OF DYNAMIC CHARACTERISTICS OF BEAM STRUCTURE WITH MULTIPLE TRANSVERSE CRACKS

It has been observed that the presence of cracks in structures or in machine members lead to operational problem as well as premature failure. A number of researchers throughout the world are working on structural dynamics and particularly on dynamic characteristics of structures with crack. The dynamic characteristic comprises of natural frequencies; the amplitude responses due to vibration and the mode shapes. Due to presence of crack the dynamic characteristics of structure changes e.g. there is a reduction in natural frequencies, an increase in modal damping.

3.1 Introduction

In the recent times, the dynamic responses of cracked structure have been analyzed effectively by different researchers. The modal parameters are found to vary due to presence of crack in the structure and the intensity of variation is a function of crack intensity and position of crack. Engineers and scientists have emphasized the effect of crack on the natural frequencies and mode shapes of dynamically vibrating structure, which in turn can be efficiently utilized for developing crack identification algorithms. The focus of this chapter is to adopt a systematic approach to formulate a theoretical model to analyze the effect of multiple cracks on the modal response of the cantilever beam structure. Stress intensity factor and strain energy release rate from linear fracture mechanics theory have been employed to derive the dimensionless compliance matrices and subsequently the local stiffness matrices. The stiffness matrix has been utilized to find out the variation in the dynamic response of the multiple cracked beams in comparison to that of the undamaged beam. In the theoretical analysis different boundary conditions have been laid down to compute the natural frequencies and mode shapes for the cantilever beam structure with various crack depths and crack locations. The modal responses obtained from the theoretical analysis have been authenticated by comparing the results with that of the experimental analysis.

3.2 Vibration characteristics of a multi cracked cantilever beam

3.2.1 Theoretical analysis

This section presents the approach adopted to build the theoretical model for measuring the modal characteristics i.e. natural frequencies and mode shapes of the cracked beam containing multiple transverse cracks for different relative crack depths and relative crack positions and undamaged beam structure. During the analysis of the theoretical results, it is observed that a noticeable change in the first three mode shapes have been marked at the vicinity of crack locations. The robustness of the proposed theoretical approach has been established by comparing the results with the experimental results.

3.2.1.1 Evaluation of local flexibility of the damaged beam under axial and bending loading

Fig. 3.1(a) presents a multi cracked cantilever beam, subjected to axial load (P_1) and bending moment (P_2). The loading provides a coupling effect resulting in both longitudinal and transverse motion of the beam. The beam contains two transverse cracks of depth ' a_1 ' and ' a_2 ' having width ' B ' and height ' W '. Due to the cracks present in the beam a local flexibility will be introduced and a 2x2 matrix is considered, which represents the flexibility of the beam. Fig. 3.1(b) represents the cross sectional view of the cantilever beam model.

At the cracked section strain energy release rate can be explained as [20];

$$J = \frac{1}{E'} (K_{I1} + K_{I2})^2, \text{ Where } \frac{1}{E'} = \frac{1 - \nu^2}{E} \text{ (for plane strain condition);} \quad (3.1a)$$

$$= \frac{1}{E} \text{ (for plane stress condition)} \quad (3.1b)$$

The Stress intensity factors K_{I1} , K_{I2} are of mode I (opening of the crack) for load P_1 and P_2 respectively. The values of stress intensity factors from earlier studies [20] are;

$$\frac{P_1}{WB} \sqrt{\pi a} (F_1(\frac{a}{W})) = K_{I1}, \frac{6P_2}{W^2 B} \sqrt{\pi a} (F_2(\frac{a}{W})) = K_{I2} \quad (3.2)$$

The expressions for F_1 and F_2 are as follows

$$\left. \begin{aligned} F_1\left(\frac{a}{W}\right) &= \left(\frac{2W}{\pi a} \tan\left(\frac{\pi a}{2W}\right)\right)^{0.5} \left\{ \frac{0.752 + 2.02(a/W) + 0.37(1 - \sin(a\pi/2W))^3}{\cos(a\pi/2W)} \right\} \\ F_2\left(\frac{a}{W}\right) &= \left(\frac{2W}{\pi a} \tan\left(\frac{\pi a}{2W}\right)\right)^{0.5} \left\{ \frac{0.923 + 0.199(1 - \sin(a\pi/2W))^4}{\cos(a\pi/2W)} \right\} \end{aligned} \right\} \quad (3.3)$$

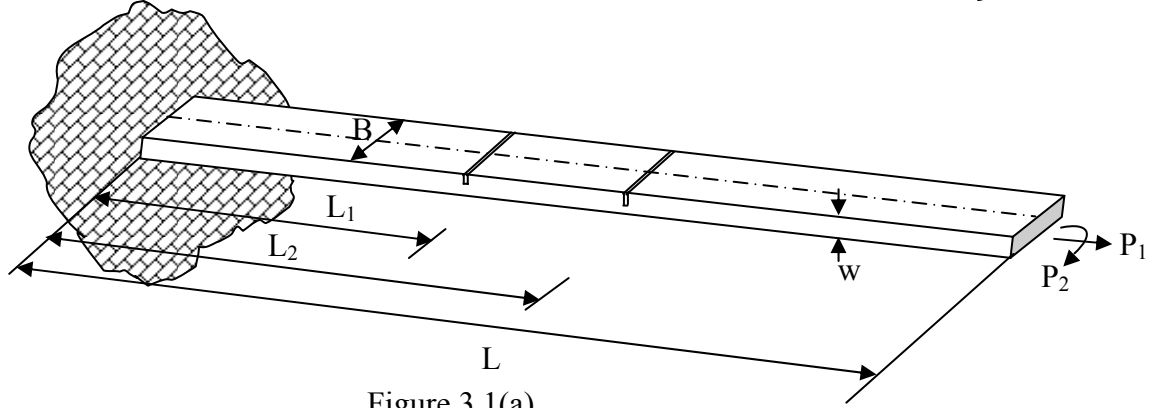


Figure 3.1(a)

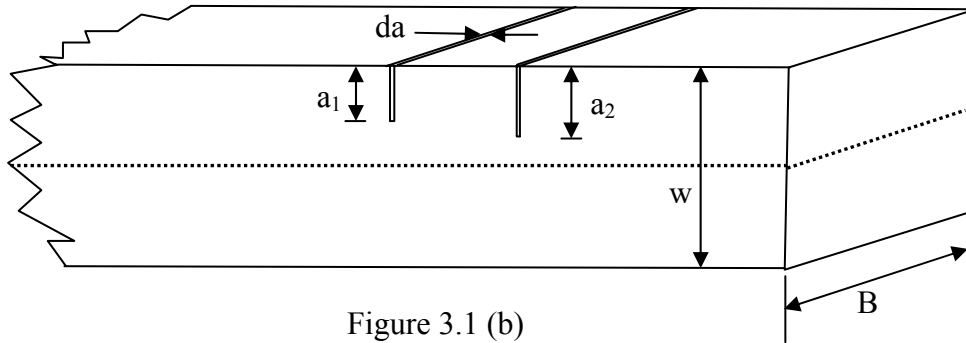


Figure 3.1 (b)

Fig. 3.1 Geometry of beam, (a) Cantilever beam, (b) Cross-sectional view of the beam.

Assuming U_t be the strain energy due to the crack. The additional displacement along the force P_i according to Castigliano's theorem is;

$$\frac{\partial U_t}{\partial P_i} = u_i \quad (3.4)$$

$$\text{The form of strain energy will have, } U_t = \int_0^{a_1} J da = \int_0^{a_1} \frac{\partial U_t}{\partial a} da \quad (3.5)$$

Where $J = \frac{\partial U_t}{\partial a}$ the strain energy density function.

Hence, from equations (3.1) and (3.3), we can have

$$\frac{\partial}{\partial P_i} \left[\int_0^{a_i} J(a) da \right] = u_i \quad (3.6)$$

C_{ij} the flexibility influence co-efficient by definition is

$$\frac{\partial u_i}{\partial P_j} = \frac{\partial^2}{\partial P_j \partial P_i} \int_0^{a_i} J(a) da = C_{ij} \quad (3.7)$$

$$\text{and can be expressed as, } \frac{WB}{E'} \frac{\partial^2}{\partial P_j \partial P_i} \int_0^{\xi_1} (K_{i2} + K_{i1})^2 d\xi = C_{ij} \quad (3.8)$$

Using equation (3.8) the compliance C_{11} , C_{22} , C_{12} ($=C_{21}$) are as follows;

$$\begin{aligned} C_{11} &= \frac{BW}{E'} \int_0^{\xi_1} \frac{\pi a}{B^2 W^2} 2(F_1(\xi))^2 d\xi \\ &= \frac{2\pi}{BE'} \int_0^{\xi_1} \xi (F_1(\xi))^2 d\xi \end{aligned} \quad (3.9)$$

$$C_{12} = C_{21} = \frac{12\pi}{E'BW} \int_0^{\xi_1} \xi F_1(\xi) F_2(\xi) d\xi \quad (3.10)$$

$$C_{22} = \frac{72\pi}{E'BW^2} \int_0^{\xi_1} \xi F_2(\xi) F_2(\xi) d\xi \quad (3.11)$$

The dimensionless form of the influence co-efficient will be;

$$\overline{C}_{11} = C_{11} \frac{BE'}{2\pi} \quad \overline{C}_{12} = C_{12} \frac{E'BW}{12\pi} = \overline{C}_{21} ; \quad \overline{C}_{22} = C_{22} \frac{E'BW^2}{72\pi} \quad (3.12)$$

The inversion of compliance matrix will lead to the formation of local stiffness matrix and can be written as;

$$K = \begin{bmatrix} C_{11} & C_{12} \\ C_{21} & C_{22} \end{bmatrix}^{-1} = \begin{bmatrix} K_{11} & K_{12} \\ K_{21} & K_{22} \end{bmatrix} \quad (3.13)$$

The stiffness matrix for the first and second crack location can be obtained as follows:

$$K' = \begin{bmatrix} k'_{11} & k'_{12} \\ k'_{21} & k'_{22} \end{bmatrix} = \begin{bmatrix} C'_{11} & C'_{12} \\ C'_{21} & C'_{22} \end{bmatrix}^{-1} \quad \text{and} \quad K'' = \begin{bmatrix} k''_{22} & k''_{23} \\ k''_{32} & k''_{33} \end{bmatrix} = \begin{bmatrix} C''_{22} & C''_{23} \\ C''_{32} & C''_{33} \end{bmatrix}^{-1}$$

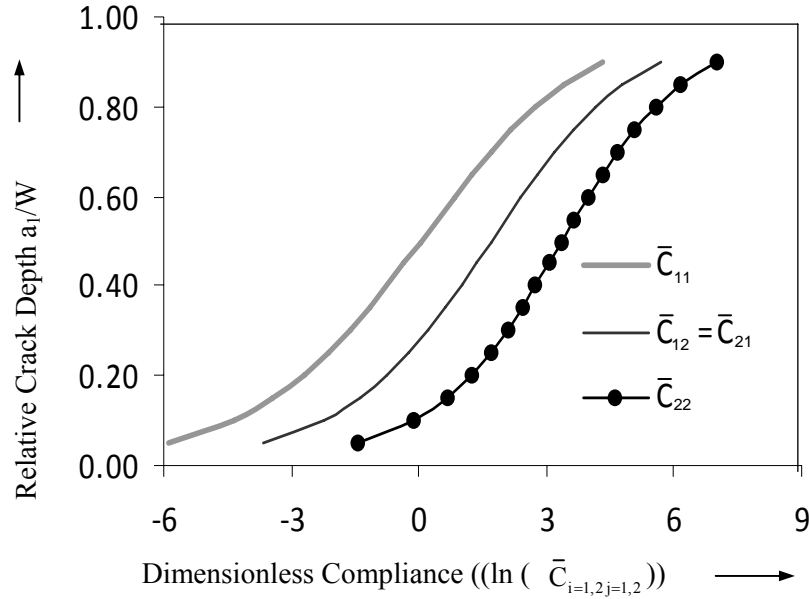


Fig. 3.2 Relative Crack Depth (a_1/W) vs. Dimensionless Compliance $((\ln(\bar{C}_{i=1,2,j=1,2})))$

The variations of dimensionless compliances with respect to relative crack depth have been shown in Fig. 3.2 and from the graph it is observed that the dimensionless compliance increases with increase in relative crack depths.

3.2.1.2 Vibration analysis of the multi cracked cantilever beam

In the present section, a cantilever beam (Fig. 3.3) with multiple crack with length 'L' width 'B' and depth 'W', having cracks at distance 'L₁' and 'L₂' with crack depths 'a₁' and 'a₂' respectively from the fixed end has been analyzed. The amplitudes of longitudinal vibration have been taken as u₁(x, t), u₂(x, t), u₃(x, t) and amplitudes of bending vibration have been considered as y₁(x, t), y₂(x, t), y₃(x, t) for the section-1(before 1st crack), section-2 (in between cracks), section-3 (after the 2nd crack) respectively as shown in Fig.3.3.

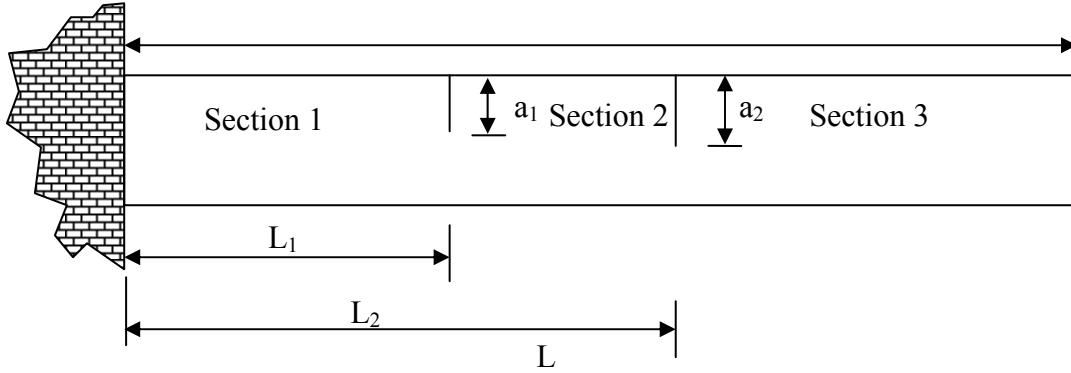


Fig. 3.3 Front view of the cracked cantilever beam

The following are the expressions of normal functions for the system

$$\bar{u}_1(\bar{x}) = A_1 \cos(\bar{K}_u \bar{x}) + A_2 \sin(\bar{K}_u \bar{x}) \quad (3.14a)$$

$$\bar{u}_2(\bar{x}) = A_3 \cos(\bar{K}_u \bar{x}) + A_4 \sin(\bar{K}_u \bar{x}) \quad (3.14b)$$

$$\bar{u}_3(\bar{x}) = A_5 \cos(\bar{K}_u \bar{x}) + A_6 \sin(\bar{K}_u \bar{x}) \quad (3.14c)$$

$$\bar{y}_1(\bar{x}) = A_7 \cosh(\bar{K}_y \bar{x}) + A_8 \sinh(\bar{K}_y \bar{x}) + A_9 \cos(\bar{K}_y \bar{x}) + A_{10} \sin(\bar{K}_y \bar{x}) \quad (3.14d)$$

$$\bar{y}_2(\bar{x}) = A_{11} \cosh(\bar{K}_y \bar{x}) + A_{12} \sinh(\bar{K}_y \bar{x}) + A_{13} \cos(\bar{K}_y \bar{x}) + A_{14} \sin(\bar{K}_y \bar{x}) \quad (3.14e)$$

$$\bar{y}_3(\bar{x}) = A_{15} \cosh(\bar{K}_y \bar{x}) + A_{16} \sinh(\bar{K}_y \bar{x}) + A_{17} \cos(\bar{K}_y \bar{x}) + A_{18} \sin(\bar{K}_y \bar{x}) \quad (3.14f)$$

Where, $\bar{x} = \frac{x}{L}$, $\bar{u} = \frac{u}{L}$, $\bar{y} = \frac{y}{L}$, $\beta_1 = \frac{L_1}{L}$, $\beta_2 = \frac{L_2}{L}$

$$\bar{K}_u = \frac{\omega L}{C_u}, C_u = \left(\frac{E}{\rho} \right)^{1/2}, \bar{K}_y = \left(\frac{\omega L^2}{C_y} \right)^{1/2}, C_y = \left(\frac{EI}{\mu} \right)^{1/2}, \mu = A\rho$$

The constants A_i , ($i=1, 18$) are to be calculated using the laid down boundary conditions. The following are the boundary conditions for the cantilever beam;

$$\bar{u}_1(0)=0; \quad 3.15(a)$$

$$\bar{y}_1(0)=0; \quad 3.15(b)$$

$$\bar{y}'_1(0)=0; \quad 3.15(c)$$

$$\bar{u}'_3(1)=0; \quad 3.15(d)$$

$$\bar{y}''_3(1)=0; \quad 3.15(e)$$

$$\bar{y}_3(1)=0 \quad 3.15(f)$$

At the fractured section:

$$\bar{u}'_1(\beta) = \bar{u}'_2(\beta); \quad 3.16(a)$$

$$\bar{y}_1(\beta_1) = \bar{y}_2(\beta_1); \quad 3.16(b)$$

$$\bar{y}'_1(\beta_1) = \bar{y}'_2(\beta_1); \quad 3.16(c)$$

$$\bar{y}''_1(\beta_1) = \bar{y}''_2(\beta_1); \quad 3.16(d)$$

$$\bar{u}'_2(\beta_2) = \bar{u}'_3(\beta_2); \quad 3.16(e)$$

$$\bar{y}_2(\beta_2) = \bar{y}_3(\beta_2); \quad 3.16(f)$$

$$\bar{y}''_2(\beta_2) = \bar{y}''_3(\beta_2); \quad 3.16(g)$$

$$\bar{y}'''_2(\beta_2) = \bar{y}'''_3(\beta_2); \quad 3.16(h)$$

The expression in equation (3.17) can be found out because of the discontinuity of axial deformation to the right and left of the first crack location at the distance L_1 from the fixed end of the cantilever beam. Also at the cracked section, we have

$$AE \frac{du_1(L_1)}{dx} = k'_{11}(u_2(L_1) - u_1(L_1)) + k'_{12} \left(\frac{dy_2(L_1)}{dx} - \frac{dy_1(L_1)}{dx} \right) \quad (3.17)$$

Multiplying $\frac{AE}{Lk'_{11}k'_{12}}$ on both sides of equation (3.17) we get ;

$$M_1 M_2 \bar{u}_1'(\beta_1) = M_2 (\bar{u}_2(\beta_1) - \bar{u}_1'(\beta_1)) + M_1 (\bar{y}_2'(\beta_1) - \bar{y}_1'(\beta_1)) \quad (3.18)$$

The expression in equation (3.19) can be found out because of the discontinuity of slope to the left and right of the crack at the crack section.

$$EI \frac{d^2 y_1(L_1)}{dx^2} = k'_{21} (u_2(L_1) - u_1(L_1)) + k'_{22} \left(\frac{dy_2(L_1)}{dx} - \frac{dy_1(L_1)}{dx} \right) \quad (3.19)$$

Multiplying $\frac{EI}{L^2 k'_{22} k'_{21}}$ on both sides of equation (3.19) we get;

$$M_3 M_4 \bar{y}_1''(\beta_1) = M_4 (\bar{y}_2'(\beta_1) - \bar{y}_1'(\beta_1)) + M_3 (\bar{u}_2(\beta_1) - \bar{u}_1(\beta_1)) \quad (3.20)$$

Similarly considering the second crack we can have;

$$M_5 M_6 \bar{u}_2'(\beta_2) = M_6 (\bar{u}_3(\beta_2) - \bar{u}_2(\beta_2)) + M_5 (\bar{y}_3'(\beta_2) - \bar{y}_2'(\beta_2)) \quad (3.21)$$

$$M_7 M_8 \bar{y}_2''(\beta_2) = M_8 (\bar{y}_3'(\beta_2) - \bar{y}_2'(\beta_2)) + M_7 (\bar{u}_3(\beta_2) - \bar{u}_2(\beta_2)) \quad (3.22)$$

Where $M_1 = AE/(Lk'_{11})$, $M_2 = AE/k'_{12}$, $M_3 = EI/(Lk'_{22})$, $M_4 = EI/(L^2 k'_{21})$

$M_5 = AE/(Lk''_{22})$, $M_6 = AE/k''_{23}$, $M_7 = EI/(Lk''_{33})$, $M_8 = EI/(L^2 k''_{32})$

By using the normal functions, equation (3.14a) to equation (3.14f) with the laid down boundary conditions as mentioned above, the characteristic equation of the system can be expressed as;

$$|Q| = 0 \quad (3.23)$$

This determinant is a function of natural frequency (ω), the relative locations of the crack (β_1, β_2) and the local stiffness matrix (K) which in turn is a function of the relative crack depth ($a_1/W, a_2/W$).

Where Q is a 18x18 matrix and is expressed as

$$[Q] = \begin{bmatrix} 0 & 0 & 0 & 0 & 0 & 0 & 0 & 0 & 0 & 0 & 0 & 0 & 1 & 0 & 0 & 0 & 0 & 0 \\ 1 & 0 & 1 & 0 & 0 & 0 & 0 & 0 & 0 & 0 & 0 & 0 & 0 & 0 & 0 & 0 & 0 & 0 \\ 0 & 1 & 0 & 1 & 0 & 0 & 0 & 0 & 0 & 0 & 0 & 0 & 0 & 0 & 0 & 0 & 0 & 0 \\ 0 & 0 & 0 & 0 & 0 & 0 & 0 & 0 & 0 & 0 & 0 & 0 & 0 & 0 & 0 & 0 & -T_1 & T_2 \\ 0 & 0 & 0 & 0 & 0 & 0 & 0 & 0 & G_3 & G_4 & -G_7 & -G_8 & 0 & 0 & 0 & 0 & 0 & 0 \\ 0 & 0 & 0 & 0 & 0 & 0 & 0 & 0 & G_4 & G_3 & G_8 & -G_7 & 0 & 0 & 0 & 0 & 0 & 0 \\ 0 & 0 & 0 & 0 & 0 & 0 & 0 & 0 & 0 & 0 & 0 & 0 & -T_6 & T_5 & T_6 & -T_5 & 0 & 0 \\ G_1 & G_2 & G_5 & G_6 & -G_1 & -G_2 & -G_5 & -G_6 & 0 & 0 & 0 & 0 & 0 & 0 & 0 & 0 & 0 & 0 \\ G_1 & G_2 & -G_5 & -G_6 & -G_1 & -G_2 & G_5 & G_6 & 0 & 0 & 0 & 0 & 0 & 0 & 0 & 0 & 0 & 0 \\ G_2 & G_1 & G_6 & -G_5 & -G_2 & -G_1 & -G_6 & G_5 & 0 & 0 & 0 & 0 & 0 & 0 & 0 & 0 & 0 & 0 \\ 0 & 0 & 0 & 0 & 0 & 0 & 0 & 0 & 0 & 0 & 0 & 0 & 0 & 0 & -T_4 & T_3 & T_4 & -T_3 \\ 0 & 0 & 0 & 0 & G_9 & G_{10} & G_{11} & G_{12} & -G_9 & -G_{10} & -G_{11} & -G_{12} & 0 & 0 & 0 & 0 & 0 & 0 \\ 0 & 0 & 0 & 0 & G_9 & G_{10} & -G_{11} & -G_{12} & -G_9 & -G_{10} & G_{11} & G_{12} & 0 & 0 & 0 & 0 & 0 & 0 \\ 0 & 0 & 0 & 0 & G_{10} & G_9 & G_{12} & -G_{11} & -G_{10} & -G_9 & -G_{12} & G_{11} & 0 & 0 & 0 & 0 & 0 & 0 \\ -S_3 & -S_4 & S_5 & -S_6 & S_3 & S_4 & -S_5 & S_6 & 0 & 0 & 0 & 0 & S_1 & -S_2 & T_5 & T_6 & 0 & 0 \\ S_7 & S_8 & -S_9 & -S_{10} & -S_{11} & -S_{12} & S_{13} & -S_{14} & 0 & 0 & 0 & 0 & S_{15} & S_{16} & -S_{15} & -S_{16} & 0 & 0 \\ 0 & 0 & 0 & 0 & V_3 & V_4 & -V_5 & V_6 & -V_3 & -V_4 & V_5 & -V_6 & 0 & 0 & V_1 & V_2 & -T_3 & -T_4 \\ 0 & 0 & 0 & 0 & V_7 & V_8 & -V_9 & -V_{10} & -V_{11} & -V_{12} & V_{13} & -V_{14} & 0 & 0 & V_{15} & V_{16} & -V_{15} & -V_{16} \end{bmatrix} \quad (3.24)$$

Where;

$$T_1 = \sin \bar{k}_u, T_2 = \cos \bar{k}_u, T_3 = \cos(\bar{k}_u \beta_2), T_4 = \sin(\bar{k}_u \beta_2), T_5 = \cos(\bar{k}_u \beta_1), T_6 = \sin(\bar{k}_u \beta_1),$$

$$G_1 = \cosh(\bar{k}_y \beta_1), G_2 = \sinh(\bar{k}_y \beta_1), G_3 = \cosh(\bar{k}_y), G_4 = \sinh(\bar{k}_y),$$

$$G_5 = \cos(\bar{k}_y \beta_1), G_6 = \sin(\bar{k}_y \beta_1), G_7 = \cos(\bar{k}_y), G_8 = \sin(\bar{k}_y), G_9 = \cosh(\bar{k}_y \beta_2),$$

$$G_{10} = \sinh(\bar{k}_y \beta_2), G_{11} = \cos(\bar{k}_y \beta_2), G_{12} = \sin(\bar{k}_y \beta_2), M_1 = AE / (Lk'_{11}), M_2 = AE / k'_{12},$$

$$M_3 = EI / (Lk'_{22}), M_4 = EI / (L^2 k'_{21}), M_{12} = M_1 / M_2, M_{34} = M_3 / M_4, S_1 = T_5 - M_1 \bar{k}_u T_6,$$

$$S_2 = T_6 + M_1 \bar{k}_u T_5, S_3 = M_{12} S_{11}, S_4 = M_{12} S_{12}, S_5 = M_{12} S_{13}, S_6 = M_{12} S_{14}, S_7 = M_3 \bar{k}_y^2 G_1 + S_{11},$$

$$S_8 = M_3 \bar{k}_y^2 G_2 + S_{12}, S_9 = M_3 \bar{k}_y^2 G_5 + S_{13}, S_{10} = M_3 \bar{k}_y^2 G_6 - S_{14},$$

$$S_{11} = \bar{k}_y G_2, S_{12} = \bar{k}_y G_1, S_{13} = \bar{k}_y G_6, S_{14} = \bar{k}_y G_5, S_{15} = M_{34} T_5, S_{16} = M_{34} T_6, M_5 = AE / (Lk''_{22}),$$

$$\begin{aligned}
M_6 &= AE/k_{23}'' , & M_7 &= EI/(Lk_{33}'') , & M_8 &= EI/(L^2k_{32}'') , & M_{56} &= M_5 / M_6 , \\
M_{78} &= M_7 / M_8 , & V_1 &= T_3 - M_5 \bar{k}_u T_4 , & V_2 &= T_4 + M_5 \bar{k}_u T_3 , & V_3 &= M_{56} V_{11} , & V_4 &= M_{56} V_{12} , \\
V_5 &= M_{56} V_{13} , & V_6 &= M_{56} V_{14} , & V_7 &= M_7 \bar{k}_y^2 G_9 + V_{11} , & V_8 &= M_7 \bar{k}_y^2 G_{10} + V_{12} , \\
V_9 &= M_7 \bar{k}_y^2 G_{11} + V_{13} , & V_{10} &= M_7 \bar{k}_y^2 G_{12} - V_{14} , & V_{11} &= \bar{k}_y G_{10} , & V_{12} &= \bar{k}_y G_9 , & V_{13} &= \bar{k}_y G_{12} , \\
V_{14} &= \bar{k}_y G_{11} , & V_{15} &= M_{78} T_3 , & V_{16} &= M_{78} T_4
\end{aligned}$$

3.2.2 Numerical analysis

The cantilever beam with multiple crack and undamaged condition has been considered for numerical analysis, to compute the relative natural frequencies and relative amplitude of vibration for different crack locations and crack severities. In the current investigation, the cantilever beam model used for the vibration analysis has the following dimensions.

Length of the Beam	= 800mm
Width of the beam	= 38mm
Height of the Beam	= 6mm
Relative crack depth (a_1/W , a_2/W)	= Varies from 0.083 to 0.416
Relative crack location (L_1/L , L_2/L)	= Varies from 0.0625 to 0.9375

3.2.2.1 Results of theoretical analysis

The theoretical analysis has been carried out to obtain the mode shapes for the first three modes of the cracked aluminum cantilever beam model with different crack locations and crack severities using the equation (3.24). A comparison of mode shapes computed for both the multiple cracked and undamaged beam member along with the magnified using views at the vicinity of crack location have been presented in Fig. (3.4a to 3.4 c).

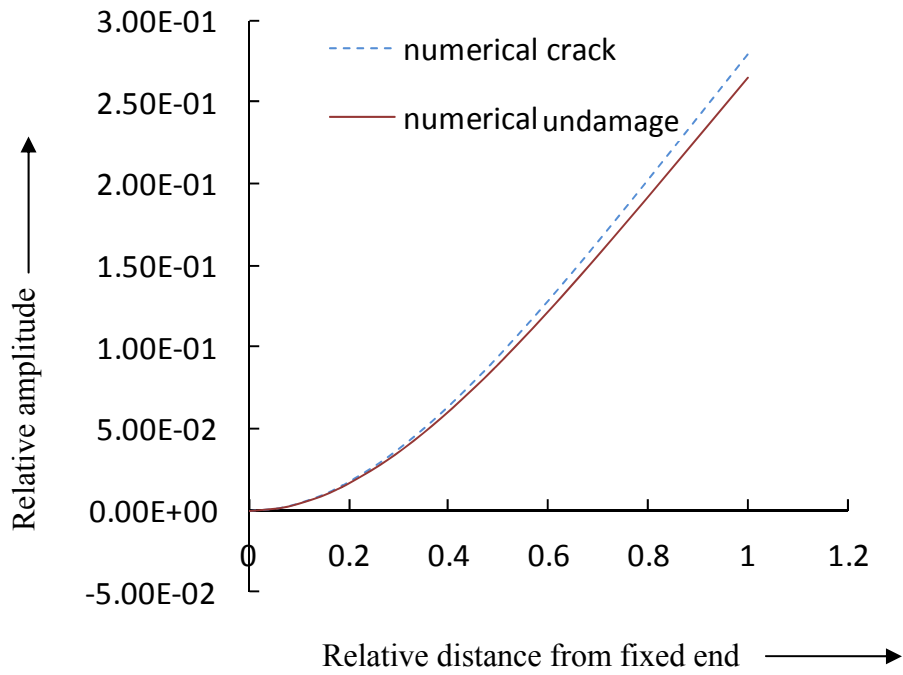


Fig. 3.4a Relative amplitude vs. relative distance from the fixed end (1st mode of vibration), $a_1/W=0.083$, $a_2/W=0.333$, $L_1/L=0.1875$, $L_2/L=0.5625$.

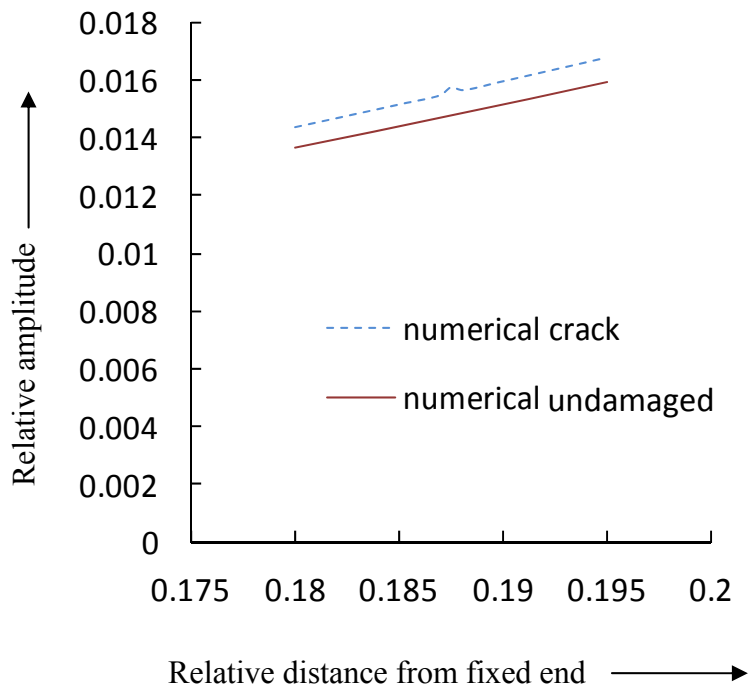


Fig. 3.4a1 Magnified view of fig. 3.4a at the vicinity of the crack location $L_1/L=0.1875$.

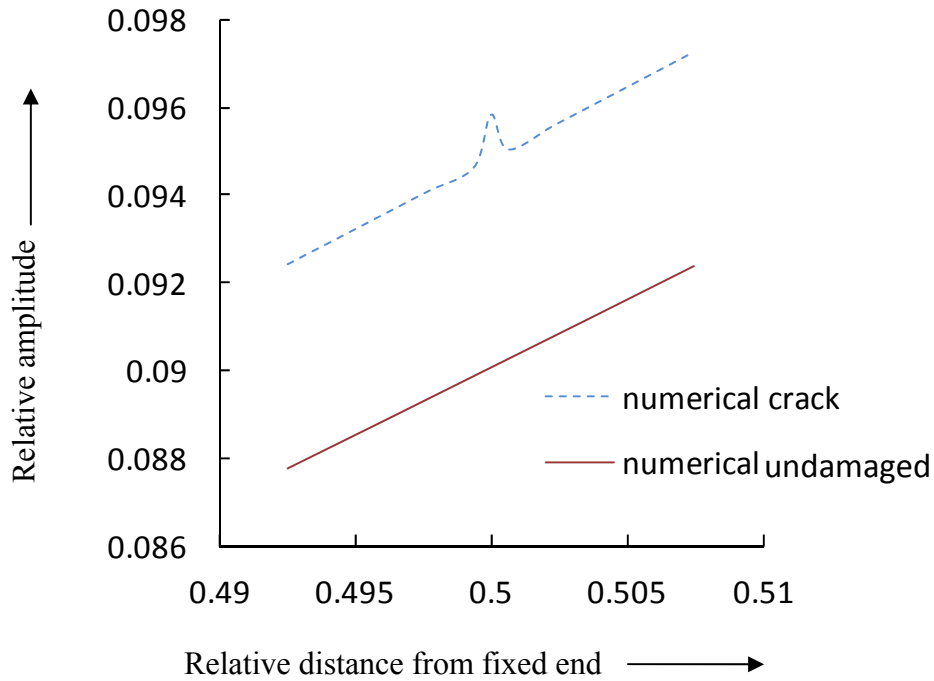


Fig. 3.4a2 Magnified view of fig. 3.4a at the vicinity of the crack location $L_2/L=0.5625$.

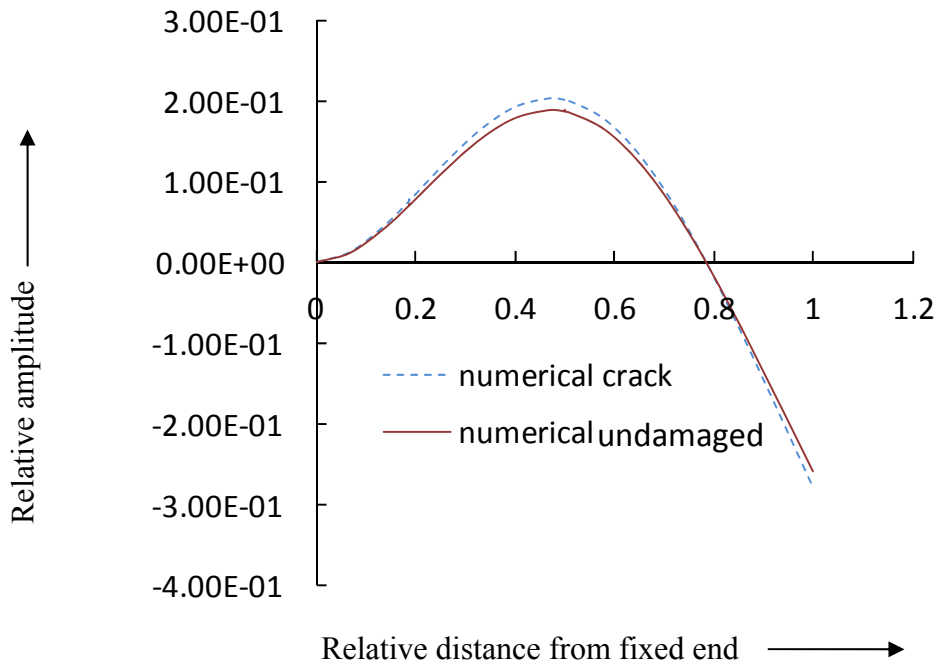


Fig. 3.4b Relative amplitude vs. relative distance from the fixed end (2nd mode of vibration), $a_1/W=0.083$, $a_2/W=0.333$, $L_1/L=0.1875$, $L_2/L=0.5625$.

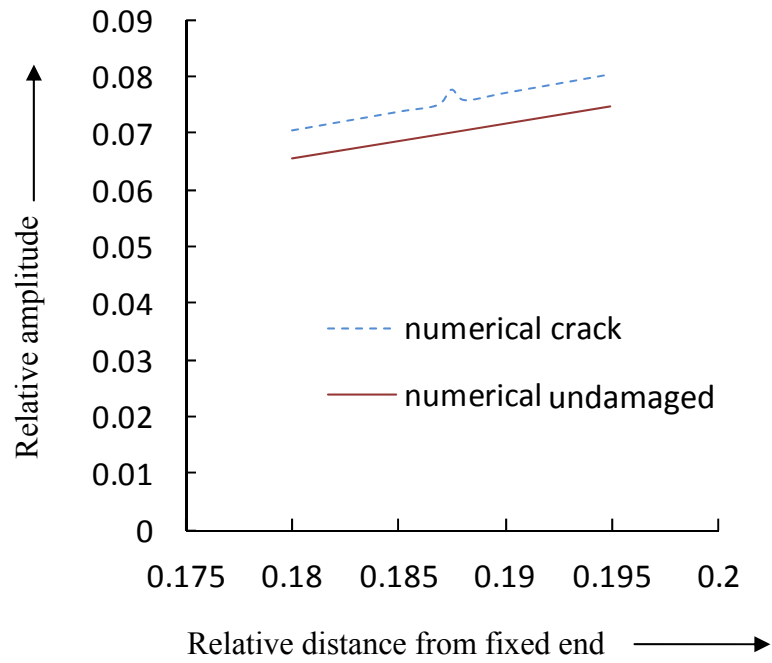


Fig. 3.4b1 Magnified view of fig. 3.4b at the vicinity of the crack location $L_1/L=0.1875$.

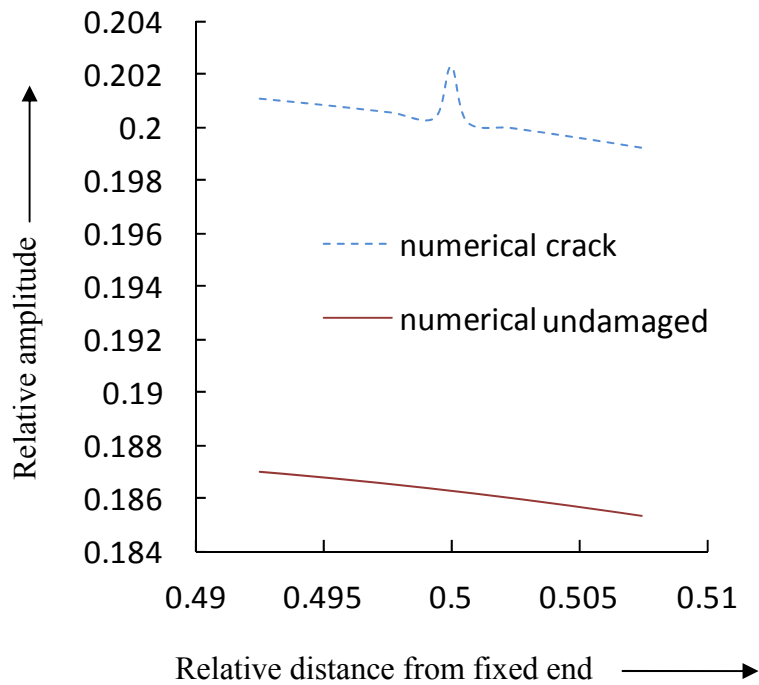


Fig. 3.4b2 Magnified view of fig. 3.4b at the vicinity of the crack location $L_2/L=0.5625$.

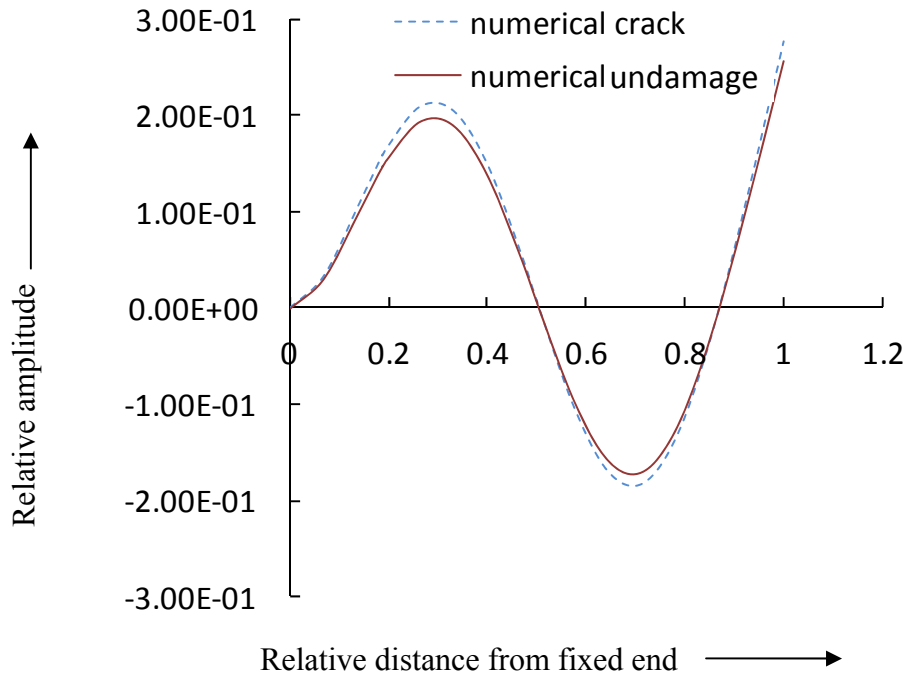


Fig. 3.4c Relative amplitude vs. relative distance from the fixed end (3rd mode of vibration), $a_1/W=0.083$, $a_2/W=0.333$, $L_1/L=0.1875$, $L_2/L=0.5625$.

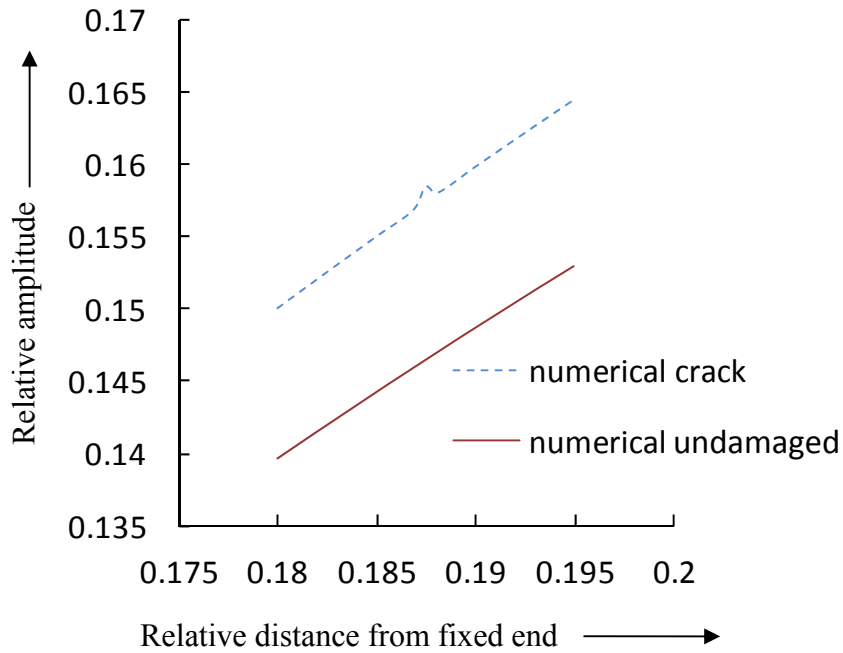


Fig. 3.4c1 Magnified view of fig. 3.4c at the vicinity of the crack location $L_1/L=0.1875$.

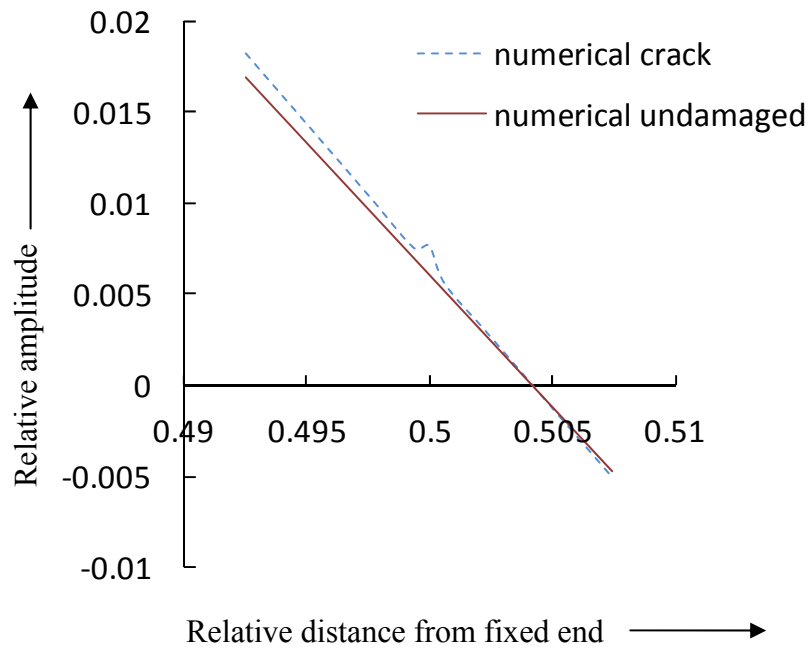


Fig. 3.4c2 Magnified view of fig. 3.4c at the vicinity of the crack location $L_2/L=0.5625$.

3.3 Analysis of experimental results

The aluminum cantilever beam with dimension (800 x 38 x 6 mm) has been considered to carry out experiments for evaluating the relative amplitude of vibration. A number of experiments have been performed on the test specimens with various configurations of crack locations and crack depths to determine the first three mode shapes and natural frequencies.

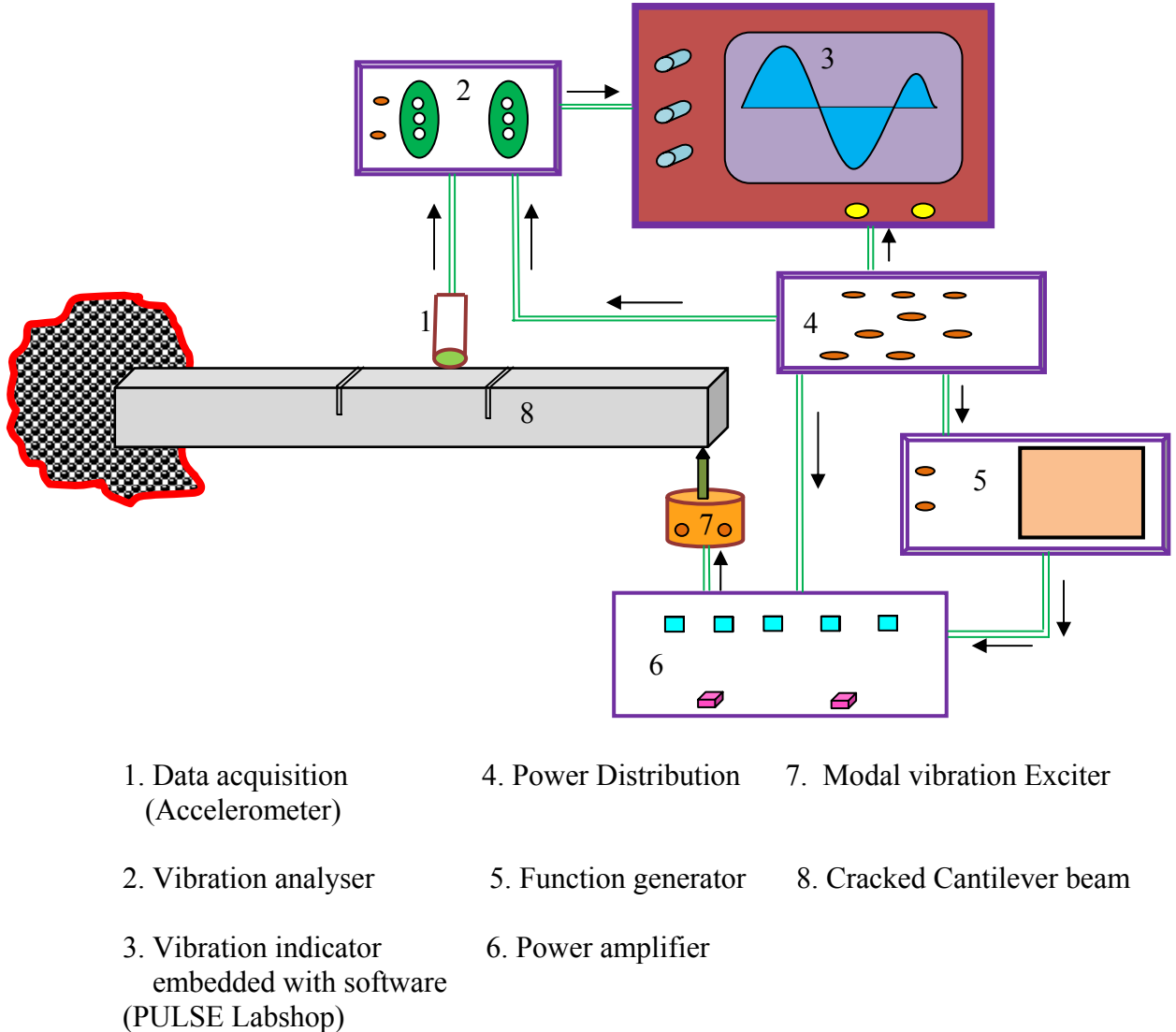


Fig. 3.5 Schematic block diagram of experimental set-up

3.3.1 Experimental results

The mode shapes obtained from experimentation (Fig. 3.5) for relative crack locations (0.25, 0.0625, 0.3125, 0.5625, 0.1875, 0.5) and relative crack depths (0.083, 0.166, 0.25, 0.333) have been compared with that of the numerical analysis for both cracked and undamaged beam. The comparisons are presented in Fig.3.6 to Fig. 3.8.

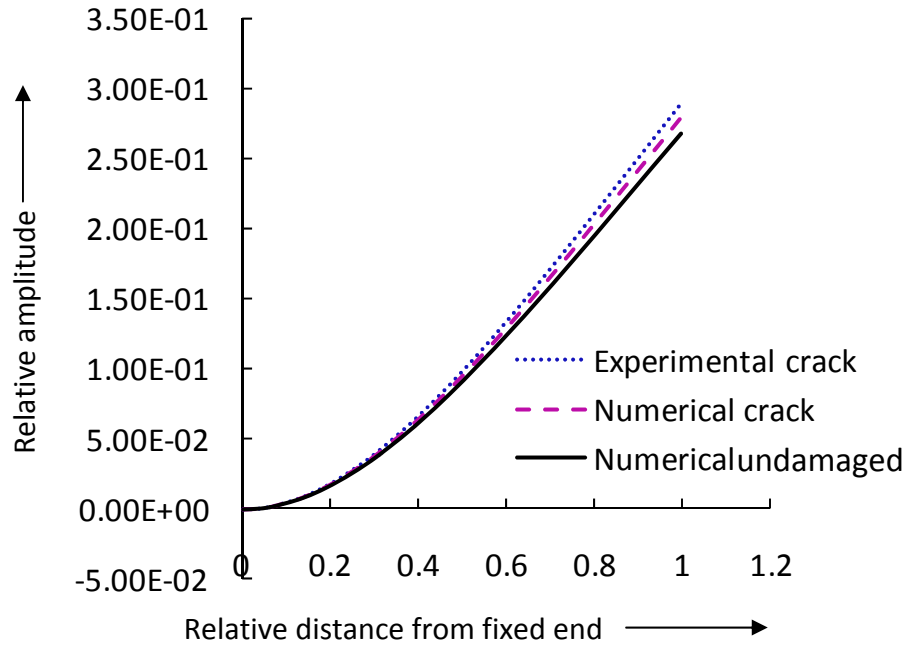


Fig.3.6 (a) Relative amplitude vs. relative distance from the fixed end (1st mode of vibration), $a_1/W=0.166$, $L_1/L=0.0625$, $a_2/W=0.25$, $L_2/L=0.3125$

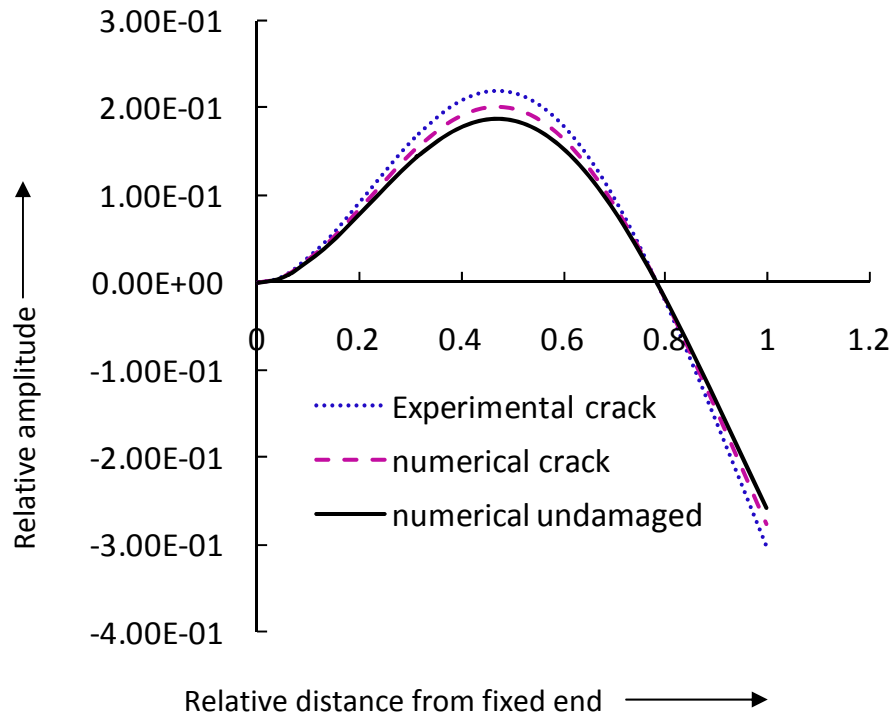


Fig.3.6 (b) Relative amplitude vs. relative distance from the fixed end (2nd mode of vibration), $a_1/W=0.166$, $L_1/L=0.0625$, $a_2/W=0.25$, $L_2/L=0.3125$

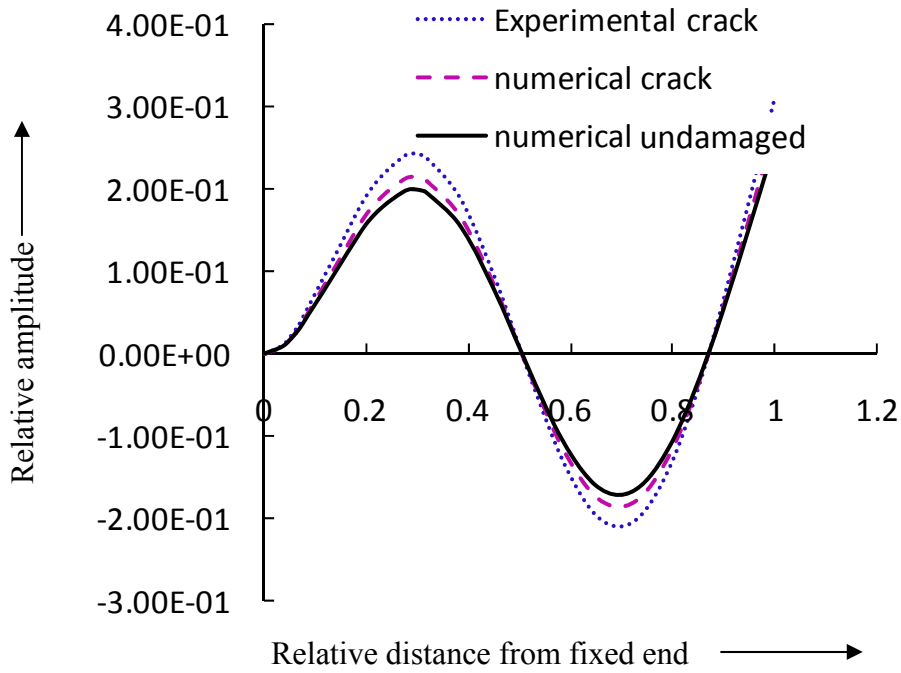


Fig.3.6 (c) Relative amplitude vs. relative distance from the fixed end (3rd mode of vibration), $a_1/W=0.166$, $L_1/L=0.0625$, $a_2/W=0.25$, $L_2/L=0.3125$

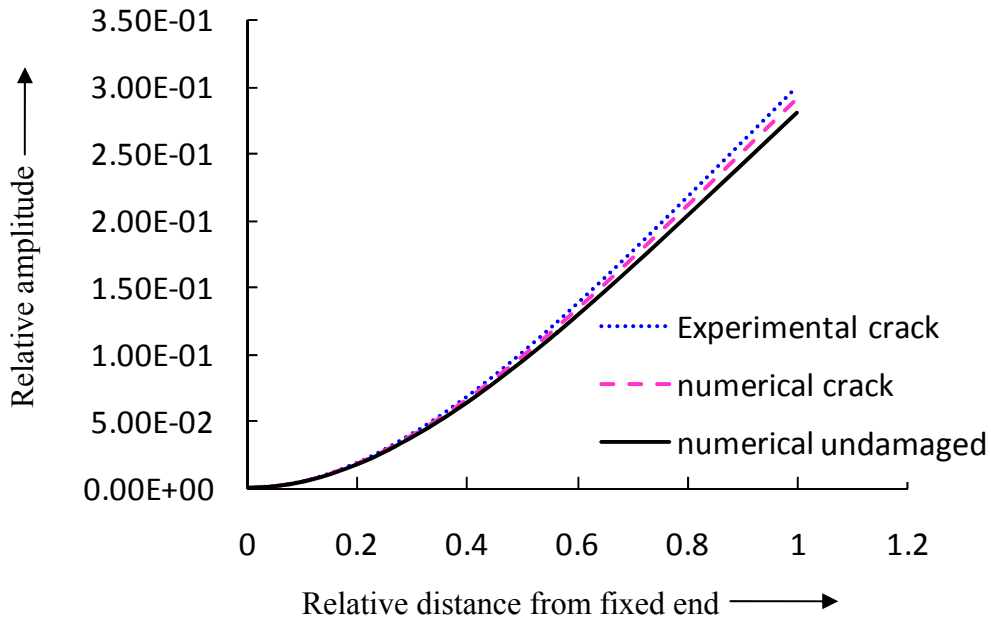


Fig.3.7 (a) Relative amplitude vs. relative distance from the fixed end (1st mode of vibration), $a_1/W=0.083$, $L_1/L=0.25$, $a_2/W=0.333$, $L_2/L=0.5625$

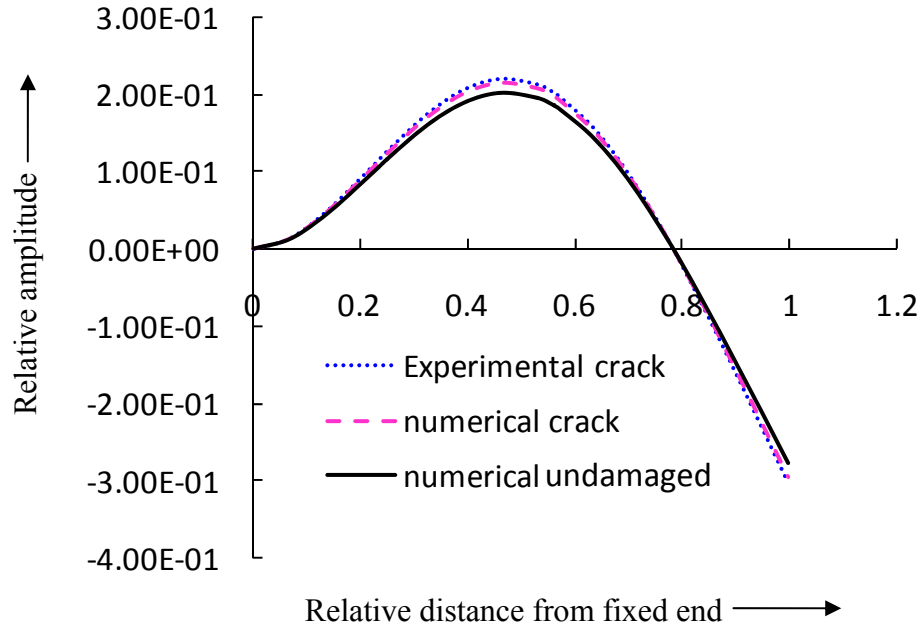


Fig.3.7 (b) Relative amplitude vs. relative distance from the fixed end (2nd mode of vibration), $a_1/W=0.083$, $L_1/L=0.25$, $a_2/W=0.333$, $L_2/L=0.5625$

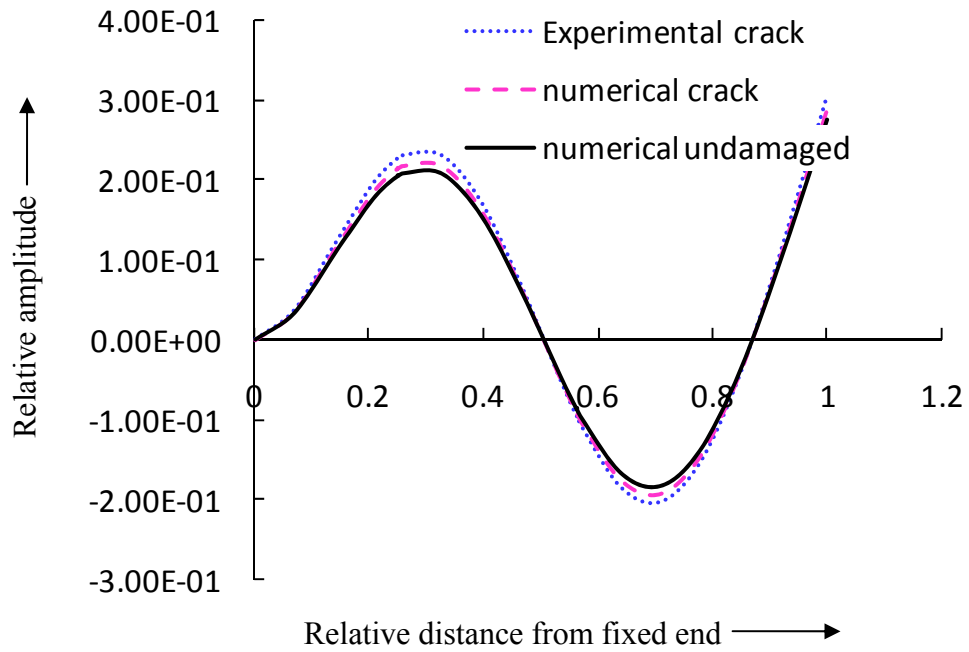


Fig.3.7(c) Relative amplitude vs. relative distance from the fixed end (3rd mode of vibration), $a_1/W=0.083$, $L_1/L=0.25$, $a_2/W=0.333$, $L_2/L=0.5625$

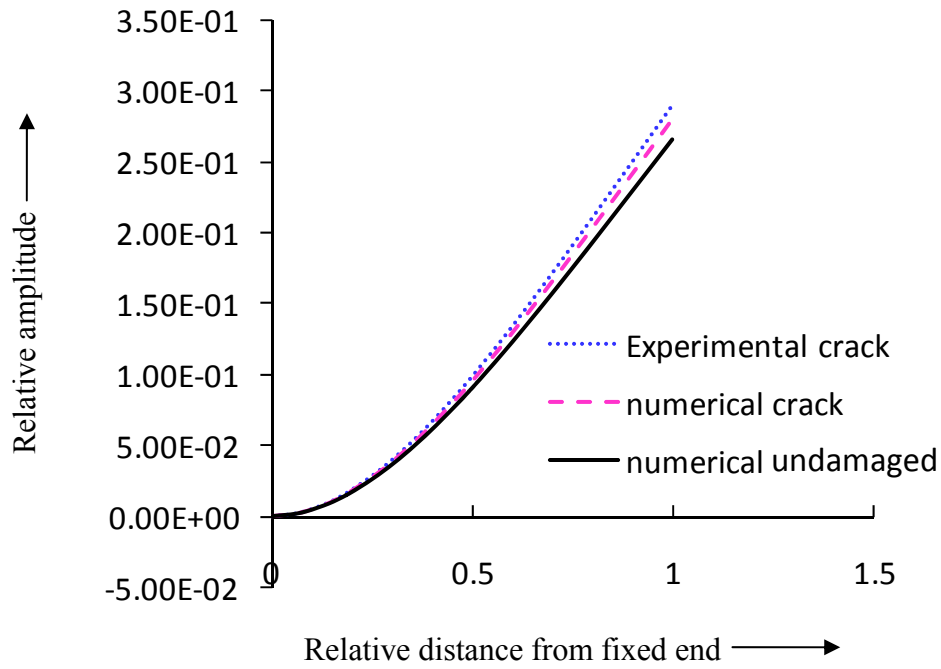


Fig.3.8 (a) Relative amplitude vs. relative distance from the fixed end (1st mode of vibration), $a_1/W=0.166$, $L_1/L=0.1875$, $a_2/W=0.083$, $L_2/L=0.5$

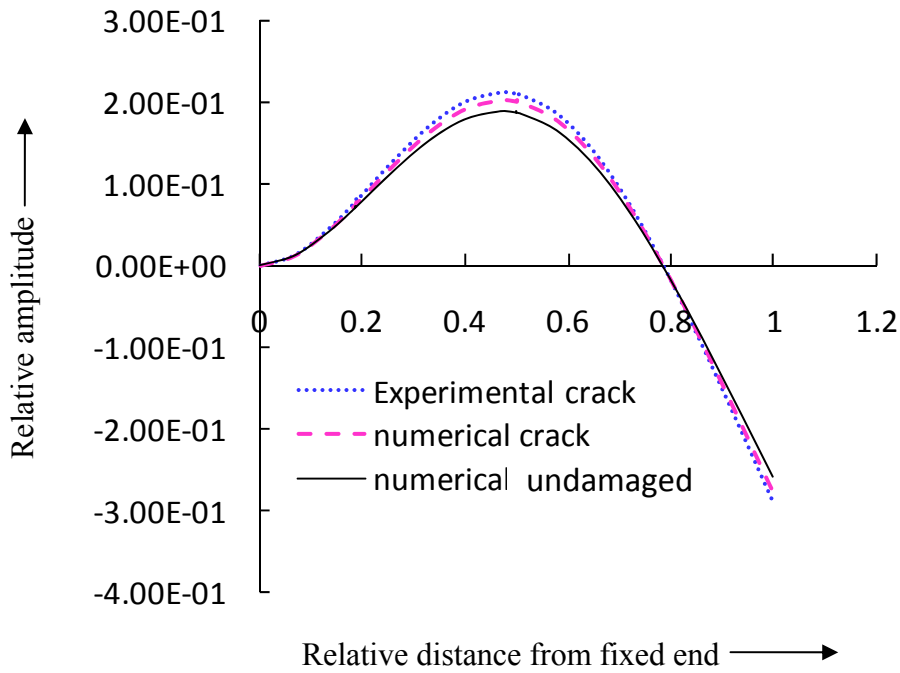


Fig.3.8 (b) Relative amplitude vs. relative distance from the fixed end (2nd mode of vibration), $a_1/W=0.166$, $L_1/L=0.1875$, $a_2/W=0.083$, $L_2/L=0.5$

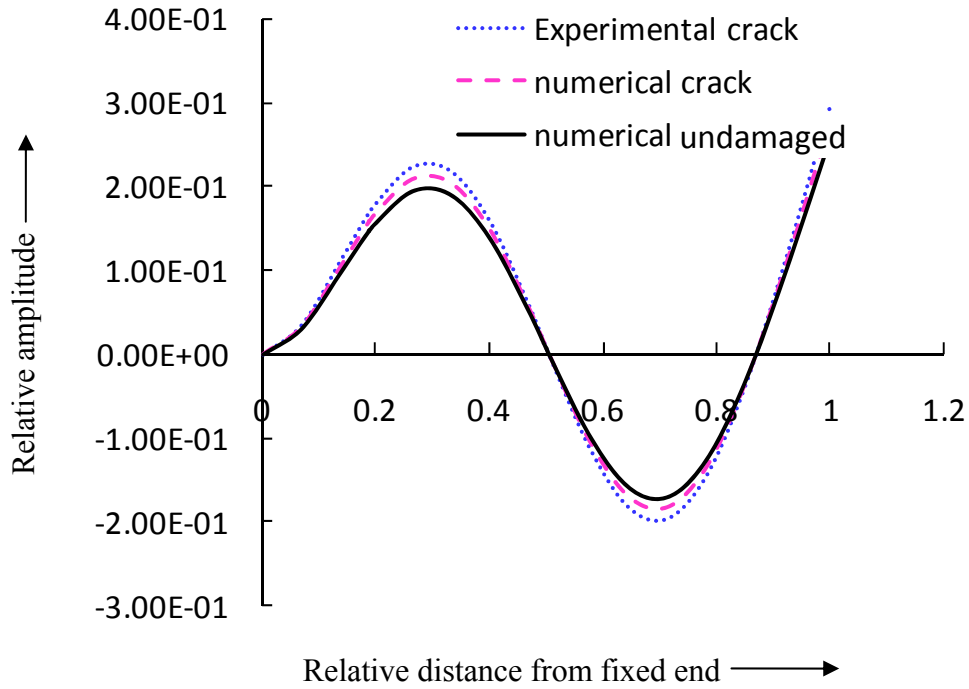


Fig.3.8 (c) Relative amplitude vs. relative distance from the fixed end (3rd mode of vibration), $a_1/W=0.166$, $L_1/L=0.1875$, $a_2/W=0.083$, $L_2/L=0.5$

3.3.2. Comparison between the results of numerical and experimental analyses

The results obtained in the form of mode shapes from theoretical analysis and experimental analyses are compared in Fig.3.6 to Fig. 3.8. The results from the several recorded data set, ten numbers are presented in Table 3.1 for systematic comparison among the theoretical and experimental results.

The relative natural frequency and relative mode shape difference used in the above analysis can be defined as follows.

$$\text{Relative natural frequency} = \frac{(\text{Natural frequency of cracked beam})}{(\text{Natural frequency of undamaged beam})}$$

Relative mode shape difference =

$$\frac{(\text{Modal amplitude of undamaged beam} - \text{Modal amplitude of cracked beam})}{\text{Modal amplitude of undamaged beam}}$$

Table 3.1 Comparison of results between numerical and experimental analysis

Relative First natural frequency "f ₁ "	Relative second natural frequency "f ₂ "	Relative third natural frequency "f ₃ "	Average Relative first mode shape difference "f _{md} "	Average Relative second mode shape difference "s _{md} "	Average Relative third mode shape difference "t _{md} "	Numerical				Experimental			
						relative 1 st crack depth "rcd1"	relative 1 st crack location "rcl1"	relative 2 nd crack depth "rcd2"	relative 2 nd crack location "rcl2"	relative 1 st crack depth "rcd1"	relative 1 st crack location "rcl1"	relative 2 nd crack depth "rcd2"	relative 2 nd crack location "rcl2"
0.9985	0.9991	0.9994	0.0090	0.0025	0.0034	0.158	0.117	0.20	0.369	0.169	0.128	0.27	0.377
0.9966	0.9994	0.9990	0.0001	0.9710	0.2257	0.324	0.118	0.408	0.44	0.336	0.129	0.420	0.52
0.9922	0.9984	0.9993	0.0147	0.01	0.0824	0.407	0.116	0.324	0.867	0.419	0.127	0.336	0.879
0.9981	0.9995	0.9984	0.002	0.0032	0.0807	0.157	0.21	0.20	0.43	0.169	0.29	0.27	0.53
0.9976	0.9960	0.9880	0.0020	0.0330	0.0130	0.20	0.21	0.407	0.70	0.29	0.29	0.418	0.79
0.9991	0.9975	0.9973	0.3719	0.3414	0.2612	0.408	0.20	0.157	0.45	0.419	0.28	0.170	0.54
0.9850	0.9983	0.9862	0.0147	.0201	0.0120	0.43	0.21	0.20	0.69	0.53	0.29	0.28	0.77
0.9992	0.9963	0.9966	0.0010	0.0011	0.0080	0.158	0.365	0.19	0.618	0.171	0.379	0.29	0.627
0.9984	0.9849	0.9883	0.0062	0.0081	0.0285	0.327	0.369	0.44	0.616	0.338	0.379	0.53	0.628
0.9989	0.99639	0.9992	0.0047	0.0031	0.0146	0.407	0.366	0.20	0.620	0.419	0.378	0.28	0.629

The first three columns of the Table 3.1 represents first three relative natural frequencies, where as the fourth, fifth and sixth number columns present the average relative mode shape difference for first three modes of vibration. The columns number seven, eight, nine and ten presents the relative crack depth for first crack position, relative crack location for first crack position, relative crack depth for second crack position, relative crack location for second crack position respectively obtained from numerical analysis. The columns number eleven, twelve, thirteen and fourteen present the relative crack depth for first crack position, relative crack location for first crack position, relative crack depth for second crack position, relative crack location for second crack position respectively obtained from experimental analysis.

3.4 Discussions

This section explains the discussions made from the analysis of the results derived from theoretical and experimental section. The cracked cantilever beam containing multiple transverse cracks and cross sectional view of the cantilever beam structure are shown in Fig. 3.1 (a) and Fig.3.1 (b) respectively. Fig.3.3 represents the front view of the cracked cantilever beam. The variation of relative crack depth with dimensionless compliances is shown in Fig. 3.2. It is observed that the due to decrease in local stiffness at the crack sections the dimensionless compliance increases with increase in relative crack depth. The graphs presented in Fig. 3.4a to Fig. 3.4c show the deviation of the first three mode shapes for the cracked and undamaged beam with magnified view at the vicinity of the crack locations obtained from theoretical analysis. From the magnified view (such as Fig. 3.4a1, Fig. 3.4a2), it is evident that there is a noticeable effect on the mode shapes due to presence of cracks in the cracked beam as compared to undamaged beam. A significant variation in the mode shapes can be seen with increase in crack depth in Fig. 3.4a to Fig. 3.4c. A comparison of results for the intact and cracked beam derived from numerical analysis and experimental set up (Fig. 3.5) have been exhibited in Fig. 3.6 to Fig. 3.8. The relative crack locations and relative crack depths corresponding to ten sets of first three natural frequencies and first three mode shape differences from numerical and experimental analysis are presented in Table 3.1.

3.5 Summary

The conclusions drawn from the above analysis are described in this section. Due to the presence of cracks the vibration parameters of the cracked beam such as natural frequencies and mode shapes shows a major deviation near the crack locations as compared to undamaged beam. This phenomenon can be seen in the magnified view. The vibration indices obtained from the numerical analysis have been validated using the results from experimental analysis and are found to be well in agreement. The deviation in the dynamic response can be used as the basis for multiple crack identification in damaged structural members and the measured vibration parameters can also be used for design and development of inverse methodologies for fault diagnosis. The proposed method can be effectively used to develop artificial intelligent techniques for online structural health monitoring. In the subsequent sections various AI techniques have been employed to formulate intelligent supervision system for multiple crack diagnosis.

Chapter 4

ANALYSIS OF FINITE ELEMENT FOR MULTIPLE CRACK DETECTION

One form of damage that can lead to catastrophic failure of the beam structures are transverse cracks if undetected in their primary stages. However, it is difficult to locate a crack using visual inspection and it may be detected usually by non-destructive techniques such as x-ray, ultrasonic test etc. However, these techniques are found to be unsuitable for various engineering systems as they require periodic inspection. In last two decades, a lot of researches have been devoted and several models have been developed to predict the damage characteristics using the vibrational behavior of the damaged beam structures. Vibration based methods for detection of crack offer some advantages over conventional methods. This methodology can help to determine the location and size of the cracks from the vibration data collected from the cracked beam structure. The crack developed in the structure generates flexibility at the vicinity of the crack which in turn, gives rise to a reduction in natural frequencies and the change in the mode shapes. Hence, it may be possible to estimate the location and size of the cracks by measuring changes in the vibration parameters. Single crack detection in beam has been studied by scientists adopting analytical model of the structure. This chapter introduces finite element analysis for identification of multiple cracks present in structural systems. The results from the finite element analysis have been compared with that of the numerical analysis and experimental analysis to establish the robustness of the proposed finite element model. Finally, it is found that the finite element technique can be suitably used for multiple crack detection in damaged structures.

4.1 Introduction

Automation of fault identification in various engineering systems can be termed as the implementation of systematic approach to detect and quantify the presence of faults present in the system. Faulty beam has been a point of major concern for failure analysts of structural systems for overall safety and performance. The modal responses of the damaged members can be potentially used for estimating the damage parameters present in the beam members. In due course of development of different crack detection technique researchers have used energy based method, wavelet analysis, numerical techniques such as finite element method,

artificial intelligent methods, etc. In last few decades scientists have addressed the problem of detecting single crack present in beam model using finite element analysis and it is cited that the performance of FEA is better as compared to theoretical model developed for crack diagnosis. So, this technique can be used to detect the presence of multiple cracks with their crack features such as crack depth and crack location in systems using the vibration response of the system.

In this present investigation for fault identification in a cracked beam containing multiple transverse cracks, finite element analysis has been carried out to identify crack depths and their positions. It has been established that a crack in a beam has an important effect on its dynamic behavior. Theoretical and experimental analyses have been done to validate the results obtained from the finite element analysis of the multi cracked cantilever beam structure. In the theoretical analysis the strain energy density function is used to evaluate the additional flexibility produced due to the presence of crack. Based on the flexibility a new stiffness matrix is deduced and subsequently that is used to calculate the natural frequencies and mode shapes of the cracked beam. The results from finite element method and experimental method are compared with the results from the numerical analysis for validation. The results are found to be in good agreement.

This chapter has been organized into five sections. Introduction, Finite Element Analysis is explained in section 4.1 and 4.2 respectively. The analysis of cracked beam using finite element analysis (FEA) is discussed in section 4.2.1. In section 4.3, the results of the finite element analysis are compared with that of experimental and numerical results to exhibit the authenticity of the proposed methodology. In the concluding section 4.4 summaries are given.

4.2 Finite element analysis

The finite element analysis is a useful numerical technique that utilizes variational and interpolation methods for modeling and solving boundary value problems such as the one described in this current chapter. The finite element analysis is very systematic and can be useful for model with complex shape. So, the finite element model can be suitably employed for solving vibration based problems with different boundary conditions. Commercial finite

element packages are available to address the practical problems. During finite element analysis, the structure is approximated in two ways. First step is employed by dividing the structure into a number of small parts. The small parts are known as finite elements and the procedure adopted to divide the structure is called as discretization. Each element on the structure has usually associated with equation of motion and that can be easily approximated. The each element on the finite element model has end points, they are known as nodes. The nodes are used for connecting one element to other element. Collectively the finite element and nodes are called as finite element mesh or finite element grid. In the second level of approximation the equation of vibration for each finite element is determined and solved. The solution for each finite element brought together to generate the global mass and stiffness matrices describing the vibrational response of the whole structure. The displacement associated with the solution represents the motion of the nodes of the finite element mesh. This global mass and stiffness matrices represent the lumped parameter approximation of the structure and can be analyzed to obtain natural frequencies and mode shapes of damaged vibrating structures.

4.2.1 Analysis of cracked beam using finite element analysis (FEA)

In the following section FEA is analyzed for vibration analysis of a cantilever cracked beam (Fig. 4.1). The relationship between the displacement and the forces can be expressed as;

$$\begin{Bmatrix} u_j - u_i \\ \theta_j - \theta_i \end{Bmatrix} = C_{ovl} \begin{Bmatrix} U_j \\ \phi_j \end{Bmatrix} \quad (4.1)$$

Where overall flexibility matrix C_{ovl} can be expressed as;

$$C_{ovl} = \begin{pmatrix} R_{11} & -R_{12} \\ -R_{21} & R_{22} \end{pmatrix}$$

The displacement vector in equation (4.1) is due to the crack.

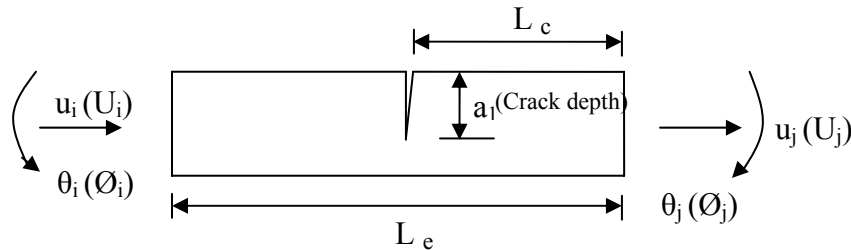


Fig. 4.1 View of a crack beam element subjected to axial and bending forces.

The forces acting on the beam element for finite element analysis are shown in Fig. 4.1.

Where,

R_{11} : Deflection in direction 1 due to load in direction 1

$R_{12}= R_{21}$: Deflection in direction 1 due to load in direction 2

R_{22} : Deflection in direction 2 due to load in direction 2.

Under this system, the flexibility matrix C_{intact} of the intact beam element can be expressed

$$\text{as; } \begin{Bmatrix} u_j - u_i \\ \theta_j - \theta_i \end{Bmatrix} = C_{\text{intact}} \begin{Bmatrix} U_j \\ \theta_j \end{Bmatrix} \quad (4.2)$$

$$\text{Where, } C_{\text{intact}} = \begin{pmatrix} Le/EA & 0 \\ 0 & Le/EI \end{pmatrix}$$

The displacement vector in equation (4.2) is for the intact beam.

The total flexibility matrix C_{tot} of the damaged beam element can now be obtained by

$$C_{\text{tot}} = C_{\text{intact}} + C_{\text{ovl}} = \begin{bmatrix} Le/EA + R_{11} & -R_{12} \\ -R_{21} & Le/EI + R_{22} \end{bmatrix} \quad (4.3)$$

Through the equilibrium conditions, the stiffness matrix K_c of a damaged beam element can be obtained as [80]

$$K_c = D C_{\text{tot}}^{-1} D^T \quad (4.4)$$

Where D is the transformation matrix and expressed as;

$$D = \begin{pmatrix} -1 & 0 \\ 0 & -1 \\ 1 & 0 \\ 0 & 1 \end{pmatrix}$$

By solving the stiffness matrix K_c , the natural frequencies and mode shapes of the multi cracked cantilever beam can be obtained. This procedure has been adopted by ALGOR package to evaluate the natural frequencies and mode shapes of beam structures. In the current investigation, ALGOR (Version 19.3) has been used to calculate the vibration signatures of damaged and undamaged cantilever beam. The FEA model of the cantilever

beam and the ALGOR generated cantilever beam model with 2nd mode of vibration are shown in the appendix section in Fig. A1 and Fig. A2 respectively. The results of the finite element analysis for the first three mode shapes of the cracked beam are compared with that of the numerical analysis and experimental analysis of the cracked beam and are presented in Fig. 4.2 to Fig. 4.4 and Table 4.1.

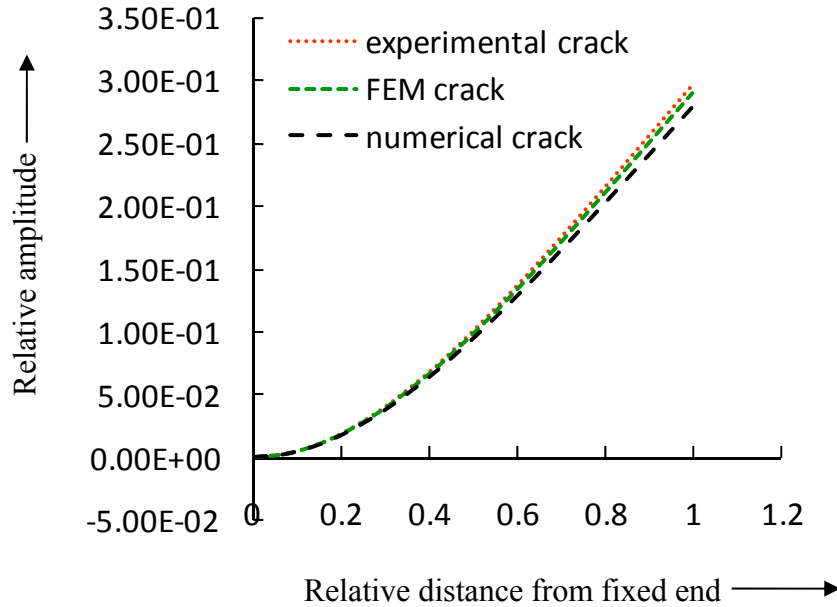


Fig.4.2 (a) Relative amplitude vs. relative distance from the fixed end (1st mode of vibration), $a_1/W=0.166$, $L_1/L=0.3125$, $a_2/W=0.083$, $L_2/L=0.625$

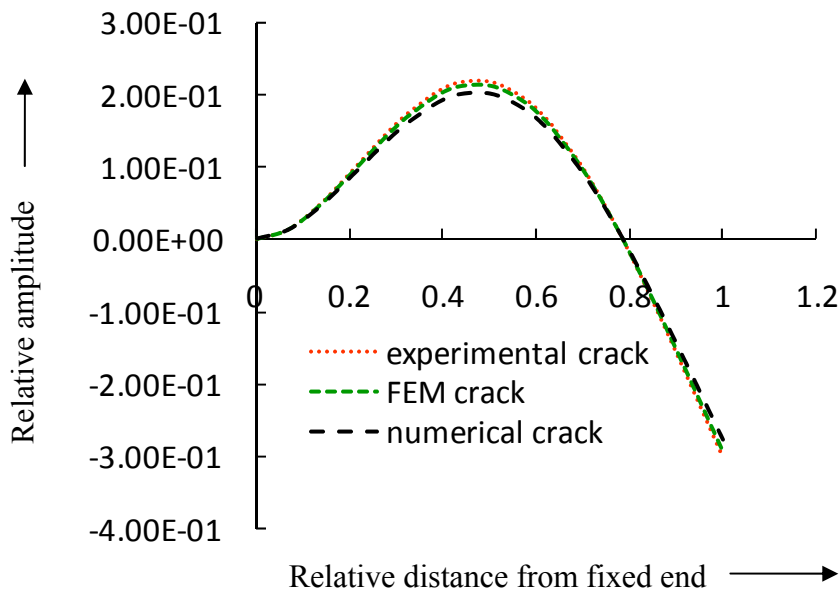


Fig. 4.2 (b) Relative amplitude vs. relative distance from the fixed end (2nd mode of vibration), $a_1/W=0.166$, $L_1/L=0.3125$, $a_2/W=0.083$, $L_2/L=0.625$

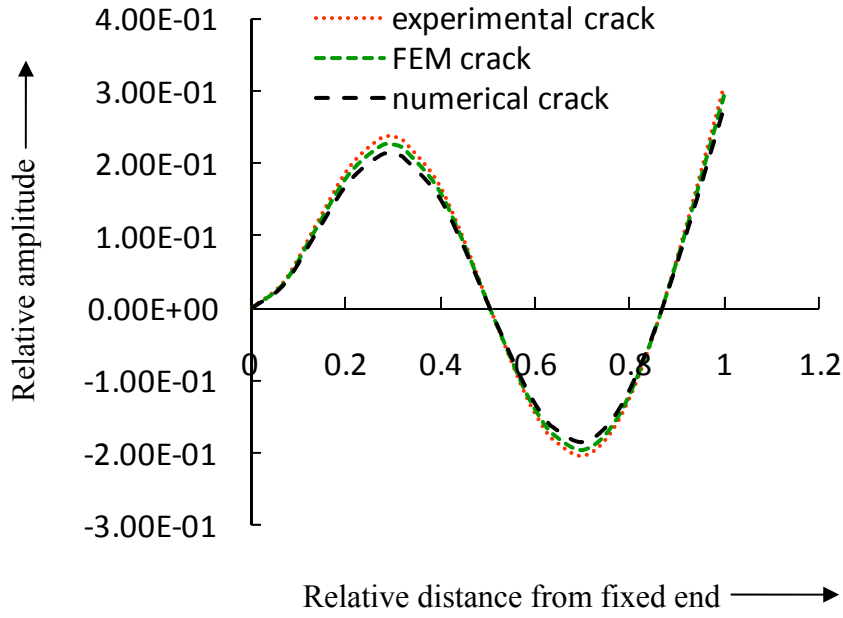


Fig. 4.2 (c) Relative amplitude vs. relative distance from the fixed end (3rd mode of vibration), $a_1/W=0.166$, $L_1/L=0.3125$, $a_2/W=0.083$, $L_2/L=0.625$

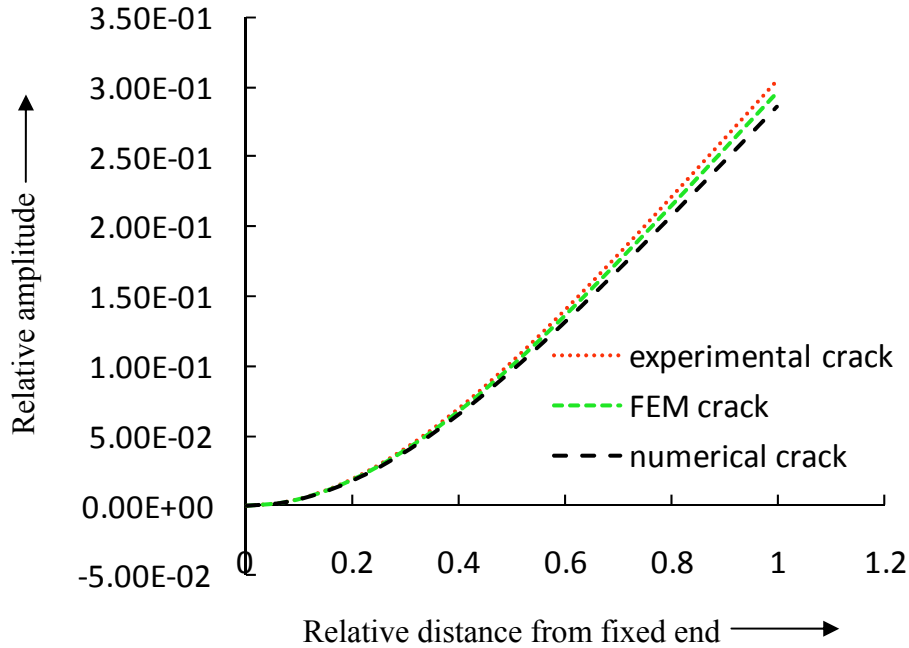


Fig. 4.3 (a) Relative amplitude vs. relative distance from the fixed end (1st mode of vibration), $a_1/W=0.25$, $L_1/L=0.4375$, $a_2/W=0.166$, $L_2/L=0.625$

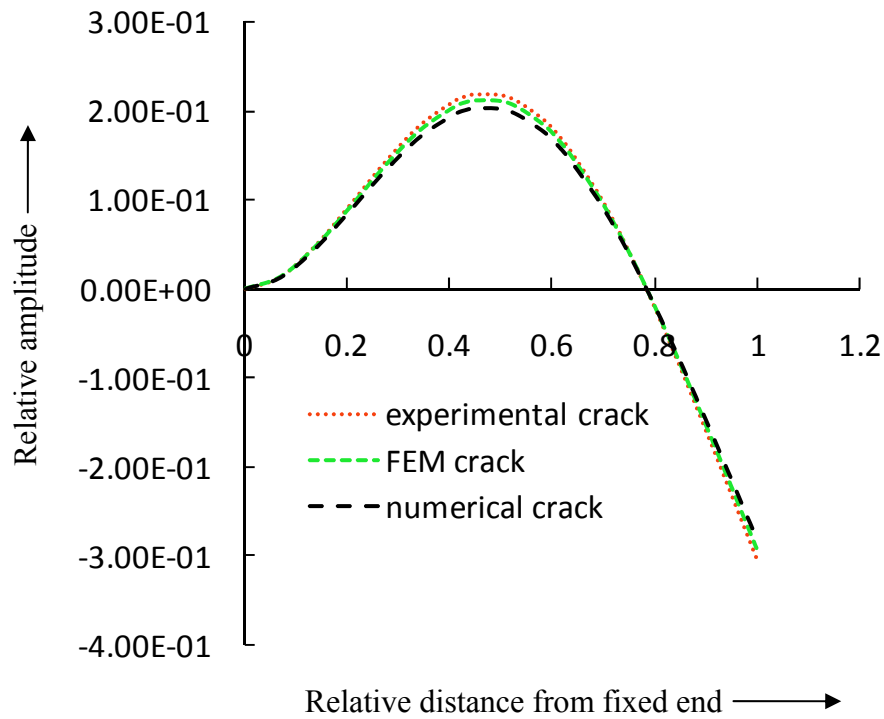


Fig.4.3 (b) Relative amplitude vs. relative distance from the fixed end (2nd mode of vibration), $a_1/W=0.25$, $L_1/L=0.4375$, $a_2/W=0.166$, $L_2/L=0.625$

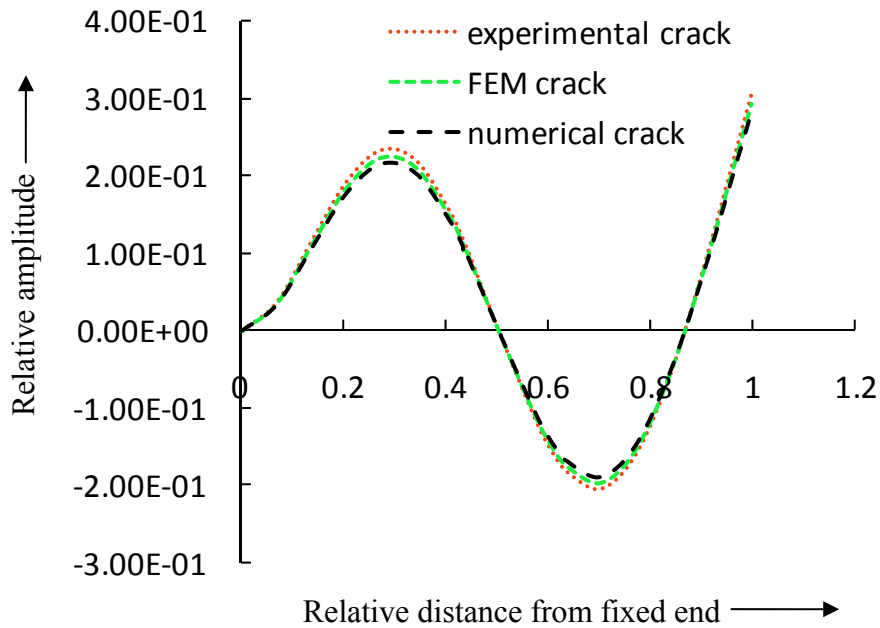


Fig. 4.3 (c) Relative amplitude vs. relative distance from the fixed end (3rd mode of vibration), $a_1/W=0.25$, $L_1/L=0.4375$, $a_2/W=0.166$, $L_2/L=0.625$

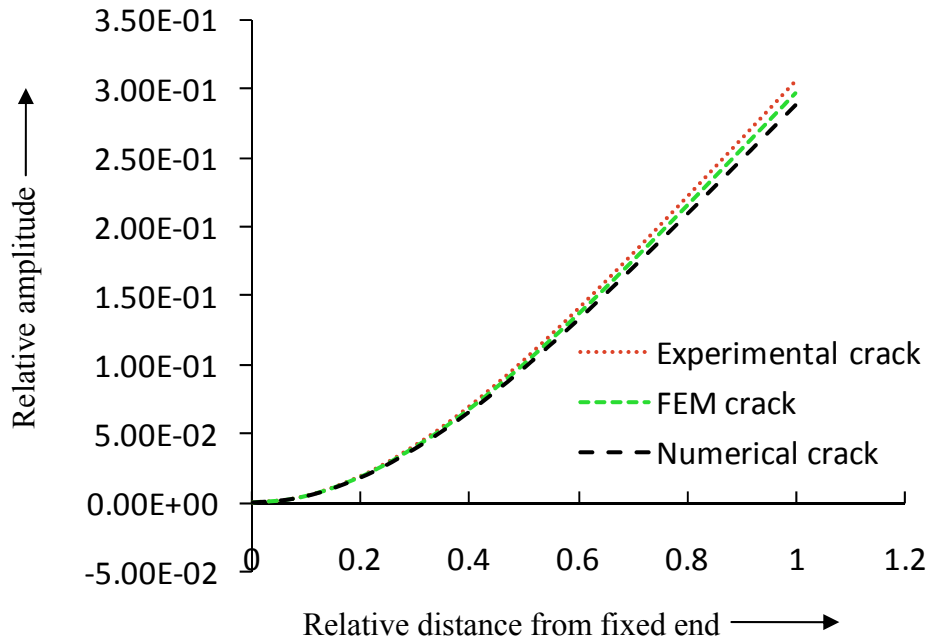


Fig.4.4 (a) Relative amplitude vs. relative distance from the fixed end (1st mode of vibration), $a_1/W=0.166$, $L_1/L=0.3125$, $a_2/W=0.083$, $L_2/L=0.625$

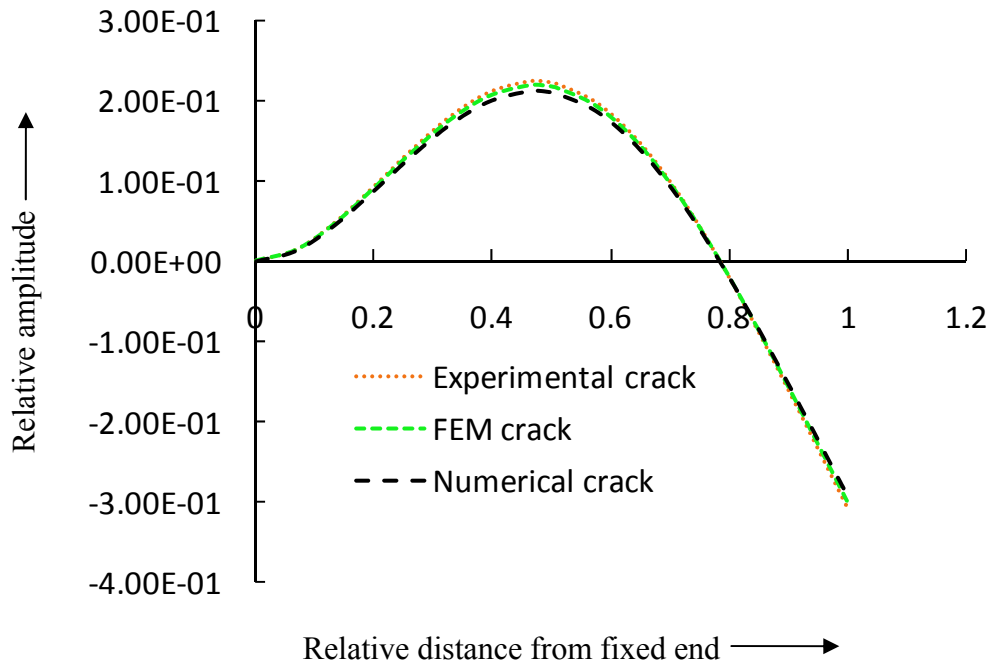


Fig. 4.4 (b) Relative amplitude vs. relative distance from the fixed end (2nd mode of vibration), $a_1/W=0.166$, $L_1/L=0.3125$, $a_2/W=0.083$, $L_2/L=0.625$

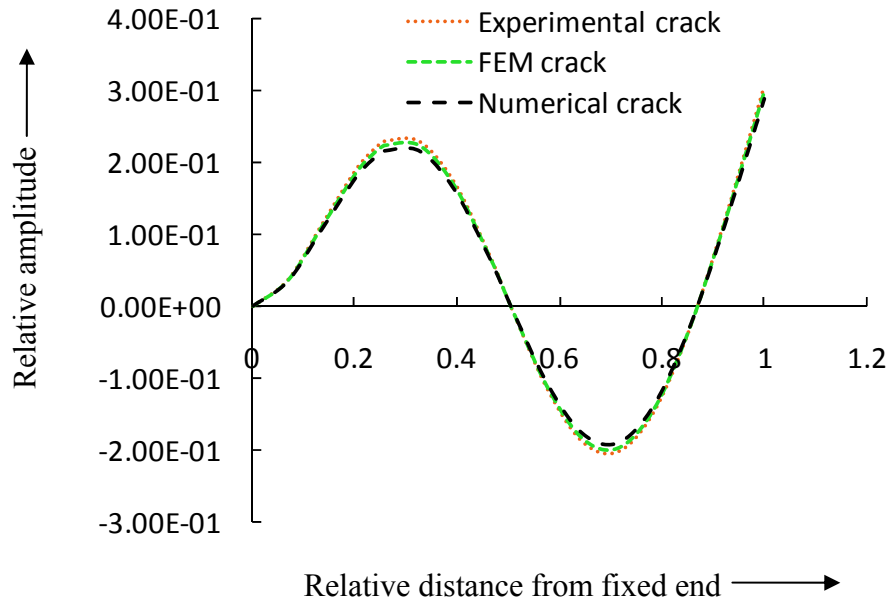


Fig.4.4 (c) Relative amplitude vs. relative distance from the fixed end (3rd mode of vibration), $a_1/W=0.166$, $L_1/L=0.3125$, $a_2/W=0.083$, $L_2/L=0.625$

4.3 Results and discussions of finite element analysis

This section presents an in depth analysis of the results obtained from finite element analysis and briefly discusses the outcome from the proposed methodologies.

It is observed that, the presence of damage in the cantilever beam model have noticeable effect on the vibration characteristics of the beam. A beam element with a crack subjected to axial and bending forces for Finite Element Analysis has been presented in Figure 4.1. The displacement vector and force vector have been applied to calculate the overall matrix. The total flexibility matrix that is produced due to the presence of cracks on the cantilever beam has been derived, which is subsequently used to formulate the stiffness matrix for the multi cracked beam. Finally, the formulated matrices are used to calculate the first three natural frequencies and first three mode shapes of the cantilever beam structure. These vibration parameters obtained from the finite element analysis have been used to estimate the crack characteristics present on the structural member. The results from the FEA have been validated using the results from experimental and theoretical analysis for multiple crack identification. The results obtained from Finite Element Analysis (FEA), theoretical analysis and experimental analyses are compared and presented in Figure 4.2 to Fig. 4.4 (mode shape comparison). Table 4.1 presents results for relative crack locations and relative crack depths

obtained from FEA, numerical analysis and experimental analysis corresponds to ten set of relative deviation of first three natural frequencies and first three mode shape differences. The results are found to be well in agreement showing the effectiveness of the developed FEA methodology.

Table 4.1 Comparison of results between FEA, numerical and experimental analysis.

Relative first natural frequency "f _{1f} "	Relative second natural frequency "f _{2f} "	Relative third natural frequency "f _{3f} "	Average Relative first mode shape difference "f _{md} "	Average Relative second mode shape difference "s _{md} "	Average Relative third mode shape difference "t _{md} "	FEA				Numerical				Experimental							
						relative 1 st crack depth "rcd1" 1 st crack location "rc1" 2 nd crack depth "rcd2", 2 nd crack location "rc2"				relative 1 st crack depth "rcd1" 1 st crack location "rc1" 2 nd crack depth "rcd2", 2 nd crack location "rc2"		relative 1 st crack depth "rcd1" 1 st crack location "rc1" 2 nd crack depth "rcd2", 2 nd crack location "rc2"									
0.9985	0.9991	0.9994	0.0090	0.0025	0.0034	rcd1	rcd2	rc1	rcd2	rcd1	rcd2	rc1	rcd2	rcd1	rcd2	rc1	rcd2	rc1	rcd2	rc1	rcd2
						0.160	0.118	0.118	0.21	0.370	0.370	0.158	0.117	0.20	0.369	0.169	0.128	0.27	0.377		
0.9966	0.9994	0.9990	0.0001	0.9710	0.2257	0.323	0.119	0.119	0.410	0.45	0.45	0.324	0.118	0.408	0.44	0.336	0.129	0.420	0.52		
0.9922	0.9984	0.9993	0.0147	0.01	0.0824	0.408	0.118	0.118	0.326	0.869	0.869	0.407	0.116	0.324	0.867	0.419	0.127	0.336	0.879		
0.9981	0.9995	0.9984	0.002	0.0032	0.0807	0.159	0.20	0.20	0.22	0.45	0.45	0.157	0.21	0.20	0.43	0.169	0.29	0.27	0.53		
0.9976	0.9960	0.9880	0.0020	0.0330	0.0130	0.21	0.19	0.19	0.409	0.70	0.70	0.20	0.21	0.407	0.70	0.29	0.29	0.418	0.79		
0.9991	0.9975	0.9973	0.3719	0.3414	0.2612	0.409	0.22	0.22	0.160	0.46	0.46	0.408	0.20	0.157	0.45	0.419	0.28	0.170	0.54		
0.9850	0.9983	0.9862	0.0147	.0201	0.0120	0.45	0.21	0.21	0.21	0.68	0.68	0.43	0.21	0.20	0.69	0.53	0.29	0.28	0.77		
0.9992	0.9963	0.9966	0.0010	0.0011	0.0080	0.160	0.367	0.367	0.21	0.620	0.620	0.158	0.365	0.19	0.618	0.171	0.379	0.29	0.627		
0.9984	0.9849	0.9883	0.0062	0.0081	0.0285	0.329	0.371	0.371	0.45	0.618	0.618	0.327	0.369	0.44	0.616	0.338	0.379	0.53	0.628		
0.9989	0.99639	0.9992	0.0047	0.0031	0.0146	0.409	0.368	0.368	0.21	0.621	0.621	0.407	0.366	0.20	0.620	0.419	0.378	0.28	0.629		

4.4 Summary

In this section, the conclusions obtained from the Finite Element Analysis are described below.

In the present study a simple and efficient method to detect multiple cracks in a beam is presented. From the analysis of the vibration signatures it is observed that there is variation of mode shapes and natural frequencies for the cracked beam with respect to undamaged beam. The vibration responses i.e. the natural frequencies and mode shapes obtained from the FE analysis are found to be in close agreement with theoretical and experimental analysis. In the future the artificial intelligent techniques (Fuzzy, Neural network, Genetic Algorithm) and hybrid artificial intelligent techniques such as fuzzy-neuro technique can be used for detection of fault in dynamic vibrating structures. The proposed method can be utilized to model any practical engineering structure and on-line condition monitoring of damaged structures.

Publication:

- D.R.K. Parhi, **Amiya Kumar Dash**, Faults detection by finite element analysis of a multi cracked beam using vibration signatures, Int. J. Vehicle Noise and Vibration, Vol. 6, No. 1, 2010, 40-54.

Chapter 5

ANALYSIS OF FUZZY INFERENCE SYSTEM FOR MULTIPLE CRACK DETECTION

Cracks present a serious threat to proper performance of structures and machines. Most of the failures are due to material fatigue and presence of cracks in structures. For this reason methods allowing early detection and localization of cracks have been the subject of intensive research for investigators. Many techniques have been adopted in the past to quantify and identify faults. Some of these are visual (e.g. dye penetrate methods) and others use sensors to detect local faults (e.g. magnetic field, eddy current, radiographs and thermal fields). These methods cannot indicate that a structure is fault-free without testing the entire structure in minute detail. Since the last two decades a number of experiments and theories have been developed to elucidate the phenomenon and determine the crack initiation and propagation conditions. In the current investigation a fuzzy logic based technique has been proposed for structural damage identification. The approach adopted in this chapter utilizes the induced vibration parameters of the beam structure using an inverse technique and predicts the position and severities of the multi crack present in the system.

5.1 Introduction

Basically, fuzzy logic (FL) is a multi valued logic, which allows interim values to be defined between linguistic expressions like yes/no, high/low, true/false. In the last few decades, researchers have used the FL methodology for applications such as feature extraction, classification and detection of geometrical features in objects etc. Fuzzy system has the capability to mimic the human behavior by following the different reasoning modes in order to make the computer program behave like humans. In traditional computing, actions are taken based on data with precision and certainty. In soft computing, imprecise data are employed for decision making. The exploration of the imprecision and uncertainty underlies the remarkable human ability to understand various engineering applications. FL can specify mapping rules in terms of words rather than numbers. Another basic concept in FL is the fuzzy if-then rule which is mostly used in development of fuzzy rule based systems. FL can model nonlinear functions of arbitrary complexity to a desired degree of accuracy. FL is a

convenient way to map an input space to an output space and is one of the tools used to model a multi-input, multi-output system. Hence the fuzzy approach can be effectively employed to develop a multi crack diagnostic tool using the vibration response of structures.

In the current chapter, a multi crack identification algorithm using fuzzy inference system has been formulated and the performance has been evaluated. The fuzzy system for crack diagnosis has been designed with six inputs (first three relative natural frequencies and first three relative mode shape differences) and four outputs (relative first and second crack locations, relative first and second crack depths). A number of fuzzy linguistic terms and fuzzy membership functions (triangular, trapezoidal and Gaussian) have been used to develop the proposed crack detection methodology. The dynamic response obtained from the numerical, finite element and experimental analyses have been used to set up the rule base for designing of the fuzzy system. The performance of the proposed fuzzy based system for crack diagnosis have been compared with the results obtained from FEA, numerical and experimental analysis and it is observed that, the current fuzzy model can be implemented successfully for structural health monitoring.

The current chapter is comprised of five different sections. Section 5.1 discusses about the introduction to Fuzzy Inference System and section 5.2 enumerates the systematic steps to be followed to design and develop a fuzzy logic system. The analysis of the fuzzy model used for multi crack identification has been explained in section 5.3. Section 5.4 discusses about the results obtained from the fuzzy logic model and finally, section 5.5 provides a summary of the fuzzy logic analysis applied for multiple crack detection in the damaged structure.

5.2 Fuzzy inference system

A fuzzy logic system (FLS) essentially takes a decision by nonlinear mapping of the input data into a scalar output, using fuzzy rules. The mapping can be done through input/output membership functions, fuzzy if-then rules, aggregation of output sets, and defuzzification. An FLS can be considered as a collection of independent multi-input, single-output systems. The FLS maps crisp inputs into crisp outputs. It can be seen from the figure that the FIS contains four components: the fuzzifier, inference engine, rule base, and defuzzifier. The rule base of the FLS system can be developed using the numeric data. Once the rules have been

established, the FLS can be viewed as a system that utilizes inputs and process them using the fuzzy rule database and fuzzy linguistic terms to get output vector. The fuzzifier takes input values and verifies the degree of association to each of the fuzzy sets via membership functions.

The fuzzy system generally consists of five steps. They are as follows,

Step 1

Inputs to fuzzy system: The fuzzy system at first is fed with the input parameters and then the system recognizes the degree of association of the data with the corresponding fuzzy set through the membership functions.

Step 2

Application of fuzzy operator: After the fuzzification of the inputs, the fuzzy model measures the degree to which each of the antecedents satisfies for each rule of the fuzzy rule data base. If the rule has a more than one part, the fuzzy operator is employed to obtain a single value for the given rule.

Step 3

Application of method for fulfillment of rules: Method is applied to reshape the output of the membership functions, which is represented by a fuzzy set. The reshaping of the output is done by a function related to the antecedent.

Step 4

Aggregation of results: The results obtained from each rule are unified to get a decision from the system. Aggregation process leads to a combined fuzzy set as output.

Step 5

Defuzzification: In this process the defuzzification layer of the fuzzy system incorporate method like centroid, maxima etc in order to convert the fuzzy set into crisp value, which will be easier to analyze.

5.2.1 Modeling of fuzzy membership functions

One of the key features in designing a fuzzy inference system is to determine the fuzzy membership functions. The membership function defines the fuzzy set and also provides a measure of degree of imprecise dependencies or similarity of an element to a fuzzy set. The membership function can take any shape, but some commonly used examples for real

applications are Gaussian, triangular, trapezoidal, bell shape etc. In a fuzzy set, elements with non zero degree membership are known as support and elements with degree of one are known as core of the fuzzy set. The membership functions are generally represented as $\mu_F(x)$. Where, μ is the degree of weight of the element x to the fuzzy set F . The height or magnitude of the membership function is usually referred to zero to one. Hence, any element from the fuzzy set belongs to the set with a degree ranging from $[0, 1]$.

From the Fig. 5.1(a) (triangular membership function) the point 'c', 'd', 'e' represents the three vertices of the triangular membership function $\mu_F(x)$ of the fuzzy set 'F'. It is observed that the element at 'c' and 'e' is having membership degree equivalent to zero and the element at 'd' is having membership degree equivalent to one. The mathematical representation of the fuzzy triangular membership function of $\mu_F(x)$ can be explained as follows.

$$\mu_F(x) = \begin{cases} 0 & \text{if } x \leq c \\ (x - c) / (d - c) & \text{if } c \leq x \leq d \\ (e - x) / (e - d) & \text{if } d \leq x \leq e \\ 0 & \text{if } x \geq e \end{cases}$$

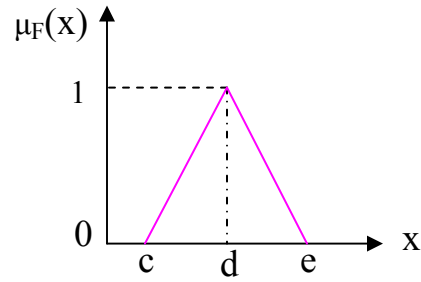


Fig. 5.1(a) Triangular membership function

The mathematical representation of the fuzzy Gaussian membership function can be expressed as follows. Where c , w , n are the center, width and fuzzification factor respectively. The graphical presentation of the fuzzy Gaussian membership function can be seen in Fig. 5.1(b).

$$\mu_F(x, c, w, n) = \text{Exp} [-0.5 \{(x - c) / w\}^n]$$

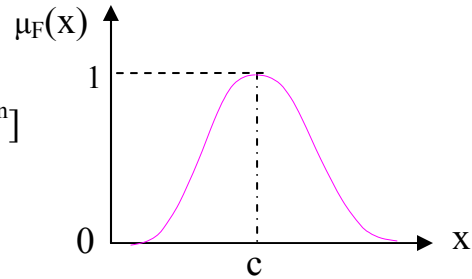


Fig. 5.1(b) Gaussian membership function

The trapezoidal membership function (Fig. 5.1 (c)) has two base points (0.2, 0.5) and two shoulder points (0.3, 0.4). A mathematical expression for the trapezoidal membership function is presented below. A graphical representation of the trapezoidal membership function has been shown in Fig. 5.1 (c).

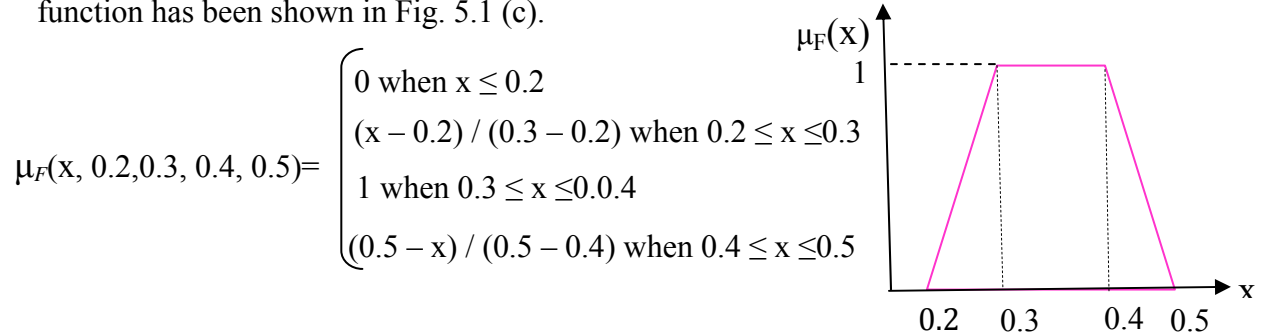


Fig.5.1(c) Trapezoidal membership function

5.2.2 Modeling of fuzzy inference system using fuzzy rules

The understanding of the input data and the output data for a real application is often vague due to the intricate dependencies of the input and output variables of the working domain. However, a good approximation of the input and output parameters is fairly favorable to address a complex problem, rather than going for a complex process, which will consume more time to get an exact result. Fuzzy inference system possesses the approximation features by the help of fuzzy membership functions and fuzzy IF-THEN rules. In the process of development of a fuzzy model, the domain knowledge helps in selecting the appropriate membership functions and development of fuzzy rules. These membership functions are designed by using the suitable fuzzy linguistic terms and fuzzy rule base. The fuzzy rule base or the conditional statements are used for fuzzification of the input parameters and defuzzification of the output parameters. The fuzzy model can be designed with single input and multi output (SIMO), multi input and single output (MISO), multi input and multi output (MIMO). During the design of the fuzzy model, the fuzzy operations like fuzzy intersection, union and complement are used to develop the membership functions. Hence, the fuzzy model takes the input parameters from the application at a certain state of condition and using the rules it will provide a controlled action as desired by the system. A general model of a fuzzy inference system (FIS) is shown in Fig. 5.2.

The inputs to the fuzzy model for crack detection in the current analysis comprises Relative first natural frequency = “fnf”; Relative second natural frequency = “snf”;

Relative third natural frequency = “tnf”; Relative first mode shape difference = “fmd”;

Relative second mode shape difference = “smd”; Relative third mode shape difference = “tmd”

The linguistic term used for the outputs are as follows;

Relative first crack location = “rc1” Relative second crack location = “rc2”

Relative first crack depth = “rcd1” Relative second crack depth = “rcd2”

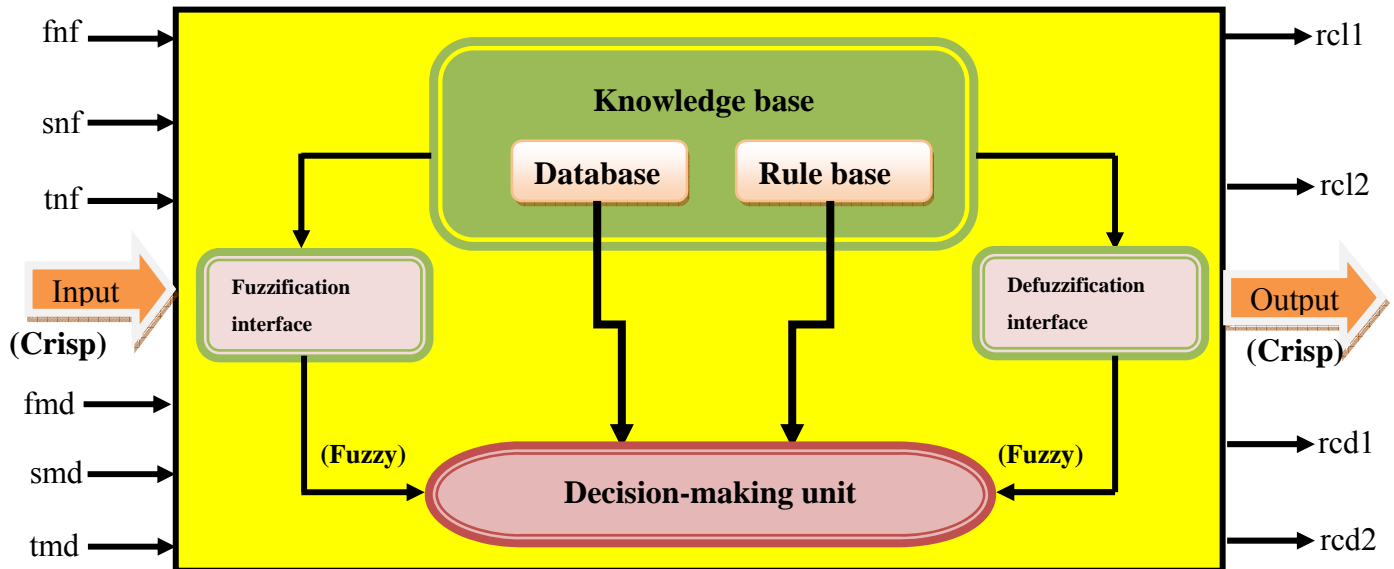


Fig. 5.2 Fuzzy inference system

5.2.3 Modelling of defuzzifier

The final step in building of a fuzzy system is to convert the fuzzy output set into a crisp output. So, the input to the defuzzifier is the aggregate output fuzzy set and output is a single number. The crisp output represents the possible distribution of the inferred fuzzy control action. Selection of the defuzzification strategy depends on the features of the application. The relationship between the fuzzy output set (F), defuzzifier and crisp output (K_0) can be established in the following equation;

$$K_0 = \text{defuzzifier}(F);$$

There are several defuzzification methods used for development of fuzzy system. Some of them are listed below;

- i- Centroid of the area,
- ii- Mean of maximum
- iii- Weighted average method
- iv- Height method

5.3 Analysis of the fuzzy model used for crack detection

The fuzzy models developed in the current analysis, based on triangular, Gaussian and trapezoidal membership functions have got six input parameters and four output parameters.

The linguistic term used for the inputs are as follows;

- Relative first natural frequency = “fnf”;
- Relative second natural frequency = “snf”;
- Relative third natural frequency = “tnf”;
- Average relative first mode shape difference = “fmd”;
- Average relative second mode shape difference = “smd”;
- Average relative third mode shape difference = “tmd”.

The linguistic term used for the outputs are as follows;

- First relative crack location = “rcl1”
- First relative crack depth = “rcd1”
- Second relative crack location = “rcl2”
- Second relative crack depth = “rcd2”

The pictorial view of the triangular membership, Gaussian membership, trapezoidal membership fuzzy models are shown in Fig. Fig. 5.3 (a), Fig. 5.3 (b) and Fig. 5.3 (c) respectively. Some of the fuzzy linguistic terms and fuzzy rules (Twenty numbers) used to design and train the knowledge based fuzzy logic systems are represented in Table 5.1 and Table 5.2 respectively. The membership functions used in developing the fuzzy inference system for crack diagnosis are shown in Fig.5.4 to Fig.5.6. Ten membership functions have been used for each input parameters to the fuzzy model. In designing the output membership functions for the output parameters such as first relative crack location (rcl1) and second relative crack location (rcl2) forty six membership functions are taken whereas for first relative crack depth (rcd1) and second relative crack depth (rcd2) nineteen membership functions have been used. The defuzzification process of the triangular, Gaussian, trapezoidal membership functions are presented in Fig 5.7, Fig. 5.8 and Fig. 5.9 respectively by activating the rule no 3 and rule no 17 from Table 5.2.

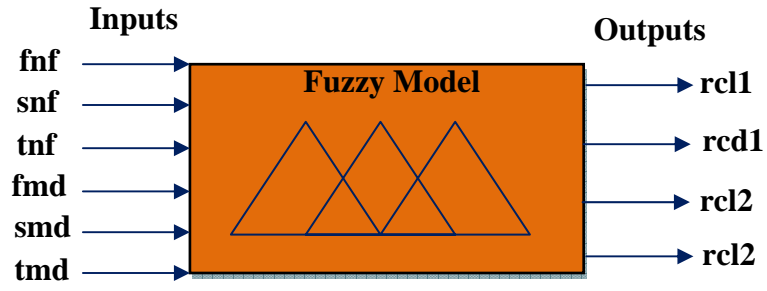


Fig. 5.3(a) Triangular fuzzy model

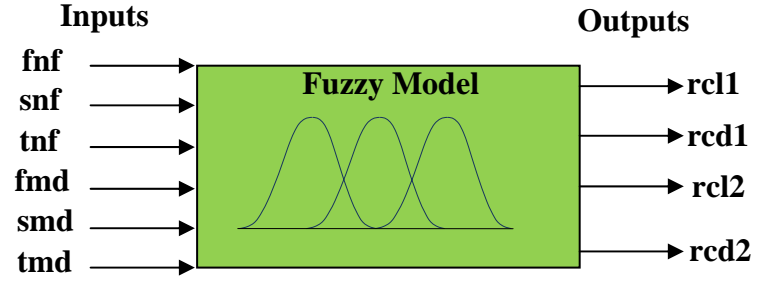


Fig. 5.3(b) Gaussian fuzzy model

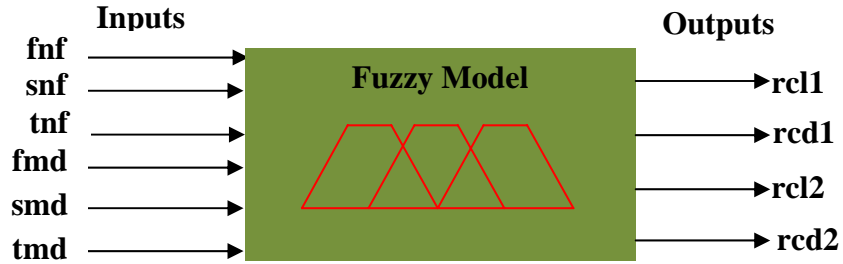


Fig. 5.3(c) Trapezoidal fuzzy model

5.3.1 Fuzzy mechanism for crack detection

Based on the above fuzzy subsets, the fuzzy control rules are defined in a general form as follows:

If (fnf is fnf_i and snf is snf_j and tnf is tnf_k and fmd is fmd_l and smd is smd_m and tmd is tmd_n)
 then rcl1 is $rcl1_{ijklmn}$ and rcd1 is $rcd1_{ijklmn}$ and rcl2 is $rcl2_{ijklmn}$ and rcd2 is $rcd2_{ijklmn}$ (4.1)
 where $i=1$ to 10, $j=1$ to 10, $k=1$ to 10, $l=1$ to 10, $m=1$ to 10, $n=1$ to 10

As “fnf”, “snf”, “tnf”, “fmd”, “smd”, “tmd” have ten membership functions each. From equation (4.1), two set of rules can be written

$$\left. \begin{array}{l} \text{If (fnf is fnf}_i \text{ and snf is snf}_j \text{ and tnf is tnf}_k \text{ and fmd is fmd}_l \text{ and smd is smd}_m \text{ and tmd is tmd}_n \text{)} \\ \text{then rcd1 is rcd1}_{ijklmn} \text{ and rcd2 is rcd2}_{ijklmn} \\ \text{If (fnf is fnf}_i \text{ and snf is snf}_j \text{ and tnf is tnf}_k \text{ and fmd is fmd}_l \text{ and smd is smd}_m \text{ and tmd is tmd}_n \text{)} \\ \text{then rcl1 is rcl1}_{ijklmn} \text{ and rcl2 is rcl2}_{ijklmn} \end{array} \right\} (4.2)$$

According to the usual fuzzy logic control method [91,205], a factor W_{ijklmn} is defined for the rules as follows:

$$W_{ijklmn} = \mu_{fnf_i}(freq_i) \wedge \mu_{snf_j}(freq_j) \wedge \mu_{tnf_k}(freq_k) \wedge \mu_{fmd_l}(moddif_l) \wedge \mu_{smd_m}(moddif_m) \wedge \mu_{tmd_n}(moddif_n)$$

Where $freq_i$, $freq_j$ and $freq_k$ are the first, second and third relative natural frequencies of the cantilever beam with crack respectively; $moddif_l$, $moddif_m$ and $moddif_n$ are the average first, second and third relative mode shape differences of the cantilever beam with crack respectively. By applying the composition rule of inference [91,205], the membership values of the relative crack location and relative crack depth, $(location)_{rclv}$ and $(depth)_{rcdv}$ ($v=1,2$) can be computed as;

$$\left. \begin{array}{l} \mu_{rclv_{ijklmn}}(location) = W_{ijklmn} \wedge \mu_{rclv_{ijklmn}}(location) \quad \forall_{length} \in rclv \\ \mu_{rcdv_{ijklmn}}(depth) = W_{ijklmn} \wedge \mu_{rcdv_{ijklmn}}(depth) \quad \forall_{depth} \in rcdv \end{array} \right\} (4.3)$$

The overall conclusion by combining the outputs of all the fuzzy rules can be written as follows:

$$\left. \begin{array}{l} \mu_{rclv}(location) = \mu_{rclv_{111111}}(location) \vee \dots \vee \mu_{rclv_{ijklmn}}(location) \vee \dots \vee \mu_{rclv_{1010101010}}(location) \\ \mu_{rcdv}(depth) = \mu_{rcdv_{111111}}(depth) \vee \dots \vee \mu_{rcdv_{ijklmn}}(depth) \vee \dots \vee \mu_{rcdv_{1010101010}}(depth) \end{array} \right\} (4.4)$$

The crisp values of relative crack location and relative crack depth are computed using the centre of gravity method [91,205] as:

$$\left. \begin{array}{l} \text{relative crack location} = rcl_{1,2} = \frac{\int (location) \cdot \mu_{rcl_{1,2}}(location) \cdot d(location)}{\int \mu_{rcl_{1,2}}(location) \cdot d(location)} \\ \text{relative crack depth} = rcd_{1,2} = \frac{\int (depth) \cdot \mu_{rcd_{1,2}}(depth) \cdot d(depth)}{\int \mu_{rcd_{1,2}}(depth) \cdot d(depth)} \end{array} \right\} (4.5)$$

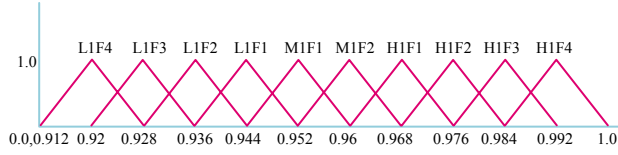


Fig. 5.4(a1) Membership functions for relative natural frequency for first mode of vibration.

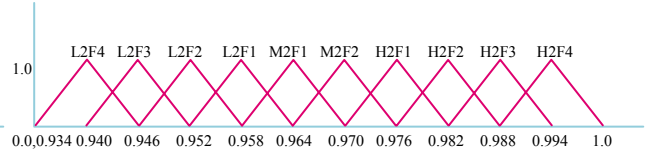


Fig. 5.4(a2) Membership functions for relative natural frequency for second mode of vibration.

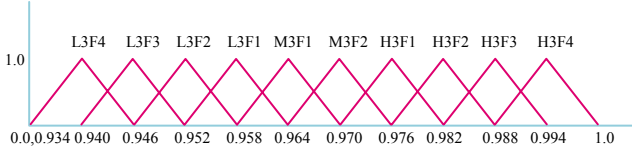


Fig. 5.4(a3) Membership functions for relative natural frequency for third mode of vibration.

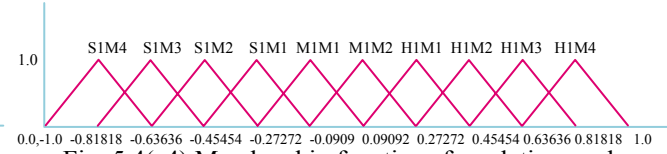


Fig. 5.4(a4) Membership functions for relative mode shape difference for first mode of vibration.



Fig. 5.4(a5) Membership functions for relative mode shape difference for second mode of vibration.

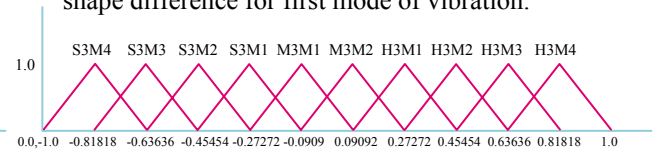


Fig. 5.4(a6) Membership functions for relative mode shape difference for third mode of vibration.

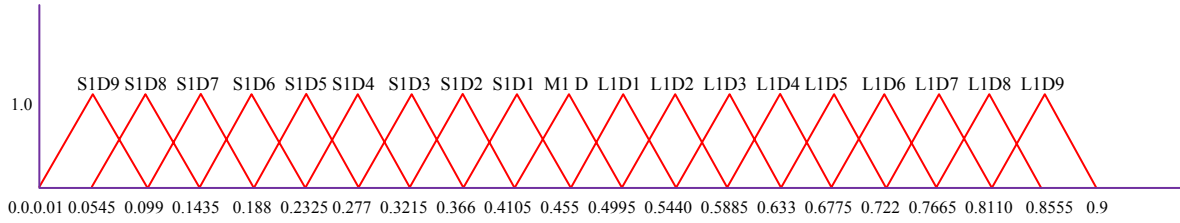


Fig. 5.4(a7) (a) Membership functions for relative crack depth1.

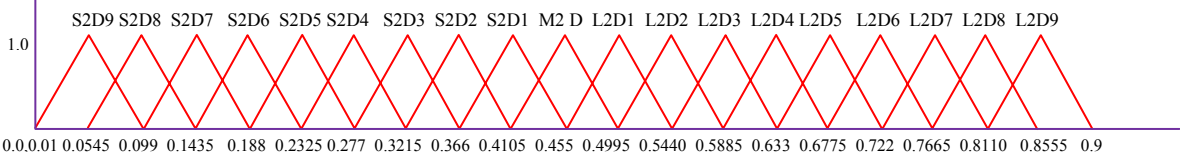


Fig. 5.4(a7) (b) Membership functions for relative crack depth2.

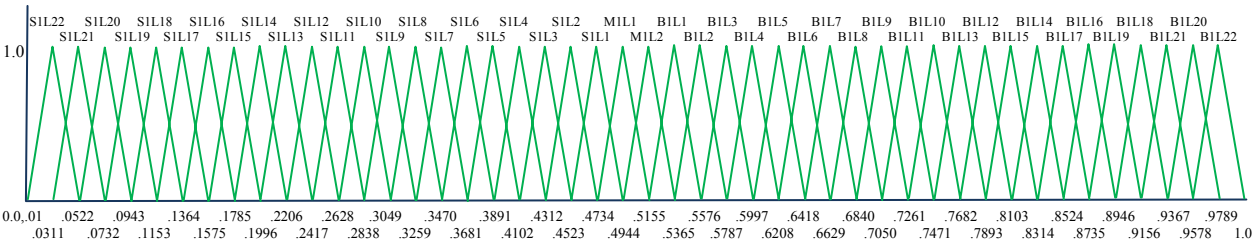


Fig. 5.4(a8) (a) Membership functions for relative crack location1.

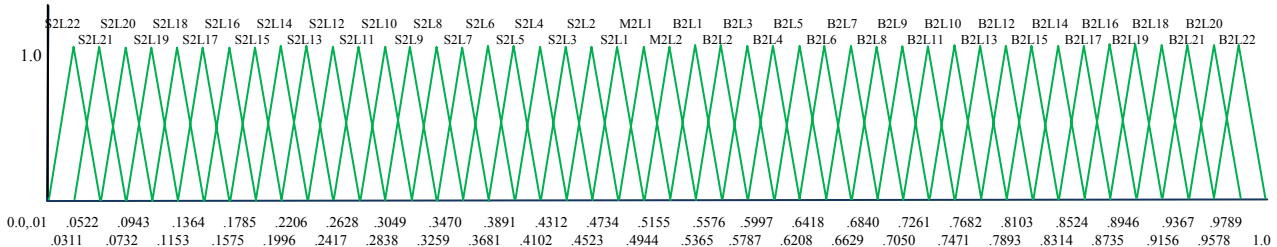


Fig. 5.4(a8) (b) Membership functions for relative crack location2.

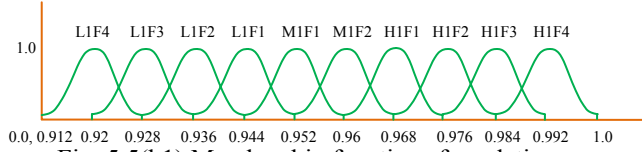


Fig. 5.5(b1) Membership functions for relative natural frequency for first mode of vibration.

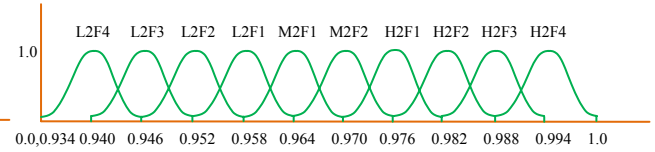


Fig. 5.5(b2) Membership functions for relative natural frequency for second mode of vibration.

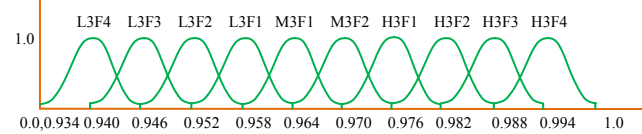


Fig. 5.5(b3) Membership functions for relative natural frequency for third mode of vibration.

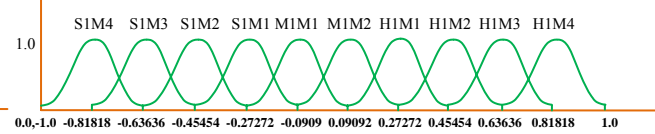


Fig. 5.5(b4) Membership functions for relative mode shape difference for first mode of vibration.

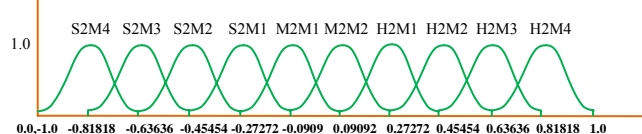


Fig. 5.5(b5) Membership functions for relative mode shape difference for second mode of vibration.

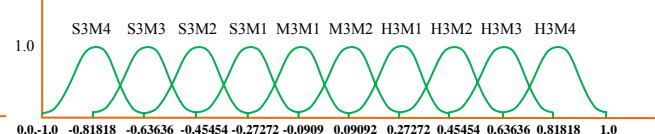


Fig. 5.5(b6) Membership functions for relative mode shape difference for third mode of vibration.

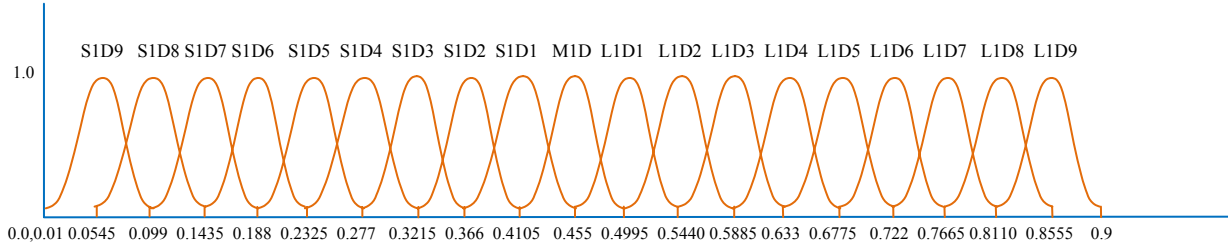


Fig. 5.5(b7) (a) Membership functions for relative crack depth1.

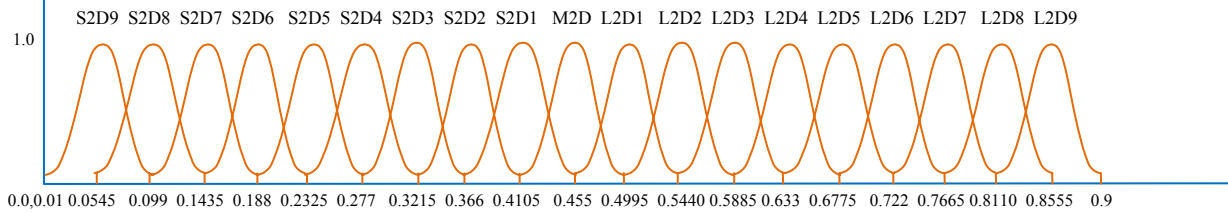


Fig. 5.5(b7) (b) Membership functions for relative crack depth2.

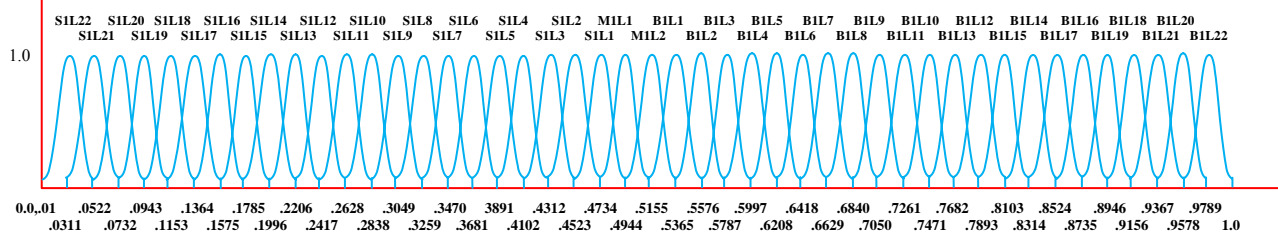


Fig. 5.5(b8) (a) Membership functions for relative crack location1.

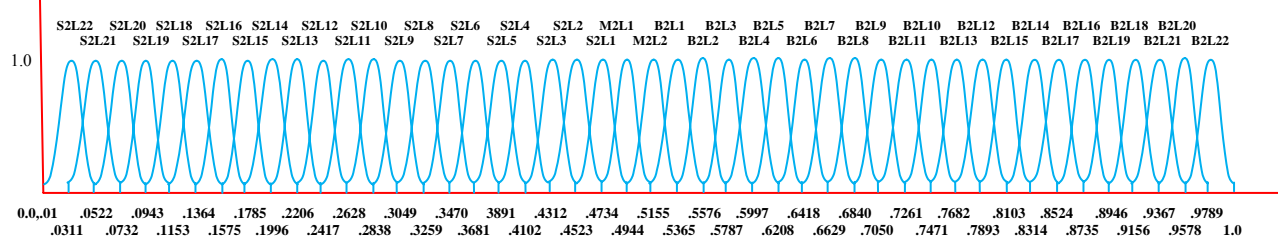


Fig. 5.5 (b8) (b) Membership functions for relative crack location2.

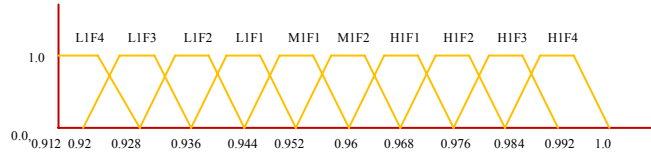


Fig. 5.6(c1) Trapezoidal membership functions for relative natural frequency for first mode of vibration.

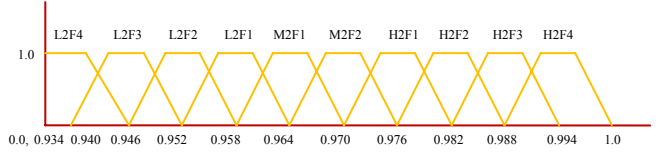


Fig. 5.6 (c2) Trapezoidal Membership functions for relative natural frequency for second mode of vibration.

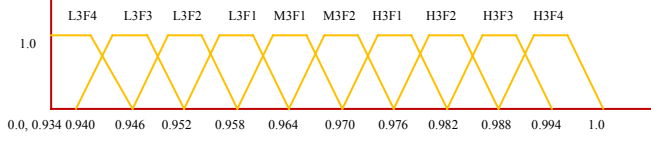


Fig. 5.6(c3) Trapezoidal membership functions for relative natural frequency for third mode of vibration.

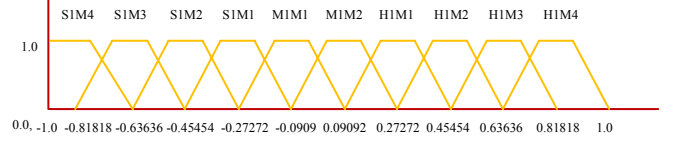


Fig. 5.6 (c4) Trapezoidal membership functions for relative mode shape difference for first mode of vibration.

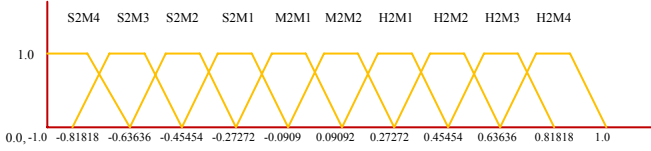


Fig.5.6 (c5) Trapezoidal membership functions for relative mode shape difference for second mode of vibration.

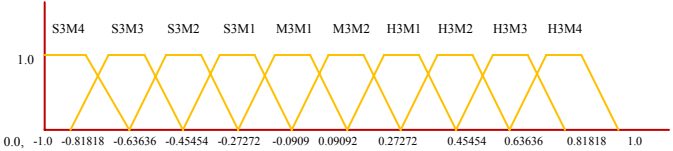


Fig. 5.6(c6) Trapezoidal membership functions for relative mode shape difference for third mode of vibration.

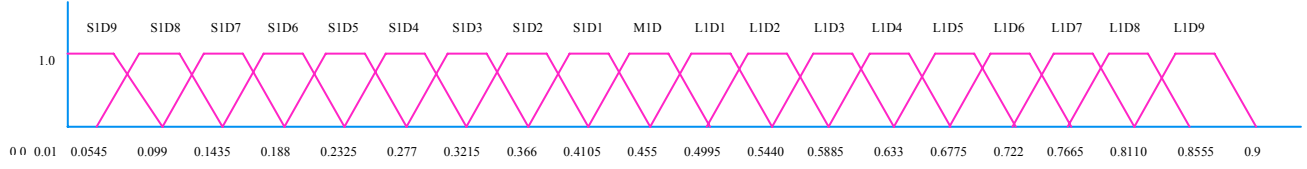


Fig. 5.6 (c7) (a) Trapezoidal membership functions for relative crack depth1.

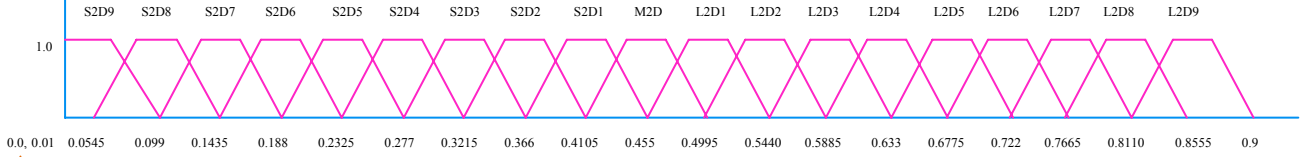


Fig. 5.6 (c7) (b) Trapezoidal membership functions for relative crack depth2.

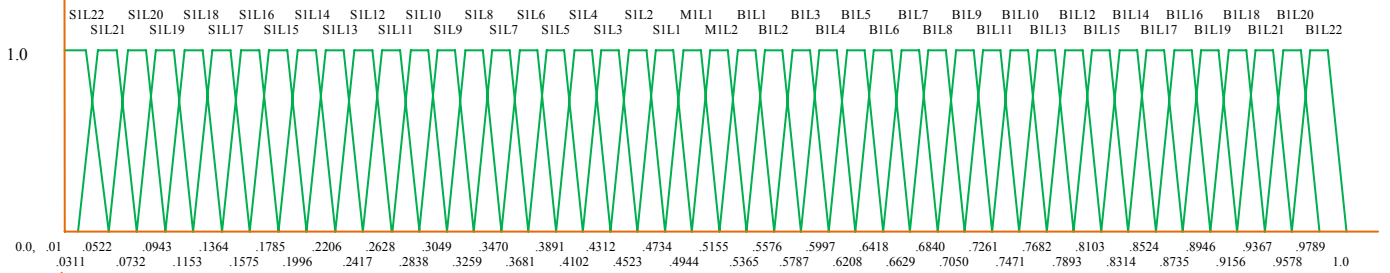


Fig. 5.6 (c8) (a) Trapezoidal membership functions for relative crack location1.

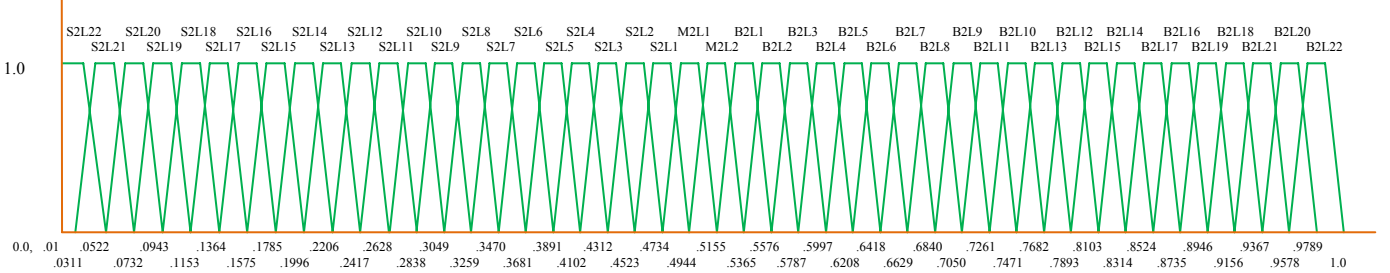


Fig. 5.6 (c8) (b) Trapezoidal membership functions for relative crack location2.

Table 5.1 Description of fuzzy linguistic terms.

Membership Functions Name	Linguistic Terms	Description and range of the Linguistic terms
L1F1,L1F2,L1F3,L1F4	$fnf_{1 \text{ to } 4}$	Low ranges of relative natural frequency for first mode of vibration in descending order respectively
M1F1,M1F2	$fnf_{5,6}$	Medium ranges of relative natural frequency for first mode of vibration in ascending order respectively
H1F1,H1F2,H1F3,H1F4	$fnf_{7 \text{ to } 10}$	Higher ranges of relative natural frequency for first mode of vibration in ascending order respectively
L2F1,L2F2,L2F3,L2F4	$snf_{1 \text{ to } 4}$	Low ranges of relative natural frequency for second mode of vibration in descending order respectively
M2F1,M2F2	$snf_{5,6}$	Medium ranges of relative natural frequency for second mode of vibration in ascending order respectively
H2F1,H2F2,H2F3,H2F4	$snf_{7 \text{ to } 10}$	Higher ranges of relative natural frequencies for second mode of vibration in ascending order respectively
L3F1,L3F2,L3F3,L3F4	$tnf_{1 \text{ to } 4}$	Low ranges of relative natural frequencies for third mode of vibration in descending order respectively
M3F1,M3F2	$tnf_{5,6}$	Medium ranges of relative natural frequencies for third mode of vibration in ascending order respectively
H3F1,H3F2,H3F3,H3F4	$tnf_{7 \text{ to } 10}$	Higher ranges of relative natural frequencies for third mode of vibration in ascending order respectively
S1M1,S1M2,S1M3,S1M4	$fmd_{1 \text{ to } 4}$	Small ranges of first relative mode shape difference in descending order respectively
M1M1,M1M2	$fmd_{5,6}$	medium ranges of first relative mode shape difference in ascending order respectively
H1M1,H1M2,H1M3,H1M4	$fmd_{7 \text{ to } 10}$	Higher ranges of first relative mode shape difference in ascending order respectively
S2M1,S2M2,S2M3,S2M4	$smd_{1 \text{ to } 4}$	Small ranges of second relative mode shape difference in descending order respectively
M2M1,M2M2	$smd_{5,6}$	medium ranges of second relative mode shape difference in ascending order respectively
H2M1,H2M2,H2M3,H2M4	$smd_{7 \text{ to } 10}$	Higher ranges of second relative mode shape difference in ascending order respectively
S3M1,S3M2,S3M3,S3M4	$tmd_{1 \text{ to } 4}$	Small ranges of third relative mode shape difference in descending order respectively
M3M1,M3M2	$tmd_{5,6}$	medium ranges of third relative mode shape difference in ascending order respectively
H3M1,H3M2,H3M3,H3M4	$tmd_{7 \text{ to } 10}$	Higher ranges of third relative mode shape difference in ascending order respectively
S1L1,S1L2.....S1L22	$rcll_{1 \text{ to } 22}$	Small ranges of relative crack location in descending order respectively
M1L1,M1L2	$rcll_{23,24}$	Medium ranges of relative crack location in ascending order respectively
B1L1,B1L2.....B1L22	$rcll_{25 \text{ to } 46}$	Bigger ranges of relative crack location in ascending order respectively
S1D1,S1D2.....S1D9	$rcd1_{1 \text{ to } 9}$	Small ranges of relative crack depth in descending order respectively
M1D	$rcd1_{10}$	Medium relative crack depth
L1D1,L1D2.....L1D9	$rcd1_{11 \text{ to } 19}$	Larger ranges of relative crack depth in ascending order respectively
S2L1,S2L2.....S2L22	$rcl2_{1 \text{ to } 22}$	Small ranges of relative crack location in descending order respectively
M2L1,M2L2	$rcl2_{23,24}$	Medium ranges of relative crack location in ascending order respectively
B2L1,B2L2.....B2L22	$rcl2_{25 \text{ to } 46}$	Bigger ranges of relative crack location in ascending order respectively
S2D1,S2D2.....S2D9	$rcd2_{1 \text{ to } 9}$	Small ranges of relative crack depth in descending order respectively
M2D	$rcd2_{10}$	Medium relative crack depth
L2D1,L2D2.....L2D9	$rcd2_{11 \text{ to } 19}$	Larger ranges of relative crack depth in ascending order respectively

Table 5.2 Examples of twenty fuzzy rules used in fuzzy model.

Sl. No.	Examples of some rules used in the fuzzy model
1	If fnf is H1F1,snf is M2F2,tnf is M3F1,fmd is H1M2,smd is H2M4,tmd is H3M3, then rcd1 is S1D6,and rcl1 is S1L17 and rcd2 is S2D4,and rcl2 is S2L6
2	If fnf is L1F4,snf is L2F4,tnf is L3F4,fmd is H1M1,smd is H2M1,tmd is H3M2, then rcd1 is S1D2,and rcl1 is S1L17 and rcd2 is S2D1,and rcl2 is M2L2
3	If fnf is L1F3,snf is L2F4,tnf is L3F4,fmd is M1M2,smd is H2M2,tmd is H3M3, then rcd1 is M1D,and rcl1 is S1L17 and rcd2 is S2D2,and rcl2 is B2L19
4	If fnf is H1F2,snf is H2F1,tnf is H3F1,fmd is H1M3,smd is H2M4,tmd is H3M4, then rcd1 is S1D6,and rcl1 is S1L11 and rcd2 is S2D4,and rcl2 is M2L2
5	If fnf is M1F1,snf is L2F2,tnf is L3F3,fmd is H1M1,smd is H2M1,tmd is H3M2, then rcd1 is S1D4,and rcl1 is S1L11 and rcd2 is S2D1,and rcl2 is B2L13
6	If fnf is L1F1,snf is L2F2,tnf is L3F3,fmd is H1M3,smd is M2M1,tmd is H3M4, then rcd1 is M1D,and rcl1 is S1L11 and rcd2 is S2D7,and rcl2 is M2L2
7	If fnf is L1F4,snf is L2F4,tnf is L3F4,fmd is M1M2,smd is H2M1,tmd is H3M1, then rcd1 is L1D1,and rcl1 is S1L11 and rcd2 is S2D4,and rcl2 is B2L10
8	If fnf is H1F1,snf is M2F2,tnf is M3F1,fmd is H1M2,smd is H2M2,tmd is H3M2, then rcd1 is S1D6,and rcl1 is S1L6 and rcd2 is S2D4,and rcl2 is B2L5
9	If fnf is L1F1,snf is L2F4,tnf is L3F4,fmd is M1M1,smd is M2M1,tmd is M3M2, then rcd1 is S1D2,and rcl1 is S1L6 and rcd2 is L2D1,and rcl2 is B2L5
10	If fnf is M1F1,snf is L2F2,tnf is L3F1,fmd is M1M2,smd is M2M2,tmd is H3M1, then rcd1 is S1D1,and rcl1 is S1L6 and rcd2 is S2D4,and rcl2 is B2L5
11	If fnf is M1F1,snf is M2F1,tnf is M3F1,fmd is H1M3,smd is H2M3,tmd is H3M4, then rcd1 is S1D6,and rcl1 is S1L18 and rcd2 is S2D5,and rcl2 is M2L2
12	If fnf is M1F1,snf is L2F1,tnf is L3F1,fmd is H1M3,smd is H2M2,tmd is H3M3, then rcd1 is S1D4,and rcl1 is S1L17 and rcd2 is S2D6,and rcl2 is S2L6
13	If fnf is M1F2,snf is M2F1,tnf is M3F1,fmd is M1M1,smd is H2M1,tmd is H3M2, then rcd1 is S1D4,and rcl1 is S1L11 and rcd2 is S2D4,and rcl2 is M2L2
14	If fnf is H1F2,snf is H2F1,tnf is H3F1,fmd is H1M4,smd is H2M1,tmd is H3M1, then rcd1 is S1D7,and rcl1 is S1L17 and rcd2 is S2D6,and rcl2 is B2L16
15	If fnf is M1F1,snf is L2F1,tnf is L3F2,fmd is S1M1,smd is S2M2,tmd is H3M1, then rcd1 is S1D2,and rcl1 is S1L11 and rcd2 is S2D6,and rcl2 is B2L10
16	If fnf is L1F4,snf is L2F4,tnf is L3F4,fmd is H1M2,smd is S2M1,tmd is H3M2, then rcd1 is L1D1,and rcl1 is S1L17 and rcd2 is S2D5,and rcl2 is M2L2
17	If fnf is M1F1,snf is L2F3,tnf is L3F1,fmd is S1M2,smd is M2M1,tmd is S3M1, then rcd1 is S1D6,and rcl1 is S1L12 and rcd2 is M2D,and rcl2 is M2L1
18	If fnf is L1F1,snf is L2F1,tnf is L3F1,fmd is H1M2,smd is H2M2,tmd is H3M2, then rcd1 is S1D2,and rcl1 is S1L12 and rcd2 is S2D4,and rcl2 is B2L13
19	If fnf is H1F2,snf is H2F1,tnf is H3F1,fmd is S1M2,smd is H2M3,tmd is H3M1, then rcd1 is S1D4,and rcl1 is S1L5 and rcd2 is S2D6,and rcl2 is B2L6
20	If fnf is L1F3,snf is L2F4,tnf is L3F4,fmd is S1M3,smd is S2M2,tmd is S3M3, then rcd1 is L1D1,and rcl1 is S1L5 and rcd2 is S2D2,and rcl2 is B2L5

Inputs

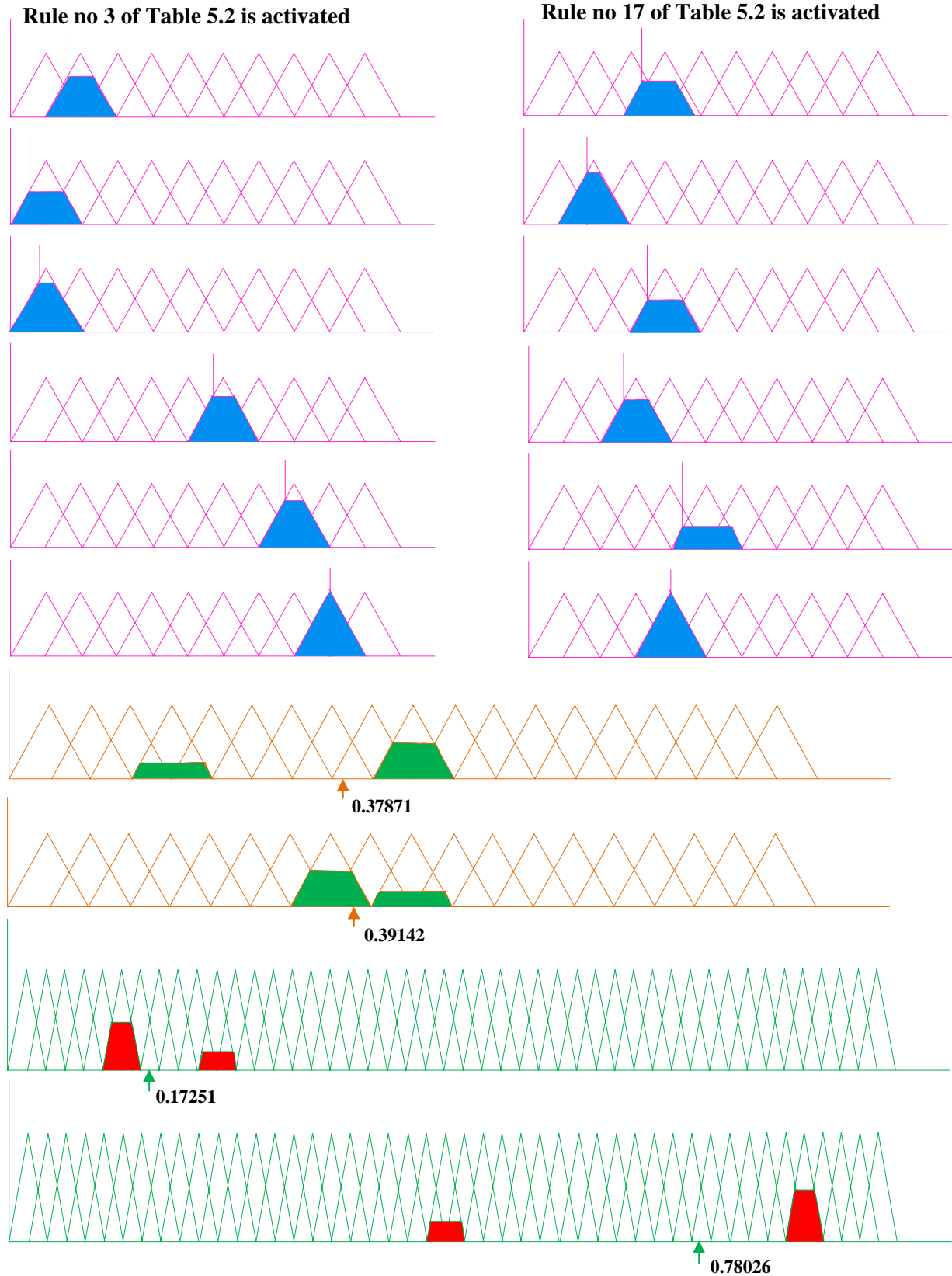


Fig. 5.7 Resultant values of relative crack depths and relative crack locations when Rules 3 and 17 of Table 5.2 are activated.

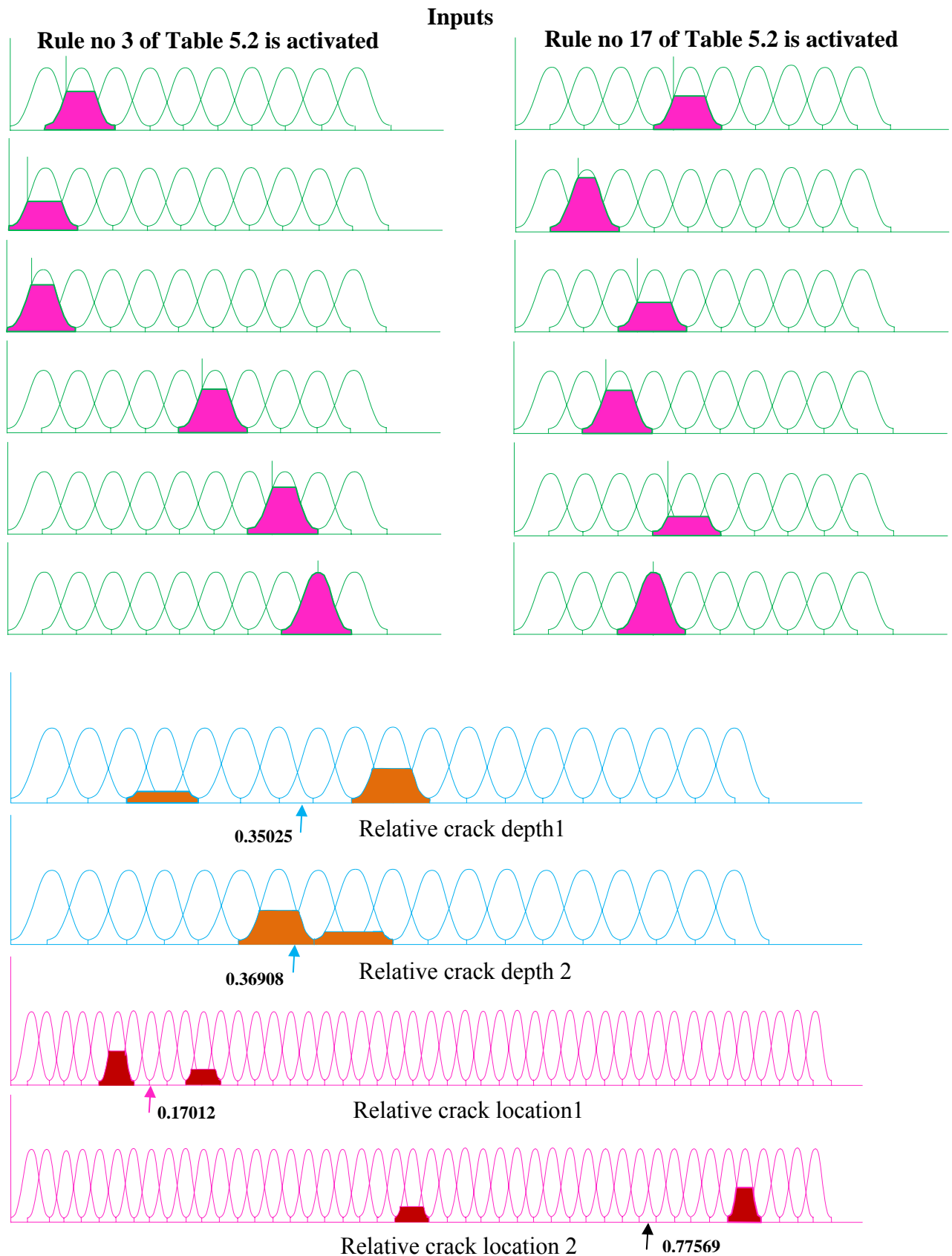


Fig. 5.8 Resultant values of relative crack depth and relative crack location when Rules 3 and 17 of Table 5.2 are activated.

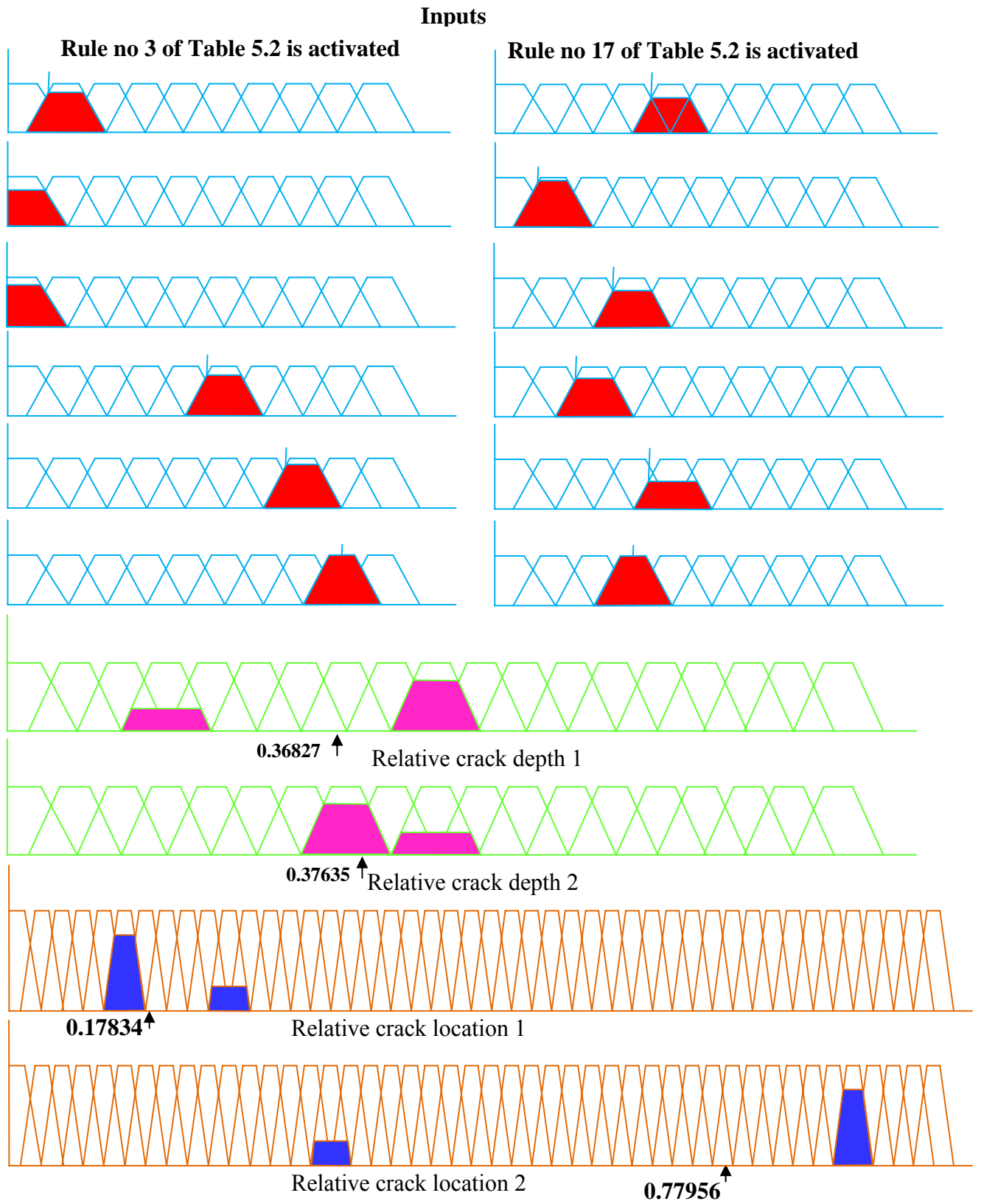


Fig. 5.9 Resultant values of relative crack depth and relative crack location from trapezoidal fuzzy model when Rules 3 and 17 of Table 5.2 are activated.

5.3.2 Results of fuzzy model

The results obtained from the proposed fuzzy system for multiple crack identification are presented in this section.

The fuzzy model (Fig. 5.2) has been designed with six inputs (relative first three natural frequencies and relative first three mode shape differences) and four outputs (relative first and second crack location, relative first and second crack depth). Three types of membership functions (triangular, Gaussian and trapezoidal) has been employed to develop the fuzzy model (Fig.5.4, Fig.5.5, Fig.5.6). Defuzzification (Fig.5.7, Fig.5.8, Fig.5.9) of the inputs using triangular, Gaussian and trapezoidal membership functions have been done by activating the rule no. 3 and rule no. 17 from the Table 5.2. The results obtained from numerical, finite element, fuzzy triangular, fuzzy Gaussian, fuzzy trapezoidal model and experimental analysis are compared in Table 5.3 (a) and Table 5.3 (b). Ten sets of data from the Table 5.3 (a), Table 5.3 (b) represents the first three relative natural frequencies and first three relative mode shape differences in the first six columns and rest of the columns represents the corresponding values of relative first and second crack locations and crack depths obtained from numerical, finite element, fuzzy triangular, fuzzy Gaussian, fuzzy trapezoidal model and experimental analysis.

5.4 Discussions

The fuzzy system designed in the current research has been adopted for multiple crack diagnosis in structural members. The various types of membership functions used for development of the knowledge based system are triangular (Fig. 5.1 (a)), Gaussian (Fig. 5.1 (b)), trapezoidal (Fig. 5.1 (c)). The different stages involved in designing of the proposed system are presented in Fig. 5.2. The various linguistic terms and some of the fuzzy rules used for developing the fuzzy crack diagnostic tool have been exhibited in Table 5.1 and Table 5.2 respectively. The different types of membership functions with the linguistic terms have been presented in Fig. 5.4 to Fig. 5.6 showing complete architecture. The results obtained from fuzzy model with triangular, Gaussian and trapezoidal membership functions and experimental analyses are compared in Table 5.3 (a). The results from numerical, finite element and Gaussian fuzzy model analysis are shown in Table 5.3 (b) and the results are found to be in close proximity. From the analysis of the results presented in Table 5.3 (a), it is seen that the percentage deviation of the results of the triangular membership function

fuzzy model is 7.84%, for Gaussian membership function fuzzy model is 5.06% and for trapezoidal membership function fuzzy model is 7.02%.

Table 5.3 (a) Comparison of results between fuzzy Gaussian model, fuzzy triangular model, fuzzy trapezoidal model and experimental analysis.

Relative first natural frequency "f ₁ "	Relative second natural frequency "f ₂ "	Relative third natural frequency "f ₃ "	Average Relative first mode shape difference "f _{md} "	Average Relative second mode shape difference "s _{md} "	Average Relative third mode shape difference "t _{md} "	Fuzzy Gaussian model				Fuzzy trapezoidal model				Fuzzy triangular model				Experimental analysis relative			
						relative 1 st crack depth "rcd1"	relative 1 st crack location "rcl1"	2 nd crack depth "rcd2"	2 nd crack location "rcl2"	relative 1 st crack depth "rcd1"	relative 1 st crack location "rcl1"	2 nd crack depth "rcd2"	2 nd crack location "rcl2"	relative 1 st crack depth "rcd1"	relative 1 st crack location "rcl1"	2 nd crack depth "rcd2"	2 nd crack location "rcl2"	1st crack depth "rcd1"	1st crack location "rcl1"	2nd crack depth "rcd2"	2nd crack location "rcl2"
0.9987	0.9979	0.9889	0.0036	0.0346	0.0132	0.24	0.25	0.413	0.74	0.22	0.23	0.412	0.73	0.21	0.21	0.410	0.72	0.29	0.29	0.418	0.79
0.9997	0.9989	0.9978	0.0017	0.0021	0.0082	0.166	0.373	0.24	0.624	0.164	0.372	0.24	0.623	0.163	0.370	0.22	0.621	0.171	0.379	0.29	0.627
0.9958	0.9944	0.9937	0.0126	0.009	0.0732	0.165	0.375	0.24	0.623	0.163	0.373	0.22	0.621	0.162	0.371	0.21	0.620	0.171	0.379	0.29	0.629
0.9981	0.9989	0.9975	0.0012	0.0026	0.0752	0.333	0.125	0.415	0.49	0.331	0.123	0.413	0.47	0.329	0.121	0.412	0.46	0.337	0.129	0.420	0.55
0.9981	0.9986	0.9881	0.0048	0.0267	0.0152	0.164	0.24	0.23	0.50	0.162	0.22	0.21	0.47	0.163	0.23	0.22	0.48	0.172	0.31	0.30	0.56
0.9987	0.9972	0.9981	0.0036	0.0028	0.0123	0.23	0.24	0.412	0.73	0.21	0.22	0.410	0.71	0.19	0.20	0.409	0.70	0.27	0.28	0.418	0.77
0.9849	0.9982	0.9869	0.0134	0.0211	0.0119	0.414	0.23	0.163	0.46	0.412	0.21	0.161	0.44	0.410	0.19	0.160	0.43	0.419	0.28	0.169	0.52
0.9989	0.9973	0.9974	0.0017	0.0025	0.0079	0.48	0.22	0.21	0.73	0.46	0.20	0.19	0.71	0.44	0.19	0.18	0.69	0.52	0.27	0.26	0.77
0.9980	0.9857	0.9871	0.0065	0.0069	0.0247	0.331	0.373	0.48	0.624	0.329	0.371	0.46	0.622	0.327	0.370	0.45	0.620	0.336	0.378	0.53	0.628
0.9993	0.9985	0.9988	0.0046	0.0019	0.0162	0.416	0.374	0.26	0.626	0.413	0.372	0.24	0.624	0.412	0.370	0.23	0.623	0.420	0.378	0.29	0.631

Table 5.3 (b) Comparison of results between Fuzzy Gaussian model, FEA and numerical analysis

Relative first natural frequency "f _{1f} "	Relative second natural frequency "s _{nf} "	Relative third natural frequency "t _{nf} "	Average Relative first mode shape difference "fmd"	Average Relative second mode shape difference "smd"	Average Relative third mode shape difference "tmd"	Fuzzy Gaussian model				FEA				Numerical			
						relative 1 st crack depth "red1"	1 st crack location "rel1"	2 nd crack depth "red2"	2 nd crack location "rel2"	relative 1 st crack depth "red1"	1 st crack location "rel1"	2 nd crack depth "red2"	2 nd crack location "rel2"	relative 1 st crack depth "red1"	1 st crack location "rel1"	2 nd crack depth "red2"	2 nd crack location "rel2"
0.9987	0.9979	0.9889	0.0036	0.0346	0.0132	0.24	0.25	0.413	0.74	0.20	0.19	0.409	0.70	0.19	0.18	0.407	0.69
0.9997	0.9989	0.9978	0.0017	0.0021	0.0082	0.166	0.373	0.24	0.624	0.162	0.369	0.20	0.618	0.161	0.367	0.18	0.616
0.9958	0.9944	0.9937	0.0126	0.009	0.0732	0.165	0.375	0.24	0.623	0.163	0.369	0.20	0.619	0.161	0.367	0.19	0.617
0.9981	0.9989	0.9975	0.0012	0.0026	0.0752	0.333	0.125	0.415	0.49	0.329	0.120	0.411	0.46	0.327	0.119	0.409	0.45
0.9981	0.9986	0.9881	0.0048	0.0267	0.0152	0.164	0.24	0.23	0.50	0.163	0.22	0.21	0.46	0.162	0.20	0.19	0.44
0.9987	0.9972	0.9981	0.0036	0.0028	0.0123	0.23	0.24	0.412	0.73	0.18	0.19	0.408	0.68	0.17	0.17	0.406	0.67
0.9849	0.9982	0.9869	0.0134	0.0211	0.0119	0.414	0.23	0.163	0.46	0.409	0.19	0.160	0.43	0.407	0.18	0.158	0.42
0.9989	0.9973	0.9974	0.0017	0.0025	0.0079	0.48	0.22	0.21	0.73	0.43	0.18	0.18	0.68	0.42	0.17	0.16	0.67
0.9980	0.9857	0.9871	0.0065	0.0069	0.0247	0.331	0.373	0.48	0.624	0.327	0.369	0.44	0.619	0.325	0.367	0.43	0.617
0.9993	0.9985	0.9988	0.0046	0.0019	0.0162	0.416	0.374	0.26	0.626	0.411	0.369	0.20	0.622	0.409	0.367	0.19	0.620

5.5 Summary

The fuzzy approach adopted in the current analysis has been studied and following conclusions are made. The presence of cracks in structural member has considerable effect on the dynamic response of the dynamic structure. The first three relative natural frequencies and first three relative mode shape differences are taken as inputs to the fuzzy model and relative crack locations and relative crack depths are the output parameters. The authenticity of the proposed approach has been established by comparing the results from the fuzzy models (Gaussian, trapezoidal, triangular) with that of the numerical, finite element and experimental analysis. The results are found to be well in agreement. From the analysis of the results obtained from the fuzzy models using various membership functions, it is observed that the fuzzy system based on Gaussian membership function provides better results in comparison to numerical, finite element analysis, trapezoidal and triangular fuzzy models. Hence, the proposed Gaussian fuzzy model can be effectively used as multiple crack diagnostic tools in dynamically vibrating structures. Since the fuzzy Gaussian model produces best results in terms of relative crack depths and relative crack locations in comparison to fuzzy triangular, fuzzy trapezoidal model, the results of fuzzy Gaussian model will be compared with other AI techniques discussed in next chapters to compare their performance in regard to Gaussian fuzzy model.

Publications:

- Amiya Kumar Dash, Dayal.R.Parhi, Development of an inverse methodology for crack diagnosis using AI technique, International Journal of Computational Materials Science and Surface Engineering (IJCMSSE) 4(2), 2011, 143-167.
- Das H. C., Dash A. K., Parhi D. R., Experimental Validation of Numerical and Fuzzy Analysis of a Faulty Structure, 5th International Conference on System of Systems Engineering (SoSE), 2010, Loughborough, U.K., 22-24 June, pp.1-6.

Chapter 6

ANALYSIS OF ARTIFICIAL NEURAL NETWORK FOR MULTIPLE CRACK DETECTION

The presence of damage in general, in a structure undermines the viability of the structure and leads to shorter life time period and opens the way for complete failure of the system. Hence, development of an automated method to identify cracks accurately in an engineering application is desirable. As it is known that, the cracks present in a mechanical element increase the flexibility, decrease the vibration frequencies and modify the amplitude of vibration. Those changes can be potentially used to locate the crack positions and crack depths. So, it is of interest to design and develop an AI based technique for online multiple crack diagnosis to avoid catastrophic failure of structural system. In the current chapter an intelligent model has been designed using artificial neural network to detect presence of multiple cracks in structural members. The proposed neural model has been modeled with feed forward network trained with back propagation technique. Finally, the results from the model have been compared with the experimental results to establish the robustness of the proposed neural method.

6.1 Introduction

This section of the thesis provides an introduction to basic neural network architectures and learning rules.

The complex biological neural network in a human body has highly interconnected set of neurons, facilitates for various kind of output such as thinking, breathing, driving etc. Generally the neurons are believed to store the biological neural functions and memory and learning of the neural system facilitates for establishment of new connections between the neurons. The most interesting feature of this artificial neural network (ANN) is the novel structure of the information processing system. It is composed of a large number of highly interconnected processing elements (neurons) working in parallel to solve specific applications, such as pattern recognition or data classification, through a learning process. Learning in biological systems involves adjustments to the synaptic weights that exist

between the neurons. Neural networks, with their remarkable ability to derive meaning from complicated or imprecise data, can be used to recognize patterns and detect trends that are too complex to be noticed by either humans or other computer techniques. McCulloch and Pitts [207] have developed models of neural networks with several assumptions about how neurons worked. The proposed networks were considered to be binary devices with fixed thresholds based on simple neurons. Rosenblatt [208] has designed and developed the Perceptron. The developed Perceptron has three layers with the middle layer known as the association layer. This system could learn to connect or associate a given input to a random output unit. According to [206] a neural network is a large parallel distributed processor made up of simple processing units, called neurons, which have a natural tendency to store experimental knowledge and making it available for use. Some of the advantages of the ANN are depicted below.

Adaptive learning: The ability of the neural system lies in the capacity to adapt to the changing environment by adjusting the synaptic weights and perform according to the situation. This feature makes the neural network a methodology to address industrial applications in dynamic environment.

Self-Organization: An artificial neural network can produce results for inputs that are not used during training by creating its own representation of the information it receives during learning time. This capability helps in solving problem of higher complexities.

Real Time Operation: The neural network is composed of a large number interconnected neurons working in parallel to solve a specific problem. Neural networks learn by example. For this special hardware devices are being designed and manufactured which take advantage of this capability.

Fault Tolerance: In case of failure of a neuron in neural network system there will be a partial destruction of a network which leads to only deterioration of quality of output rather than collapsing the system as a whole.

Research has been carried out in last few decades to develop system for online condition monitoring of structural systems. As the presence of cracks reduces the service life of the structures and also responsible for economic loss and in some of the cases may be loss of human life, the development of a fault diagnostic methodology is of paramount importance

for science community. Although at the present time different non destructive techniques (e.g. acoustic emission, sensor) are available for identification of crack present in a system, the response of the techniques are very poor in terms of accuracy and computational time for complex system. Moreover, development of a mathematical model for a complex system with changing environment becomes impossible. In this scenario, the use of ANN with its parallel computing and pattern recognition capabilities are well suitable to design an intelligent system for damage assessment in cracked structures with higher accuracy and faster computational time. In the recent times a lot of effort have been made by scientists to develop crack diagnostic tool using ANN. Schlechtingen et al. [96] have presented a comparison of results among the regression based model and two artificial neural network based approaches, which are a full signal reconstruction and an autoregressive normal behavior model used for condition monitoring of bearings in a wind turbine. From the comparison of results they have revealed all three models were capable of detecting incipient faults. They have concluded that the neural network model provides the best result with a faster computational time with comparison to regression based model. Ghate et al. [97] have proposed a multi layer perceptron neural network based classifier for fault detection in induction motors which is inexpensive, reliable by employing more readily available information such as stator current. They have used simple statistical parameters as input feature space and principal component analysis has been used for reduction of input dimensionality. They have also verified their methodology to noise and found the performance of the proposed technique encouraging.

This section introduces a feed forward multilayer neural network trained with back propagation technique for online multiple damage detection in beam members. The proposed neural network system has been designed with six input parameters (first three relative natural frequencies, first three relative mode shape differences) and four output parameters (relative first crack location, relative first crack depth, relative second crack location and relative second crack depth). A comparison of results obtained from fuzzy, numerical, FEA, neural and experimental analysis have been carried out and it is observed that the developed neural network provides more accurate results as compared to other mentioned methods. The robustness of the neural system has been validated using the experimental set up.

The present chapter has been arranged into five different sections. The first section i.e. introduction (Section 6.1) gives a brief introduction to neural network algorithm. Section 6.2 provides an in depth view of the feed forward neural network trained with back propagation technique. The analysis of the neural network model used for multiple crack diagnosis is presented in section 6.3. The results and discussions of the results obtained from the neural model and the summary of the chapter are described in section 6.4 and section 6.5 respectively.

6.2 Neural network technique

Given this the description of neural network, it has been successfully implemented in many industrial applications such as industrial process control, sales forecasting, electronic noses, modeling, diagnosing the Cardiovascular System and etc. The parallel computing capability and the ability to perform under changing environment make the neural network a potential tool to address applications, which are hard to solve using analytical or numerical methods.

6.2.1 Model of a neural network

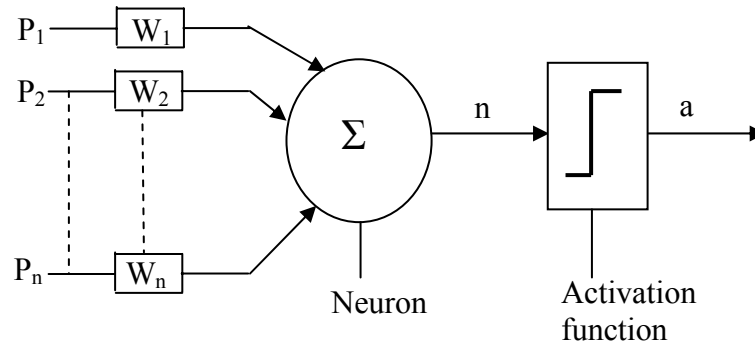


Fig. 6.1 Neuron model

A neuron which can be used in a dynamic environment is shown in Fig. 6.1. An artificial neuron is a device with many inputs and one output. The neuron has two modes of operation; the training mode and the using mode. In the training mode, the neuron can be trained to fire (or not), for particular input patterns. In the using mode, when a taught input pattern is detected at the input, its associated output becomes the current output. If the input pattern does not belong in the taught list of input patterns, the firing rule is used to determine whether to fire or not.

The main features of the neural model are as follows,

1. The inputs to the neuron are assigned with synaptic weights, which in turn affect the decision making ability of the neural network. The inputs to the neuron are called weighted inputs.
2. These weighted inputs are then summed together in an adder and if they exceed a pre-set threshold value, the neuron fires. In any other case the neuron does not fire.
3. An activation function for limiting the amplitude of the output of a neuron. Generally the normalized amplitude range of the output of a neuron is given as the closed unit interval $[0,1]$ or alternatively $[-1,1]$.

Learning process of ANN:

The learning for a neural network means following a methodology for modifying the weights to make the network adaptive in nature to changing environment. The learning rules may be broadly divided into three categories,

1. Supervised learning: The supervised learning rule is provided with set of training data for proper network behavior. When the inputs are applied to the network, the outputs from the network are compared with the targets. Through the learning process the network will adjust the weights of the network in order to bring the outputs closer to the targets.
2. Unsupervised learning: In this type of learning the network modifies the weights in response to the inputs to the network. This is suitable for applications requiring vector quantization.
3. Reinforcement learning: In the reinforcement learning instead of being provided with the correct output, for each network input, the algorithm is only given a score. The score is the measure of network performance over some sequence of inputs.

In mathematical terms, we can describe a neuron k by writing the following pair of equations:

$$u_k = \sum_{j=1}^p w_{kj} x_j \quad (6.1)$$

$$y_k = f(u_k) \quad (6.2)$$

Where x_1, x_2, \dots, x_p are the input signals; $w_{k1}, w_{k2}, \dots, w_{kp}$ are the synaptic weights of neuron k ; u_k is the linear combined output; $f(\cdot)$ is the activation function; and y_k is the output signal of the neuron.

6.2.2 Use of back propagation neural network

The back propagation technique (Fig. 6.2) can be used to train the multilayer networks. This technique is an approximate steepest gradient algorithm in which the performance of the network is based on mean square error. In order to train the neural network, the weights for each input to the neural system should be so adjusted that the error between the actual output and desired output is minimum. The multilayer neural system would calculate the change in error due to increase or decrease in the weights. The algorithm first computes each error weight by computing the rate of the error changes with the change in synaptic weights. The error in each hidden layer just before the output layer in a direction opposite to the way activities propagate through the network have to be computed and fed to the network by back propagation algorithm to minimize the error in the actual output and desired output by adjusting the parameters of the network.

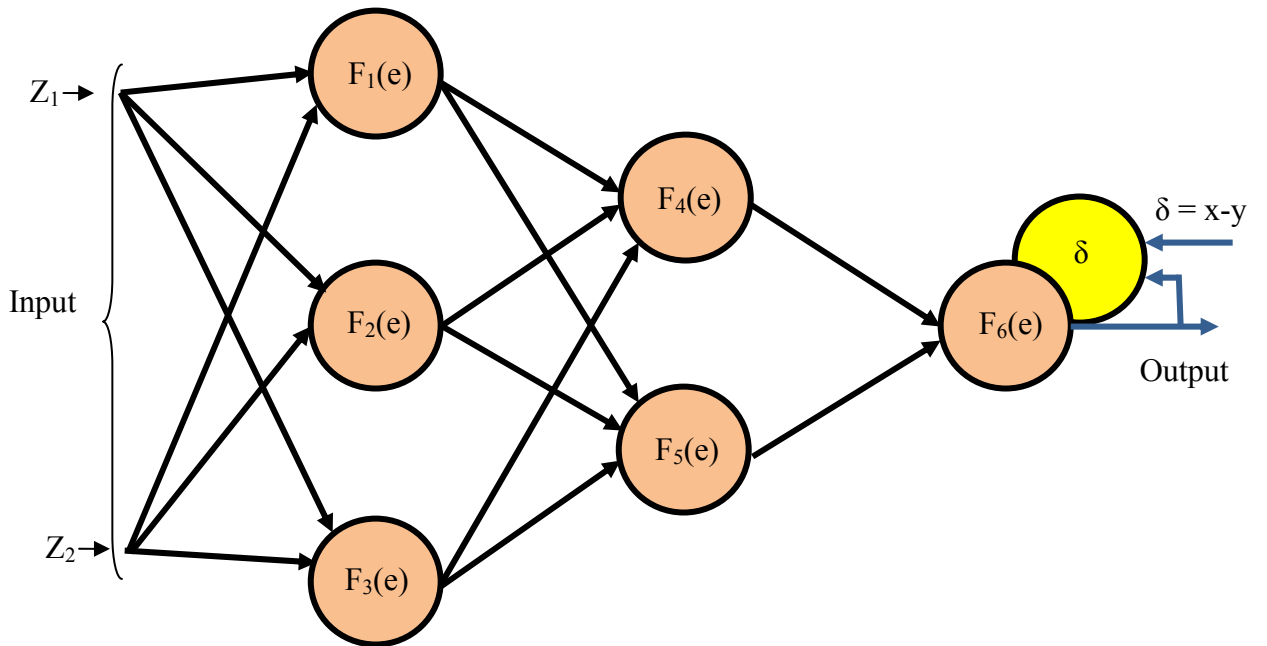


Fig. 6.2 Back propagation technique

6.3 Analysis of neural network model used for crack detection

A back propagation neural model has been proposed for identification of multiple cracks (i.e. relative crack locations, relative crack depths) of a cantilever beam structure (Fig.6.3).The neural model has been designed with six input parameters and four output parameters.

The inputs to the neural network model are fnf, snf, tnf, fmd, smd and tmd.

The outputs from the neural model are as follows;

first relative crack location = “rcl1” and first relative crack depth = “rcd1”

second relative crack location = “rcl2” and first relative crack depth = “rcd2”

The back propagation neural network has been made with one input layer, one output layer and eight hidden layers. The input layer contains six neurons, where as the output layer contains four neurons. The number of neurons in each hidden layers are different in order to give the neural network a diamond shape and for better convergence of results (Fig.6.4). The neurons associated with the input layer of the network represent the first three relative natural frequencies and first three average relative mode shape difference. The first relative crack location, first relative crack depth, second relative crack location, second relative crack depth are represented by the four neurons of the output layer of the neural network.

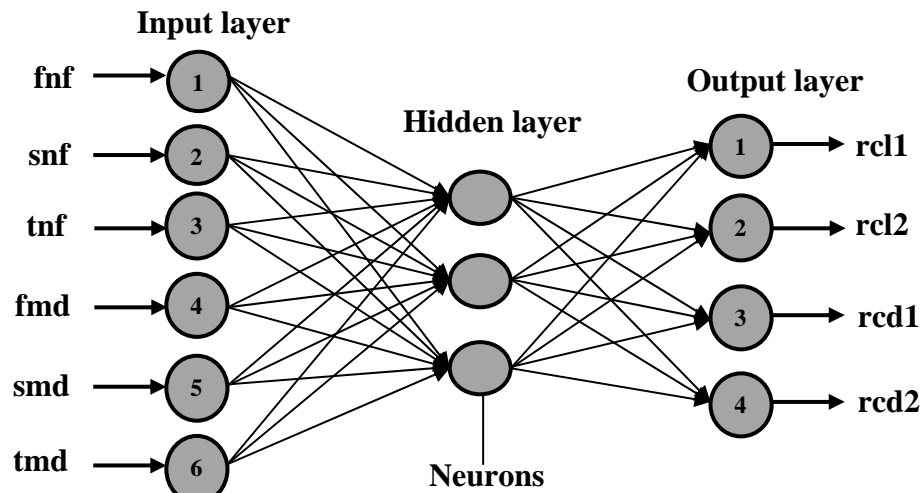


Fig. 6.3 Neural model

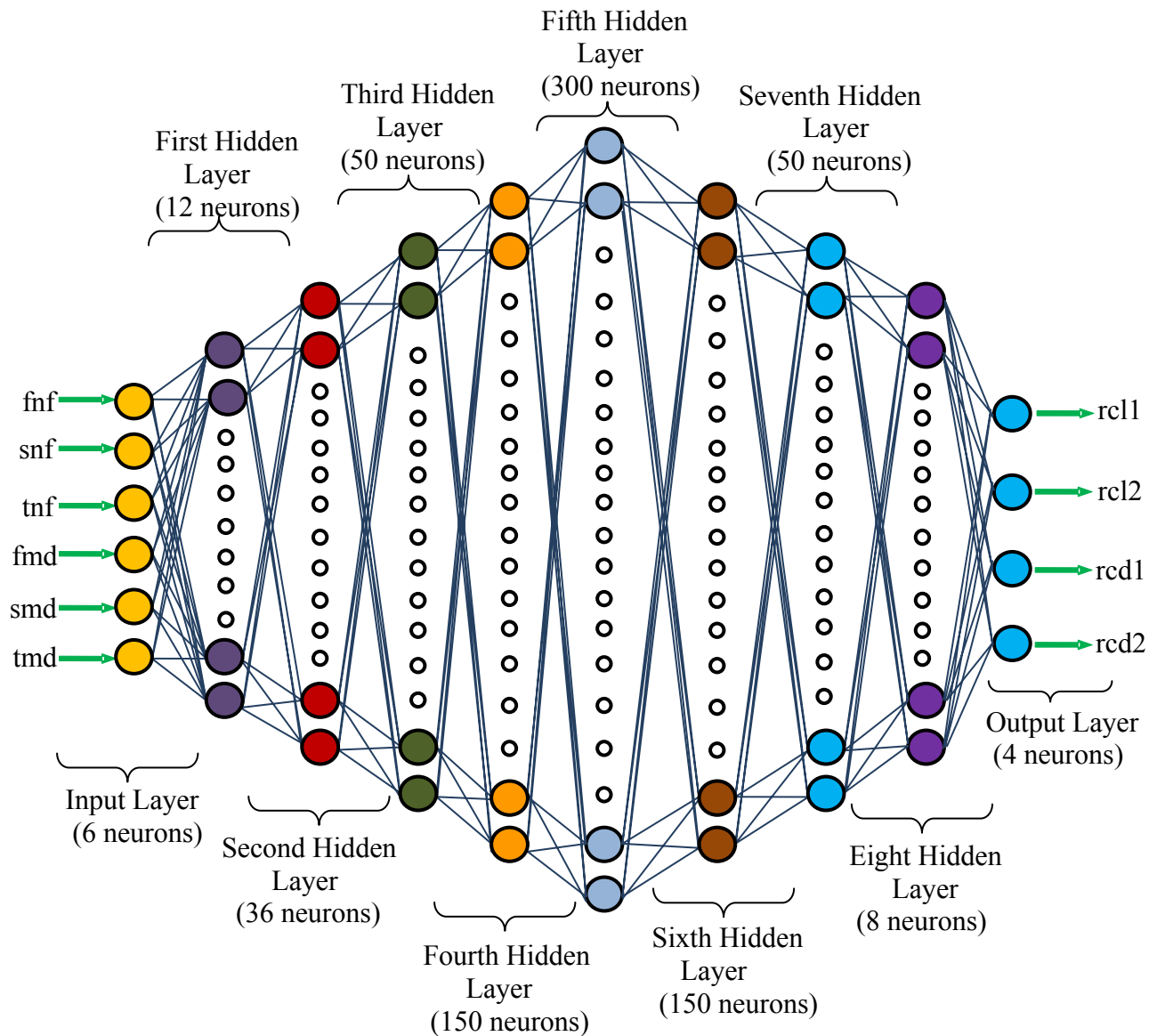


Fig. 6.4 Multi Layer feed forward back propagation Neural model for damage detection

6.3.1 Neural model mechanism for crack detection

The neural network used in the current investigation is a ten-layer feed forward neural network model trained with back propagation technique [206]. The chosen number of layers was found empirically to facilitate training. The first three relative natural frequencies and first three relative mode shape difference are the neurons representing the input layer of the network and relative crack locations and relative crack depths are represented by the four neurons of the output layer. The hidden layers i.e. 2nd, 3rd, 4th, 5th, 6th, 7th and 8th layer of the network comprises 12 neurons, 36 neurons, 50 neurons, 150 neurons, 300 neurons, 150 neurons, 50 neurons, 8 neurons respectively. The number of neurons in each hidden layer has been decided using the empirical relation. Fig. 6.4 depicts the neural network with its input and output signals.

The proposed neural network model for multiple crack detection has been trained with 900 patterns of data featuring various conditions of the structural system. Out of the several hundred testing data, some of them are presented in Table 6.1. During the training, the model is fed with six input parameters i.e. first three relative natural frequencies and first three mode shape differences (e.g. 0.9924, 0.9937, 0.9987, 0.0025, 0.0047, 0.0051). The outputs are relative crack depths and relative crack locations (e.g. 0.164, 0.23, 0.0622, and 0.3123).

During training and during normal operation, the input patterns fed to the neural network comprise the following components:

$$y_1^{\{1\}} = \text{relative deviation of first natural frequency} \quad (6.3(a))$$

$$y_2^{\{1\}} = \text{relative deviation of second natural frequency} \quad (6.3(b))$$

$$y_3^{\{1\}} = \text{relative deviation of third natural frequency} \quad (6.3(c))$$

$$y_4^{\{1\}} = \text{relative deviation of first mode shape difference} \quad (6.3(d))$$

$$y_5^{\{1\}} = \text{relative deviation of second mode shape difference} \quad (6.3(e))$$

$$y_6^{\{1\}} = \text{relative deviation of third mode shape difference} \quad (6.3(f))$$

The outputs generated due to the distribution of the input to the hidden neurons are given by [206]:

$$f(V_j^{\{lay\}}) = y_j^{\{lay\}} \quad (6.4)$$

Where,

$$\sum_i W_{ji}^{\{lay\}} \cdot y_i^{\{lay-1\}} = V_j^{\{lay\}} \quad (6.5)$$

layer number (2 or 9) = lay

label for j^{th} neuron in hidden layer ‘lay’= j

label for i^{th} neuron in hidden layer ‘lay-1’= i

Weight of the connection from neuron i in layer ‘lay-1’ to neuron j in layer ‘lay’= $W_{ji}^{\{lay\}}$

Activation function, chosen in this work as the hyperbolic tangent function = $f(.)$, where,

$$\frac{e^x - e^{-x}}{e^x + e^{-x}} = f(x) \quad (6.6)$$

In the process of training, the network output $\theta_{\text{actual}, n}$ ($i=1$ to 4) may differ from the desired output $\theta_{\text{desired}, n}$ ($n=1$ to 4) as specified in the training pattern presented to the network. The measure of performance of the network is the instantaneous sum-squared difference between $\theta_{\text{desired}, n}$ and $\theta_{\text{actual}, n}$ for the set of presented training patterns:

$$\text{Err} = \frac{1}{2} \sum_{\text{all training patterns}} (\theta_{\text{desired}, n} - \theta_{\text{actual}, n})^2 \quad (6.7)$$

Where $\theta_{\text{actual}, n}$ ($n=1$) represents relative crack location (“rcl1”)

$\theta_{\text{actual}, n}$ ($n=2$) represents relative crack depth (“rcd1”)

$\theta_{\text{actual}, n}$ ($n=3$) represents relative crack location (“rcl2”)

$\theta_{\text{actual}, n}$ ($n=4$) represents relative crack depth (“rcd2”)

During the development of the neural model, the error back propagation method is employed to train the network [206]. This method requires the computation of local error gradients in

order to determine appropriate weight corrections to reduce error. For the output layer, the error gradient $\delta^{\{10\}}$ is:

$$\delta^{\{10\}} = f'(V_1^{\{10\}}) (\theta_{\text{desired},n} - \theta_{\text{actual},n}) \quad (6.8)$$

Hence, the local gradient for neurons in hidden layer $\{\text{lay}\}$ is given by:

$$\delta_j^{\{\text{lay}\}} = f'(V_j^{\{\text{lay}\}}) \left(\sum_k \delta_k^{\{\text{lay}+1\}} W_{kj}^{\{\text{lay}+1\}} \right) \quad (6.9)$$

Synaptic weights are updated according to the following expressions:

$$W_{ji}(t+1) = W_{ji}(t) + \Delta W_{ji}(t+1) \quad (6.10)$$

$$\text{and } \Delta W_{ji}(t+1) = \alpha \Delta W_{ji}(t) + \eta \delta_j^{\{\text{lay}\}} y_i^{\{\text{lay}-1\}} \quad (6.11)$$

Where

Momentum coefficient (chosen statistically as 0.2 in this work) = α

Learning rate (chosen statistically as 0.35 in this work) = η

Iteration number, each iteration consisting of the presentation of a training pattern and correction of the weights = t

Following expression shows, the final output from the neural network as;

$$\theta_{\text{actual},n} = f(V_n^{\{10\}}) \quad (6.12)$$

$$\text{where } V_n^{\{10\}} = \sum_i W_{ni}^{\{10\}} y_i^{\{9\}} \quad (6.13)$$

η = learning rate (chosen empirically as 0.35 in this work)

t = iteration number, each iteration consisting of the presentation of a training pattern and correction of the weights.

Table 6.1 Test patterns for NN model other than training data

Input to the NN model						Output from the NN			
Relative first natural frequency (fnf)	Relative second natural frequency (snf)	Relative third natural frequency (tnf)	Average relative first mode shape differences (fmd)	Average relative first mode shape differences (fmd)	Average relative first mode shape differences (fmd)	Relative first crack depth (rcd1)	Relative first crack location (rc11)	Relative second crack depth (rcd2)	Relative second crack location (rc12)
0.9924	0.9937	0.9987	0.0025	0.0047	0.0051	0.164	0.0622	0.23	0.3123
0.9962	0.9973	0.9981	0.0154	0.026	0.0324	0.081	0.122	0.163	0.48
0.9947	0.9965	0.9985	0.0068	0.0255	0.0287	0.23	0.3122	0.33	0.623
0.9955	0.9972	0.9992	0.0037	0.0157	0.0253	0.331	0.23	0.22	0.872
0.9974	0.9982	0.9996	0.0074	0.0097	0.0166	0.163	0.622	0.331	0.9372
0.9934	0.9958	0.9978	0.0026	0.0035	0.0124	0.082	0.621	0.162	0.873
0.9942	0.9964	0.9988	0.0012	0.0031	0.0049	0.161	0.24	0.332	0.23
0.9918	0.9945	0.9992	0.0021	0.0041	0.0058	0.413	0.3124	0.22	0.6872
0.9957	0.9979	0.9996	0.0015	0.0034	0.0064	0.081	0.22	0.414	0.8123
0.9951	0.9977	0.9989	0.0019	0.0028	0.0059	0.23	0.123	0.332	0.872

6.3.2 Neural model for finding out crack depth and crack location

The feed forward network has been trained with 900 different patterns of parameters to obtain the objective. Some of the test patterns are depicted in Table 6.1. The intelligent neural system has six numbers of input parameters in the input layer i.e. first three relative natural frequencies and first three average mode shape difference. The output layer has four outputs and they are first and second relative crack locations and first and second relative crack depths.

6.4 Results and discussions of neural model

The ten layer feed forward neural network model with back propagation technique for crack prediction is shown with the complete architecture in Fig.6.4. This has been designed to predict the relative crack locations and relative crack depths. The first three relative natural frequencies and first three average relative mode shape differences have been used as inputs to the input layer of the proposed network. These inputs are processed in the eight hidden layers and finally the output layer provides the results for relative crack locations and relative crack depths. The block diagram of the neural model with the input and output parameters are presented in Fig.6.3. Out of several hundred training patterns that have been used to train the neural model some of them along with the outputs from the model are shown in Table 6.1. Experiments have been carried out to validate the results obtained from different analyses performed on the cracked cantilever beam. Comparison among the results obtained from neural model, fuzzy Gaussian model and experimental analysis are presented in Table 6.2 (a). The results from theoretical, finite element and fuzzy Gaussian model have been expressed in Table 6.2 (b) and are found to be in close agreement. The different parameters presented in various columns of the Table 6.2 (a) and Table 6.2 (b) are expressed as, the first column relative first natural frequency (fnf), the second column relative second natural frequency (snf), the third column relative of 3rd natural frequency (tnf), the fourth column relative first mode shape difference (fmd), the fifth column relative second mode shape difference (smd), the sixth column represents the relative third mode shape difference (tmd) as inputs and the rest columns represents the outputs as relative crack location and relative crack depth obtained from corresponding analyses. The percentage of deviation of the results from neural model with respect to experimental results observed during the analysis of the data given in Table 6.2 (a) is about 4.53%, which is better than the performance of fuzzy Gaussian model. A plot of graph for epochs vs mean squared error from NN has been shown in Fig. A3 of the appendix section showing the convergence of results. The graph for actual values vs predicted values from the neural model has been presented in Fig. A4 of appendix section showing the robustness of the neural network.

Table 6.2 (a) Comparison of results between neural model, fuzzy Gaussian model and experimental analysis.

Relative first natural frequency "f1"	Relative second natural frequency "snf"	Relative third natural frequency "tnf"	Average Relative first mode shape difference "fmd"	Average Relative second mode shape difference "smd"	Average Relative third mode shape difference "tmd"	Neural Model relative				Fuzzy Gaussian model				Experimental analysis			
						1 st crack depth "rcd1"	1 st crack location "rc11"	2 nd crack depth "rcd2"	2 nd crack location "rc12"	relative 1 st crack depth "rcd1"	1 st crack location "rc11"	2 nd crack depth "rcd2"	2 nd crack location "rc12"	relative 1 st crack depth "rcd1"	1 st crack location "rc11"	2 nd crack depth "rcd2"	2 nd crack location "rc12"
0.9979	0.9985	0.9993	0.0087	0.0036	0.0042	0.48	0.123	0.22	0.46	0.46	0.121	0.21	0.45	0.52	0.127	0.27	0.51
0.9962	0.9989	0.9991	0.0036	0.9729	0.2263	0.414	0.123	0.330	0.873	0.412	0.122	0.328	0.871	0.418	0.127	0.335	0.877
0.9936	0.9976	0.9987	0.0138	0.014	0.0832	0.164	0.373	0.23	0.622	0.163	0.372	0.22	0.621	0.168	0.377	0.27	0.627
0.9976	0.9991	0.9988	0.0014	0.0041	0.0812	0.332	0.123	0.414	0.49	0.330	0.121	0.412	0.48	0.335	0.127	0.418	0.53
0.9978	0.9983	0.9878	0.0036	0.0329	0.0141	0.164	0.24	0.23	0.49	0.162	0.22	0.21	0.47	0.169	0.28	0.27	0.53
0.9987	0.9972	0.9981	0.2936	0.3428	0.2623	0.24	0.24	0.414	0.73	0.23	0.22	0.412	0.73	0.27	0.28	0.418	0.77
0.9849	0.9982	0.9869	0.0134	0.0211	0.0119	0.414	0.372	0.22	0.622	0.415	0.373	0.23	0.623	0.418	0.376	0.27	0.627
0.9989	0.9973	0.9974	0.0017	0.0025	0.0079	0.46	0.21	0.20	0.71	0.47	0.22	0.22	0.73	0.52	0.27	0.26	0.77
0.9977	0.9847	0.9881	0.0079	0.0077	0.0292	0.329	0.371	0.46	0.621	0.330	0.372	0.45	0.622	0.335	0.377	0.52	0.627
0.9988	0.9974	0.9991	0.0057	0.0023	0.0155	0.413	0.22	0.163	0.46	0.414	0.23	0.162	0.47	0.419	0.28	0.169	0.52

Table 6.2 (b) Comparison of results between neural model, FEA analysis and Numerical analysis.

Relative first natural frequency "f1"	Relative second natural frequency "sf"	Relative third natural frequency "tf"	Average Relative first mode shape difference "fmd"	Average Relative second mode shape difference "smd"	Average Relative third mode shape difference "umd"	Neural Model				FEA				Numerical			
						relative 1 st crack location "rcd1"	relative 1 st crack depth "rcd1"	relative 2 nd crack location "rcd2"	relative 2 nd crack depth "rcd2"	relative 1 st crack location "rcd1"	relative 1 st crack depth "rcd1"	relative 2 nd crack location "rcd2"	relative 2 nd crack depth "rcd2"	relative 1 st crack location "rcd1"	relative 1 st crack depth "rcd1"	relative 2 nd crack location "rcd2"	relative 2 nd crack depth "rcd2"
0.9979	0.9985	0.9993	0.0087	0.0036	0.0042	0.48	0.123	0.22	0.46	0.43	0.119	0.18	0.42	0.41	0.117	0.16	0.40
0.9962	0.9989	0.9991	0.0036	0.9729	0.2263	0.414	0.123	0.330	0.873	0.409	0.118	0.326	0.868	0.407	0.117	0.324	0.866
0.9936	0.9976	0.9987	0.0138	0.014	0.0832	0.164	0.373	0.23	0.622	0.159	0.368	0.18	0.618	0.157	0.367	0.16	0.616
0.9976	0.9991	0.9988	0.0014	0.0041	0.0812	0.332	0.123	0.414	0.49	0.327	0.119	0.410	0.45	0.325	0.117	0.409	0.43
0.9978	0.9983	0.9878	0.0036	0.0329	0.0141	0.164	0.24	0.23	0.49	0.161	0.19	0.18	0.44	0.159	0.17	0.16	0.42
0.9987	0.9972	0.9981	0.2936	0.3428	0.2623	0.24	0.24	0.414	0.73	0.19	0.20	0.409	0.68	0.18	0.19	0.407	0.66
0.9849	0.9982	0.9869	0.0134	0.0211	0.0119	0.414	0.372	0.22	0.622	0.410	0.367	0.19	0.618	0.408	0.365	0.18	0.616
0.9989	0.9973	0.9974	0.0017	0.0025	0.0079	0.46	0.21	0.20	0.71	0.44	0.18	0.18	0.68	0.42	0.17	0.16	0.66
0.9977	0.9847	0.9881	0.0079	0.0077	0.0292	0.329	0.371	0.46	0.621	0.326	0.368	0.44	0.619	0.324	0.366	0.43	0.617
0.9988	0.9974	0.9991	0.0057	0.0023	0.0155	0.413	0.22	0.163	0.46	0.410	0.19	0.160	0.45	0.408	0.17	0.158	0.44

6.5 Summary

This section expresses the final conclusions drawn from the analysis carried out in the present chapter. The neural network model has been designed on the basis of change of vibration signatures such as natural frequencies and modes shapes due to presence of cracks in structural members. The input parameters to the diamond shaped feed forward neural network model is the first three natural frequencies and first three average mode shapes. The outputs from the model are relative crack locations and relative crack depths. Hundreds of training patterns have been developed to train the neural model for crack prediction. The neural system has different numbers of neurons in all the ten layers for processing the inputs to the model. By adopting the back propagation algorithm, it is observed that the difference between the actual output and desired output has been successfully reduced. The results derived from the proposed neural network have been compared with the results obtained from numerical, FEA, fuzzy Gaussian model and experimental analysis to check the effectiveness of the model. From the analysis of the performance of the developed neural system for multiple crack diagnosis, it is seen that, the model can predict the crack locations and their intensities very close to the actual results as compared to fuzzy Gaussian model. In the next chapters, the neural model have been used to fabricate various hybrid technique such as fuzzy- neuro, GA-neural and MANFIS methodology for online structural health monitoring.

Publication

- Dayal.R.Parhi, Amiya K. Dash, Application of neural network and finite element for condition monitoring of structures, Proceedings of the Institution of Mechanical Engineers, Part C: Journal of Mechanical Engineering Science. Vol. 225, pp. 1329-1339, 2011.

Chapter 7

ANALYSIS OF GENETIC ALGORITHM FOR MULTIPLE CRACK DETECTION

Machines and beam like structures require continuous monitoring for the fault identification for ensuring uninterrupted service. Different non destructive techniques (NDT) are generally used for this purpose, but they are costly and time consuming. Vibration based methods can be useful to detect cracks in structures using various artificial intelligence (AI) techniques. The modal parameters from the dynamic response of the structure are used for this purpose. In the current analysis, the vibration characteristics of a cracked cantilever beam having different crack locations and depths have been studied. Numerical and finite element methods have been used to extract the diagnostic indices (natural frequencies, mode shapes) from cracked and intact beam structure. An intelligent Genetic Algorithm (GA) based model has been designed to automate the fault identification and location process. Single point crossover and in some cases mutation procedure have been followed to find out the optimal solution from the search space. The model has been trained in offline mode using the simulation and experimental results (initial data pool) under various healthy and faulty conditions of the structure. The outcome from the developed model shows that the system could not only detect the cracks but also predict their locations and severities. Good agreement between the simulation, experimental and GA model results confirms the effectiveness of the proposed model.

7.1 Introduction

Genetic algorithms are inspired by Darwin's theory for evolution. With the application of GA the solution to a problem has been evolved. The adoptions of natural process like reproduction, mutation [126] are the base for development of GA. Finding an optimization solution in various problems is the strength of this evolutionary algorithm. Hence GA has evolved as a potential tool for different optimization problems for a large variety of applications. In most of the optimization problems, the objective is to either maximizing/minimizing an objective function from the search space of arbitrary dimension. An algorithm which will examine every possible inputs in the search space in order to determine the element for which objective function is optimal is most desirable. GA follows

a heuristic way of searching the input space for optimal value that approximates without enumerating all the elements by exhaustive search. During application of GA, at the beginning a large population of random chromosomes is created. Subsequently the genes of the chromosomes are decoded to get different solution to the problem at hand. The genetic algorithms perform a randomized search in solution space using a genotypic. The steps followed in GA are systematically listed below.

1. Each solution is encoded as a chromosome in a population (a binary, integer, or real-valued string). Each string's element represents a particular feature of the solution.
2. The string is evaluated by a fitness function to determine the solution's quality. Better-fit solutions survive and produce offspring. Less-fit solutions are removed from the population.
3. Strings are evolved using mutation & recombination operators.
4. New individuals created by these operators form next generation of solutions.

This chapter has been organized into four sections. The introduction section describes the generalized features of the GA methodology in section 7.1. The analysis of the crack diagnostic tool using GA has been discussed in section 7.2. The results and discussions and summary of the chapter are presented in section 7.3 and 7.4 respectively.

7.2. Analysis of crack diagnostic tool using GA

7.2.1. Approach of GA for crack identification

The generalized procedures of genetic algorithm are shown in He et al. [120]. Genetic algorithm is based on the mechanics of nature selection and natural genetics, which is designed to efficiently search large, non-linear, discrete and poorly understood search space, where expert knowledge is scarce or difficult to model and where traditional optimization techniques fail. The genetic algorithm consists of an array of gene values, its 'chromosome', and as in nature, an individual that is optimized for its environment is created by successive modification over a number of generations. Genetic algorithm have been frequently accepted as optimization methods in various fields, and have also proved their excellence in solving complicated, non-linear, discrete and poorly understood optimization problem. This is why we use it to solve our inverse problem for the multiple crack detection in a cracked cantilever beam.

The developed genetic methodology discusses the prediction of cracks in a cantilever beam containing multiple transverse cracks using the chromosomes representing the parameters of vibration responses. The parameters i.e. (natural frequencies, mode shapes, relative crack locations, relative crack depths) indirectly define the predicted values of cracks locations and crack depths. The vibration signatures from theoretical, FEA and experimental analysis are used to get the data pool for the GA methodology. The proposed GA model utilizes hundreds of chromosomes in the data pool to act as parents. Each parents consists of ten parameters such as first three relative natural frequencies, first three average relative mode shapes, relative crack locations (two numbers), relative crack depths (two numbers). The steps used in the genetic algorithm have been presented in the form of flow chart in Fig. 7.3. The procedure followed to find out the crack depths and crack locations are systematically described below in stages.

Stage 1: Data pool set for prediction of multiple cracks

The calculated values of the fnf, snf, tnf, fmd, smd, tmd, relative crack location 1, relative crack location 2, relative crack depth 1, relative crack depth 2 from theoretical, finite element and experimental analysis are used for creating the initial data pool of predetermined size. Each individual data set from the created data pool represents the chromosomes of the GA model. In this investigation the field data set is used to find the optimized solution. The generated data pool set is the search space for the problem under study and relative crack locations, relative crack depths are the solutions from the developed methodology.

The initial population with size n can be presented as follows:

Initial Population = $\langle P_1, P_2, \dots, P_n \rangle$

Each structure have the elements $p_{(i, j)}$ which are simply an integer string of length L, in general.

Each population members have 10-sets of genes which are represented by Element numbers 1 to 10.

$$P_1 = \{ p_{1,1} \quad p_{1,2} \quad p_{1,3} \quad p_{1,4} \quad p_{1,5} \quad p_{1,6} \quad p_{1,7} \quad p_{1,8} \quad p_{1,9} \quad p_{1,10} \}$$

$$P_2 = \{ p_{2,1} \quad p_{2,2} \quad p_{2,3} \quad p_{2,4} \quad p_{2,5} \quad p_{2,6} \quad p_{2,7} \quad p_{2,8} \quad p_{2,9} \quad p_{2,10} \}$$

.....

$$P_n = \{ p_{n,1} \quad p_{n,2} \quad p_{n,3} \quad p_{n,4} \quad p_{n,5} \quad p_{n,6} \quad p_{n,7} \quad p_{n,8} \quad p_{n,9} \quad p_{n,10} \}$$

Where,

Element No. 1 ($p_{1,1}$ to $p_{n,1}$) represents the relative first natural frequency (fnf)

Element No. 2 ($p_{1,2}$ to $p_{n,2}$) represents the relative second natural frequency (snf)

Element No. 3 ($p_{1,3}$ to $p_{n,3}$) represents the relative third natural frequency (tnf)

Element No. 4 ($p_{1,4}$ to $p_{n,4}$) represents the average relative first mode shape (fmd)

Element No. 5 ($p_{1,5}$ to $p_{n,5}$) represents the average relative second mode shape (smd)

Element No. 6 ($p_{1,6}$ to $p_{n,6}$) represents the average relative third mode shape (tmd)

Element No. 7 ($p_{1,7}$ to $p_{n,7}$) represents the relative crack location 1 (rcl1)

Element No. 8 ($p_{1,8}$ to $p_{n,8}$) represents the relative crack depth 1 (rcd1)

Element No. 9 ($p_{1,9}$ to $p_{n,9}$) represents the relative crack location 2 (rcl2)

Element No. 10 ($p_{1,10}$ to $p_{n,10}$) represents the relative crack depth 2 (rcd2)

The crack prediction technique using GA uses the natural frequencies, mode shapes, relative crack locations and relative crack depths to identify the crack locations and their severities. For better understanding of the method 10 population members have been shown in tabular form in Table 7.1.

Table 7.1 Examples of initial data pool for the genetic algorithm model

Sl. no.	Some of the examples of initial data pool for the genetic algorithm model									
	Relative first natural frequency “fnf”	Relative second natural frequency “snf”	Relative third natural frequency “tnf”	Average Relative first mode shape difference “fmd”	Average Relative second mode shape difference “smd”	Average Relative third mode shape difference “tmd”	Relative first crack depth “rcd1”	Relative first crack location “rcl1”	Relative second crack depth “rcd2”	Relative second crack location “rcl2”
1	0.9997	0.9959	0.9971	0.0022	0.0021	0.0072	0.169	0.127	0.168	0.877
2	0.9993	0.9968	0.9989	0.0053	0.0034	0.0157	0.52	0.378	0.335	0.627
3	0.9992	0.9977	0.9975	0.0026	0.0059	0.0132	0.419	0.128	0.337	0.877
4	0.9858	0.9982	0.9869	0.0201	0.0189	0.0131	0.335	0.127	0.417	0.52
5	0.9988	0.9857	0.9887	0.0075	0.0077	0.0292	0.338	0.379	0.53	0.628
6	0.9991	0.9987	0.9977	0.0087	0.0025	0.0029	0.336	0.28	0.27	0.77
7	0.9975	0.9993	0.9981	0.001	0.0046	0.0862	0.28	0.127	0.169	0.378
8	0.9974	0.9997	0.9995	0.0011	0.0052	0.0124	0.169	0.27	0.420	0.52
9	0.9972	0.9959	0.9886	0.0032	0.0289	0.0114	0.29	0.29	0.418	0.79
10	0.9936	0.9975	0.9989	0.0154	0.021	0.0146	0.27	0.27	0.28	0.53

Stage 2: objective function for crack localization:

The optimize solution from a GA based methodology can be drawn by proper formulation of an objective function. The appropriate formulation of the objective function can lead to optimal solution. In the current analysis the minimization of the objective function gives the best result in the search space. So, the cracks can be properly quantified by the proposed GA knowledge based model with the help of objective function.

The objective function used in the developed GA model is depicted below:

Objective function (rcl1, rcd1, rcl2, rcd2) =

$$\begin{aligned} & ((fnf_{fld} - fnf_{x1,i})^2 + (snf_{fld} - snf_{x1,i})^2 + (tnf_{fld} - tnf_{x1,i})^2 \\ & + (fmd_{fld} - fmd_{x1,i})^2 + (smd_{fld} - smd_{x1,i})^2 + (tmd_{fld} - tmd_{x1,i})^2)^{0.5} \end{aligned} \quad (7.1)$$

fnf_{fld} = Relative first natural frequency of the field

fnf_x = Relative first natural frequency

snf_{fld} = Relative second natural frequency of the field

snf_x = Relative second natural frequency

tnf_{fld} = Relative third natural frequency of the field

tnf_x = Relative third natural frequency

fmd_{fld} = Average relative first mode shape difference of the field

fmd_x = Average relative first mode shape difference

smd_{fld} = Average relative second mode shape difference of the field

smd_x = Relative average second mode shape difference

tmd_{fld} = Average relative third mode shape difference of the field

tmd_x = Average relative third mode shape difference

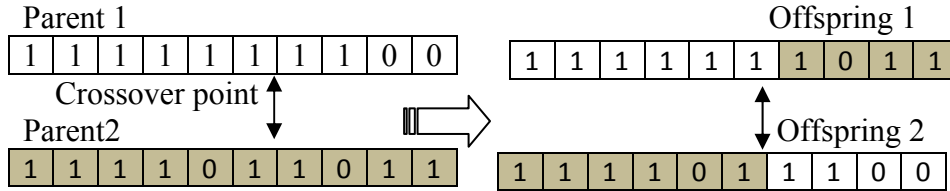
i = number of iterations

Stage 3: Crossover for offspring and their analysis

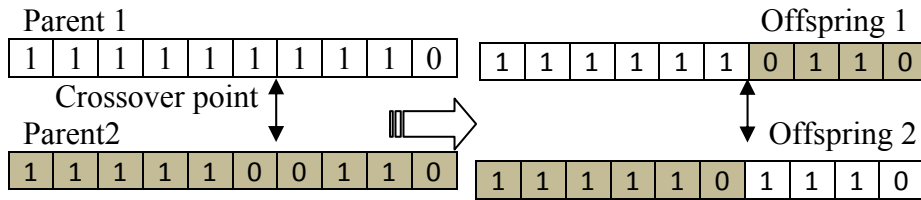
In the present work the reproduction process has been introduced by using the cross over operation to produce the offspring by choosing the proper parent chromosomes from the search space. The chosen parent chromosomes are combined by single cross point with the encoded values of the gene information to produce two numbers of offspring chromosomes. Finally, the offspring chromosomes are analyzed to find the optimal solution. In the current developed GA based methodology the crossover of gene information leads to calculation of relative first natural frequency (fnf), relative second natural frequency (snf), relative third

natural frequency (tnf), average relative first mode shape (fmd), average relative second mode shape (smd), average relative third mode shape (tmd), relative crack location 1, relative crack location 2, relative crack depth 1, relative crack depth 2. The details of the crossover operation are exhibited in Figure 7.1.

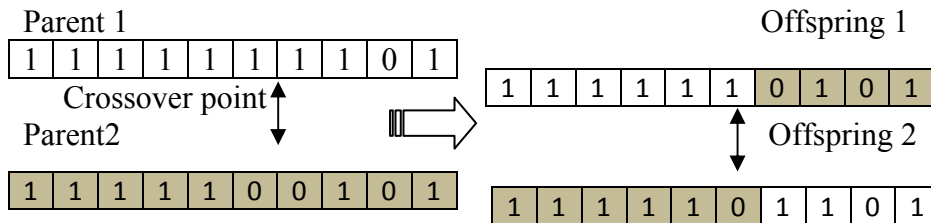
Cross over for fnf



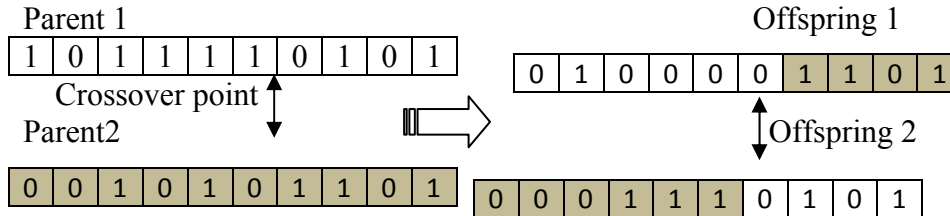
Cross over for snf



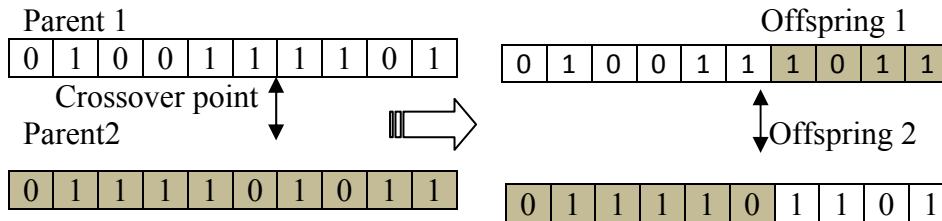
Cross over for tnf



Cross over for fmd



Cross over for smd



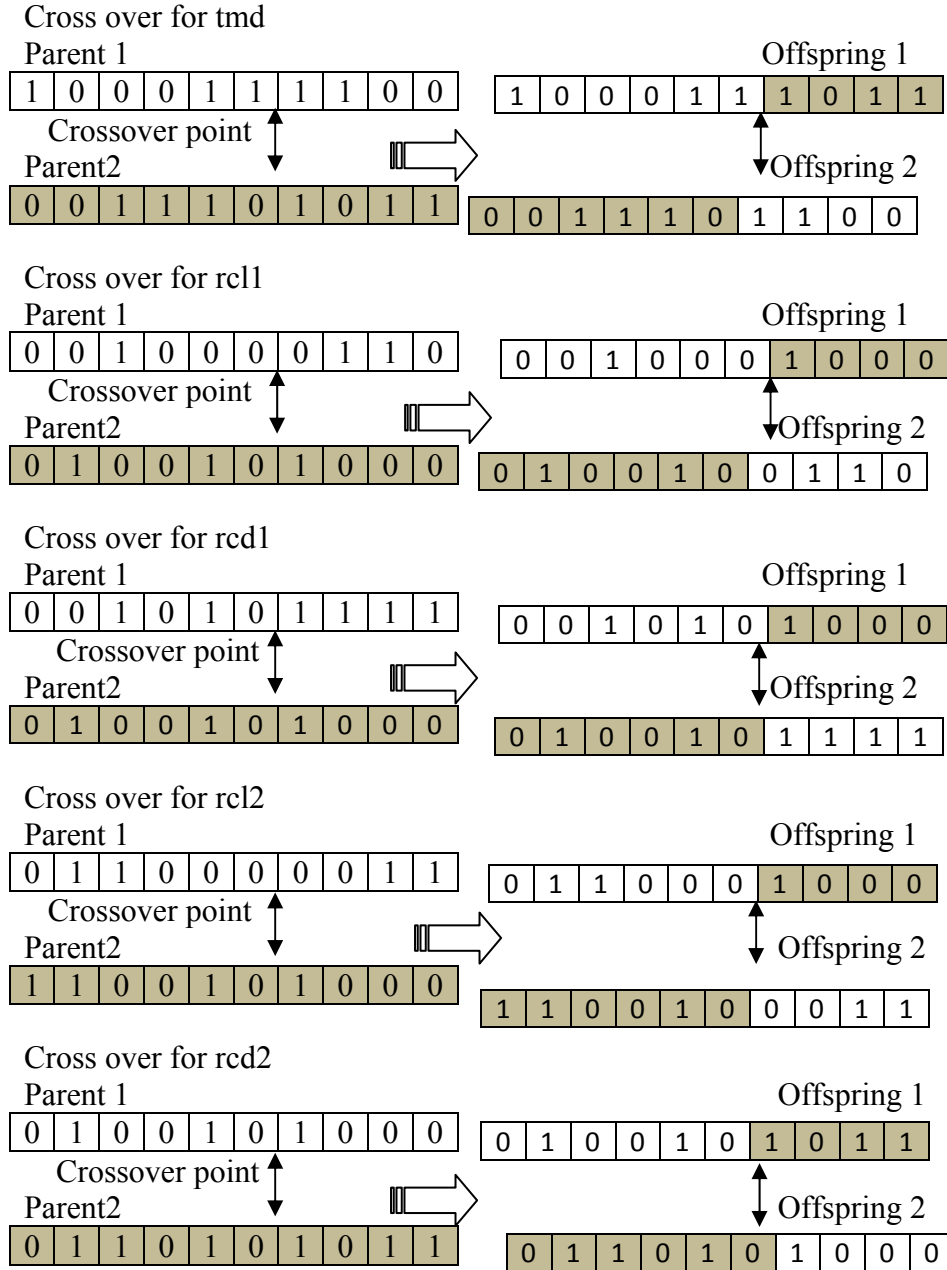


Fig.7.1 Single cross point, value encoding crossover for fnf, snf, tnf, fmd, smd, tmd, rcl1,rcd1,rcl2,rcd2

Stage 4: Mutation of the genes

The mutation process is followed to get new sequence of genes by altering the binary code of the existing genes. Hence this procedure introduces new genetic patterns in the search space. Then, the fitness of the chromosome with the muted genes is evaluated for finding the optimal solution. Natural selection will determine the fate of the mutated chromosome. If the fitness of the mutated chromosome is higher than the general population, it will survive and

likely be allowed to mate with other chromosomes. If the genetic mutation produces an undesirable feature, then natural selection will ensure that the chromosome does not live to mate.

In the current analysis, a new set for fnf,snf, tn timer, fmd, smd, tmd, rcl1, rcd1, rcl2, rcd2 are produced from the mutation process by changing the sequence of binary code of the genes. For better understanding of the mutation process few examples are illustrated below in Fig. 17;

Mutation for fnf										Mutation of fmd									
Parent 1										parent1									
1	1	1	1	0	1	1	0	1	1	0	0	1	0	1	0	1	1	0	1
Mutated gene										Mutated gene									
1	1	0	1	1	0	1	0	1	1	0	1	1	0	1	1	1	0	1	1
Mutation for snf										Mutation of smd									
Parent 1										Parent 1									
1	1	1	1	1	0	0	1	1	0	0	1	1	1	1	0	1	0	1	1
Mutated gene										Mutated gene									
1	0	1	1	1	0	1	0	1	1	0	0	1	0	1	1	0	0	1	1
Mutation for tn timer										Mutation of tmd									
Parent 1										Parent 1									
1	1	1	1	1	0	0	1	0	1	0	0	1	1	1	0	1	0	1	1
Mutated gene										Mutated gene									
1	0	0	1	1	1	1	0	1	1	0	0	0	1	1	1	0	1	1	0

Fig.7.2 Mutation of genes for fnf, snf, tn timer, fmd, smd, tmd

Stage 5: Evaluation of fittest child

The crossover and mutation process produce new chromosomes with newly formulated genes. These new chromosomes are evaluated to find the optimal solution. Out of the off springs from the crossover and the newly produced chromosome from the mutation process are compared with the results from data pool to find the fittest child. The evaluation of fittest child is computed using the equation (7.1).

The applied genetic algorithm based model have six inputs (fnf, snf, tnf, fmd, smd, tmd) and have four outputs (relative crack location 1, relative crack location 2, relative crack depth 1, relative crack depth 2).

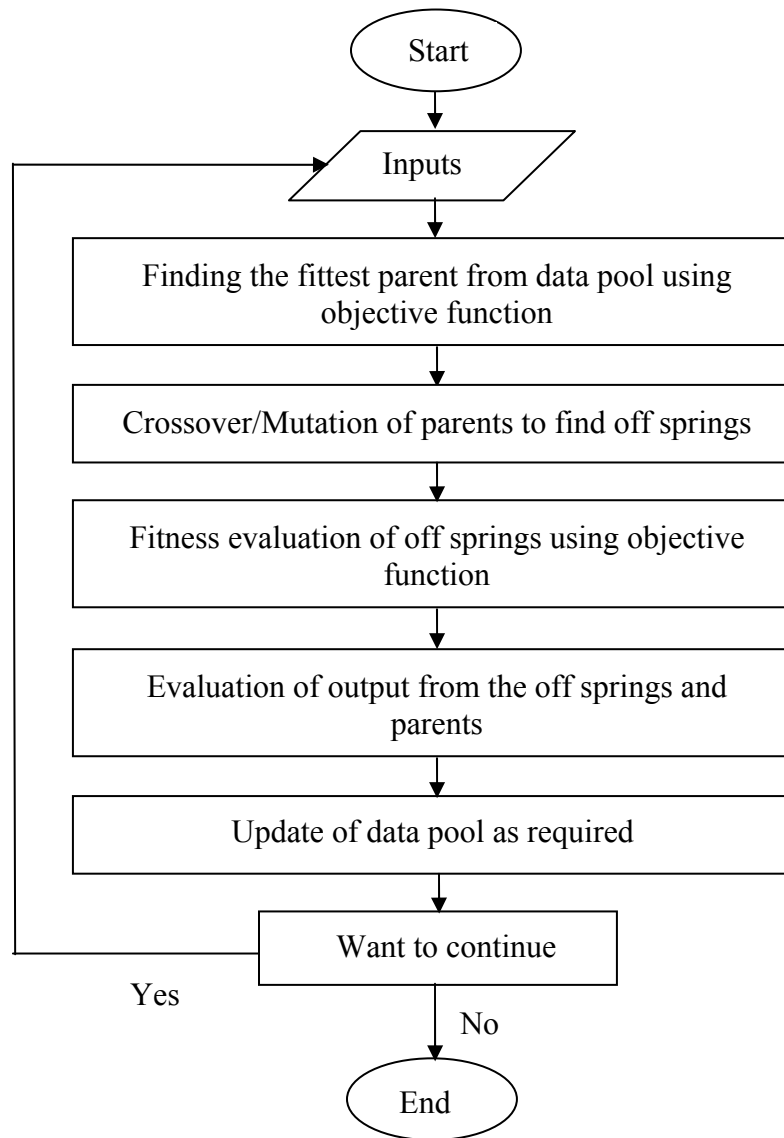


Fig.7.3 Flow chart for the proposed Genetic Algorithm

Table 7.2 (a) Comparison of results between GA model, neural model, fuzzy Gaussian model and experimental analysis.

Relative first natural frequency "f ₁ "	Relative second natural frequency "f ₂ "	Relative third natural frequency "f ₃ "	Average Relative first mode shape difference "fmd"	Average Relative second mode shape difference "smd"	Average Relative third mode shape difference "tmd"	GA Model relative				Neural model relative				Fuzzy Gaussian model relative				Experimental analysis relative			
						rcd1	rcd2	rcd1	rcd2	rcd1	rcd2	rcd1	rcd2	rcd1	rcd2	rcd1	rcd2	rcd1	rcd2	rcd1	rcd2
0.9979	0.9985	0.9993	0.0087	0.0036	0.0042	0.47	0.122	0.21	0.44	0.47	0.123	0.22	0.46	0.46	0.121	0.21	0.45	0.52	0.127	0.27	0.51
0.9962	0.9989	0.9991	0.0036	0.9729	0.2263	0.415	0.124	0.331	0.874	0.414	0.123	0.330	0.873	0.412	0.122	0.328	0.871	0.418	0.127	0.335	0.877
0.9936	0.9976	0.9987	0.0138	0.014	0.0832	0.163	0.371	0.22	0.621	0.164	0.373	0.23	0.622	0.163	0.372	0.22	0.621	0.168	0.377	0.27	0.627
0.9976	0.9991	0.9988	0.0014	0.0041	0.0812	0.333	0.124	0.415	0.50	0.332	0.123	0.414	0.49	0.330	0.121	0.412	0.48	0.335	0.127	0.418	0.53
0.9978	0.9983	0.9987	0.0036	0.0329	0.0141	0.163	0.23	0.21	0.48	0.164	0.24	0.23	0.49	0.162	0.22	0.21	0.47	0.169	0.28	0.27	0.53
0.9987	0.9972	0.9981	0.2936	0.3428	0.2623	0.25	0.25	0.415	0.74	0.24	0.24	0.414	0.73	0.23	0.22	0.412	0.73	0.27	0.28	0.418	0.77
0.9849	0.9982	0.9869	0.0134	0.0211	0.0119	0.413	0.373	0.23	0.621	0.414	0.372	0.22	0.622	0.415	0.373	0.23	0.623	0.418	0.376	0.27	0.627
0.9989	0.9973	0.9974	0.0017	0.0025	0.0079	0.47	0.20	0.19	0.70	0.46	0.21	0.20	0.71	0.47	0.22	0.22	0.73	0.52	0.27	0.26	0.77
0.9977	0.9847	0.9881	0.0079	0.0077	0.0292	0.328	0.376	0.47	0.619	0.329	0.371	0.46	0.621	0.330	0.372	0.45	0.622	0.335	0.377	0.52	0.627
0.9988	0.9974	0.9991	0.0057	0.0023	0.0155	0.412	0.21	0.162	0.47	0.413	0.22	0.163	0.46	0.414	0.23	0.162	0.47	0.419	0.28	0.169	0.52

Table 7.2 (b) Comparison of results between GA model, FEA and numerical analysis.

Relative first natural frequency "f ₁ "	Relative second natural frequency "s ₁ "	Relative third natural frequency "t ₁ "	Average Relative first mode shape difference "f _{md} "	Average Relative second mode shape difference "s _{md} "	Average Relative third mode shape difference "t _{md} "	GA Model relative				FEA relative				Numerical relative			
						rcd1	rcd2	rcd1	rcd2	rcd1	rcd2	rcd1	rcd2	rcd1	rcd2	rcd1	rcd2
0.9979	0.9985	0.9993	0.0087	0.0036	0.0042	0.47	0.122	0.21	0.44	0.43	0.118	0.18	0.42	0.42	0.117	0.16	0.40
0.9962	0.9989	0.9991	0.0036	0.9729	0.2263	0.415	0.124	0.331	0.874	0.418	0.118	0.326	0.868	0.416	0.116	0.324	0.866
0.9936	0.9976	0.9987	0.0138	0.014	0.0832	0.163	0.371	0.22	0.621	0.159	0.369	0.18	0.627	0.156	0.366	0.17	0.625
0.9976	0.9991	0.9988	0.0014	0.0041	0.0812	0.333	0.124	0.415	0.50	0.327	0.119	0.410	0.45	0.325	0.117	0.408	0.44
0.9978	0.9983	0.9878	0.0036	0.0329	0.0141	0.163	0.23	0.21	0.48	0.160	0.19	0.18	0.45	0.158	0.17	0.16	0.43
0.9987	0.9972	0.9981	0.2936	0.3428	0.2623	0.25	0.25	0.415	0.74	0.18	0.19	0.410	0.68	0.16	0.17	0.408	0.66
0.9849	0.9982	0.9869	0.0134	0.0211	0.0119	0.413	0.373	0.23	0.621	0.409	0.368	0.19	0.618	0.407	0.366	0.17	0.616
0.9989	0.9973	0.9974	0.0017	0.0025	0.0079	0.47	0.20	0.19	0.70	0.43	0.19	0.18	0.68	0.41	0.17	0.16	0.66
0.9977	0.9847	0.9881	0.0079	0.0077	0.0292	0.328	0.376	0.47	0.619	0.326	0.369	0.44	0.619	0.324	0.367	0.42	0.617
0.9988	0.9974	0.9991	0.0057	0.0023	0.0155	0.412	0.21	0.162	0.47	0.411	0.21	0.160	0.44	0.409	0.19	0.158	0.42

7.3 Results and discussion

The analyses of the results obtained from genetic algorithm model have been expressed in the current section. It is observed that the presence of cracks have noticeable effects on the vibration characteristics of a structural member and the vibration parameters can be used to predict the crack locations and their severities in cracked structures. Numerical, finite element and experimental analyses have been performed on the cantilever beam with different boundary conditions to extract the vibration signatures, which are later used for designing the GA system. A flow chart representing the various steps followed to design the GA model has been shown in Fig. 7.3. Experimental analysis has been carried out to validate the simulated results from the proposed crack diagnostic methodology. The use of single point crossover operator has been shown in Fig. 7.1 to find the optimal solution. In some cases the mutation operation (Fig. 7.2) has been presented to find the best fit child with in the search space for solution. Table 7.1 represents some of the examples of initial data pool used for the designing of the GA based model. The results for relative crack depths and relative crack locations from GA model, neural network, fuzzy Gaussian model and experimental analysis are shown in Table 7.2 (a) and the results from GA model have been proved to be the best to other AI techniques mentioned in the Table 7.2 (a). A comparison of results from GA model, finite element, numerical is presented in Table 7.2 (b) and the outcomes are found to be in agreement. The percentage of deviation of the predicted results from the GA model has been found as 4.33%. The graph for estimation error vs number of generations for the GA model has been shown in Fig. A5 of the Appendix section.

7.4. Summary

The following conclusions can be made by analyzing the results obtained from the GA model for multiple crack diagnosis in cantilever beam structure. This section presents a technique for automatic detection of crack locations and their severities of structural members using GA based model. Analysis of vibration parameters i.e. (natural frequencies, mode shapes) of the cracked structure have been done through numerical, finite element and experimental analysis and the extracted vibration signatures are used to create the initial data pool of the GA system, for multiple crack identification. Single point cross over and mutation procedure have been followed to find out the best possible solution with in the search space. The first

three relative natural frequencies and first three average relative mode shape differences are used as inputs to the GA crack identification method. Relative crack depths and relative crack locations are the output parameters from the proposed GA based technique. A close agreement between the results from simulation, experimental and GA model shows the effectiveness of the developed methodology for multiple crack diagnosis. The developed GA model can be used for automated condition monitoring of structural systems.

Publication:

- D.R.K.Parhi, Amiya Kumar Dash, H.C. Das Formulation of a GA based methodology for multiple crack detection in a beam structure, Australian journal of structural engineering, Vol. 12 (2), pp. 59-71, 2011.

Chapter 8

ANALYSIS OF HYBRID FUZZY-NEURO SYSTEM FOR MULTIPLE CRACK DETECTION

Integration of Neural networks (NN) and Fuzzy logic (FL) have brought researchers from various scientific and engineering domains for the need of developing adaptive intelligent systems to address real time applications. NN learns by adjusting the synaptic weights of neurons between layers. FL is a potential computing model based on the concept of fuzzy set, fuzzy rules, and fuzzy reasoning. It is known that fuzzy logic and NN have the ability to perceive the working environment and mimic the human behavior, thus the advantages of combining neural network and fuzzy logic are immense. There are different procedures to integrate NN and FL and mostly it depends on the types of application. The integration of NN and FL can be classified broadly into three categories namely concurrent model, cooperative model and fully fused model. In the current chapter fuzzy logic and neural network have been adopted to form a multiple crack identification tool for structural health monitoring.

8.1 Introduction

Fuzzy-Neuro hybrid computing technique is a potential tool for solving problems with complexity. If the parameters representing a system can be expressed in terms of linguistic rules, a fuzzy inference system can be build up. A neural network can be built, if data required for training from simulations are available. From the analysis of NN and FL it is observed that drawbacks of the two methods are complementary and therefore it is desirable to build an integrated system combining the two techniques. The learning capability is an advantage for NN, while the formation of linguistic rule base is an advantage for fuzzy logic. Hence, the hybrid fuzzy-neuro technique can be used for identifying cracks present in a structural system using vibration data.

In this chapter, a novel identification algorithm (hybrid intelligent system) using inverse analysis of the vibration response of a cracked cantilever beam has been proposed. The crack identification algorithm utilizes the vibration signatures of the cracked beam derived from finite element and theoretical analysis. The hybrid model is designed to predict the crack

locations and their severities by integrating the capabilities of fuzzy logic and neural network technique. The reliability of the proposed crack identification algorithm is established by comparing the results obtained from the experimental analysis.

The current chapter has been arranged into five sections. The introduction section (Section 8.1) presents a discussion about the hybrid intelligent technique such as fuzzy-neuro used for fault diagnosis. Section 8.2 depicts the analysis of the fuzzy and neural part of the hybrid intelligent system proposed for crack identification. The discussions made by analyzing the results obtained from fuzzy-neural model are depicted in section 8.4. The conclusions drawn from the current chapter is expressed in section 8.4.

8.2 Analysis of the fuzzy-neuro model

The current chapter introduces a hybrid intelligent method for prediction of crack locations and their intensities in a beam structure having multiple transverse cracks using inverse analysis. As the presence of cracks alters the dynamic behavior of the beam, the first three relative natural frequencies and first three average relative mode shape differences of the cracked and undamaged beam for different crack locations and depths are calculated using numerical, finite element and experimental analysis. The calculated modal frequencies, mode shapes, relative crack locations and relative crack depths are used to design the fuzzy neural model. The measured vibration signatures are used as inputs to the fuzzy segment of the hybrid model and initial relative crack depths and initial crack locations are the output parameters. The first three relative natural frequencies, first three average relative mode shape difference and the output from the fuzzy model are used as inputs to the neural part of the hybrid model and final crack depths and locations are the output parameters. The measured vibration signatures are used to formulate series of fuzzy rules and training patterns for the fuzzy and neural model. Finally, the validation of the proposed method is carried out dynamically by means of experimental results from the developed experimental setup. The fuzzy segment of the hybrid model for multiple crack prediction has been developed using triangular, Gaussian and trapezoidal membership functions. The triangular membership function based hybrid model, Gaussian membership function based hybrid model and trapezoidal membership function based hybrid model are shown in Fig.8.1, Fig.8.2, Fig.8.3 respectively.

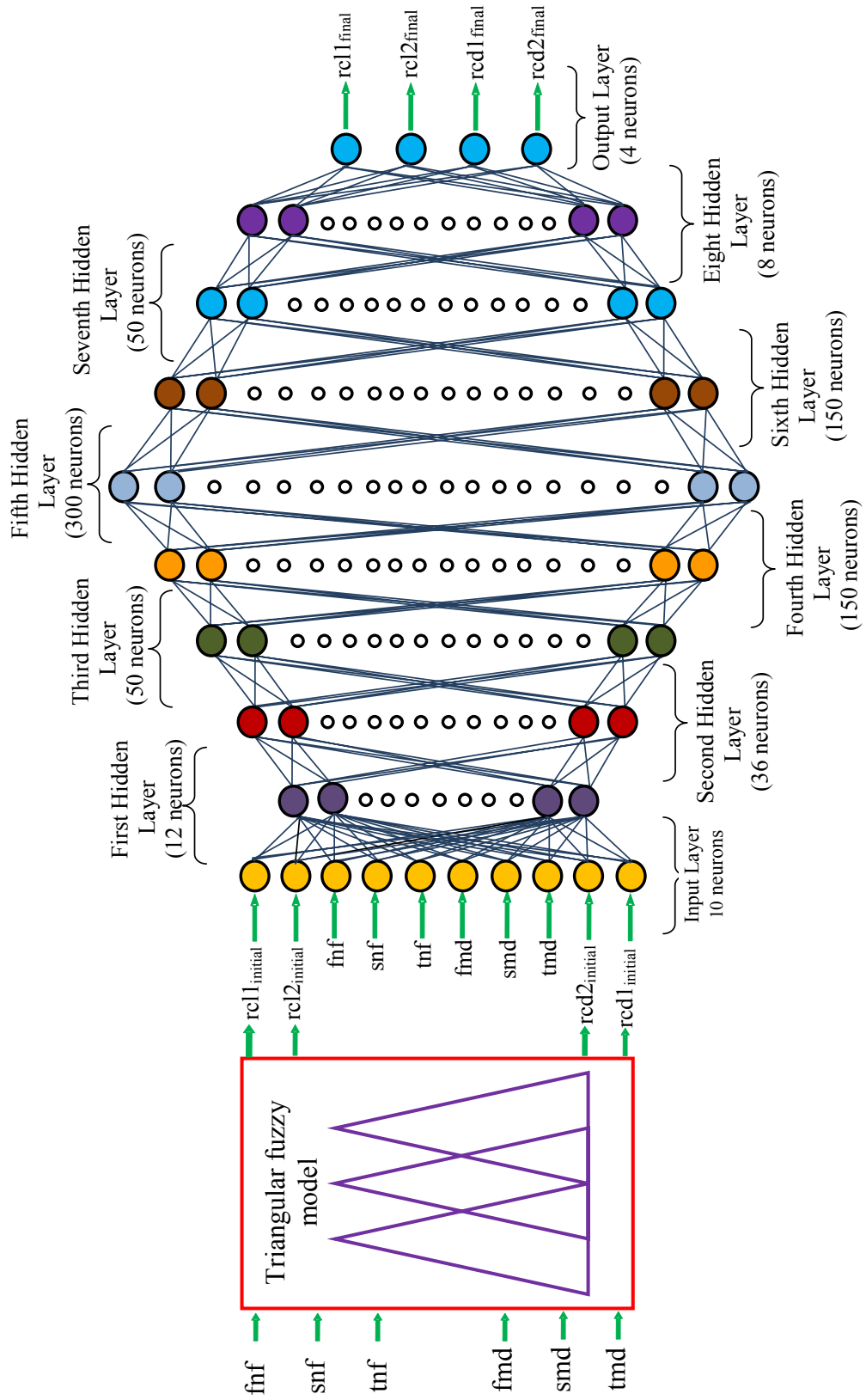


Fig. 8.1 Triangular fuzzy-neural system for damage detection

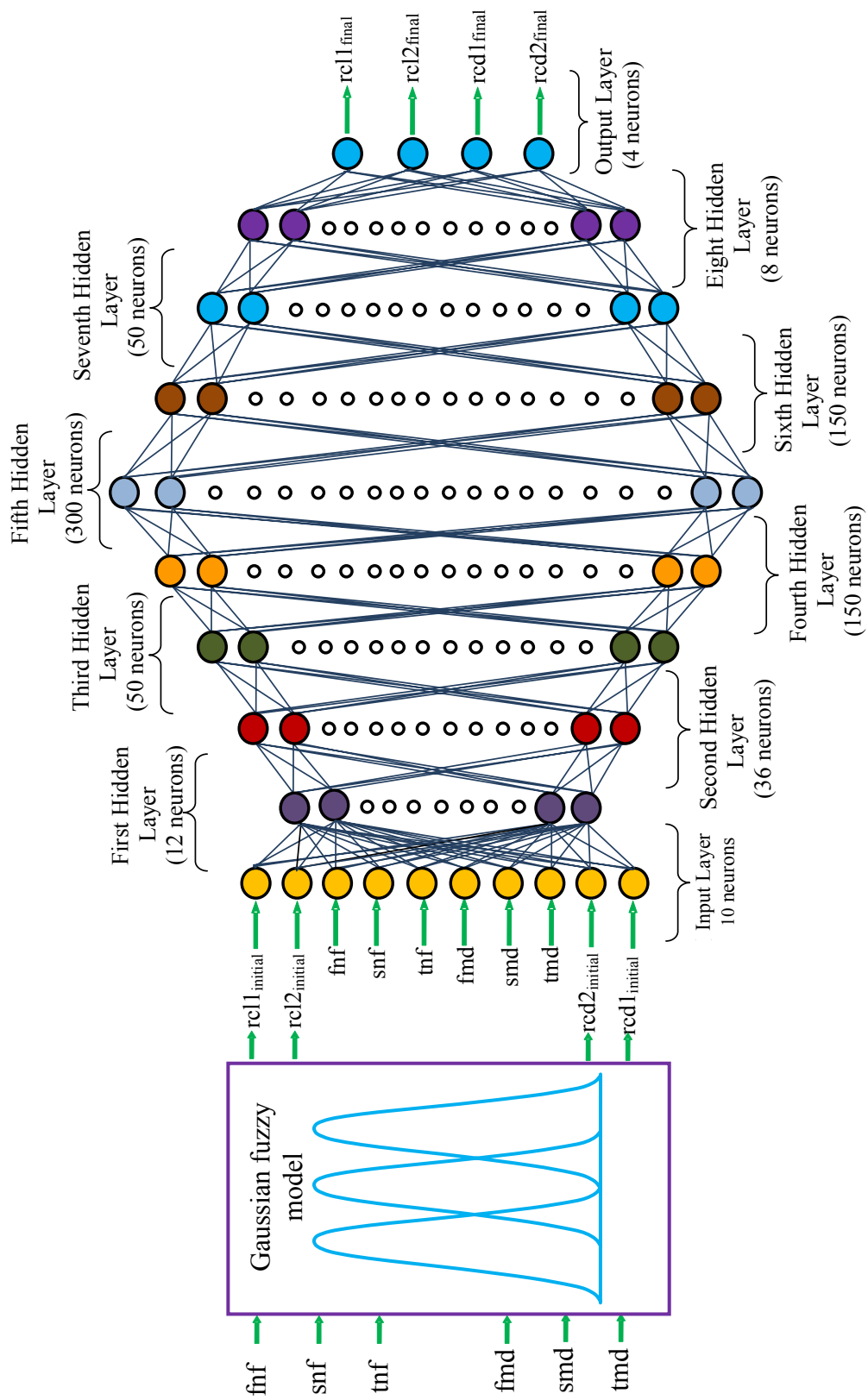


Fig. 8.2 Gaussian fuzzy-neural system for damage detection

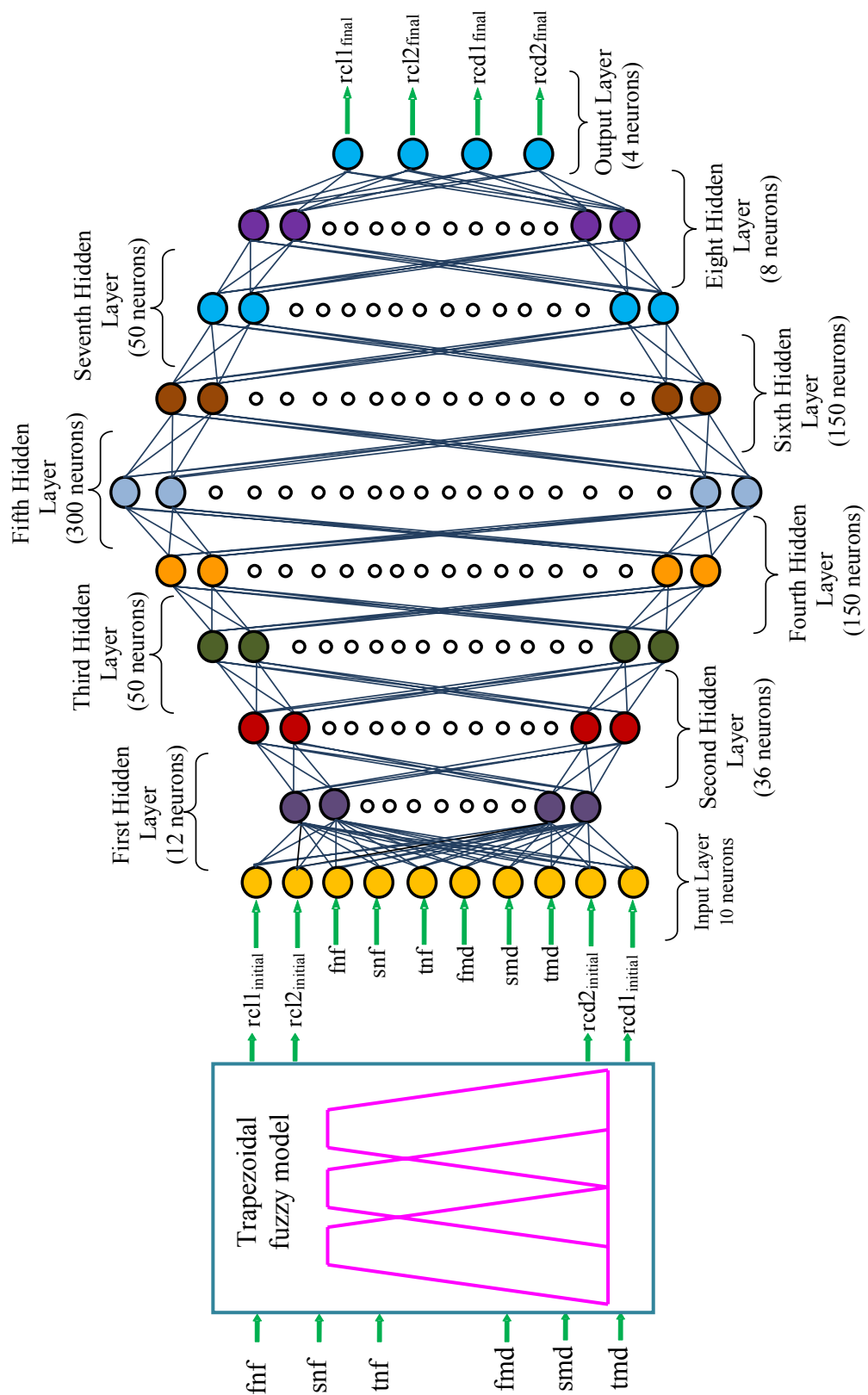


Fig. 8.3 Trapezoidal fuzzy-neural system for damage detection

8.2.1 Analysis of the fuzzy segment of the fuzzy-neuro model

The first layer of the fuzzy-neuro hybrid model i.e. the fuzzy segment has six inputs and four interim output parameters. The linguistic terms representing the inputs are fnf, snf, tnf, fmd, smd and tmd. The interim outputs from the fuzzy part of the hybrid crack diagnostic system are as follows;

Initial first relative crack location = “rcl1_{initial}”, Initial first relative crack depth = “rcd1_{initial}”

Initial second relative crack location = “rcl2_{initial}”, Initial second relative crack depth = “rcd2_{initial}”

The different types of membership functions such as triangular, Gaussian and trapezoidal have been used for designing the fuzzy part of the fuzzy-neural model. The fuzzy rules and fuzzy linguistics terms used for designing the fuzzy layer of the fuzzy-neuro model follows the rule and linguistics terms pattern mentioned in Table 5.1 and Table 5.2 of chapter 5. The fuzzy methodology to develop the fuzzy-neuro crack identification tool has been inherited from section 5.2 and 5.3 of chapter 5.

8.2.2 Analysis of the neural segment of fuzzy-neuro model

The model of the neural segment has been discussed in this section. The neural model of the proposed fuzzy-neural hybrid system for crack diagnosis is a ten layer feed forward network trained with back propagation technique for multiple crack diagnosis in structural members. The results obtained from the fuzzy analysis will be used as inputs to the neural segment of the hybrid fuzzy-neuro model. The diamond shape neural network comprises of ten inputs and four output parameters. The various inputs to the neural network are fnf, snf, tnf, fmd, smd, tmd and initial first relative crack location (rcl1_{initial}), initial first relative crack depth (rcd1_{initial}), initial second relative crack location (rcl2_{initial}), initial first relative crack depth (rcd2_{initial}). The final outputs from the neural network are depicted below;

final first relative crack location = “rcl1_{final}”, final first relative crack depth = “rcd1_{final}”,

final second relative crack location = “rcl2_{final}”, final second relative crack depth = “rcd2_{final}”

The number of neurons present in each layer (i.e. 2nd layer to 8th layer) of the neural model is twelve, thirty-six, fifty, one hundred fifty, three hundred, one hundred fifty, fifty and eight respectively. The numbers of neurons have been selected to make the neural model a diamond shape for better convergence of results. The complete working principle of the neural model has been described in sections 6.2 and 6.3 of chapter 6.

8.3 Results and discussions of fuzzy-neuro model

This section depicts the analysis of the results obtained from the fuzzy-neuro model used for multiple crack identification in structural systems.

A comparison of results from the triangular membership based fuzzy-neural model (Fig 8.1), Gaussian membership based fuzzy-neural model (Fig. 8.2), trapezoidal membership based fuzzy-neural model (Fig. 8.3) with that of the experimental analysis are presented in Table 8.1 (a). By studying the results mentioned in Table 8.1 (a), the deviation of Gaussian fuzzy-neural model from the actual results is found to be least as compared to triangular fuzzy-neural model, trapezoidal fuzzy-neural model. Again the results from the Gaussian fuzzy-neural model are compared with the outcome from GA, neural network and fuzzy Gaussian model in Table 8.1(b) and the results are in close agreement. Six numbers of inputs i.e. first three relative natural frequencies and first three relative mode shape differences have been considered to measure the relative crack locations and relative crack depths by the proposed fuzzy-neuro models. The corresponding outputs have been presented to evaluate the accuracy of the results from the various methodologies mentioned. The parameter presented in column number one to six in the Table 8.1(a) and Table 8.1(b) are first three relative natural frequencies and first three relative mode shape differences. The rest of the column represents the relative first crack location, relative second crack location, relative first crack depth and relative second crack depth obtained from the different methodologies being performed on the multiple cracked cantilever beam model. From the analysis of the results, it is found that the percentage of deviation of the prediction values of relative crack locations and relative crack depths for the triangular fuzzy-neuro model, Gaussian fuzzy-neuro model and trapezoidal membership fuzzy-neuro model are 6.48%, 4% and 5% respectively.

Table 8.1 (a) Comparison of results between trapezoidal fuzzy neural model, triangular fuzzy neural model, Gaussian fuzzy neural model and experimental analysis.

Relative first natural frequency "fnf"	Relative second natural frequency "snf"	Relative third natural frequency "tnf"	Average Relative first mode shape difference "fmd"	Average Relative second mode shape difference "smd"	Average Relative third mode shape difference "tmd"	Triangular fuzzy Neural Model relative				Trapezoidal fuzzy Neural Model relative				Gaussian fuzzy Neural Model relative				Experimental analysis relative			
						1 st crack depth "rcd1"	1 st crack location "rcel1"	2 nd crack depth "rcd2"	2 nd crack location "rcel2"	1 st crack depth "rcd1"	1 st crack location "rcel1"	2 nd crack depth "rcd2"	2 nd crack location "rcel2"	1 st crack depth "rcd1"	1 st crack location "rcel1"	2 nd crack depth "rcd2"	2 nd crack location "rcel2"	1 st crack depth "rcd1"	1 st crack location "rcel1"	2 nd crack depth "rcd2"	2 nd crack location "rcel2"
0.9979	0.9985	0.9993	0.0087	0.0036	0.0042	0.45	0.120	0.20	0.44	0.47	0.122	0.22	0.46	0.48	0.124	0.23	0.47	0.52	0.127	0.27	0.51
0.9962	0.9989	0.9991	0.0036	0.9729	0.2263	0.412	0.121	0.329	0.871	0.413	0.122	0.330	0.872	0.414	0.123	0.331	0.873	0.418	0.127	0.335	0.877
0.9936	0.9976	0.9987	0.0138	0.014	0.0832	0.162	0.371	0.21	0.621	0.163	0.372	0.22	0.622	0.165	0.373	0.23	0.623	0.168	0.377	0.27	0.627
0.9976	0.9991	0.9988	0.0014	0.0041	0.0812	0.329	0.120	0.412	0.47	0.331	0.122	0.413	0.48	0.332	0.124	0.415	0.49	0.335	0.127	0.418	0.53
0.9978	0.9983	0.9878	0.0036	0.0329	0.0141	0.163	0.21	0.21	0.46	0.164	0.23	0.22	0.48	0.165	0.24	0.23	0.49	0.169	0.28	0.27	0.53
0.9987	0.9972	0.9981	0.2936	0.3428	0.2623	0.21	0.22	0.412	0.70	0.22	0.23	0.413	0.72	0.23	0.24	0.415	0.73	0.27	0.28	0.418	0.77
0.9849	0.9982	0.9869	0.0134	0.0211	0.0119	0.412	0.370	0.21	0.621	0.413	0.371	0.22	0.622	0.414	0.372	0.23	0.623	0.418	0.376	0.27	0.627
0.9989	0.9973	0.9974	0.0017	0.0025	0.0079	0.46	0.21	0.20	0.71	0.47	0.22	0.22	0.72	0.48	0.24	0.23	0.73	0.52	0.27	0.26	0.77
0.9977	0.9847	0.9881	0.0079	0.0077	0.0292	0.329	0.371	0.46	0.621	0.330	0.372	0.47	0.622	0.331	0.373	0.48	0.623	0.335	0.377	0.52	0.627
0.9988	0.9974	0.9991	0.0057	0.0023	0.0155	0.413	0.22	0.163	0.46	0.414	0.23	0.164	0.47	0.415	0.24	0.165	0.48	0.419	0.28	0.169	0.52

Table 8.1 (b) Comparison of results between Gaussian fuzzy neural model, GA model, neural model and fuzzy Gaussian model

Relative first natural frequency "fnf"	Relative second natural frequency "snf"	Relative third natural frequency "tnf"	Average Relative first mode shape difference "fnd"	Average Relative second mode shape difference "smd"	Average Relative third mode shape difference "tmd"	Gaussian fuzzy Neural Model relative				GA Model relative				Neural Model relative				Fuzzy Gaussian model relative			
						1 st crack depth "rcd1"	1 st crack location "rc11"	2 nd crack depth "rcd2"	2 nd crack location "rc12"	1 st crack depth "rcd1"	1 st crack location "rc11"	2 nd crack depth "rcd2"	2 nd crack location "rc12"	1 st crack depth "rcd1"	1 st crack location "rc11"	2 nd crack depth "rcd2"	2 nd crack location "rc12"	1 st crack depth "rcd1"	1 st crack location "rc11"	2 nd crack depth "rcd2"	2 nd crack location "rc12"
0.9979	0.9985	0.9993	0.0087	0.0036	0.0042	0.48	0.124	0.23	0.47	0.47	0.122	0.21	0.45	0.47	0.123	0.22	0.46	0.46	0.121	0.21	0.45
0.9962	0.9989	0.9991	0.0036	0.9729	0.2263	0.414	0.123	0.331	0.873	0.415	0.124	0.331	0.874	0.414	0.123	0.330	0.873	0.412	0.122	0.328	0.871
0.9936	0.9976	0.9987	0.0138	0.014	0.0832	0.165	0.373	0.23	0.623	0.163	0.371	0.22	0.621	0.164	0.373	0.23	0.622	0.163	0.372	0.22	0.621
0.9976	0.9991	0.9988	0.0014	0.0041	0.0812	0.332	0.124	0.415	0.49	0.333	0.124	0.415	0.50	0.332	0.123	0.414	0.49	0.330	0.121	0.412	0.48
0.9978	0.9983	0.9878	0.0036	0.0329	0.0141	0.165	0.24	0.23	0.49	0.163	0.23	0.21	0.48	0.164	0.24	0.23	0.49	0.162	0.22	0.21	0.47
0.9987	0.9972	0.9981	0.2936	0.3428	0.2623	0.23	0.24	0.415	0.73	0.25	0.25	0.415	0.74	0.24	0.24	0.414	0.73	0.23	0.22	0.412	0.73
0.9849	0.9982	0.9869	0.0134	0.0211	0.0119	0.414	0.372	0.23	0.623	0.413	0.373	0.23	0.621	0.414	0.372	0.22	0.622	0.415	0.373	0.23	0.623
0.9989	0.9973	0.9974	0.0017	0.0025	0.0079	0.48	0.24	0.23	0.73	0.47	0.20	0.19	0.70	0.46	0.21	0.20	0.71	0.47	0.22	0.22	0.73
0.9977	0.9847	0.9881	0.0079	0.0077	0.0292	0.331	0.373	0.48	0.623	0.328	0.376	0.47	0.619	0.329	0.371	0.46	0.621	0.330	0.372	0.45	0.622
0.9988	0.9974	0.9991	0.0057	0.0023	0.0155	0.415	0.24	0.165	0.48	0.412	0.21	0.162	0.47	0.413	0.22	0.163	0.46	0.414	0.23	0.162	0.47

8.4 Summary

The following conclusions can be drawn by investigating the results from the fuzzy-neural analysis carried out for multiple crack identification.

From the analysis, it has been observed that both crack locations and crack depths have noticeable effects on the modal parameters of the cracked beam. The hybrid intelligent model is developed with the computed values of modal parameters of the cracked beam with various crack depths and crack locations as inputs and final relative crack depths and final relative crack locations as output parameters. The authenticity of the hybrid system has been verified from the predicted values of the crack locations and depths by comparing the results from neural network model, GA, fuzzy Gaussian and experimental analysis. The Gaussian fuzzy neuro model produces best results in terms of relative crack depths and relative crack locations in comparison to triangular fuzzy neuro, trapezoidal fuzzy neuro model. This modular Gaussian fuzzy-neural architecture can be used as a non-destructive procedure for health monitoring of structures. Evolution algorithm has also been used in next chapters to develop hybrid system for easy diagnosis of faults in dynamically vibrating structures. Since the Gaussian fuzzy neuro model performance is better than the other two fuzzy-neuro model, in the next chapters the results from Gaussian fuzzy neuro model will be compared with other AI techniques (MANFIS, GA-fuzzy, GA-neural, GA-neuro-fuzzy) to compare their performance.

Publication

- Amiya Kumar Dash, D.R.K.Parhi, A vibration based inverse hybrid intelligent method for structural health monitoring, International Journal of Mechanical and Materials Engineering. Vol.6 (2), pp. 212-230, 2011.

Chapter 9

ANALYSIS OF MANFIS FOR MULTIPLE CRACK DETECTION

The presence of a transverse crack in shaft, rotor and structures incurs a potential risk of destruction or collapse. This produces high costs of production and maintenance. Detection of multiple cracks in their early stages may save the system for use after repair. By monitoring the system, depending upon the type and severity of the cracks, it may be possible in some cases to extend the use of a flawed member without risking a catastrophic failure. This section of the thesis presents an inverse technique using multiple adaptive neuro-fuzzy-evolutionary system (MANFIS) methodology for identification of multiple transverse cracks present in structural members. The proposed MANFIS model utilizes six inputs the first three natural frequencies and first three mode shapes from the system and provides outputs relative crack locations and relative crack depths, there by identifying the position and severities of the cracks. The developed technique has been found to be suitable for diagnosis of cracks present in the beam structures.

The MANFIS system introduced in this chapter is comprises five layers. The first layer is an adaptive layer which has six inputs. The second and third layers are fixed layers. The fourth and fifth layers are adaptive layers. Relative first crack location, relative second crack location, relative first crack depth and relative second crack depth are the output parameters from the fifth layer of the MANFIS model. MANFIS is an extended version of ANFIS to produce multiple real responses of the required system. This technique can be utilized effectively for modeling functions with nonlinearities and complexity without the application of accurate quantitative analyses. The Takagi and Sugeno's model can be employed to extract the input and output pairs of data which are used to train the fuzzy logic system [205]. ANFIS has been developed by integrating the best features of Fuzzy Systems and Neural Networks. The fuzzy part represents the prior knowledge into a set of constraints (network topology) to reduce the optimization search space. The proposed MANFIS methodology has

been found to be in good agreement with the results from experimentation, thereby showing its authenticity.

9.1 Introduction

A lot of research has been carried out by scientists to develop techniques for structural health monitoring. It is observed that the artificial intelligence techniques such as fuzzy inference system, neural network and genetic algorithm have been applied to design the more robust expert systems for crack diagnosis in damaged structures. Recently multiple adaptive neuro-fuzzy-inference system has drawn attention of science community to design intelligent systems. The advantage of the MANFIS system is that, it integrates the positive features of both fuzzy logic and neural network and provides a more robust platform to develop systems for different engineering applications.

The current chapter exhibits a methodology based on multiple adaptive neuro-fuzzy-inference system which is an extension of ANFIS system to diagnose multiple cracks present in a cantilever beam model. The developed MANFIS model is comprising of five layers i.e. one input layer, three hidden layer and one output layer. Out of five layers, the input layer has been designed using fuzzy inference system and the rest four layers are designed using neural network. Various fuzzy linguistic terms and several hundred fuzzy rules have been developed from the derived values of first three relative natural frequencies, first three average relative mode shape difference, relative crack locations and relative crack depths to train the fuzzy layer of the MANFIS model. Similarly several hundred training patterns have been developed to design and train the neural based layers of the proposed system. The fuzzy segment uses the first three relative natural frequencies, first three average relative mode shape difference as the inputs and the hidden layer process the outputs from the fuzzy model. Finally relative crack locations and relative crack depths are outputs from the developed MANFIS model. It is observed that the predicted values of relative crack locations and relative crack depths from the formulated technique are well in agreement with the results from experimental analysis. The proposed methodology demonstrates its capability to be a suitable non destructive technique for fault identification in vibrating structures.

The current chapter of the thesis has been divided into four sections. The first section, which is the introduction section of this chapter explain the use of MANFIS in advanced

computing. The analysis of the MANFIS applied for fault diagnosis has been discussed in section 9.2. The results obtained from MANFIS system has been compared with the results obtained from the methods discussed in the previous chapters and discussion about the same has been expressed in section 9.3. The conclusions made by analyzing the results from the MANFIS model have been explained in section 9.4.

9.2 Analysis of multiple adaptive neuro-fuzzy inference system for crack detection

The MANFIS (multiple adaptive neuro fuzzy inference system) technique is known as a multiple ANFIS system. It integrates the capabilities of the neural network and fuzzy logic. The ANFIS model used for designing the MANFIS model is a first order Takagi Sugeno Fuzzy Model [205]. In the present investigation, six parameters are used as inputs to the MANFIS system and four parameters are the outputs from the system. The inputs are (x1) fnf, (x2) snf, (x3) tnf, (x4) fmd, (x5) smd and (x6) tmd. The output parameters are as follows;

First relative crack location = “rcl1”; First relative crack depth = “rcd1”

Second relative crack location = “rcl2”; Second relative crack depth = “rcd2”

In the current analysis, the MANFIS model has four output parameters; based on this logic the system has been fabricated.

The if then rules for the MANFIS architecture is defined as follows;

$$\left. \begin{array}{l} \text{IF } x_1 \text{ is } A_j, x_2 \text{ is } B_k, x_3 \text{ is } C_m, x_4 \text{ is } D_n, x_5 \text{ is } E_o, x_6 \text{ is } F_p \\ \text{THEN} \\ f_{e,i} = p_{e,i} x_1 + r_{e,i} x_2 + s_{e,i} x_3 + t_{e,i} x_4 + u_{e,i} x_5 + v_{e,i} x_6 + z_{e,i} \end{array} \right\} \quad (9.1)$$

Where;

$$\left. \begin{array}{l} f_{1,i} = rcl1_{,i} = p_{1,i} x_1 + r_{1,i} x_2 + s_{1,i} x_3 + t_{1,i} x_4 + u_{1,i} x_5 + v_{1,i} x_6 + z_{1,i} \quad ; \text{ for relative crack length1.} \\ f_{2,i} = rcd1_{,i} = p_{2,i} x_1 + r_{2,i} x_2 + s_{2,i} x_3 + t_{2,i} x_4 + u_{2,i} x_5 + v_{2,i} x_6 + z_{2,i} \quad ; \text{ for relative crack depth1.} \\ f_{3,i} = rcl2_{,i} = p_{1,i} x_1 + r_{1,i} x_2 + s_{1,i} x_3 + t_{1,i} x_4 + u_{1,i} x_5 + v_{1,i} x_6 + z_{1,i} \quad ; \text{ for relative crack length2.} \\ f_{4,i} = rcd2_{,i} = p_{2,i} x_1 + r_{2,i} x_2 + s_{2,i} x_3 + t_{2,i} x_4 + u_{2,i} x_5 + v_{2,i} x_6 + z_{2,i} \quad ; \text{ for relative crack depth2.} \end{array} \right\} \quad (9.2)$$

$e = 1 \text{ to } 4; j = 1 \text{ to } q_1; k = 1 \text{ to } q_2; m = 1 \text{ to } q_3; n = 1 \text{ to } q_4; o = 1 \text{ to } q_5 \text{ and } p = 1 \text{ to } q_6 \text{ and } i = 1 \text{ to } q_1, q_2, q_3, q_4, q_5, q_6$

A, B, C, D, E and F are the fuzzy membership sets defined for the input variables x_1 (fnf), x_2 (snf), x_3 (tnf), x_4 (fmd), x_5 (smd) and x_6 (tmd). q_1, q_2, q_3, q_4, q_5 and q_6 are the number of member ship functions for the fuzzy systems of the inputs x_1, x_2, x_3, x_4, x_5 and x_6 respectively.

“rcl1”, “rcl2”, “rcd1” and “rcd2” are the linear consequent functions defined in terms of the inputs (x_1, x_2, x_3, x_4, x_5 and x_6) . $p_{1,i}, r_{1,i}, s_{1,i}, t_{1,i}, u_{1,i}, v_{1,i}, z_{1,i}, p_{2,i}, r_{2,i}, s_{2,i}, t_{2,i}, u_{2,i}, v_{2,i}$ and $z_{2,i}$ are the consequent parameters of the ANFIS fuzzy model. In the ANFIS model nodes of the same layer have similar functions. The output signals from the nodes of the previous layer are the input signals for the current layer. The output obtained with the help of the node function will be the input signals for the subsequent layer.

Layer 1: Every node in this layer is an adaptive node (square node) with a particular fuzzy membership function (node function) specifying the degrees to which the inputs satisfy the quantifier. For six inputs the outputs from nodes are given as follows;

$$\begin{aligned}
 O_{1,g,e} &= \mu_{Ag}(x) \quad \text{for } g = 1, \dots, q1 && \text{(for input } x1) \\
 O_{1,g,e} &= \mu_{Bg}(x) \quad \text{for } g = q1+1, \dots, q1+q2 && \text{(for input } x2) \\
 O_{1,g,e} &= \mu_{Cg}(x) \quad \text{for } g = q1+q2+1, \dots, q1+q2+q3 && \text{(for input } x3) \\
 O_{1,g,e} &= \mu_{Dg}(x) \quad \text{for } g = q1+q2+q3+1, \dots, q1+q2+q3+q4 && \text{(for input } x4) \\
 O_{1,g,e} &= \mu_{Eg}(x) \quad \text{for } g = q1+q2+q3+q4+1, \dots, q1+q2+q3+q4+q5 && \text{(for input } x5) \\
 O_{1,g,e} &= \mu_{Fg}(x) \quad \text{for } g = q1+q2+q3+q4+q5+1, \dots, q1+q2+q3+q4+q5+q6 && \text{(for input } x6)
 \end{aligned} \tag{9.3}$$

Here the membership functions for A, B, C, D, E and F considered are the bell shaped function. The membership function for A,B,C,D,E and F considered in “layer 1” are the bell shaped function (Fig. 9.1) and are defined as follows;

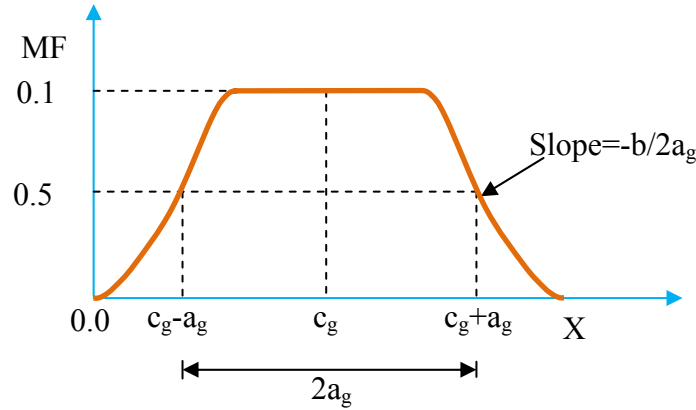


Fig. 9.1 Bell-shaped membership function

$$\mu_{Ag}(x) = \frac{1}{1 + \left\{ \left(\frac{x - c_g}{a_g} \right)^2 \right\}^{b_g}} ; \quad g = 1, \dots, q1 \tag{9.4 (i)}$$

$$\mu_{Bg}(x) = \frac{1}{1 + \left\{ \left(\frac{x - c_g}{a_g} \right)^2 \right\}^{b_g}} ; \quad g = q1+1, \dots, q1+q2 \quad (9.4 \text{ (ii)})$$

$$\mu_{Cg}(x) = \frac{1}{1 + \left\{ \left(\frac{x - c_g}{a_g} \right)^2 \right\}^{b_g}} ; \quad g = q1+q2+1, \dots, q1+q2+q3 \quad (9.4 \text{ (iii)})$$

$$\mu_{Dg}(x) = \frac{1}{1 + \left\{ \left(\frac{x - c_g}{a_g} \right)^2 \right\}^{b_g}} ; \quad g = q1+q2+q3+1, \dots, q1+q2+q3+q4 \quad (9.4 \text{ (iv)})$$

$$\mu_{Eg}(x) = \frac{1}{1 + \left\{ \left(\frac{x - c_g}{a_g} \right)^2 \right\}^{b_g}} ; \quad g = q1+q2+q3+q4+1, \dots, q1+q2+q3+q4+q5 \quad (9.4 \text{ (v)})$$

$$\mu_{Fg}(x) = \frac{1}{1 + \left\{ \left(\frac{x - c_g}{a_g} \right)^2 \right\}^{b_g}} ; \quad g = q1+q2+q3+q4+q5+1, \dots, q1+q2+q3+q4+q5+q6 \quad (9.4 \text{ (vi)})$$

Where a_g, b_g and c_g are the parameters for the fuzzy membership function. The bell-shaped function changes its pattern as per the change of the parameters. This change will give the various contour of bell shaped function as needed in accord with the data set for the problem considered.

Layer 2: Every node in this layer is a fixed node (circular) labeled as “II”. The output denoted by $O_{2,i,e}$. The output is the product of all incoming signal.

$$O_{2,i,e} = w_{i,e} = \mu_{Ag}(x) \mu_{Bg}(x) \mu_{Cg}(x) \mu_{Dg}(x) \mu_{Eg}(x) \mu_{Fg}(x) ; \quad (9.5)$$

for $i = 1, \dots, q1.q2.q3.q4.q5.q6$ and $g = 1, \dots, q1+q2+q3+q4+q5+q6$

The output of each node of the second layer represents the firing strength (degree of fulfillment) of the associated rule. The T-nom operator algebraic product $\{ T_{ap}(a,b) = ab\}$, has been used to obtain the firing strength ($w_{i,e}$).

Layer 3: Every node in this layer is a fixed node (circular) labeled as “N”. The output of the i th. node is calculated by taking the ratio of firing strength of i th. rule ($w_{i,e}$) to the sum of all rules’ firing strength.

$$O_{3,i,e} = \bar{w}_{i,e} = \frac{w_{i,e}}{\sum_{r=1}^{r=q1.q2.q3.q4.q5.q6} w_{r,e}} \quad (9.6)$$

This output gives a normalized firing strength.

Layer 4: Every node in this layer is an adaptive node (square node) with a node function.

$$O_{4,i,e} = \bar{w}_{i,e} f_{e,i} = \bar{w}_{i,e} (p_{e,i} x1 + r_{e,i} x2 + s_{e,i} x3 + t_{e,i} x4 + u_{e,i} x5 + v_{e,i} x6 + z_{e,i}) \quad (9.7)$$

Where $\bar{w}_{i,e}$ is a normalized firing strength form (output) from layer 3 and $\{p_{e,i}, r_{e,i}, s_{e,i}, t_{e,i}, u_{e,i}, v_{e,i}, z_{e,i}\}$ is the parameter set for relative crack location($e=1,2$) and relative crack depth ($e=1,2$). Parameters in this layer are referred to as consequent parameters.

Layer 5: The single node in this layer is a fixed node (circular) labeled as “Σ”, which computes the overall output as the summation of all incoming signals.

$$O_{5,1,e} = \sum_{i=1}^{i=q1.q2.q3.q4.q5.q6} \bar{w}_{i,e} f_{e,i} = \frac{\sum_{i=1}^{i=q1.q2.q3.q4.q5.q6} w_{i,e} f_{e,i}}{\sum_{i=1}^{i=q1.q2.q3.q4.q5.q6} w_{i,e}} \quad (9.8)$$

In the current developed ANFIS structure there are six dimensional space partition and has “ $q_1 \times q_2 \times q_3 \times q_4 \times q_5 \times q_6$ ” regions. Each region is governed by a fuzzy if then rule. The first layer (consists of premise or antecedent parameters) of the ANFIS is dedicated to fuzzy sub space. The parameters of the fourth layer are referred as consequent parameters and are used to optimize the network. During the forward pass of the hybrid learning algorithm node outputs go forward until layer four and the consequent parameters are identified by least square method. In the backward pass, error signals propagate backwards and the premise parameters are updated by a gradient descent method. The MANFIS architectures are presented in Fig. 9.2 (a) & Fig. 9.2 (b).

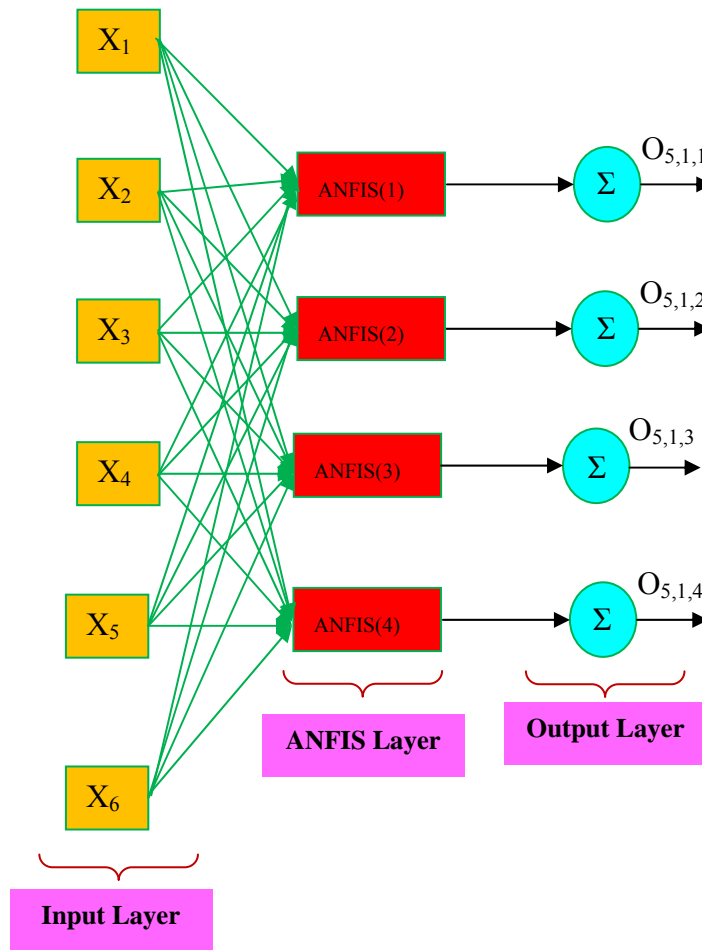


Fig. 9.2 (a) Multiple ANFIS (MANFIS) Model for crack detection

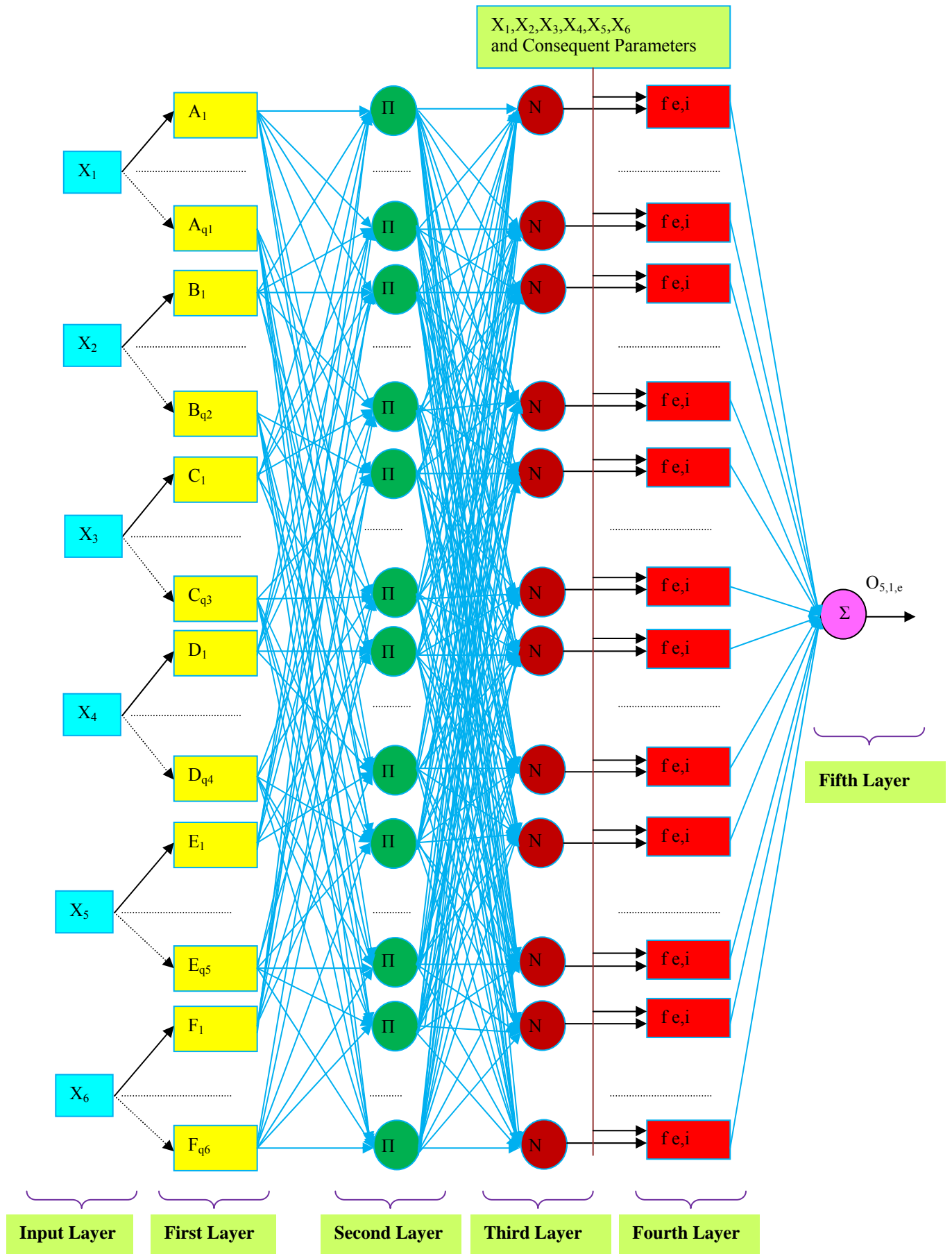


Fig. 9.2 (b) Adaptive-Neuro-Fuzzy-Inference System (ANFIS) for crack detection

9.3 Results and discussions of MANFIS model

The following discussions can be made from the analysis of the results of the multiple adaptive neuro-fuzzy inference system to predict the relative crack locations and relative crack depths.

The simulation results in current analysis indicate that the impact of crack locations and depths on the vibrational characteristics of the cantilever beam is quiet evident. This is an important outcome of the numerical, finite element and experimental analysis which is used as a baseline for formulation of a multiple crack diagnostic tool using MANFIS technique. The Bell shaped membership function used for designing the ANFIS model has been shown in Fig. 9.1. The architecture of the proposed MANFIS model for multiple crack diagnosis and the detailed architecture showing the different layers of the ANFIS system for crack detection have been presented in Fig. 9.2 (a) and Fig. 9.2 (b) respectively. The suitability of the MANFIS technique has been checked by comparing the results with that of the Gaussian fuzzy-neuro model of chapter-8, GA model of chapter-7, experimental analysis of chapter-12 and the comparison has been presented in Table 9.1 (a). The results obtained from MANFIS, numerical analysis and finite element analysis have been compared and presented in Table 9.1 (b). Ten sets of inputs (relative first three natural frequencies and relative first three mode shape differences) out of the several hundred inputs have been considered for the above mentioned techniques and the corresponding outputs in terms of relative first crack location (rcl1), relative second crack location (rcl2), relative first crack depth (rcd1), relative second crack depth (rcd2) are presented in the Table 9.1 (a) and Table 9.1 (b). The first six columns of both the Table (Table 9.1 (a), Table 9.1 (b)) presents the inputs for the above mentioned methodologies i.e. relative 1st natural frequency (fnf), relative 2nd natural frequency (snf), relative 3rd natural frequency (tnf), relative 1st mode shape difference (fmd), relative 2nd mode shape difference (smd) and relative 3rd mode shape difference (tmd) respectively. The rest columns from the Table represent the outputs such as relative crack locations and relative crack depths from the respective techniques. From the analysis of the results presented in Tables 9.1(a) it is found that, the percentage deviation of the results of MANFIS is 2.53%.

Table 9.1 (a) Comparison of results between MANFIS model, Gaussian fuzzy neural model, GA model and experimental analysis.

Relative first natural frequency "f ₁ "	Relative second natural frequency "f ₂ "	Relative third natural frequency "f ₃ "	Average Relative first mode shape difference "f _{md} "	Average Relative second mode shape difference "s _{md} "	Average Relative third mode shape difference "t _{md} "	MANFIS Model relative				Gaussian Fuzzy Neural Model relative				GA model relative				Experimental analysis relative			
						1 st crack depth "rcd1"	1 st crack location "rc1"	2 nd crack depth "rcd2"	2 nd crack location "rc2"	1 st crack depth "rcd1"	1 st crack location "rc1"	2 nd crack depth "rcd2"	2 nd crack location "rc2"	1 st crack depth "rcd1"	1 st crack location "rc1"	2 nd crack depth "rcd2"	2 nd crack location "rc2"	1 st crack depth "rcd1"	1 st crack location "rc1"	2 nd crack depth "rcd2"	2 nd crack location "rc2"
0.9991	0.9987	0.9977	0.0087	0.0025	0.0029	0.333	0.26	0.25	0.74	0.332	0.24	0.23	0.73	0.331	0.23	0.22	0.72	0.336	0.28	0.27	0.77
0.9974	0.9997	0.9995	0.0011	0.9852	0.2314	0.165	0.24	0.417	0.49	0.166	0.23	0.416	0.48	0.164	0.22	0.415	0.47	0.169	0.27	0.420	0.52
0.9936	0.9975	0.9989	0.0154	0.02	0.0746	0.24	0.24	0.25	0.50	0.23	0.23	0.24	0.49	0.22	0.22	0.23	0.48	0.27	0.27	0.28	0.53
0.9975	0.9993	0.9981	0.001	0.0046	0.0862	0.25	0.124	0.166	0.375	0.24	0.123	0.165	0.374	0.22	0.122	0.164	0.373	0.28	0.127	0.169	0.378
0.9972	0.9959	0.9886	0.0032	0.0289	0.0114	0.26	0.27	0.415	0.76	0.25	0.25	0.414	0.75	0.23	0.24	0.413	0.74	0.29	0.29	0.418	0.79
0.9992	0.9977	0.9975	0.3826	0.2359	0.2311	0.416	0.125	0.334	0.874	0.414	0.123	0.332	0.872	0.412	0.122	0.331	0.871	0.419	0.128	0.337	0.877
0.9858	0.9982	0.9869	0.0201	0.0189	0.0131	0.332	0.124	0.414	0.49	0.330	0.122	0.412	0.48	0.328	0.121	0.411	0.47	0.335	0.127	0.417	0.52
0.9997	0.9959	0.9971	0.0022	0.0021	0.0072	0.166	0.124	0.165	0.874	0.164	0.122	0.163	0.872	0.163	0.121	0.162	0.870	0.169	0.127	0.168	0.877
0.9988	0.9858	0.9887	0.0075	0.0077	0.0292	0.335	0.376	0.51	0.625	0.333	0.374	0.49	0.623	0.331	0.372	0.48	0.621	0.338	0.379	0.53	0.628
0.9993	0.9968	0.9989	0.0053	0.0035	0.0157	0.49	0.375	0.332	0.624	0.48	0.373	0.330	0.622	0.47	0.371	0.329	0.620	0.52	0.378	0.335	0.627

Table 9.1 (b) Comparison of results between MANFIS model, FEA and numerical analysis.

Relative first natural frequency "f _{1f} "	Relative second natural frequency "f _{2n} "	Relative third natural frequency "f _{3n} "	Average Relative first mode shape difference "f _{md} "	Average Relative second mode shape difference "s _{md} "	Average Relative third mode shape difference "t _{md} "	MANFIS Model relative				FEA relative				Numerical analysis relative			
						1 st crack depth "rcd1"	1 st crack location "rc1"	2 nd crack depth "rcd2"	2 nd crack location "rc2"	1 st crack depth "rcd1"	1 st crack location "rc1"	2 nd crack depth "rcd2"	2 nd crack location "rc2"	1 st crack depth "rcd1"	1 st crack location "rc1"	2 nd crack depth "rcd2"	2 nd crack location "rc2"
0.9991	0.9987	0.9977	0.0087	0.0025	0.0029	0.333	0.26	0.25	0.74	0.327	0.19	0.19	0.69	0.325	0.17	0.18	0.66
0.9974	0.9997	0.9995	0.0011	0.9852	0.2314	0.165	0.24	0.417	0.49	0.160	0.18	0.411	0.44	0.159	0.16	0.409	0.42
0.9936	0.9975	0.9989	0.0154	0.02	0.0746	0.24	0.24	0.25	0.50	0.18	0.18	0.19	0.44	0.16	0.17	0.17	0.43
0.9975	0.9993	0.9981	0.001	0.0046	0.0862	0.25	0.124	0.166	0.375	0.19	0.118	0.160	0.369	0.17	0.116	0.158	0.367
0.9972	0.9959	0.9886	0.0032	0.0289	0.0114	0.26	0.27	0.415	0.76	0.20	0.21	0.409	0.70	0.18	0.19	0.407	0.68
0.9992	0.9977	0.9975	0.3826	0.2359	0.2311	0.416	0.125	0.334	0.874	0.411	0.120	0.328	0.869	0.408	0.117	0.326	0.866
0.9858	0.9982	0.9869	0.0201	0.0189	0.0131	0.332	0.124	0.414	0.49	0.326	0.118	0.408	0.43	0.324	0.116	0.406	0.41
0.9997	0.9959	0.9971	0.0022	0.0021	0.0072	0.166	0.124	0.165	0.874	0.161	0.119	0.160	0.868	0.158	0.116	0.157	0.867
0.9988	0.9858	0.9887	0.0075	0.0077	0.0292	0.335	0.376	0.51	0.625	0.338	0.371	0.44	0.620	0.328	0.369	0.43	0.618
0.9993	0.9968	0.9989	0.0053	0.0035	0.0157	0.49	0.375	0.332	0.624	0.43	0.370	0.327	0.619	0.42	0.368	0.325	0.617

9.4 Summary

Based on the results from MANFIS technique the following conclusions are drawn for multiple crack diagnosis in the beam structure.

In the current investigation a methodology based on measurement of natural frequencies and mode shapes of the system has been presented for identification of crack locations and their severities in a beam structure using MANFIS model having one input (fuzzy) layer, four hidden layers and one output layer. Analyzing the results obtained from experimental, finite element and numerical methods, it is clear that the natural frequencies and mode shapes shows a noticeable change due to presence of cracks on the beam structure. The first three relative natural frequencies and mode shapes differences from the numerical, finite element and experimental analysis are used as inputs to the fuzzy segment (input layer) of the MANFIS model. Relative crack locations and relative crack depths are the output from the developed model. The predicted results of the MANFIS model has been validated using the results from the developed experimental setup and the results are found to be in close agreement. From the analysis of the results obtained from the newly designed model it is observed that the MANFIS model predicts the position and severities of cracks with more accuracy than the other AI techniques discussed in this thesis and can be suitably utilized for online multiple crack diagnosis in the dynamically vibrating structures.

Publications

- Amiya Kumar Dash, Dayal R.Parhi, Development of a crack diagnostic application using MANFIS technique, International journal of acoustics and vibration (IJAV), In Press.

Chapter 10

ANALYSIS OF GENETIC FUZZY MODEL FOR MULTIPLE CRACK DETECTION

Detection faults before it affects the performance of the system become essential for efficient, reliable and safe operation in engineering systems. Traditional techniques for fault detection have limitations due to non accurate mathematical model used for simulating the actual conditions. Moreover, generation of an accurate mathematical model for a non linear system becomes very complex. Therefore, knowledge based system and evolutionary techniques become more appropriate to address modeling uncertainties. Fuzzy inference system is one of the knowledge based methodology, to resolve fault detection problem. Genetic algorithms (GAs) are search algorithm based on the mechanism of natural selection and genetic reproduction. It can be employed effectively to find the optimize solution in [163] many control systems. In the present study, genetic algorithm and fuzzy logic based hybrid technique (GA-fuzzy model) has been designed for diagnosis of multiple cracks in vibrating structures. The proposed method represents a suitable alternative method to neural network and genetic algorithm based method in the domain of fault diagnosis for damaged structures.

10.1 Introduction

The presence of vibrations on structures and machine components are used by engineers and scientists to formulate methodologies for identification of crack in damaged structures. So, the vibration parameters can be used to design techniques based on artificial intelligence for fault diagnosis.

To develop a robust fault diagnostic tool based on genetic algorithm and fuzzy logic, the current chapter explores the use of dynamic responses of cracked and intact cantilever beam structure. Theoretical, finite element and experimental analyses have been carried out to find the combined impact of crack locations and crack depths on the vibrational characteristics (natural frequencies, mode shapes) of the cantilever beam. The calculated vibration signatures are used to design and train the GA-fuzzy model. The viability of the proposed

technique has been investigated both analytically and experimentally for the cantilever beam containing multiple cracks.

This chapter has been organized into four sections. Section 10.1, the introduction part of the current chapter gives an outline about the application of AI techniques used for fault detection. The analysis of the GA-fuzzy model has been described in section 10.2. Section 10.2.1 and section 10.2.2 gives a detail picture about the GA methodology and fuzzy methodology adopted for developing the hybrid intelligent model. Section 10.3 explains about the results from the GA-fuzzy system and also explains the performance of the system in comparison to numerical, FEA, Gaussian fuzzy-neuro, MANFIS and experimental technique. The summary of the chapter is expressed in section 10.4.

10.2 Analysis of genetic- fuzzy system for crack detection

This section discusses about the mechanism of the proposed genetic-fuzzy system for identification of multiple cracks in structural members. To identify the locations and depths of multiple cracks in structural members, a new hybrid GA-fuzzy model has been designed. The computed vibration signatures from theoretical, finite element and experimental analysis are used to train the hybrid model. The first three relative natural frequencies, first three relative mode shape differences are used as inputs to the GA model and `rcl1_interim`, `rcl2_interim`, `rcl3_interim` are the outputs from the GA model. The fuzzy system takes the interim outputs from the GA model along with the first three relative natural frequencies, first three relative mode shape differences as inputs. Finally, `rcl1_final`, `rcl2_final`, `rcl3_final` are the output parameters from the hybrid GA-fuzzy technique. A comparison of results obtained from theoretical, finite element, Gaussian fuzzy-neuro, MANFIS, GA-fuzzy model and experimental analysis have been presented in Table 10.4 (a), Table 10.4 (b) and the results are found to be in close agreement. The detail architecture of the hybrid GA- fuzzy (Gaussian membership based) model has been shown in Fig. 10.3. The proposed hybrid GA-fuzzy system can be used as a robust technique to identify multiple cracks in damaged structures. The mechanism of GA segment and the fuzzy segment of the hybrid model inherits the steps followed in section 7.2, section 5.3 respectively.

10.2.1 Analysis of the GA segment of GA-fuzzy model

This section presents the approach adopted for formulating the GA segment of the developed hybrid GA-fuzzy model to identify presence of multiple cracks in the cantilever beam model. The GA model has got six inputs such as fnf, snf, tnf, fmd, smd and tmd. The output parameters from the GA model are interim first relative crack location (rcl1_interim), interim first relative crack depth (rcd1_interim), interim second relative crack location (rcl2_interim) and interim first relative crack depth (rcd2_interim).

The GA system utilizes reproduction, mutation and objective function to process the input parameters and provide interim outputs (interim relative crack locations and interim relative crack depths). The steps followed to formulate the GA model have been inherited from section 7.2 of the thesis.

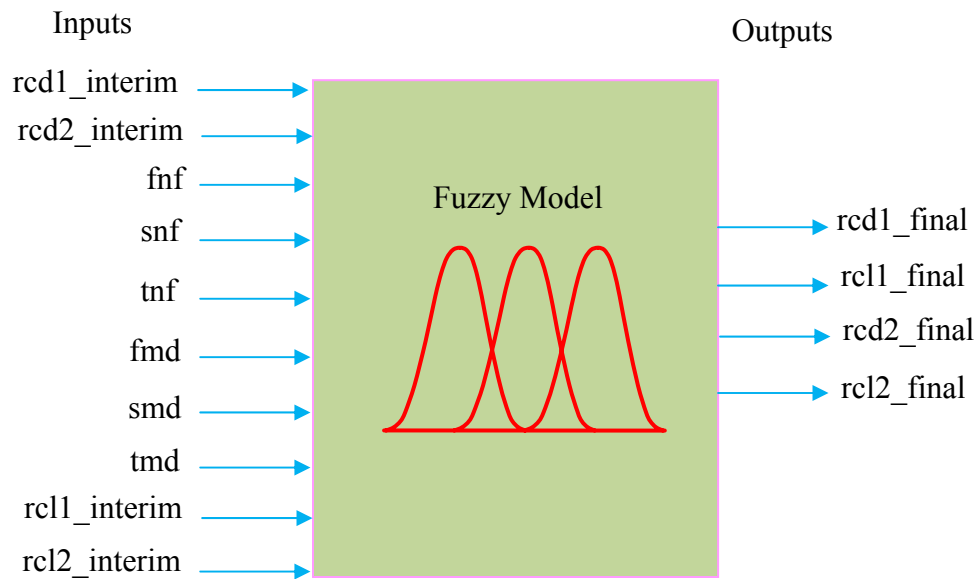


Fig. 10.1 Fuzzy Gaussian model for crack detection

10.2.2 Analysis of the fuzzy segment of GA-fuzzy model

This section analyses the knowledge based fuzzy inference system used for designing the fuzzy model used to detect multiple cracks present in the cracked cantilever beam structure. The vibration signatures extracted from the healthy and faulty beam model using numerical, finite and experimental techniques have been used for formulation of the fuzzy rule base and fuzzy linguistic terms of the Gaussian membership based fuzzy inference system of the proposed hybrid system.

The ten numbers inputs to the fuzzy layer of the hybrid GA-fuzzy system are fnf, snf, tnf, fmd, smd, tmd, interim first relative crack location (rcl1_interim), interim first relative crack depth (rcd1_interim), interim second relative crack location (rcl2_interim) and interim first relative crack depth (rcd2_interim). The four numbers of output parameters from the fuzzy segment are final first relative crack location (rcl1_final), final first relative crack depth (rcd1_final), final second relative crack location (rcl2_final), final first relative crack depth (rcd2_final).

The Gaussian membership based fuzzy model with inputs and outputs has been shown in Fig.10.1. The membership functions used for fuzzification of the system are shown in Fig. 10.2. Some of the fuzzy linguistic terms used for input and output parameters and fuzzy rules for development of the fuzzy segment are presented in Table 10.1, Table 10.2 and Table 10.3 respectively.

The detail architecture of the developed GA-fuzzy based intelligent system has been presented in Fig. 10.3. Subsequently, results from the developed intelligent hybrid system have been validated by experimental method. The methodology for development of the fuzzy system has been adopted as explained in section 5.3 of the thesis.

Membership functions for input parameters

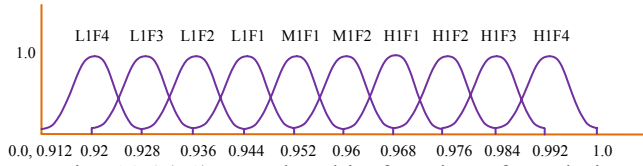


Fig. 10.2(a1) Membership functions for relative natural frequency for first mode of vibration.

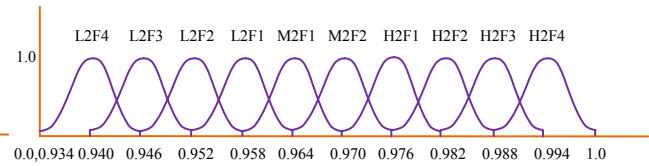


Fig. 10.2(a2) Membership functions for relative natural frequency for second mode of vibration.

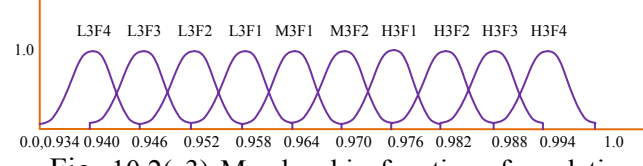


Fig. 10.2(a3) Membership functions for relative natural frequency for third mode of vibration.

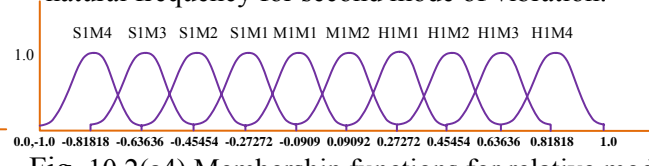


Fig. 10.2(a4) Membership functions for relative mode shape difference for first mode of vibration.

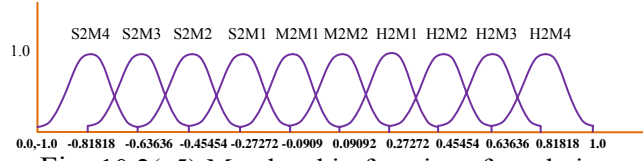


Fig. 10.2(a5) Membership functions for relative mode shape difference for second mode of vibration.

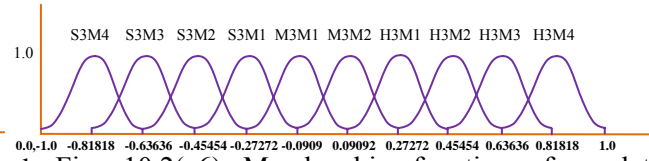


Fig. 10.2(a6) Membership functions for relative mode shape difference for third mode of vibration.

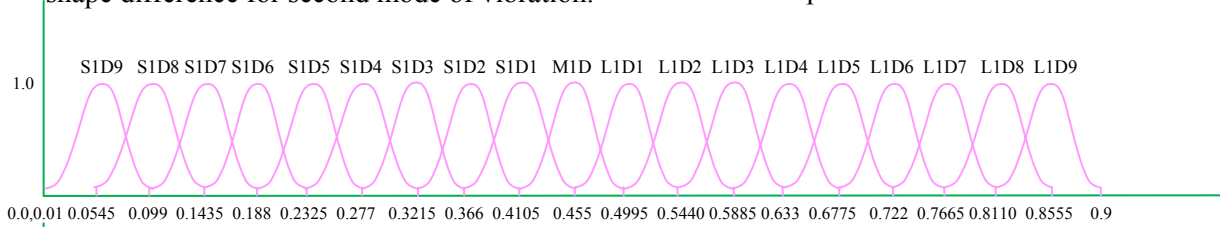


Fig. 10.2a7 (a) Membership functions for interim relative crack depth1.

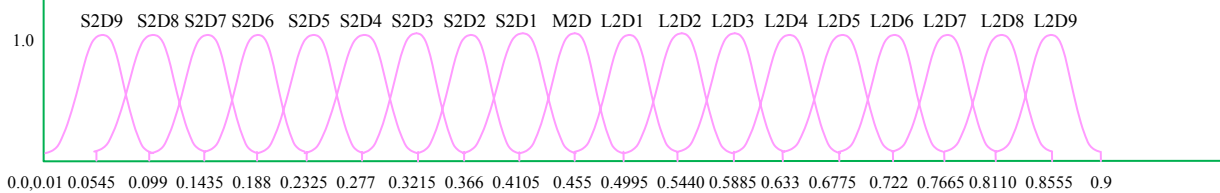


Fig. 10.2a7 (b) Membership functions for interim relative crack depth2.

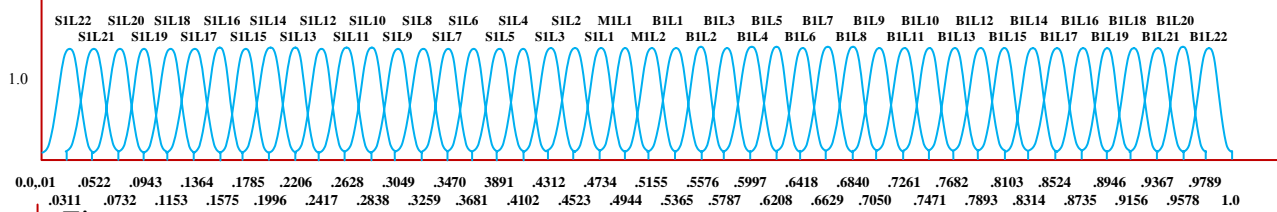


Fig. 10.2a8 (a) Membership functions for interim relative crack location1.

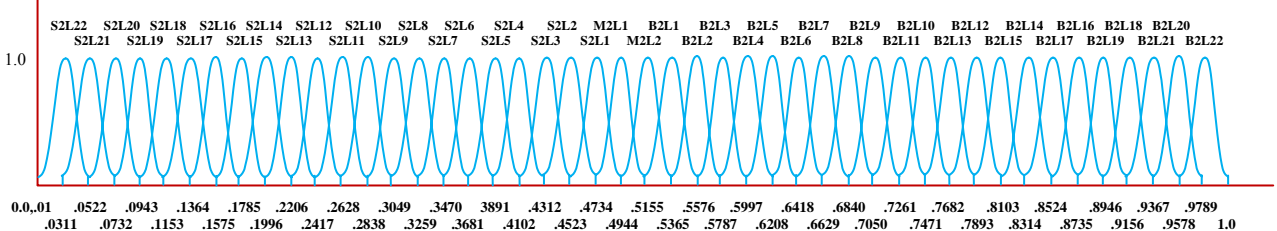


Fig. 10.2a8 (b) Membership functions for interim relative crack location2.

Membership functions for output parameters

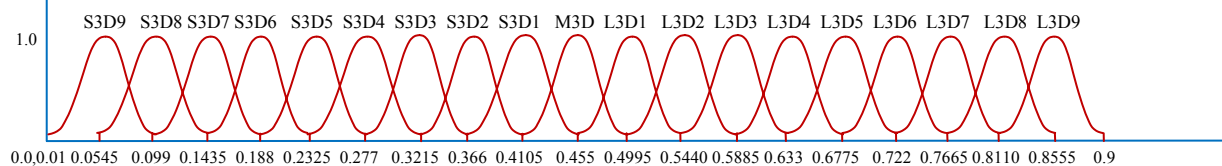


Fig. 10.2a9 (a) Membership functions for final relative crack depth1.

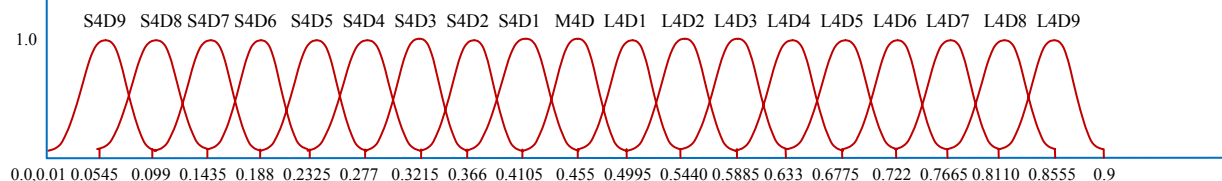


Fig. 10.2a9 (b) Membership functions for final relative crack depth2.

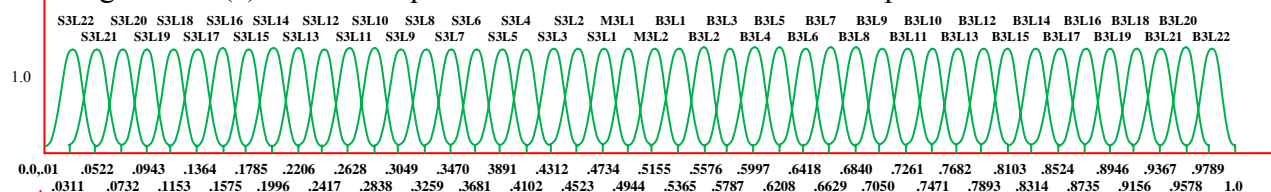


Fig. 10.2a10 (a) Membership functions for final relative crack location1.

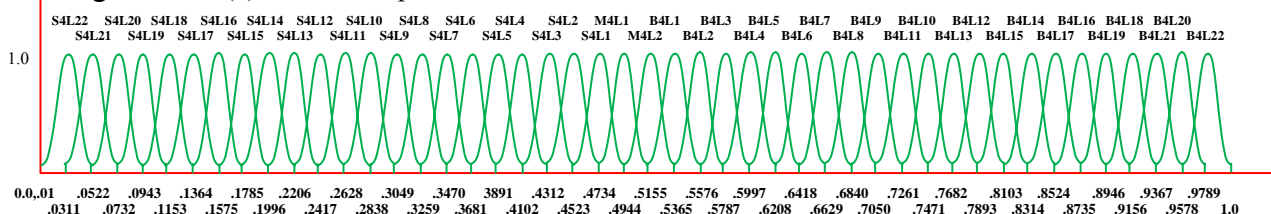


Fig. 10.2a10 (b) Membership functions for final relative crack location2.

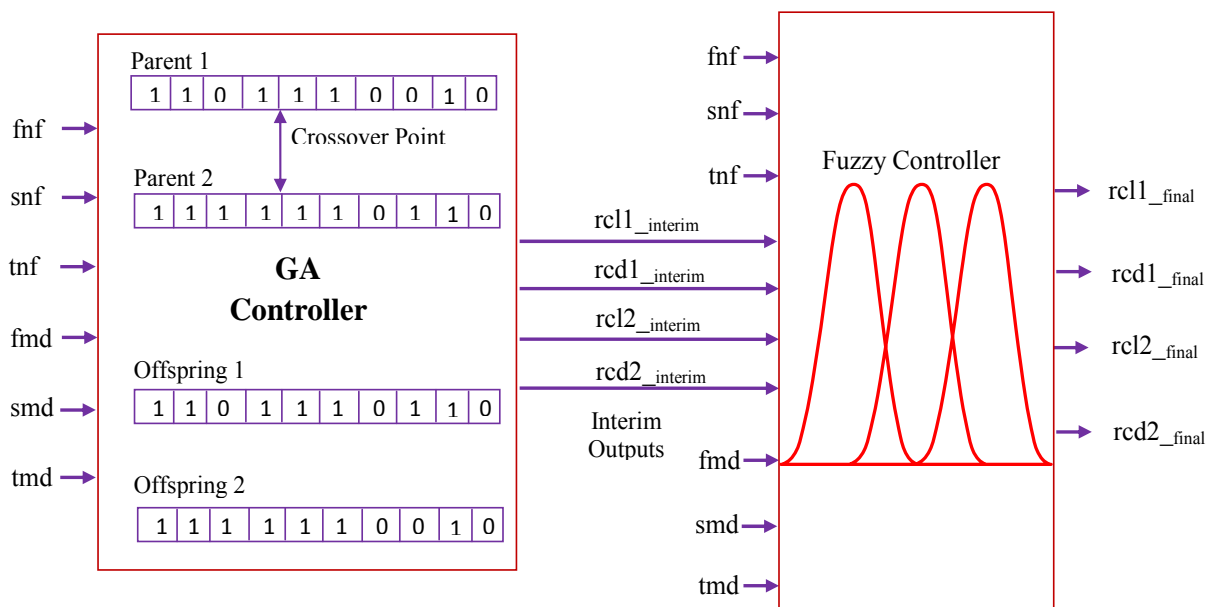


Fig. 10.3 Genetic-Fuzzy system for fault detection

Table 10.1 Description of fuzzy Linguistic terms for input parameters of fuzzy segment for GA-fuzzy Model

Membership Functions Name	Linguistic Terms	Description and range of the Linguistic terms
L1F1,L1F2,L1F3,L1F4	fnf _{1 to 4}	Low ranges of relative natural frequency for first mode of vibration in descending order respectively
M1F1,M1F2	fnf _{5,6}	Medium ranges of relative natural frequency for first mode of vibration in ascending order respectively
H1F1,H1F2,H1F3,H1F4	fnf _{7 to 10}	Higher ranges of relative natural frequency for first mode of vibration in ascending order respectively
L2F1,L2F2,L2F3,L2F4	snf _{1 to 4}	Low ranges of relative natural frequency for second mode of vibration in descending order respectively
M2F1,M2F2	snf _{5,6}	Medium ranges of relative natural frequency for second mode of vibration in ascending order respectively
H2F1,H2F2,H2F3,H2F4	snf _{7 to 10}	Higher ranges of relative natural frequencies for second mode of vibration in ascending order respectively
L3F1,L3F2,L3F3,L3F4	tnf _{1 to 4}	Low ranges of relative natural frequencies for third mode of vibration in descending order respectively
M3F1,M3F2	tnf _{5,6}	Medium ranges of relative natural frequencies for third mode of vibration in ascending order respectively
H3F1,H3F2,H3F3,H3F4	tnf _{7 to 10}	Higher ranges of relative natural frequencies for third mode of vibration in ascending order respectively
S1M1,S1M2,S1M3,S1M4	fmd _{1 to 4}	Small ranges of first relative mode shape difference in descending order respectively
M1M1,M1M2	fmd _{5,6}	medium ranges of first relative mode shape difference in ascending order respectively
H1M1,H1M2,H1M3,H1M4	fmd _{7 to 10}	Higher ranges of first relative mode shape difference in ascending order respectively
S2M1,S2M2,S2M3,S2M4	smd _{1 to 4}	Small ranges of second relative mode shape difference in descending order respectively
M2M1,M2M2	smd _{5,6}	medium ranges of second relative mode shape difference in ascending order respectively
H2M1,H2M2,H2M3,H2M4	smd _{7 to 10}	Higher ranges of second relative mode shape difference in ascending order respectively
S3M1,S3M2,S3M3,S3M4	tmd _{1 to 4}	Small ranges of third relative mode shape difference in descending order respectively
M3M1,M3M2	tmd _{5,6}	medium ranges of third relative mode shape difference in ascending order respectively
H3M1,H3M2,H3M3,H3M4	tmd _{7 to 10}	Higher ranges of third relative mode shape difference in ascending order respectively
S1L1,S1L2.....S1L22	rcll _{1 to 22}	Small ranges of relative crack location in descending order respectively
M1L1,M1L2	rcll _{23,24}	Medium ranges of relative crack location in ascending order respectively
B1L1,B1L2.....B1L22	rcll _{25 to 46}	Bigger ranges of relative crack location in ascending order respectively
S1D1,S1D2.....S1D9	rcd1 _{1 to 9}	Small ranges of relative crack depth in descending order respectively
M1D	rcd1 ₁₀	Medium relative crack depth
L1D1,L1D2.....L1D9	rcd1 _{11 to 19}	Larger ranges of relative crack depth in ascending order respectively
S2L1,S2L2.....S2L22	rcl2 _{1 to 22}	Small ranges of relative crack location in descending order respectively
M2L1,M2L2	rcl2 _{23,24}	Medium ranges of relative crack location in ascending order respectively
B2L1,B2L2.....B2L22	rcl2 _{25 to 46}	Bigger ranges of relative crack location in ascending order respectively
S2D1,S2D2.....S2D9	rcd2 _{1 to 9}	Small ranges of relative crack depth in descending order respectively
M2D	rcd2 ₁₀	Medium relative crack depth
L2D1,L2D2.....L2D9	rcd2 _{11 to 19}	Larger ranges of relative crack depth in ascending order respectively

Table 10.2 Description of fuzzy Linguistic terms for output parameters of fuzzy segment for GA-fuzzy Model

S3L1,S3L2.....S3L22	(Interim) rcl1 _{1 to 22}	Small ranges of relative crack location in descending order respectively
M3L1,M3L2	(Interim) rcl1 _{23,24}	Medium ranges of relative crack location in ascending order respectively
B3L1,B3L2.....B3L22	(Interim) rcl1 _{25 to 46}	Bigger ranges of relative crack location in ascending order respectively
S3D1,S3D2.....S3D9	(Interim) rcd1 _{1 to 9}	Small ranges of relative crack depth in descending order respectively
M3D	(Interim) rcd1 ₁₀	Medium relative crack depth
L3D1,L3D2.....L3D9	(Interim) rcd1 _{11 to 19}	Larger ranges of relative crack depth in ascending order respectively
S4L1,S4L2.....S4L22	(Interim) rcl2 _{1 to 22}	Small ranges of relative crack location in descending order respectively
M4L1,M4L2	(Interim) rcl2 _{23,24}	Medium ranges of relative crack location in ascending order respectively
B4L1,B4L2.....B4L22	(Interim) rcl2 _{25 to 46}	Bigger ranges of relative crack location in ascending order respectively
S4D1,S4D2.....S4D9	(Interim) rcd2 _{1 to 9}	Small ranges of relative crack depth in descending order respectively
M4D	(Interim) rcd2 ₁₀	Medium relative crack depth
L4D1,L4D2.....L4D9	(Interim) rcd2 _{11 to 19}	Larger ranges of relative crack depth in ascending order respectively

Table 10.3 Examples of ten fuzzy rules used in fuzzy segment of GA-fuzzy Model

Sl.No.	Examples of some rules used in the fuzzy model
1	If fnf is H1F1,snf is M2F2,tnf is M3F1,fmd is H1M2,smd is H2M4,tmd is H3M3, then rcd1 is S1D6,and rcl1 is S1L17 and rcd2 is S2D4,and rcl2 is S2L6, interim rcd1 is S3D4,and interim rcl1 is S3L15 and interim rcd2 is S4D5,and interim rcl2 is S4L8
2	If fnf is L1F4,snf is L2F4,tnf is L3F4,fmd is H1M1,smd is H2M1,tmd is H3M2, then rcd1 is S1D2,and rcl1 is S1L17 and rcd2 is S2D1,and rcl2 is M2L2, interim rcd1 is S3D1,and interim rcl1 is S3L15 and interim rcd2 is S4D3,and interim rcl2 is M2L1
3	If fnf is L1F3,snf is L2F4,tnf is L3F4,fmd is M1M2,smd is H2M2,tmd is H3M3, then rcd1 is M1D,and rcl1 is S1L17 and rcd2 is S2D2,and rcl2 is B2L19, interim rcd1 is M1D,and interim rcl1 is S3L15 and interim rcd2 is S4D3,and interim rcl2 is B4L21
4	If fnf is H1F2,snf is H2F1,tnf is H3F1,fmd is H1M3,smd is H2M4,tmd is H3M4, then rcd1 is S1D6,and rcl1 is S1L11 and rcd2 is S2D4,and rcl2 is M2L2, interim rcd1 is S3D5,and interim rcl1 is S3L13 and interim rcd2 is S4D5,and interim rcl2 is M2L1
5	If fnf is M1F1,snf is L2F2,tnf is L3F3,fmd is H1M1,smd is H2M1,tmd is H3M2, then rcd1 is S1D4,and rcl1 is S1L11 and rcd2 is S2D1,and rcl2 is B2L13, interim rcd1 is S3D2,and interim rcl1 is S3L14 and interim rcd2 is S4D5,and interim rcl2 is B4L15
6	If fnf is L1F1,snf is L2F2,tnf is L3F3,fmd is H1M3,smd is M2M1,tmd is H3M4, then rcd1 is M1D,and rcl1 is S1L11 and rcd2 is S2D7,and rcl2 is M2L2, interim rcd1 is S3D1,and interim rcl1 is S3L13 and interim rcd2 is S4D5,and interim rcl2 is M3L1
7	If fnf is L1F4,snf is L2F4,tnf is L3F4,fmd is M1M2,smd is H2M1,tmd is H3M1, then rcd1 is L1D1,and rcl1 is S1L11 and rcd2 is S2D4,and rcl2 is B2L10, interim rcd1 is L3D3,and interim rcl1 is S3L13 and interim rcd2 is S4D7,and interim rcl2 is B4L15
8	If fnf is H1F1,snf is M2F2,tnf is M3F1,fmd is H1M2,smd is H2M2,tmd is H3M2, then rcd1 is S1D6,and rcl1 is S1L6 and rcd2 is S2D4,and rcl2 is B2L5, interim rcd1 is S3D9,and interim rcl1 is S3L3 and interim rcd2 is S4D7,and interim rcl2 is B4L7
9	If fnf is L1F1,snf is L2F4,tnf is L3F4,fmd is M1M1,smd is M2M1,tmd is M3M2, then rcd1 is S1D2,and rcl1 is S1L6 and rcd2 is L2D1,and rcl2 is B2L5, interim rcd1 is S3D1,and interim rcl1 is S3L8 and interim rcd2 is L4D4,and interim rcl2 is B4L7
10	If fnf is M1F1,snf is L2F2,tnf is L3F1,fmd is M1M2,smd is M2M2,tmd is H3M1, then rcd1 is S1D1,and rcl1 is S1L6 and rcd2 is S2D4,and rcl2 is B2L5, interim rcd1 is S3D3,and interim rcl1 is S3L7 and interim rcd2 is S4D6,and interim rcl2 is B4L3

Table 10.4 (a) Comparison of results between GA-fuzzy model, MANFIS model, Gaussian fuzzy neural model, and experimental analysis.

Relative first natural frequency "f _{1f} "	Relative second natural frequency "snf"	Relative third natural frequency "tnf"	Average Relative first mode shape difference "fmd"	Average Relative second mode shape difference "smd"	Average Relative third mode shape difference "tmd"	GA-fuzzy Model relative				MANFIS Model relative				Gaussian Fuzzy Neural Model relative				Experimental analysis relative			
						1 st crack depth "rcd1"	1 st crack location "rcl1"	2 nd crack depth "rcd2"	2 nd crack location "rcl2"	1 st crack depth "rcd1"	1 st crack location "rcl1"	2 nd crack depth "rcd2"	2 nd crack location "rcl2"	1 st crack depth "rcd1"	1 st crack location "rcl1"	2 nd crack depth "rcd2"	2 nd crack location "rcl2"	1 st crack depth "rcd1"	1 st crack location "rcl1"	2 nd crack depth "rcd2"	2 nd crack location "rcl2"
0.9991	0.9987	0.9977	0.0087	0.0025	0.0029	0.334	0.27	0.26	0.75	0.333	0.26	0.25	0.74	0.332	0.24	0.23	0.73	0.336	0.28	0.27	0.77
0.9974	0.9997	0.9995	0.0011	0.9852	0.2314	0.164	0.23	0.416	0.48	0.165	0.24	0.417	0.49	0.166	0.23	0.416	0.48	0.169	0.27	0.420	0.52
0.9936	0.9975	0.9989	0.0154	0.02	0.0746	0.25	0.25	0.26	0.51	0.24	0.24	0.25	0.50	0.23	0.23	0.24	0.49	0.27	0.27	0.28	0.53
0.9975	0.9993	0.9981	0.001	0.0046	0.0862	0.24	0.123	0.165	0.374	0.25	0.124	0.166	0.375	0.24	0.123	0.165	0.374	0.28	0.127	0.169	0.378
0.9972	0.9959	0.9886	0.0032	0.0289	0.0114	0.27	0.26	0.416	0.77	0.26	0.27	0.415	0.76	0.25	0.25	0.414	0.75	0.29	0.29	0.418	0.79
0.9992	0.9977	0.9975	0.3826	0.2359	0.2311	0.415	0.126	0.333	0.875	0.416	0.125	0.334	0.874	0.414	0.123	0.332	0.872	0.419	0.128	0.337	0.877
0.9858	0.9982	0.9869	0.0201	0.0189	0.0131	0.333	0.123	0.415	0.48	0.332	0.124	0.414	0.49	0.330	0.122	0.412	0.48	0.335	0.127	0.417	0.52
0.9997	0.9959	0.9971	0.0022	0.0021	0.0072	0.167	0.125	0.166	0.873	0.166	0.124	0.165	0.874	0.164	0.122	0.163	0.872	0.169	0.127	0.168	0.877
0.9988	0.9858	0.9887	0.0075	0.0077	0.0292	0.336	0.375	0.50	0.626	0.335	0.376	0.51	0.625	0.333	0.374	0.49	0.623	0.338	0.379	0.53	0.628
0.9993	0.9968	0.9989	0.0053	0.0035	0.0157	0.48	0.374	0.333	0.625	0.49	0.375	0.332	0.624	0.48	0.373	0.330	0.622	0.52	0.378	0.335	0.627

Table 10.4 (b) Comparison of results between GA-fuzzy model, FEA and numerical analysis.

Relative first natural frequency "f ₁ "	Relative second natural frequency "s _{nf} "	Relative third natural frequency "tnf"	Average Relative first mode shape difference "fmd"	Average Relative second mode shape difference "smd"	Average Relative third mode shape difference "tmd"	GA-fuzzy Model relative				FEA relative				Numerical relative			
						red1	rel1	red2	rel2	red1	rel1	red2	rel2	red1	rel1	red2	rel2
0.9991	0.9987	0.9977	0.0087	0.0025	0.0029	0.334	0.27	0.26	0.75	0.327	0.19	0.19	0.69	0.325	0.17	0.18	0.66
0.9974	0.9997	0.9995	0.0011	0.9852	0.2314	0.164	0.23	0.416	0.48	0.160	0.18	0.411	0.44	0.159	0.16	0.409	0.42
0.9936	0.9975	0.9989	0.0154	0.02	0.0746	0.25	0.25	0.26	0.51	0.18	0.18	0.19	0.44	0.16	0.17	0.17	0.43
0.9975	0.9993	0.9981	0.001	0.0046	0.0862	0.24	0.123	0.165	0.374	0.19	0.118	0.160	0.369	0.17	0.116	0.158	0.367
0.9972	0.9959	0.9886	0.0032	0.0289	0.0114	0.27	0.26	0.416	0.77	0.20	0.21	0.409	0.70	0.18	0.19	0.407	0.68
0.9992	0.9977	0.9975	0.3826	0.2359	0.2311	0.415	0.126	0.333	0.875	0.411	0.120	0.328	0.869	0.408	0.117	0.326	0.866
0.9858	0.9982	0.9869	0.0201	0.0189	0.0131	0.333	0.123	0.415	0.48	0.326	0.118	0.408	0.43	0.324	0.116	0.406	0.41
0.9997	0.9959	0.9971	0.0022	0.0021	0.0072	0.167	0.125	0.166	0.873	0.161	0.119	0.160	0.868	0.158	0.116	0.157	0.867
0.9988	0.9858	0.9887	0.0075	0.0077	0.0292	0.336	0.375	0.50	0.626	0.338	0.371	0.44	0.620	0.328	0.369	0.43	0.618
0.9993	0.9968	0.9989	0.0053	0.0035	0.0157	0.48	0.374	0.333	0.625	0.43	0.370	0.327	0.619	0.42	0.368	0.325	0.617

10.3 Results and discussions of GA-fuzzy model

The current section of this chapter analyses the results obtained from the developed GA-fuzzy inverse technique used for multiple crack diagnosis.

The hybrid model has been designed with the vibration indices i.e. first three relative natural frequencies, first three relative mode shape differences, relative crack locations and relative crack depths obtained from numerical, finite element and experimental techniques. The proposed GA-fuzzy hybrid system comprises of two layers. The first layer is the GA model, where as the second layer is the fuzzy model. In the genetic algorithm section, the initial data pool has been created using the vibration signatures obtained from numerical, finite element, experimental analysis. Crossover operation has been followed as mentioned in Fig.7.1 of section 7.2 of chapter 7, for designing the GA model to find the best fit child with in the search space. In some of the cases mutation procedure (Fig. 7.2 of section 7.2) has been carried out to find the optimal solution. The inputs to the GA layer of the hybrid system are first three relative natural frequencies, first three relative mode shape differences. The interim outputs from the GA model are, rcl1_interim, rcd1_interim, rcl2_interim, rcd2_interim. The Gaussian membership based fuzzy segment (Fig. 10.1) of the hybrid model has been developed using the set of fuzzy rules, fuzzy linguistic terms, first three relative natural frequencies, first three relative mode shape differences and the interim outputs from the GA model. The description of the fuzzy linguistic terms for the input and output parameters are shown in Table 10.1 and Table 10.2 respectively. Table 10.3 represents ten numbers of the fuzzy rules out of the several hundred fuzzy rules used for designing the fuzzy membership functions. The detail architecture of the intelligent hybrid system (GA-Fuzzy model) has been shown in Fig. 10.3. The results obtained from the various analyses carried out on the cracked cantilever beam have been validated using the developed experimental set up. A comparison of results between GA- fuzzy model, Gaussian membership based fuzzy-neuro model, MANFIS model and experimental analysis have been presented in Table 10.4 (a). The predicted results for crack locations and crack depths from GA- fuzzy analysis, numerical analysis, finite element analysis have been presented in Table 10.4 (b). Six numbers of inputs i.e. first three relative natural frequencies and first three relative mode shape differences have been considered to measure the relative crack locations and relative crack depths by GA-fuzzy model and other techniques as mentioned for crack identification. The corresponding

outputs have been presented in Table 10.4 (a) and Table 10.4 (b) to measure the accuracy of the results from the various methodologies mentioned. During the analysis of the results, it is observed that the percentage of deviation of the prediction values for relative crack locations and relative crack depths of the Gaussian membership based GA- Fuzzy model is 2.36%.

10.4 Summary

The conclusions made by analyzing the results from the developed GA-fuzzy model have been presented in this section.

In the current chapter a method for multiple crack prediction in beam like structures has been designed using genetic algorithm and fuzzy logic. It is found that the presence of cracks has a remarkable effect on the natural frequencies and mode shapes of the beam under consideration. Numerical, finite element and experimental analysis have been carried out to calculate the vibration signatures. The extracted vibration signatures are used to create the initial data pool and subsequently designing of the GA segment of the proposed hybrid system. Crossover and mutation operation have been used to find the best fit interim output from the GA system. The interim outputs from the GA model along with the first three natural frequencies and first three mode shape differences are used to develop the fuzzy layer of the hybrid system. From the analysis of the results obtained from GA- Fuzzy model, Gaussian membership based fuzzy-neuro model, MANFIS model, numerical analysis, finite element analysis and experimental analysis confirms that the developed method can identify the crack positions and their severities with higher accuracy. It is concluded that the proposed GA-fuzzy hybrid methodology can be used as an online crack diagnostic tool for vibrating structures. In next chapter genetic algorithm and neural network can be used to design a hybrid model for multiple crack detection in the domain of vibrating complex structures. The percentage of deviation in the prediction values of relative first crack location, relative second crack location, relative first crack depth, relative second crack depth for GA-fuzzy model is found to be 2.36%.

Paper Accepted in International Journal

1. A.K. Dash, D.R. Parhi, “Analysis of an intelligent hybrid system for fault diagnosis in cracked structure” Arabian Journal for Science and Engineering.

Chapter 11

ANALYSIS OF GENETIC-NEURO-FUZZY MODEL FOR MULTIPLE CRACK DETECTION

Researches in the field of damage or fault detection in engineering applications have been carried out for last few decades by engineers and scientists. In this regard, various techniques such as energy method, wavelet method, finite element method and many other numerical methods have been applied to design fault diagnostic tool. Besides the few methods as mentioned above, the knowledge based system has been evolved as one of the best technique for addressing problems with non linear characteristics. The knowledge based systems are generally designed with the help of artificial intelligent methods such as genetic algorithm, neural network, fuzzy inference system and etc. In due course for development of the system based on AI techniques, hybridization of artificial intelligent methodologies have been used successfully for automation of control system and other applications and to simulate the applications to match the real conditions. Hybridization of methodologies facilitates for integration of the best features of AI techniques, which enables to develop intelligent system for adapting to dynamic environment and to get the optimal solution. The search based algorithm GA, the adaptive neural network and rule based fuzzy logic can be fused together to design and train a multiple crack diagnostic tool for structural system. Intelligent hybrid systems (GA-neural model and GA-neuro-fuzzy model) have been presented in the current investigation for multiple crack diagnosis in structural system using the vibration characteristics obtained from theoretical, finite element, experimental analysis. Genetic algorithm, neural network, fuzzy logic have been used to design and develop the hybrid system. From the comparison of the results, obtained from theoretical, finite element, GA-fuzzy model, GA-neural model, GA-neuro-fuzzy model and experimental analysis it is observed that the results from the GA-neuro-fuzzy model are in close proximity with the results obtained from the experimental analysis as compared to other methodologies mentioned above. The developed technique can be effectively used for online health monitoring of industrial systems.

11.1 Introduction

Over the years damage detection in structures is being given prior attention. The presence of cracks is one of the main causes of failure of the structural systems. So, early crack detection is important to avoid catastrophic failure. Different non-destructive inspection techniques are usually applied for detection of crack in engineering applications. In the current research, the vibration parameters of the cracked and undamaged beam structure has been considered for development of two layer (GA-neural) and three layer (GA-neuro-fuzzy) inverse intelligent system for multiple crack diagnosis in beam like structures.

In this current section, efficient methods have been presented to identify both locations and severities of the damages in structural systems based on genetic algorithm, neural network, and fuzzy logic. The results from the proposed inverse methodologies have been validated by comparing with the results obtained from theoretical, finite element and experimental analysis. From the analysis of the results obtained from the two layer and three layer hybrid intelligent models, it is observed that these proposed methodologies can be used as an efficient online condition monitoring tool for faulty structures.

The present chapter is arranged into four sections. An over view of fault detection methodologies and the application of GA, neural network and fuzzy logic for development of crack diagnostic tool have been explained in section 11.1. The section 11.2 describes the analysis of GA-neural and GA-neuro-fuzzy model used for fault detection. Results obtained from the proposed models have been compared with that of the theoretical, finite element, GA-fuzzy and experimental analysis in section 11.3 to exhibit the effectiveness of the methodology. The summary of the current chapter is discussed in section 11.4.

11.2 Analysis of GA-neural and Genetic- neuro-fuzzy system for crack detection

This section presents the analysis of the architecture of the proposed GA-neural and GA-neuro-fuzzy model and provides a detail insight of the multiple crack diagnostic methodology.

In the current section, multiple crack diagnostic hybrid techniques based on genetic algorithm, neural network, and fuzzy logic have been proposed for beam like structures. To

detect the cracks parameters and to find the relation between the cracks and the induced vibration parameters theoretical, finite element and experimental methods are applied. The GA segment of the hybrid models monitors the changes in the vibration signatures due to the presence of multiple cracks and predicts the interim crack location and crack depths i.e. $rcl1_{interim}$, $rcl1_{interim}$, $rcl2_{interim}$, $rcl2_{interim}$ for GA-neural system and $rcl1_{interim1}$, $rcl1_{interim1}$, $rcl2_{interim1}$, $rcl2_{interim1}$ for GA-neuro-fuzzy system. The interim out puts from the GA model along with the first three relative natural frequencies, first three relative mode shape differences are used as inputs to the neural segment of the hybrid system. Finally the outputs from the GA-neural hybrid system are $rcl1_{final}$, $rcl1_{final}$, $rcl2_{final}$ and $rcl2_{final}$. Outputs from the neural model of GA-neruo-fuzzy system are $rcl1_{interim2}$, $rcl1_{interim2}$, $rcl2_{interim2}$, $rcl2_{interim2}$. The outputs from the neural segment with the first three relative natural frequencies, first three relative mode shape differences are used as inputs to the fuzzy model and the finally the output parameters from the GA-Neuro-fuzzy hybrid model are $rcl1_{final}$, $rcl1_{final}$, $rcl2_{final}$ and $rcl2_{final}$. The effectiveness of the developed hybrid models have been established by comparing the results obtained from theoretical, finite element, GA-fuzzy model, GA-neural model, GA-neuro-fuzzy model and experimental analysis. The comparisons of results are presented in Table 11.1(a), Table 11.1(b), Table 11.1(c), Table 11.1(d). The results are found to be encouraging for establishing the fact that, the intelligent two layer (GA-neural) and three layer (GA-neuro-fuzzy) hybrid models can predict the relative crack locations and their severities with higher accuracy. The detail architecture of the developed GA-neural and GA-neuro-fuzzy models with all input and output parameters for all the segments have been shown in Fig. 11.1 and Fig.11.2 respectively. By analyzing the results from Table 11.1 (c) it is observed that, the GA-neural technique can detect fault in cracked beams effectively. From the analysis of the results shown in Table 11.1 (a), it can be concluded that the three layer hybrid network is capable of identifying faults in dynamically vibrating damaged beam structures better than the GA-neural model. The methodologies followed to formulate the GA segment; neural segment and fuzzy segment of the hybrid GA-neural and GA-neuro-fuzzy model have been inherited from section 7.2, 6.3 and section 5.3 respectively.

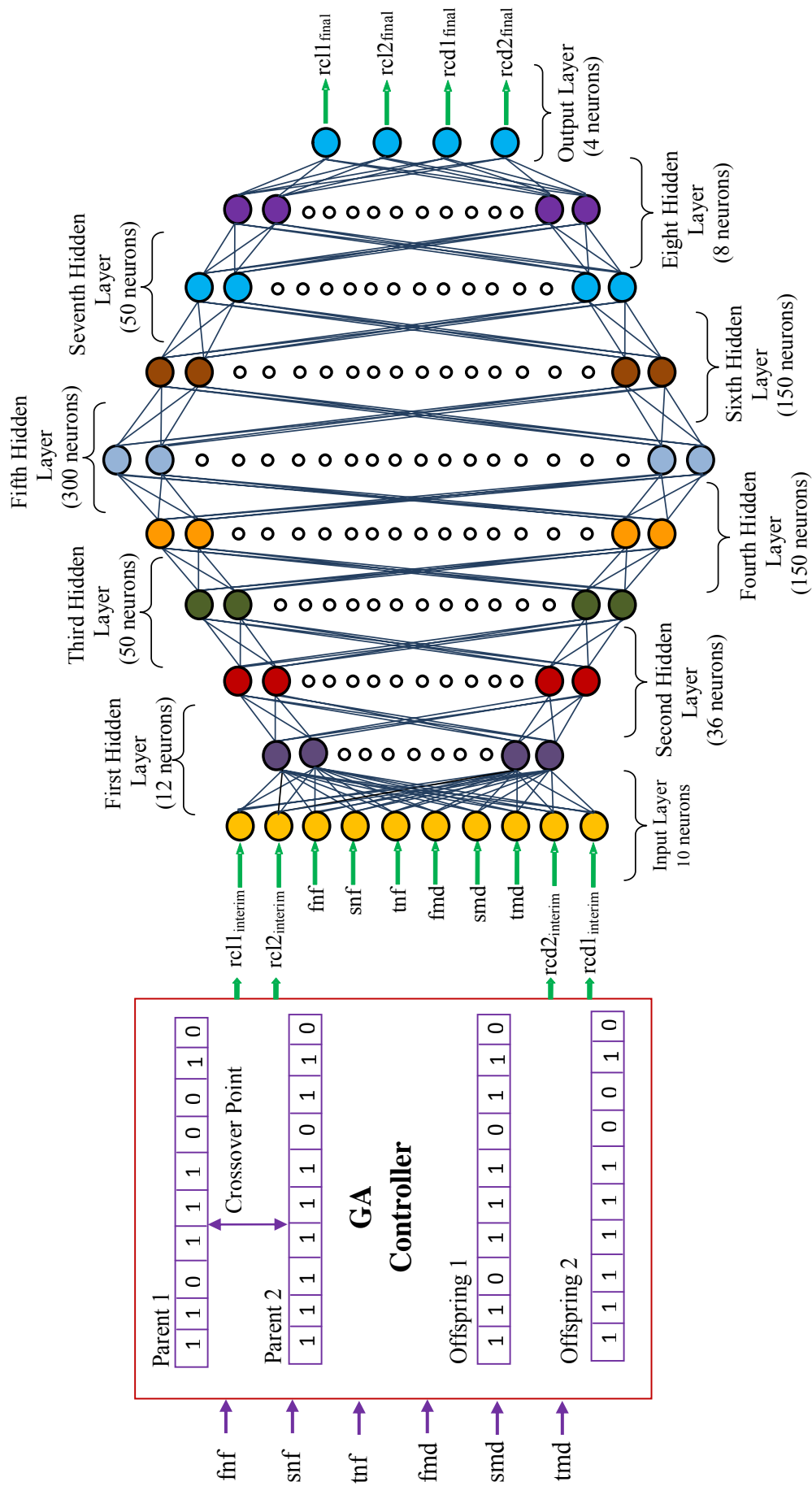


Fig. 11.1 GA-neural system for fault detection

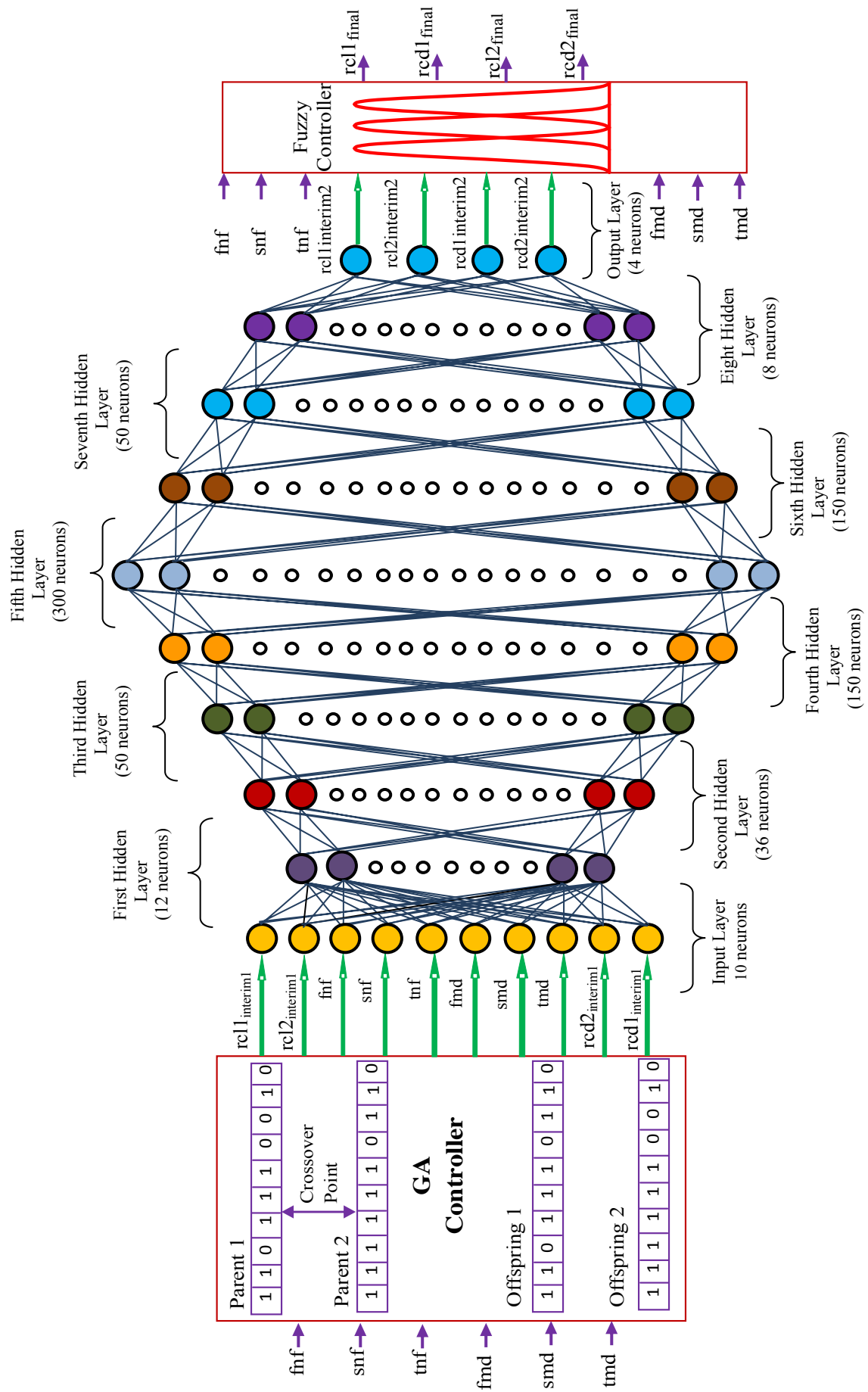


Fig. 11.2 GA-neuro-fuzzy system for fault detection

Table 11.1 (a) Comparison of results between GA-neuro-fuzzy model, GA-neural model, GA-fuzzy model, and experimental analysis.

Relative first natural frequency "f _{1f} "	Relative second natural frequency "snf"	Relative third natural frequency "tnf"	Average Relative first mode shape difference "fmd"	Average Relative second mode shape difference "smd"	Average Relative third mode shape difference "tmd"	GA-neuro-fuzzy Model relative				GA-neural Model relative				GA-fuzzy Model relative				Experimental analysis relative			
						rcd1	rcd2	rcd1	rcd2	rcd1	rcd2	rcd1	rcd2	rcd1	rcd2	rcd1	rcd2	rcd1	rcd2	rcd1	rcd2
0.9991	0.9987	0.9977	0.0087	0.0025	0.0029	0.335	0.27	0.334	0.26	0.334	0.25	0.334	0.26	0.334	0.27	0.336	0.27	0.336	0.28	0.27	0.77
0.9974	0.9997	0.9995	0.0011	0.9852	0.2314	0.168	0.26	0.167	0.25	0.167	0.418	0.50	0.416	0.164	0.23	0.416	0.48	0.169	0.27	0.420	0.52
0.9936	0.9975	0.9989	0.0154	0.02	0.0746	0.26	0.26	0.25	0.25	0.25	0.26	0.51	0.25	0.25	0.25	0.27	0.51	0.27	0.27	0.28	0.53
0.9975	0.9993	0.9981	0.001	0.0046	0.0862	0.27	0.126	0.26	0.125	0.26	0.167	0.376	0.24	0.123	0.165	0.28	0.374	0.127	0.127	0.169	0.378
0.9972	0.9959	0.9886	0.0032	0.0289	0.0114	0.28	0.30	0.27	0.27	0.27	0.416	0.77	0.27	0.26	0.416	0.29	0.77	0.29	0.29	0.418	0.79
0.9992	0.9977	0.9975	0.3826	0.2359	0.2311	0.418	0.127	0.417	0.126	0.417	0.335	0.875	0.415	0.126	0.333	0.419	0.875	0.128	0.128	0.337	0.877
0.9858	0.9982	0.9869	0.0201	0.0189	0.0131	0.334	0.126	0.333	0.125	0.333	0.415	0.50	0.333	0.123	0.415	0.335	0.48	0.335	0.127	0.417	0.52
0.9997	0.9959	0.9971	0.0022	0.0021	0.0072	0.168	0.126	0.167	0.125	0.167	0.166	0.875	0.167	0.125	0.166	0.169	0.873	0.169	0.127	0.168	0.877
0.9988	0.9858	0.9887	0.0075	0.0077	0.0292	0.337	0.378	0.336	0.377	0.336	0.51	0.626	0.336	0.375	0.50	0.626	0.626	0.338	0.379	0.53	0.628
0.9993	0.9968	0.9989	0.0053	0.0035	0.0157	0.51	0.377	0.50	0.376	0.50	0.333	0.625	0.333	0.48	0.333	0.52	0.625	0.52	0.378	0.335	0.627

Table 11.1 (b) Comparison of results between GA-neural-fuzzy model, FEA and numerical analysis.

Relative first natural frequency "f ₁ "	Relative second natural frequency "s _{nf} "	Relative third natural frequency "t _{nf} "	Average Relative first mode shape difference "f _{md} "	Average Relative second mode shape difference "s _{md} "	Average Relative third mode shape difference "t _{md} "	GA-neural-fuzzy Model relative				FEA relative				Numerical relative			
						rcd1	rcd2	rcd1	rcd2	1 st crack depth "rcd1"	1 st crack location "rc1"	2 nd crack depth "rcd2"	2 nd crack location "rc2"	1 st crack depth "rcd1"	1 st crack location "rc1"	2 nd crack depth "rcd2"	2 nd crack location "rc2"
0.9991	0.9987	0.9977	0.0087	0.0025	0.0029	0.335	0.27	0.327	0.19	0.327	0.19	0.19	0.69	0.325	0.17	0.18	0.66
0.9974	0.9997	0.9995	0.0011	0.9852	0.2314	0.168	0.26	0.160	0.18	0.160	0.18	0.411	0.44	0.159	0.16	0.409	0.42
0.9936	0.9975	0.9989	0.0154	0.02	0.0746	0.26	0.26	0.18	0.18	0.18	0.18	0.19	0.44	0.16	0.17	0.17	0.43
0.9975	0.9993	0.9981	0.001	0.0046	0.0862	0.27	0.126	0.19	0.118	0.19	0.118	0.160	0.369	0.17	0.116	0.158	0.367
0.9972	0.9959	0.9886	0.0032	0.0289	0.0114	0.28	0.30	0.20	0.21	0.20	0.21	0.409	0.70	0.18	0.19	0.407	0.68
0.9992	0.9977	0.9975	0.3826	0.2359	0.2311	0.418	0.127	0.338	0.878	0.411	0.120	0.328	0.869	0.408	0.117	0.326	0.866
0.9858	0.9982	0.9869	0.0201	0.0189	0.0131	0.334	0.126	0.418	0.51	0.326	0.118	0.408	0.43	0.324	0.116	0.406	0.41
0.9997	0.9959	0.9971	0.0022	0.0021	0.0072	0.168	0.126	0.169	0.877	0.161	0.119	0.160	0.868	0.158	0.116	0.157	0.867
0.9988	0.9858	0.9887	0.0075	0.0077	0.0292	0.337	0.378	0.338	0.627	0.338	0.371	0.44	0.620	0.328	0.369	0.43	0.618
0.9993	0.9968	0.9989	0.0053	0.0035	0.0157	0.51	0.377	0.43	0.626	0.43	0.370	0.327	0.619	0.42	0.368	0.325	0.617

Table 11.1 (c) Comparison of results between GA-neural model, GA-fuzzy model, MANFIS model and experimental analysis.

Relative first natural frequency "f _{1f} "	Relative second natural frequency "snf"	Relative third natural frequency "tnf"	Average Relative first mode shape difference "fmd"	Average Relative second mode shape difference "smd"	Average Relative third mode shape difference "tmd"	GA-neural Model relative				GA-fuzzy Model relative				MANFIS Model relative				Experimental analysis relative			
						rcd1	rcd2	rcd1	rcd2	rcd1	rcd2	rcd1	rcd2	rcd1	rcd2	rcd1	rcd2	rcd1	rcd2	rcd1	rcd2
0.9991	0.9987	0.9977	0.0087	0.0025	0.0029	0.334	0.26	0.334	0.27	0.334	0.27	0.334	0.27	0.333	0.26	0.333	0.26	0.336	0.28	0.27	0.77
0.9974	0.9997	0.9995	0.0011	0.9852	0.2314	0.167	0.25	0.167	0.25	0.164	0.23	0.164	0.23	0.165	0.24	0.165	0.24	0.169	0.27	0.420	0.52
0.9936	0.9975	0.9989	0.0154	0.02	0.0746	0.25	0.25	0.25	0.25	0.25	0.25	0.25	0.26	0.24	0.24	0.24	0.24	0.27	0.27	0.28	0.53
0.9975	0.9993	0.9981	0.001	0.0046	0.0862	0.26	0.125	0.26	0.125	0.24	0.123	0.24	0.123	0.25	0.124	0.25	0.124	0.28	0.127	0.169	0.378
0.9972	0.9959	0.9886	0.0032	0.0289	0.0114	0.27	0.27	0.27	0.416	0.77	0.26	0.27	0.416	0.26	0.27	0.26	0.27	0.29	0.29	0.418	0.79
0.9992	0.9977	0.9975	0.3826	0.2359	0.2311	0.417	0.126	0.417	0.126	0.875	0.126	0.415	0.126	0.416	0.125	0.416	0.125	0.419	0.128	0.337	0.877
0.9858	0.9982	0.9869	0.0201	0.0189	0.0131	0.333	0.125	0.333	0.125	0.50	0.333	0.123	0.415	0.332	0.124	0.332	0.124	0.335	0.127	0.417	0.52
0.9997	0.9959	0.9971	0.0022	0.0021	0.0072	0.167	0.125	0.167	0.125	0.875	0.125	0.166	0.873	0.166	0.124	0.166	0.124	0.169	0.127	0.168	0.877
0.9988	0.9858	0.9887	0.0075	0.0077	0.0292	0.336	0.377	0.336	0.375	0.51	0.336	0.375	0.50	0.335	0.376	0.335	0.376	0.338	0.379	0.53	0.628
0.9993	0.9968	0.9989	0.0053	0.0035	0.0157	0.50	0.376	0.50	0.376	0.625	0.374	0.333	0.625	0.49	0.375	0.49	0.375	0.52	0.378	0.335	0.627

Table 11.1 (d) Comparison of results between GA-neural model, FEA and numerical analysis.

Relative first natural frequency "fnf"	Relative second natural frequency "snf"	Relative third natural frequency "tnf"	Average Relative first mode shape difference "fmd"	Average Relative second mode shape difference "smd"	Average Relative third mode shape difference "tmd"	GA-neural Model relative				FEA relative				Numerical analysis relative			
						red1	red1	red2	red2	red1	red1	red2	red2	red1	red1	red2	red2
0.9991	0.9987	0.9977	0.0087	0.0025	0.0029	0.334	0.26	0.25	0.75	0.327	0.19	0.19	0.69	0.325	0.17	0.18	0.66
0.9974	0.9997	0.9995	0.0011	0.9852	0.2314	0.167	0.25	0.418	0.50	0.160	0.18	0.411	0.44	0.159	0.16	0.409	0.42
0.9936	0.9975	0.9989	0.0154	0.02	0.0746	0.25	0.25	0.26	0.51	0.18	0.18	0.19	0.44	0.16	0.17	0.17	0.43
0.9975	0.9993	0.9981	0.001	0.0046	0.0862	0.26	0.125	0.167	0.376	0.19	0.118	0.160	0.369	0.17	0.116	0.158	0.367
0.9972	0.9959	0.9886	0.0032	0.0289	0.0114	0.27	0.27	0.416	0.77	0.20	0.21	0.409	0.70	0.18	0.19	0.407	0.68
0.9992	0.9977	0.9975	0.3826	0.2359	0.2311	0.417	0.126	0.335	0.875	0.411	0.120	0.328	0.869	0.408	0.117	0.326	0.866
0.9858	0.9982	0.9869	0.0201	0.0189	0.0131	0.333	0.125	0.415	0.50	0.326	0.118	0.408	0.43	0.324	0.116	0.406	0.41
0.9997	0.9959	0.9971	0.0022	0.0021	0.0072	0.167	0.125	0.166	0.875	0.161	0.119	0.160	0.868	0.158	0.116	0.157	0.867
0.9988	0.9858	0.9887	0.0075	0.0077	0.0292	0.336	0.377	0.51	0.626	0.338	0.371	0.44	0.620	0.328	0.369	0.43	0.618
0.9993	0.9968	0.9989	0.0053	0.0035	0.0157	0.50	0.376	0.333	0.625	0.43	0.370	0.327	0.619	0.42	0.368	0.325	0.617

11.2.1 Analysis of the GA segment of GA-neural model

In the current section, the working principle of GA part of the hybrid model has been analyzed. The GA part has been designed with six inputs i.e. fnf, snf, tnf, fmd, smd and tmd. The four output parameters from the GA model are relative first crack location ($rcl1_{interim}$), relative first crack depth ($rcl1_{interim}$), relative second crack location ($rcl2_{interim}$), relative second crack depth ($rcl2_{interim}$). The extracted vibration characteristics from numerical, finite element and experimental techniques such as relative natural frequencies, relative mode shape differences, relative crack locations and relative crack depths have been used to create the initial data pool of the GA system of the multiple crack diagnostic method.

The mechanism followed to develop the GA model of the GA-neural crack diagnostic system has been inherited from section 7.2 of the thesis.

11.2.2 Analysis of the GA segment of GA-neuro-fuzzy model

There are six inputs and four output parameters used to formulate the GA part of the damage detection hybrid system. The inputs to the GA part are fnf, snf, tnf, fmd, smd, tmd. The first interim outputs from the GA model comprises of interim first relative crack location ($rcl1_{interim1}$), interim first relative crack depth ($rcl1_{interim1}$), interim second relative crack location ($rcl2_{interim1}$) and interim first relative crack depth ($rcl2_{interim1}$). The neural segment has got the interim outputs from the GA model along with the first three relative natural frequencies, first three relative mode shape differences as inputs.

The mechanism adopted to form the GA segment of the proposed GA-neural-fuzzy model for crack diagnosis has been inherited from section 7.2 of Chapter 7.

11.2.3 Analysis of the neural segment of GA-neural model

This section describes the design principle of neural segment of the proposed hybrid crack diagnostic methodology. In the GA-neural model, the GA segment of the hybrid model will give the intermittent result for initial relative crack depths and initial relative crack locations. The neural segment of the GA-neural model has ten neurons representing fnf, snf, tnf, fmd, smd, tmd, interim first relative crack location ($rcl1_{interim1}$), interim first relative crack depth ($rcl1_{interim1}$), interim second relative crack location ($rcl2_{interim1}$) and interim first relative crack

depth ($r_{cd2_interim1}$). The final outputs (four neurons) from the GA-neural model are final first relative crack location (r_{cl1_final}), final first relative crack depth (r_{cd1_final}), final second relative crack location (r_{cl2_final}) and final first relative crack depth (r_{cd2_final}).

The neural network used in the GA-neural model is a ten-layer perceptron. The neural network is trained to give outputs such as relative crack depths and relative crack locations. Fig. 11.1 depicts the GA-neural model with its input and output signals.

11.2.4 Analysis of the neural segment of GA-neuro-fuzzy model

The diamond shape neural model of the three layers intelligent multiple crack detection method has been designed with ten input and four output parameters. The ten inputs comprise of f_{nf} , s_{nf} , t_{nf} , f_{md} , s_{md} , t_{md} and interim first relative crack location ($r_{cl1_interim1}$), interim first relative crack depth ($r_{cd1_interim1}$), interim second relative crack location ($r_{cl2_interim1}$), interim second relative crack depth ($r_{cd2_interim1}$).

The final outputs from the neural segment of the GA-neural-fuzzy model are;

final first relative crack location = “ $r_{cl1_interim2}$ ”

final first relative crack depth = “ $r_{cd1_interim2}$ ”

final second relative crack location = “ $r_{cl2_interim2}$ ”

final second relative crack depth = “ $r_{cd2_interim2}$ ”

Fig. 11.2 presents the GA-neural-fuzzy model with layer wise input and output signals.

The complete architecture of the proposed neural model for multi crack diagnosis mentioned in section 11.2.3 and section 11.2.4 has been formulated using the steps from section 6.3 of the thesis.

11.2.5 Analysis of the fuzzy segment of GA-neuro-fuzzy model

The procedure followed to develop the fuzzy part of the GA-neural-fuzzy model used for crack identification is analyzed in the present section.

The fuzzy layer has ten inputs and four outputs. The inputs to the fuzzy segment of the GA-neuro-fuzzy model are f_{nf} , s_{nf} , t_{nf} , f_{md} , s_{md} , t_{md} with the second interim output from the neural segment i.e. interim first relative crack location ($r_{cl1_interim2}$), interim first relative crack depth ($r_{cd1_interim2}$), interim second relative crack location ($r_{cl2_interim2}$), interim second relative crack depth ($r_{cd2_interim2}$). The final four outputs from the fuzzy segment of the GA-neural-fuzzy model are final first relative crack location (r_{cl1_final}), final first relative crack depth

($rcl1_{final}$), final second relative crack location ($rcl2_{final}$) and final second relative crack depth ($rcl2_{final}$). Fuzzy linguistic terms and fuzzy rule base of the fuzzy model have been made by using the vibration parameters derived from numerical, finite element, experimental analysis and the outputs (relative crack locations and relative crack depths) from the neural segment of the developed hybrid multiple crack diagnosis models. Fuzzification and defuzzification of the data have been carried out to get the final results of relative crack locations and relative crack depths. The mechanism used to fabricate the fuzzy segment has been adopted from section 5.3 of chapter 5.

The pictorial view of the fuzzy segment of the proposed three layer inverse GA-neural-fuzzy model has been presented in Fig. 11.2.

11.3 Results and discussions of GA-neural and GA-neuro-fuzzy models

This section presents and analyses the results from the developed GA-neural and GA-neuro-fuzzy models during the vibration analysis of the cantilever beam structure for multiple crack diagnosis.

From the analysis of the results it is found that the cracks present on the structure affects the vibration signatures of the beam structure. The extracted vibration features from the healthy and damaged beam structures can be used to design crack diagnostic tool. Theoretical, finite element and experimental analysis have been carried out on the cracked beam structure to measure the first three relative natural frequencies and first three average relative mode shape differences, which are subsequently used for designing of the GA, neural and fuzzy segment of the hybrid multiple crack diagnosis inverse technique. The creation of initial data pool, formation of fitness function, crossover and mutation operation to find the best fit solution from the search space have been inherited from section 7.2. The GA segment which is the first layer of the proposed hybrid systems have got six inputs (fnf , snf , tnf , fmd , smd , tmd). The interim outputs from the GA segment of the GA-neural model are relative first crack location ($rcl1_{interim}$), relative first crack depth ($rcl1_{interim}$), relative second crack location ($rcl2_{interim}$), relative second crack depth ($rcl2_{interim}$) where as relative first crack location ($rcl1_{interim1}$), relative first crack depth ($rcl1_{interim1}$), relative second crack location ($rcl2_{interim1}$), relative second crack depth ($rcl2_{interim1}$) are the first interim outputs from the GA segment of

the GA-neuro-fuzzy model . The interim outputs from the GA model along with the first three relative natural frequencies and first three average relative mode shape differences have been used as inputs to the neural i.e. the second layer of the inverse hybrid intelligent models. The ten numbers of inputs to the neural system are processed in the diamond shape ten layer feed forward neural network trained with back propagation algorithm to give the results. The training patterns used for the neural model follow the same pattern as discussed in Table 6.1 of chapter 6. The final results from the GA-neural model are relative first crack location ($rcl1_{final}$), relative first crack depth ($rcl1_{final}$), relative second crack location ($rcl2_{final}$), relative second crack depth ($rcl2_{final}$). The complete architecture of the GA-neural model with all the input and output parameters have been shown in Fig. 11.1. The four interim outputs from the neural segment of the GA-neuro-fuzzy model are relative first crack location ($rcl1_{interim2}$), relative first crack depth ($rcl1_{interim2}$), relative second crack location ($rcl2_{interim2}$), relative second crack depth ($rcl2_{interim2}$). The fuzzy Gaussian model i.e. the third layer of the GA-neuro-fuzzy system has ten input and four output parameters and the fuzzy layer has been developed in accordance to the fuzzy mechanisms cited in chapter 10. The detail architecture of the GA-Neuro-Fuzzy model with inputs and output parameters are shown in Fig. 11.2. Finally the three layer (GA-neuro-fuzzy) proposed crack diagnostic method provides the results of $rcl1_{final}$, $rcl1_{final}$, $rcl2_{final}$ and $rcl2_{final}$. An experimental set up has been developed to check the authenticity the results obtained from the proposed GA-neural and GA-neuro-fuzzy intelligent systems. A comparison of results among GA-neural model, GA-fuzzy model, MANFIS model and experimental analysis are presented in Table 11.1 (c). The results for relative crack depths and relative crack locations from numerical analysis, finite element analysis and GA-neural model have been presented in Table 11.1 (d). Comparison of results from GA- neural-fuzzy model, GA- neural model, GA-fuzzy and experimental analysis is presented in Table 11.1(a) to establish the accuracy of the hybrid model. The predicted values of crack parameters from the GA- neural-fuzzy model, numerical analysis, finite element analysis are expressed in Table 11.1 (b). The first six columns of the Table 11.1 (a) to Table 11.1 (d)) represents the six numbers of inputs i.e. first three relative natural frequencies and first three relative mode shape differences to be used as inputs to the methodologies as mentioned above to measure the relative crack locations and relative crack depths. The corresponding outputs in terms of relative crack locations and relative crack

depths have been presented in rest of the columns of the Table 11.1 (a) to Table 11.1 (d). The comparison of results among the mentioned techniques has been done to measure the accuracy of the methodologies. From the analysis of the results mentioned in Table 11.1 (c) and Table 11.1 (a) it is observed that, the percentage of deviation of the prediction values for relative crack locations and relative crack depths of the GA- neural, GA-neuro-fuzzy models are 1.68%, 0.18% respectively.

11.4 Summary

This section depicts the conclusions drawn based on the results obtained from the GA-neural and GA-neuro-fuzzy analysis carried out on the beam structure.

In the current analysis hybrid intelligent methods are presented for multiple cracks diagnosis in beam like structures based on the combination of genetic algorithm, neural network and fuzzy logic. The extracted vibration features for the cracked and undamaged beam structures using theoretical, finite element and experimental analysis have been used to design and train the GA, neural and fuzzy segments of GA-neural and GA-neuro-fuzzy model. The computed vibration parameters are used to set up the initial data pool of the GA model. Selection (evaluation of each solution), reproduction (crossover and mutation) and replacement of unfit population with new one have been used to find the optimal solution (interim outputs) from the search space for the GA segment of the hybrid models. The results obtained from GA-neuro-fuzzy model, GA- neural model, GA-fuzzy model, MANFIS model, numerical analysis, finite element analysis and experimental analysis indicate that the proposed approaches i.e. GA-neuro-fuzzy model and GA- neural model can be efficiently used for the analysis and diagnosis of multiple cracks present in beam structures. During the analysis of the results presented in Table 11.1 (c) and Table 11.1 (a) it is observed that, the percentage of deviation in the prediction values of relative first crack location, relative second crack location, relative first crack depth, relative second crack depth from GA-neural and GA-neuro-fuzzy system are found to be 1.68% and 0.18% respectively. By analyzing the results from the proposed GA-Neural-Fuzzy and GA-neural methodologies, it is observed that the developed hybrid models can be used as online crack diagnostic tools for vibrating structures.

In future the proposed methodologies can be used for health monitoring of dynamically vibrating complex structures.

Paper communicated to International Journal:

1. D.R. Parhi, A.K. Dash, "Analyzing the GA, NN and FL for development of a hybrid vibration system for condition monitoring of cracked structure" Proceedings of the Institution of Mechanical Engineers, Part E: Journal of Process Mechanical Engineering.

Chapter 12

ANALYSIS AND DESCRIPTION OF EXPERIMENTAL SETUP

The experimental analysis has been carried out to measure the natural frequencies and mode shapes of the cracked beam structure. The experimental set up has been shown in Fig.12.1. Experiments have been performed on the cracked beam structures with different crack locations and crack depths to validate the results obtained from theoretical, finite element and other artificial intelligent techniques used for multiple crack detection as discussed in the previous chapters of the thesis. This chapter briefly describes the systematic procedures adopted for experimental investigation and the required instrumentation for measuring the vibration characteristics of the cantilever beam structures.

13.1 Detail specifications of the vibration measuring instruments

Experiments have been performed using the developed experimental set up (Fig. 12.1) for measuring the dynamic response (natural frequencies and amplitude of vibration) of the cantilever beam specimens made from Aluminum with dimension 800mm*38mm*6mm. During the experiment the cracked and undamaged beams have been vibrated at their 1st, 2nd and 3rd mode of vibration by using an exciter and a function generator. The vibrations characteristics of the beams correspond to 1st, 2nd and 3rd mode of vibration have been recorded by placing the accelerometer along the length of the beams. The signals from the accelerometer which contains the vibration parameters such as natural frequencies and mode shapes are analyzed and shown on the vibration indicator. The Table 12.1 shown below gives the detail specifications of the instruments used in the current experimental analysis.

Table 12.1 Specifications of the instruments used in the experimental set up

SL NO	Name of the Instrument	Description
1	Vibration Analyzer	Type : 3560L Product Name : Pocket front end Make : Bruel & kjaer Frequency : 7 Hz to 20 Khz Range ADC Bits : 16 Simultaneous Channels : 2 Inputs, 2 Tachometer Input Type : Direct/CCLD
2	Delta Tron Accelerometer	Type : 4513-001 Make : Bruel & kjaer Sensitivity : 10mv/g-500mv/g Frequency Range : 1Hz-10KHz Supply voltage : 24volts Operating temperature Range : -50 ⁰ C to +100 ⁰ c
3	Vibration indicator	PULSE LabShop Software Version 12 Make : Bruel & kjaer
4	Vibration Exciter	Type : 4808 Permanent Magnetic Vibration Exciter Force rating 112N (25 lbf) sine peak (187 N (42 lbf) with cooling) Frequency Range : 5Hz to 10 kHz First axial resonance : 10 kHz Maximum bare table Acceleration : 700 m/s ² (71 g) Continuous 12.7 mm (0.5 in) peak-to-peak displacement with over travel stops Two high-quality, 4-pin Neutrik® Speakon® connectors Make : Bruel & kjaer
5	Power Amplifier	Type : 2719 Power Amplifier : 180VA Make : Bruel & kjaer
6	Test specimen	Cracked (Multiple crack) cantilever beams made from Aluminum with dimension 800mmx38mmx6mm
7	Power Distribution	220V power supply, 50Hz

8	Function Generator	Model : FG200K Frequency Range : 0.2Hz to 200 KHz VCG IN connector for Sweep Generation Sine, Triangle, Square, TTL outputs Output Level : 15Vp-p into 600 ohms Rise/Fall Time : <300nSec Make : Aplab
---	---------------------------	--



Fig. 12.1 View of the experimental set-up

12.2 Experimental procedure and its architecture

The authenticity of the results obtained from theoretical, finite element and AI based techniques for multiple crack identification have been established by measuring the dynamic response of the undamaged and cracked Aluminum beam specimen through experimentation. The cracks at various locations with different depths in the beam were introduced by a saw perpendicular to the longitudinal axis of the beam. The test specimen made from Aluminum is of 800 mm length and has a cross section of 38mmx6 mm. The cantilever beam test sample was clamped at its one end by two clamping devices as shown in the Fig. 12.1. The free end of the beam specimen was excited by an appropriate signal from the function generator, which was amplified by the amplifier. The cantilever was excited at first three modes of vibration, and the corresponding natural frequencies and mode shapes were recorded by the hard ware support i.e. miniature accelerometer by suitable positioning, data acquisition system and tuning the vibration generator at the corresponding resonant frequencies. Finally, the analysis of the vibration parameters from the intact and cracked beam were done by the PULSE Labshop Software loaded in the laptop of the vibration analyzer. The pictorial views of the various instruments used in the current experimental analysis are shown in Fig. 12.2(a) to Fig. 12.2(h). The PCMCIA card is used to connect the vibration analyzer with the PULSE Labshop Software



Fig.12.2 (a) Vibration analyzer

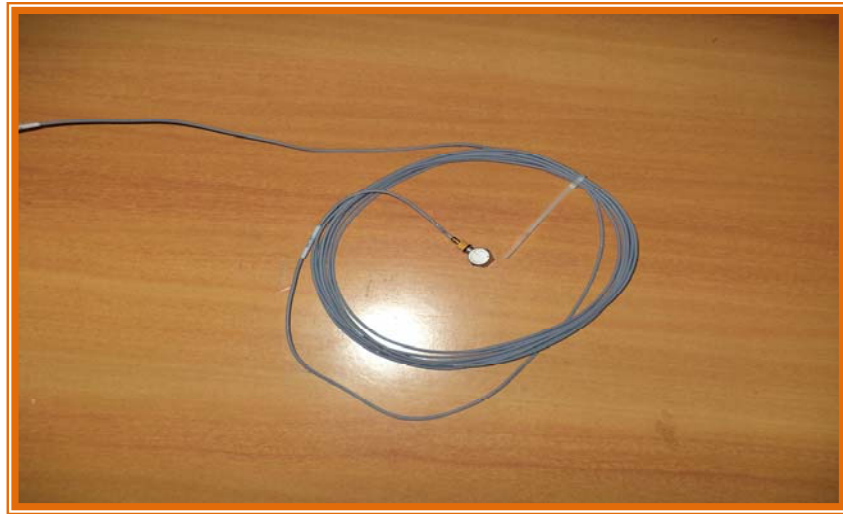


Fig.12.2 (b) Data acquisition (accelerometer)



Fig.12.2 (c) Concrete foundation with beam specimen



Fig.12.2 (d) Function generator



Fig.12.2 (e) Power amplifier



Fig.12.2 (f) Vibration exciter



Fig.12.2 (g) Vibration indicator (PULSE labShop software)



Fig.12.2 (h) PCMCIA card

12.3 Results and discussions of experimental analysis

This section depicts the analysis of the results obtained from the developed experimental set up.

The cracked beam with different crack depths and crack locations have been tested to obtain the mode shape and natural frequency to validate the results from the various techniques cited above. In chapter three Fig. 3.6 to Fig. 3.8 represents the comparison of mode shapes of a multiple cracked beam with crack parameters $a_1/W=0.166$, $L_1/L=0.0625$, $a_2/W=0.25$, $L_2/L=0.3125$ from experimental and numerical analysis. The mode shape for an undamaged beam is also compared in the same figure i.e. Fig. 3.6 to Fig.3.8 to establish the fact that, the mode shape of an undamaged beam behaves differently than a cracked beam. Table 3.1 has been presented in chapter 3 to show the comparison of results from experimental and numerical analysis for a multiple cracked beam and the results are found to be in close agreement. The mode shapes obtained from the finite element analysis in chapter 4 for a multiple cracked cantilever structure ($a_1/W=0.166$, $L_1/L=0.3125$, $a_2/W=0.083$, $L_2/L=0.625$) is compared with the results from numerical and experimental analysis in Fig.4.2 to Fig.4.4. Ten sets of results for relative crack locations and relative crack depths have been presented in Table 4.1 in chapter 4 to show the comparison between the experimental and finite

element analysis. The results are found to be well in agreement. In chapter five, the results for relative crack locations and relative crack depths from experimental analysis is compared with that of the fuzzy Gaussian, fuzzy triangular and fuzzy trapezoidal model in Table 5.3 and they are observed to be well in agreement. The results for relative crack locations and relative crack depths from the neural model as discussed in chapter six are compared with that of the experimental set up and presented in Table 6.2. The results are found to be in close proximity. The results of 1st, 2nd relative crack locations and relative crack depths for ten sets of different inputs from the GA model in chapter seven are compared with the results from experimental analysis in Table 7.2. The results are in good agreement. The results for relative crack depths and crack locations of the Gaussian based fuzzy-neuro, Triangular based fuzzy-neuro, trapezoidal based fuzzy-neuro model are compared with the results from experimental analysis in table 8.1 in chapter eight and they are found to be in close agreement. The Table 9.1 presents the comparison of results for relative crack locations and crack depths derived from the developed MANFIS technique with that of the experimental technique, showing the effectiveness of the MANFIS model. The predicted values of relative crack depths and crack locations from the GA-fuzzy, GA-neural and GA-neuro-fuzzy methodology have been compared with that of the experimental values in Table 10.4, Table 11.1(c) and Table 11.1(a) in chapter 10 and chapter 11 respectively and the values are in good agreement.

Chapter 13

RESULTS AND DISCUSSIONS

13.1 Introduction

Investigation of the feasibility of the methods as mentioned in the thesis have been carried out, in the current chapter by systematically studying and presenting the performance of each methodology used for prediction of multiple crack in a cracked cantilever beam structure. The vibration response of the multi cracked beam members have been considered to develop the crack diagnostic applications. The various techniques applied in the current research for identification of cracks in damaged structures are eleven in numbers and they are theoretical analysis (Chapter-3), finite element analysis (Chapter-4), Fuzzy Inference System (Chapter-5), Artificial neural network (Chapter-6), Genetic Algorithm (Chapter-7), Fuzzy-Neuro technique (Chapter-8), MANFIS technique (Chapter-9), GA-fuzzy technique (Chapter-10), GA-neural and GA-neuro-fuzzy technique (Chapter-11), Experimental technique (Chapter-12).

13.2 Analysis of results

In the present investigation, for development of multiple crack detection methodologies in structural systems eleven different techniques (Chapter 3 to chapter 12) have been employed as cited in the introduction section of the current chapter. Besides the eleven chapters, the thesis comprises of two other introductory chapters and they are chapter 1- Introduction and chapter 2-Literature review. This section depicts the analysis of the results from different chapters of the current research.

Chapter one the introduction section of the thesis presents the motivation factors to carry out the present research along with the aim and objective of the present investigation. Finally, the outlines of the research work have been discussed.

In chapter two various methodologies applied by researchers since last few decades for fault detection in engineering systems have been discussed. Applications of AI techniques for damage and fault diagnosis in different mechanical and electrical systems have also been

discussed. This section in particular, provides the knowledge for finalizing the direction of research.

The analytical model used to compute the vibration parameters of multiple cracked and un-crack cantilever beam structure (Fig. 3.1) and an in depth discussion of the theoretical model have been made in chapter three of the thesis. During the vibration analysis of the multi cracked cantilever beam (Fig. 3.3) the first three relative natural frequencies and first three relative mode shape differences of the cracked and undamaged beam have been measured. From the results it is evident that, the dimensionless compliances increase with increase with the relative crack depths, due to the introduction of local flexibility which have been established graphically in Fig. 3.2. Comparison of the mode shapes obtained from the numerical analysis for the cracked and undamaged beam have been shown in Fig. 3.4. A noticeable effect on the mode shapes of the cracked beam as compared to the undamaged beam at the vicinity of the crack locations can be seen in the magnified view of Fig. 3.4. The experimental validation of the results from the theoretical model has been carried out in this chapter by using the developed experimental set up as shown in Fig. 3.5. The comparison of the mode shapes from the experimental analysis with that of the numerical analysis for the cracked and undamaged beam are presented in Fig. 3.6 to Fig. 3.8 and they are found to be in close proximity. A comparison of relative crack locations and relative crack depths from the numerical and experimental analysis have been presented in Table 3.1, which shows the robustness of the analytical model developed for crack detection.

In chapter four finite element analysis has been applied to measure the dynamic response (natural frequencies, mode shapes) of the cracked cantilever beam structure. A cracked beam element (Fig. 4.1) has been considered to perform the finite element analysis to evaluate the first three natural frequencies and first three mode shapes. The mode shapes of the cracked beam obtained from the finite element analysis has been compared with the theoretical and experimental method in Fig. 4.2 to Fig. 4.4, and they are found to be very close. A comparison of results for relative crack locations and relative crack depths from FEA, numerical analysis and experimental analysis have been shown in Table 4.1, and they are found to be in close agreement.

Chapter five describes the steps used to design and develop fuzzy inference system to diagnose the damage parameters (locations, depths) present in beam like structures in section

5.2. The fuzzy models have been designed with the help of Gaussian membership function (Fig.5.1 (a)), triangular membership function (Fig.5.1 (b)) and trapezoidal membership functions (Fig.5.1(c)). Detail architecture of the fuzzy inference system with the input and output parameters are shown in Fig. 5.2. The fuzzy models used in the current research for prediction of crack locations and their severities are fuzzy Gaussian (Fig. 5.3 (a)), fuzzy triangular (Fig. 5.3 (b)) and fuzzy trapezoidal (Fig. 5.3 (c)) models. The fuzzification mechanism using the Gaussian, triangular and trapezoidal membership functions with fuzzy linguistic terms in details are graphically presented in Fig. 5.4, Fig. 5.5 and Fig. 5.6 respectively. The fuzzy linguistic terms used for formulation of the fuzzy inference system is expressed in Table 5.1. Out of several hundred fuzzy rules used for fabrication of the fuzzy system for crack detection, twenty numbers are presented in Table 5.2. The defuzzification process adopted to predict the relative crack locations and relative crack depths by activating the rule no 3 and rule no 17 from Table 5.2 for Gaussian, triangular and trapezoidal fuzzy model are shown in Fig. 5.7, Fig. 5.8 and Fig. 5.9 respectively. Center of gravity procedure has been followed to get the crisp value of the relative crack depths and crack locations. The results for the crack parameters such as relative crack locations and relative crack depths from the developed fuzzy models (Gaussian, triangular, trapezoidal) are compared with that of the numerical, finite element and experimental analysis for validation in Table 5.3 (a) and Table 5.3 (b). From the analysis of results in Table 5.3 (a), it is evident that the fuzzy Gaussian model provides the best results in comparison to other two fuzzy models, theoretical analysis and finite element analysis.

Chapter six enumerates the development of an artificial neural network model trained with back propagation technique for multiple crack diagnosis in beam structures. The working principles with the main features of the neuron model (Fig. 6.1) and the back propagation technique (Fig. 6.2) have been discussed in section 6.2.1. A schematic diagram representing the proposed neural network model with input and output parameters is shown in Fig. 6.3. The working model of the ten layer neural network (Diamond shape) used in the current research for fault detection in beam members with the detail architecture has been exhibited in Fig. 6.4. Table 6.1 presents the test patterns required to train the neural model to predict the relative crack locations and relative crack depths. The results obtained from the neural model for predicting the crack locations and their severities are compared with the results

obtained from the fuzzy models described in the above chapter, theoretical, FEA and experimental analysis in Table 6.2 (a) and Table 6.2 (b). By analyzing the results provided in Table 6.2 (a, b), it can be concluded that the proposed neural network gives better results in comparison to the fuzzy techniques mentioned in the Table 6.2 (a, b).

The genetic algorithm technique has been introduced in chapter seven for multiple damage detection in beam like members. The systematic procedures adopted to design the GA system for damage identification is presented in section 7.2. In the development of evolutionary algorithm natural process like crossover (Fig. 7.1) and mutation (Fig. 7.2) have been adopted to find the fittest solution from the search space. A flow chart (Fig. 7.3) has been presented in section 7.2 to show the flow of data in the developed GA model for crack diagnosis. Table 7.1 presents the initial data pool created to train the GA model from theoretical, FEA and experimental methods. A comparison of results for relative crack depths and relative crack locations among the GA model, neural network, Gaussian fuzzy model, theoretical, FEA and experimental analysis have been carried out in Table 7.2 (a), Table 7.2 (b) and the results are in good agreement. From the analysis of the data provided in Table 7.2 (a), it is clear that, the proposed GA model provides more accurate results in comparison to other techniques such as neural and fuzzy models.

A hybrid fuzzy-neuro technique has been proposed for multiple crack identification and is briefly discussed in chapter eight. The hybrid model has been designed by fusing the features of both fuzzy inference system and artificial neural network. Gaussian membership fuzzy-neuro model (Fig. 8.1), triangular membership fuzzy-neuro model (Fig. 8.2) and trapezoidal membership fuzzy-neuro model (Fig. 8.3) have been designed in the current research to measure the crack locations and their severities. The fuzzy segment of the fuzzy-neuro model has six inputs (first three natural frequencies and first three mode shape difference) and four outputs (initial relative first and second crack locations). The neural network has ten inputs (first three natural frequencies and first three mode shape difference along with the initial output from the fuzzy model) and four outputs (final relative first and second crack locations). The outcome from the hybrid fuzzy-neuro model in the form of relative crack locations and relative crack depths have been compared with that of the experimental, GA model, neural model and Gaussian fuzzy model in Table 8.1 (a) and Table 8.1 (b) . From the

data given in the Table 8.1 (a), it is observed that, the performance of Gaussian fuzzy-neuro model is best as compared to other techniques cited in the Table 8.1 (a). The proposed fuzzy-neuro model can be potentially used as a condition monitoring tool in dynamically vibrating structures.

The multiple adaptive neuro fuzzy inference system has been analyzed in chapter nine for checking the effectiveness of the MANFIS methodology in crack identification. The formulation of the MANFIS technique has been based on the data derived from the theoretical, FEA and experimental techniques. A bell shaped function (Fig. 9.1) has been used in the designing of the proposed model. The MANFIS system used for fault detection in damaged beams is also known as multiple ANFIS system and it is presented in Fig. 9.2 (a). The complete architecture of the MANFIS model used for multiple crack diagnosis in cantilever beam member with different layers has been shown in Fig. 9.2 (b). The superiority of the MANFIS technique has been established by comparing its predicted results with the outputs (relative crack locations and relative crack depths) from Gaussian fuzzy-neuro model, GA model, theoretical analysis, finite element analysis and experimental analysis in Table 9.1 (a) and Table 9.1 (b).

The genetic fuzzy hybrid model (GA-fuzzy) for multiple crack detection has been discussed in chapter ten of the thesis. This damage identification system comprises of two segment i.e. genetic model (first layer) and fuzzy model (second layer). The hybrid model incorporates the characteristics of both genetic algorithm and fuzzy inference system. The genetic model has been designed using the crossover and mutation operator as shown in Fig. 7.1 and Fig. 7.2 of chapter seven. The fuzzy segment model is based on Gaussian membership functions as shown in Fig. 10.1. The Gaussian membership functions for the input and output parameters used for designing of the fuzzy segment of the hybrid system for multiple crack diagnosis are presented in Fig. 10.2. The detail architecture of the proposed model is shown in Fig. 10.3. The fuzzy linguistic terms used for development of the fuzzy segment for the input and output parameters are shown in Table 10.1 and Table 10.2 respectively. Out of several hundred fuzzy rules, ten fuzzy rules are shown in Table 10.3. Finally, the relative crack depths and relative crack locations i.e. the outputs from the GA-fuzzy model have been compared with the results from MANFIS model, Gaussian fuzzy-neuro model, theoretical

analysis, finite element analysis and experimental analysis in Table 10.4 (a) and Table 10.4 (b). From the comparison, it is observed that the GA-fuzzy gives least error output from the actual as compared to other techniques cited in the Table 10.4 (a, b).

Chapter eleven discusses about two layers (GA-neural) and three layers (GA-neuro-fuzzy) hybridized techniques based on genetic algorithm, neural network and fuzzy logic. The GA-neuro-fuzzy and GA-neural model have been devised to diagnose multiple transverse cracks present in beam like structures. The proposed intelligent models integrate the capabilities of genetic algorithm, artificial neural network and fuzzy inference system. The first layer of the proposed models is a GA model. The first layer has been designed based on the steps followed in chapter seven of the thesis using the crossover and mutation operations. Initial data pool has been created to train the GA model in off line mode. A suitable objective function has been formulated to find the best fit solution from the search space. The detail architecture of the GA-neural and GA-neuro-fuzzy model has been shown in Fig. 11.1 and Fig. 11.2 respectively. The GA segment has six inputs (first three relative natural frequencies and first three relative mode shape differences) and four outputs (first interim relative first and second crack locations, first interim relative first and second crack depths for GA-neuro-fuzzy model and interim relative first and second crack locations, interim relative first and second crack depths for GA-neural model). The neural model is a multi layer perceptron trained with back propagation technique and it has been designed following the methodologies mentioned in chapter six of the thesis. The outputs from the GA model along with the first three relative natural frequencies and first three relative mode shape differences are act as inputs to the neural segment (first layer with ten neurons) of the hybrid models. The final outputs from GA-neural model are final relative first and second crack location, final relative first and second crack depth. The interim outputs from the neural model of the GA-neuro-fuzzy system are second interim relative first and second crack locations, second interim relative first and second crack depths (last layer with four neurons). The fuzzy Gaussian model, which is the third layer of the proposed GA-neuro-fuzzy crack diagnostic method, has been designed following the steps used in chapter five and chapter ten of the thesis. The outputs from the neural system with the first three relative natural frequencies and first three relative mode shape differences are used as inputs to the fuzzy system and finally

the outputs from the fuzzy segment are final relative first and second crack locations, final relative first and second crack depths. The results for relative crack depths and relative crack locations from the GA-neuro-fuzzy model have been compared with that of the GA-neural model, GA-fuzzy model, theoretical analysis, finite element analysis and experimental analysis in Table 11.1(a) to Table 11.1(d). By analyzing the data exhibited, it is revealed that, the three layer GA-neuro-fuzzy technique is faster and accurate in predicting the multiple crack parameters as compared to the other methods mentioned in the Table 11.1 (a) and Table 11.1 (c). Hence, the GA-neuro-fuzzy system can be effectively used as crack diagnostic tool in vibrating structural members.

The experimental analysis for validation of the results obtained from GA-neuro-fuzzy model GA-neural model, GA-fuzzy model, MANFIS model, fuzzy-neuro models, neural model, fuzzy models, theoretical analysis, finite element analysis has been discussed in chapter thirteen. The schematic view and photo graphic view of the experimental set up with all the instruments and test specimen is shown in Fig. 3.5 and Fig. 12.1 respectively. The developed experimental set up comprises of the following instruments; 1- Vibration analyzer, 2- Accelerometer, 3- Concrete foundation with test specimen, 4- Function Generator, 5- Power Amplifier, 6- Modal Vibration Exciter, 7- Vibration indicator (embedded with PULSE Labshop software, 8- PCMCIA card and are given in Fig. 12.2(a) to Fig. 12.2(h) respectively. Section 12.2 presents the procedures adopted to carry out the experiments to evaluate the natural frequencies and mode shapes of multi cracked and undamaged cantilever beam structures. Efforts have made to reduce the effect of external parameter such as noise on the vibration signatures of the cracked beam during experimentation.

The author contributions, conclusions drawn from the current research and future directions for further investigation of the present analysis for development of multi crack diagnostic tool have been explained in the next chapter.

Chapter 14

CONCLUSIONS AND FUTURE WORK

In the current investigation, identification and quantification of cracks present in structural members from the measured dynamic response has been addressed. In the quest, to design and develop a multiple crack diagnostic tool a vibrating structural member with multiple transverse cracks has been considered. During the analysis, analytical method, finite element method and experimental method have been adopted to simulate the actual working condition. The measured natural frequencies and mode shapes at different modes of vibration, which are known as sensitive structural integrity indicators have been used to develop inverse methodologies based AI techniques such as fuzzy logic, neural network, genetic algorithm, fuzzy-neuro, MANFIS, GA-fuzzy, GA-neural, GA-neuro-fuzzy techniques for prediction of relative crack locations and relative crack depths.

From the analysis and discussion of the results from the various methodologies cited in the chapters above, the following contributions and conclusions have been depicted in section 14.1, 14.2 and section 14.3 respectively.

14.1 Contributions

It is a fact that, the cracks present in structural systems induces a local flexibility, which is a function of crack parameters such as crack depths and crack locations. This flexibility changes the structural integrity sensitive indicators like frequency response and amplitude of vibration. In previous research, in the domain of crack identification of damaged structures the researchers have studied the effect of crack on the natural frequencies and mode shapes, where as in the current research effort has been made to design artificial intelligent inverse models to predict the crack locations and their severities present in structural systems using the natural frequencies and mode shapes.

In the current investigation for designing multiple crack identification tool an analytical model has been developed using stress intensity factors and strain energy release rate to evaluate the changes made to the vibration indicators due to the cracks present in the damaged structures. Finite element analysis and experimental analysis have also been carried out on the cracked beam member to find out the influence of cracks on the vibration signatures of the beam. Different AI models have been formulated for multiple crack identification using fuzzy inference system, artificial neural network, genetic algorithm and various hybrid techniques such as fuzzy-neuro, MANFIS, GA-fuzzy, GA-neural and GA-neuro-fuzzy

14.2 Conclusions

The conclusions are drawn on the basis of results obtained from various analyses as discussed above are depicted below.

- ❖ Theoretical and finite element analyses have been presented to identify characteristics (natural frequencies, mode shapes) of the system response that is directly attributed to the presence of transverse cracks.
- ❖ During the analysis it is observed that, the change in frequency response due to the presence of cracks (least crack depth ratio) is not so prominent, thereby decreasing the chances of identifying the cracks accurately. But the crack depths have substantial effect on the mode shapes of the vibrating structures even with the presence of small crack depths. So, it can be concluded that the cracks can be efficiently identified with their locations and severities if change in frequency response and change in mode shapes both are taken into account.
- ❖ The deviations in mode shape contours at the vicinity of the crack locations are very significant and can be seen during the comparison of mode shapes obtained from the numerical analysis performed on the cracked and intact beam in Fig. 3.4. From the observations of the mode shapes of the cracked cantilever beam with different crack locations and crack depths, a significant pattern has been identified i.e. the magnitude of deviation in mode shapes increases with increase in crack depths.

- ❖ Experimentations on the cracked cantilever beams with different configuration of crack depths and crack locations have been performed to compare the modal parameters obtained from the analytical and finite element model (Fig. 4.2 to Fig. 4.4) and the results are found to be in close agreement.
- ❖ The vibration signatures from the first three modes of the cantilever beam model and the corresponding relative crack depths and crack locations have been used as the platform to design the fuzzy inference system for multiple crack identification in structural members.
- ❖ The fuzzy system has six inputs and four outputs. The fuzzy models are based on fuzzy Gaussian, fuzzy triangular and fuzzy trapezoidal membership functions. From the analysis of results, it has been found that, the proposed fuzzy inverse technique predicts the relative crack locations and their severities faster and more accurately than the theoretical and finite element analysis. Experimental data have also been used to check the authenticity of the results from the fuzzy models.
- ❖ From the analysis of the results of the three fuzzy models for relative crack depths and relative crack locations, it is observed that the fuzzy model with Gaussian membership function yields better results than the fuzzy model with triangular membership function, fuzzy model with trapezoidal membership function. Hence, the fuzzy Gaussian model was found to be most suitable to diagnose cracks in online mode for cracked vibrating engineering applications.
- ❖ A multi layer artificial neural network model with six inputs and four outputs has been fabricated for crack diagnosis in damaged beam structures. The training patterns for the proposed neural model have been derived from theoretical, finite element and experimental analysis. The results predicted by the neural network for relative crack locations and relative crack depths are quite nearer to the experimental results, thereby establishing the fact that the neural model can be successfully used for multiple crack detection in damaged beam structures.
- ❖ From the comparison of results (relative crack depths and relative crack locations) among the fuzzy models and neural model, it is clear that the predicted results from neural system are closer to the actual results as compared to the developed fuzzy models.

- ❖ Genetic algorithm has been adopted to develop a crack diagnostic model in structural members. The GA model comprises of six inputs and four output parameters. The proposed evolutionary algorithm provides results for crack locations and their depths in close proximity to the experimental results.
- ❖ From the analysis of its performance it can be stated that, the GA model can be used as a robust multiple crack identification tool in industrial environment. When the results are compared with that of the fuzzy and neural models, it is observed that the GA gives better results as compared to fuzzy and neural model used for crack identification.
- ❖ A fuzzy-neuro analysis has been carried out to design a hybrid technique for damage detection in beam structures. Three fuzzy-neuro models have been designed with Gaussian, triangular and trapezoidal membership functions. The fuzzy-neuro models have been designed for prediction of relative crack location and their depths of the cracks present in the damaged structures.
- ❖ From the analysis of the results, the performance of fuzzy-neuro model (based on Gaussian membership function) gives results with better accuracy than the independent GA, neural and fuzzy system designed for multiple crack identification. Hence, the fuzzy-neuro model can be used as a condition monitoring tool for faulty structures.
- ❖ Multiple adaptive neuro fuzzy inference system has been applied to develop a fault identification tool in cracked structures. Based on the observations of the predicted results from the MANFIS model, it is revealed that, the MANFIS technique can identify the crack parameters with higher accuracy as compared to fuzzy-neuro, fuzzy, neural and GA model and the results are in close proximity with the experimental analysis. So, the developed crack diagnostic method is capable of identifying faults in a faulty system.
- ❖ The GA-fuzzy two layer hybrid methodology has been designed with six input and four output parameters. By analyzing the results from GA-fuzzy model, it is noticed that the GA-fuzzy results are more accurate in comparison to GA, neural, fuzzy, fuzzy-neuro and MANFIS technique. So, the developed GA-fuzzy technique can be used efficiently and effectively for structural health monitoring in online mode.

- ❖ The genetic algorithm and neural network have been adopted to develop a hybrid method (GA-Neural) for multiple damage identification in cracked beam members. The predicted results for relative crack depths and relative crack locations from the GA-neural model demonstrate its applicability for multiple crack diagnosis.
- ❖ By comparing the results from the GA-neural model with that of the GA-fuzzy, MANFIS and experimental technique, it is observed that, GA-neural model delivers results in close proximity to the actual working condition as regard to other AI techniques mentioned earlier. The proposed methodology can be successfully used for condition monitoring of vibrating structures.
- ❖ A three layer (GA-neuro-fuzzy) hybrid intelligent system has been proposed to identify both locations and severities of the damages in structural systems based on the dynamic response of cracked vibrating cantilever structure. The calculated vibration parameters from theoretical, finite element and experimental analysis are used to develop the initial data pool of the GA model, training patterns of the neural segment and to design the fuzzy membership functions.
- ❖ The results from the proposed inverse methodology have been validated by comparing with the results obtained from theoretical, finite element and experimental analysis. The results obtained from GA-neuro-fuzzy technique confirms that the developed method can identify the crack positions and their severities with higher accuracy as compared to all other AI based techniques discusses earlier in the thesis and the proposed methodology can be used as an efficient online condition monitoring tool for faulty structures.
- ❖ Finally, the GA-neuro-fuzzy model is found to be best suitable artificial intelligent model to identify multiple cracks in damaged vibrating structures with least error.
- ❖ The developed crack diagnostic intelligent system can be utilized for online condition monitoring of turbine shafts, cantilever type bridges, cantilever type cranes used for mega structures, mechanical structures, beam like structures, marine structures, engineering applications, etc.

14.3 Future work

- The artificial intelligent techniques may be developed to diagnose faults in complex engineering structures.
- The application of the artificial intelligent techniques may be extended for multiple damage detection in bi material and composite material elements.
- More robust hybrid techniques may be developed and employed for fault detection of various vibrating parts in dynamic systems such as cone crusher, railway tracks, over head cranes, oil rigs, turbine shafts etc.
- The artificial intelligence techniques may be embedded and integrated with the vibrating systems to make on line condition monitoring easier.

REFERENCES:

1. E. Z. Moore, K.D. Murphy , J. M. Nichols , Crack identification in a freely vibrating plate using Bayesian parameter estimation, *Mechanical Systems and Signal Processing* (2011), 25(6),pp.2125-2134,2011.
2. Z.Q. Lang, G. Park, C.R. Farrar, M.D. Todd, Z. Mao, L. Zhao, K. Worden, Transmissibility of non-linear output frequency response functions with application in detection and location of damage in MDOF structural systems, *Int. J. Non-Linear Mech.* (2011), 46(6),pp.841-853,2011
3. H. Hein, L. Feklistova, Computationally efficient delamination detection in composite beams using Haar wavelets, *Mechanical Systems and Signal Processing*, 25(6), pp.2257-2270, 2011.
- 4.Y. C. Huh, T.Y. Chung, S. J. Moon, H. G. Kil, J. K. Kim, Damage detection in beams using vibratory power estimated from the measured accelerations, *Journal of Sound and Vibration* ,330(15),pp.3645-3665,2011.
5. A. Salam, Y. Alsabbagh, O.M. Abuzeid , Mohammad H. Dado, Simplified stress correction factor to study the dynamic behavior of a cracked beam”, *Applied Mathematical Modelling*, 33, pp. 127–139,2009.

- 6.E. Douka, S. Loutridis, A. Trochidis, Crack identification in beams using wavelet analysis, *International Journal of Solids and Structures*, 40, pp. 3557–3569, 2003.
7. H. Nahvi and M. Jabbari, Crack detection in beams using experimental modal data and finite element mode, *International Journal of Mechanical Sciences*, 47, pp. 1477-1497, 2005.
8. M.M. R. Tahaa and J. Lucero, Damage identification for structural health monitoring using fuzzy pattern recognition, *Engineering Structures*, 27, pp.1774–1783, 2005.
9. A.K. Mahamad, S. Saon and T. Hiyama, Predicting remaining useful life of rotating machinery based artificial neural network, *Computers and Mathematics with Applications*, 60, pp.1078-1087, 2010.
10. F. Kong and R. Chen, A combined method for triplex pump fault diagnosis based on wavelet transform, fuzzy logic and neuro-networks, *Mechanical Systems and Signal Processing*, 18, pp.161–168, 2004.
11. W. Liu, W. Gao, Y. Sun, and M. Xu, Optimal sensor placement for spatial lattice structure based on genetic algorithms, *Journal of Sound and Vibration*, 317, pp. 175–189, 2008.
12. J. Sanza, R. Pererab ,C. Huertab, Fault diagnosis of rotating machinery based on auto-associative neural networks and wavelet transforms, *Journal of Sound and Vibration*, 302, pp.981–999, 2007.
13. A.J. Hoffman and N.T. van der Merwe, The application of neural networks to vibrational diagnostics for multiple fault conditions, *Computer Standards & Interfaces*, 24, pp.139–149, 2002.
14. S.M. Murigendrappa, S.K. Maiti and H.R. Srirangarajan, Experimental and theoretical study on crack detection in pipes filled with fluid, *Journal of Sound and Vibration*, 270, pp.1013–1032, 2004.

15. A.K. Darpe, K. Gupta and A. Chawla, Experimental investigations of the response of a cracked rotor to periodic axial excitation, *Journal of Sound and Vibration*, 260, pp. 265–286, 2003.
16. T. Curry and E.G. Collins, Robust Fault Detection and Isolation Using Robust ℓ_1 Estimation, *Proceeding of the 2004 American Control Conference Boston*, Massachusetts, June 30 - July 2, 2004.
17. P. C. Muller, J. Bajkowski and D. Söffker, Chaotic motions and fault detection in a cracked rotor, *Nonlinear Dynamics*, 5, pp.233-254, 1994.
18. G. M. Owolabi, A. S. J. Swamidas and R. Seshadri, Crack detection in beams using changes in frequencies and amplitudes of frequency response functions, *Journal of Sound and Vibration*, 265, pp.1-22, 2003.
19. S. Chinchalkar, Determination of crack location in beams using natural frequencies, *Journal of Sound and Vibration*, 247, pp. 417-429, 2001.
20. H. Tada, P.C. Paris and G.R. Irwin, *The stress analysis of cracks hand book*. Del Research Corp. Hellertown, Pennsylvania, 1973.
21. S. Loutridis, E. Douka and L.J. Hadjileontiadis, Forced vibration behaviour and crack detection of cracked beams using instantaneous frequency”, *NDT&E International*, 38, pp. 411–419, 2005.
22. O. Song, T.W. Ha and L. Librescu, Dynamics of anisotropic composite cantilevers weakened by multiple transverse open cracks, *Engineering Fracture Mechanics*, 70, pp. 105–123, 2003.
23. D. Ravi and K.M. Liew, A study of the effect of micro crack on the vibration mode shape, *Engineering Structures*, 22, pp. 1097–1102, 2000.
24. S.S. Law and Z.R. Lu, Crack identification in beam from dynamic responses, *Journal of Sound and Vibration*, 285, pp. 967–987, 2005.

25. M. H. Dado, A Comprehensive Crack Identification Algorithm for Beams Under Different End Conditions, *Applied Acoustics*, 51, pp. 381-398, 1997.
26. E. Douka and L.J. Hadjileontiadis, Time–frequency analysis of the free vibration response of a beam with a breathing crack, *NDT&E International*, 38, pp. 3–10, 2005.
27. S. Benfratello, P. Cacciola, N. Impollonia, A. Masnata and G. Muscolino, Numerical and experimental verification of a technique for locating a fatigue crack on beams vibrating under Gaussian excitation, *Engineering Fracture Mechanics*, 74, pp. 2992–3001, 2007.
28. M.Fledman, Hilbert transform in vibration analysis, *Mechanical systems and signal processing*, Vol. 25(3), pp.735–802, 2011.
29. R. Ruotolo, C. Surace, P. Crespu and D. Storer, Harmonic analysis of the vibrations of a cantilevered beam with a closing crack, *Computers & Structures*, 61(6), pp. 1057-1074, 1996.
- 30.M. Behzad, A. Ebrahimi and A. Meghdari, A Continuous Vibration Theory for Beams with a Vertical Edge Crack, *Scientia Iranica*, 17, pp. 194-204, 2010.
31. R.S. Prasad, SC Roy and KP Tyagi, Effect of Crack Position along Vibrating Cantilever Beam on Crack Growth Rate, *International Journal of Engineering Science and Technology*, 2, pp.837-839, 2010.
32. M. Rezaee and R.Hassannejad, free vibration analysis of simply supported beam with breathing crack using perturbation method”, *Acta Mechanica Solida Sinica*, 23, pp.459-470, 2010.
33. A.D. Dimarogonas and C.A. Papadopoulos, Vibration of cracked shafts in bending, *Journal of Sound and Vibration*, 91, pp- 583-593,1983.
34. B. Faverjon and J.J. Sinou, Identification of open crack in a beam using an a posteriori error estimator of the frequency response functions with noisy measurements, *European Journal of Mechanics*,28, pp.75-85,2009

35. K. Mazanoglu, I. Yesilyurt and M. Sabuncu, Vibration analysis of multiple cracked non-uniform beams, *Journal of sound and vibration*, 320, pp.977-989, 2009.
36. K.Wang, J.D.Inman and R.F.Charles, Modeling and analysis of a cracked composite cantilever beam vibrating in coupled bending and torsion, *Journal of sound and vibration*, 284, pp.23-49, 2004.
37. S. M. Al-said , Crack detection in stepped beam carrying slowly moving mass, *Journal of sound and vibration*, 14, pp-1903-1920,2008.
38. J. H. Lee, Identification of multiple cracks in a beam using natural frequencies, *Journal of sound and vibration*, 320, pp-482-490, 2009.
39. H.Yumin, Y. Junjie, C. Xuefeng and H. Zhengjia ,Discussion on calculation of local flexibility due to crack in a pipe, *Mechanical systems and signal processing*, 23, pp.804-810,2009.
40. J. Zou, J. Chen, J.C. Niu, and Z.M. Geng ,Discussion on the local flexibility due to the crack in a cracked rotor system, *Journal of sound and vibration*, 262, pp.365-369,2003.
41. M.N. Cerri, M. Dilella, and G.C. Ruta, Vibration and damage detection in undamaged and cracked circular arches: Experimental and Analytical results', *Journal of sound and vibration*, 314, pp.83-94,2008.
42. L. Nobile, C. Carloni, and M. Nobile ,Strain energy density prediction of crack initiation and direction in cracked T beams and pipes, *Theoretical and Applied fracture mechanics*, 41, pp.137-145,2004.
43. J. Humar, A. Bagchi, and H. Xu , Performance of vibration based techniques for the identification of structural damage, *Structural health monitoring*,5, pp-215-241,2006.
44. E. Voila, M. Dilella and F. Tornabene, Analytical and Numerical Results for Vibration Analysis of multi-stepped and multi-damaged circular arches, *Journal of Sound and vibration*, 299, pp.143-163,2007.

45. Y.J. Shin , K.M. Kwon, and J.H. Yun, Vibration analysis of a circular arch with variable cross section using differential transformation and generalized differential quadrature, *Journal of Sound and Vibration* ,309, pp-9-19,2008.
46. M.N. Cerri, and G.C. Ruta, Detection of localized damage in plane circular arches by frequency data, *Journal of Sound and vibration* , 270, pp.39-59,2004.
47. A. Labuschagne, N.F.J. Van Rensburg and A.J.V. Merwe, Comparison of linear beam theories, *Mathematical and Computer Modeling*, 79, pp-20-30, 2009.
48. T.R. Babu, and A.S. Sekhar, Detection of two cracks in a rotor-bearing system using amplitude deviation curve, *Journal of Sound and Vibration*, 314, pp.457-464, 2008.
49. Y. Xia and H. Hao, Measurement Selection for vibration based Structural damage identification, *Journal of Sound and Vibration*, 236, pp. 89-104, 2009.
50. E. Douka, G. Bamnios and A. Trochidis, A method for determining the location and depth of cracks in double cracked beams, *Applied Acoustics*, 65, pp.997-1008, 2009.
51. J.K. Sinha, Higher order spectra for crack and misalignment identification in the shaft of rotating machine, *Structural health Monitoring*, 6 , pp-325-334,2007.
52. D.P. Patil and S.K. Maiti, Detection of multiple cracks using frequency measurements, *Engineering Fracture Mechanics*, 70, pp.1553-1572, 2003.
53. J.T. Kim and M. Stubbs ,Improved Damage Identification Method based on modal information, *Journal of Sound and Vibration*, 252, pp. 223-238,2002.
54. S. Ebersbach and Z. Peng, Expert system development for vibration analysis in machine condition monitoring, *Expert systems with Applications*, 34, pp-291-299, 2008.
55. G.D. Gounaris and C.A. PapadoPoulos ,Analytical and experimental crack identification of beam structures in air or in fluid, *Computers and Structures*, 65, pp.633-639,1997.

56. M. H. H. Shen and Y.C. Chu, Vibrations of beams with a fatigue crack, *Computers & Structures*, 45, pp. 79-93, 1992.
57. A. Ebrahimi, M.Behzad and A.Meghdari, A bending theory for beams with vertical edge crack, *International Journal of Mechanical Sciences*, 52, pp.904–913, 2010.
58. M.Jasinski, S.Radkowski, Use of the higher spectra in the low-amplitude fatigue testing, *Mechanical Systems and Signal Processing*, 25, pp.704–716, 2011.
59. M. H.Seyyed, G. Behnam, M.Yaser and A.Saeed, Free transverse vibrations of cracked nano beams with surface effects, *Thin Solid Films*, 519 pp.2477–2482, 2011.
- 60.L. Rubio, B.M. Abella, G.Loaliza, Static behavior of a shaft with an elliptical crack, *Mechanical Systems and Signal Processing* ,25 ,pp.1674–1686,2011.
61. I. Argatov and E.Butcher, On the separation of internal and boundary damage in slender bars using longitudinal vibration frequencies and equivalent linearization of damaged bolted joint response, *Journal of Sound and Vibration* ,330 ,3245–3256,2011
62. R. Farshidi, D. Trieu, S.S. Park and T. Freiheit, Non-contact experimental modal analysis using air excitation and a microphone array, *Measurement*, 43, 755–765, 2010.
63. P.Casini and F. Vestroni, Characterization of bifurcating on linear normal modes in piecewise linear mechanical systems, *International Journal of Non-Linear Mechanics*, 46, 142–150, 2011.
- 64.G.E. Carr, M.D. Chapetti , On the detection threshold for fatigue cracks in welded steel beams using vibration analysis, *International Journal of Fatigue* ,33 , 642–648,2011.
65. M. Fontul, A.M.R. Ribeiro, and J.M.M. Silva, Transmissibility matrix in harmonic and random processes, *Journal Shock and Vibration*, 11, pp. 563-571, 2004.
66. P.N. Saavedra and L.A.Cuitino,Crack detection and Vibration behavior of Cracked beams ,*Computers and Structures*, 79, pp.1451-1459, 2001.

67. G. L. Qian, S. N. Gu and J. S. Jiang, The dynamic behaviour and crack detection of a beam with a crack, *Journal of Sound and Vibration*, 138, pp. 233-243, 1990.
68. U. Andreaus, P. Casini, and F. Vestroni, Non-linear dynamics of a cracked cantilever beam under harmonic excitation, *International Journal of Non-Linear Mechanics*, 42, pp. 566–575, 2007.
69. E. Viola, L. Federici, and L. Nobile, Detection of crack location using cracked beam element method for structural analysis, *Theoretical and Applied Fracture Mechanics*, 36, pp. 23-35, 2001.
70. T.G. Chondros and G.N. Labeas, Torsional vibration of a cracked rod by vibrational formulation and numerical analysis, *Journal of Sound and Vibration*, 301, pp. 994–1006, 2007.
71. A. Ariaei, S. Ziaei-Rad and M. Ghayour, Vibration analysis of beams with open and breathing cracks subjected to moving masses, *Journal of Sound and Vibration*, 326, pp. 709–724, 2009.
72. G.P. Potirniche, J. Hearndon, S.R. Daniewicz, D. Parker, P. Cuevas, P.T. Wang and M.F. Horstemeyer, A two-dimensional damaged finite element for fracture applications, *Engineering Fracture Mechanics*, 75, pp. 3895–3908, 2008.
73. Y. Narkis, Identification of crack location in vibrating simply supported beams, *Journal of sound and vibration*, 172, pp. 549-558, 1994.
74. W. M. Ostachowicz, and M. Krawczuk, Vibration analysis of a cracked beam, *Computers & Structures*, 36, pp. 245-250, 1990.
75. D.Y. Zheng and N.J. Kessissoglou, Free vibration analysis of a cracked beam by finite element method, *Journal of Sound and Vibration*, 273, pp. 457–475, 2004.

76. M. Kisa, and M. G.Arif ,Free vibration analysis of uniform and stepped cracked beams with circular cross sections, *International journal of engineering science*, 45, pp.364-380,2007.
77. M. Karthikeyan, R. Tiwari, and S. Talukdar, Crack localization and sizing in a beam based on free and forced response measurements , *Journal of mechanical systems and signal processing*, 21, pp-1362-1385,2007.
78. J.L. Hearndon, , G.P. Potirniche, D. Parker, P.M. Wevas, H. Rinehart, P.T. Wang and, M.F.H. Meyer ,Monitoring structural damage of components using an effective modulus approach, *Theoretical and applied fracture mechanics*, 50, pp.23-29,2008.
79. S. M. Al-Said , Crack Identification in a stepped beam carrying a rigid disk, *Journal of Sound and Vibration*, 300, pp. 863-876,2007.
80. A.S. Shekhar and B.S. Prabhu, Crack detection and vibration characteristics of cracked shafts, *Journal of sound and vibration*, 157, pp. 375-381, 1992.
81. S. K Panigrahi, Damage analyses of adhesively bonded single lap joints due to delaminated FRP composite adherends, *Applied Composite Materials*, 4, pp. 211-223, 2009.
82. R.P.R. Hasanzadeh, S.H.H. Sadeghi, M. Ravan , A.R. Moghaddamjoo and R.Moini, A fuzzy alignment approach to sizing surface cracks by the AC field measurement technique, *NDT&E International* ,44, 75–83,2011.
83. M. Chandrashekhar and Ranjan Ganguli, Damage assessment of structures with uncertainty by using mode- shape curvatures and fuzzy logic, *Journal of Sound and Vibration*, 26, pp. 939–957,2009.
84. Y. M. Kim, C.K. Kim and G. H. Hong, Fuzzy set based crack diagnosis system for reinforced concrete structures, *Computers and Structures*, 85, pp.1828–1844, 2007.
85. N.Saravanan, S.Cholairajan and K.I.Ramachandran, Vibration-based fault diagnosis of spur bevel gear box using fuzzy technique, *Expert Systems with Applications*, 36, pp.3119–3135, 2009.

86. T. Boutros and M. Liang, Mechanical fault detection using fuzzy index fusion, *International Journal of Machine Tools & Manufacture*, 47, pp. 1702–1714, 2007.
87. Q. Wu and R. Law, Complex system fault diagnosis based on a fuzzy robust wavelet support vector classifier and an adaptive Gaussian particle swarm optimization, *Information Sciences*, 180, pp. 4514–4528, 2010.
88. V. Sugumaran and K.I. Ramachandran, Fault diagnosis of roller bearing using fuzzy classifier and histogram features with focus on automatic rule learning, *Expert Systems with Applications*, 38(5), pp. 4901–4907, 2011.
89. L. J. de Miguel and L. F. Blazquez, Fuzzy logic-based decision-making for fault diagnosis in a DC motor, *Engineering Applications of Artificial Intelligence*, 18, pp. 423–450, 2005.
90. K. Wada, N. Hayano, and H. Oka, Application of the fuzzy control method for level control of a hopper, *Advanced Powder Technology*, 2, pp. 163–172, 1991.
91. D. R. Parhi, Navigation of mobile robot using a fuzzy logic model. *Journal of Intelligent and Robotic Systems: Theory and Applications*, 42, pp. 253–273, 2005.
92. J. Fox, Some observations on fuzzy diagnosis and medical computing, *International Journal of Bio-Medical Computing*, 8, pp. 269–275, 1977.
93. H.J. Zimmermann, Fuzzy programming and linear programming with several objective functions, *Fuzzy Sets and Systems*, 1, pp. 45–55, 1978.
94. P. Angelov, E. Lughofer, X. Zhou, Evolving fuzzy classifiers using different model architectures, *Fuzzy Sets and Systems*, 159, pp. 3160–3182, 2008.
95. D. K. Mohanta, P. K. Sadhu, R. Chakrabarti, Fuzzy Markov Model for Determination of Fuzzy State Probabilities of Generating Units Including the Effect of Maintenance Scheduling, *IEEE Transactions on Power Systems*, 20, pp. 2117–2124, 2005.

96. M. Schlechtingen and I. F. Santos, Comparative analysis of neural network and regression based condition monitoring approaches for wind turbine fault detection, *Mechanical Systems and Signal Processing*, 25, pp.1849–1875, 2011.
97. V. N. Ghate, S.V. Dudul, Optimal MLP neural network classifier for fault detection of three phase induction motor, *Expert Systems with Applications*, 37, pp.3468–3481, 2010.
98. I. Eski,S. Erkaya,S. Savas, S. Yildirim, Fault detection on robot manipulators using artificial neural networks, *Robotics and Computer-Integrated Manufacturing*, 27 ,pp. 115–123,2011.
99. B. Fan, Z. Du, X. Jin, X. Yang, Y. Guo, A hybrid FDD strategy for local system of AHU based on artificial neural network and wavelet analysis, *Building and Environment* ,45, pp.2698-2708.
100. G. Paviglianiti, F. Pierri, F. Caccavale and M. Mattei, Robust fault detection and isolation for proprioceptive sensors of robot manipulators, *Mechatronics*, 20, 162–170, 2010.
101. C.C.Wang, Y. Kang, P.C. Shen, Y.P. Chang and Y.L.Chung, Applications of fault diagnosis in rotating machinery by using time series analysis with neural network, *Expert Systems with Applications*, 37, 1696–1702, 2010.
102. S. Suresh,S.N. Omkar, R. Ganguli and V. Mani, Identification of crack location and depth in a cantilever Beam Using a Modular Neural Network Approach, *Smart Materials and Structures*, 13, pp. 907-916,2004.
103. W. A. Little and G. L. Shaw, Analytic study of the memory storage capacity of a neural network, *Mathematical Biosciences*, 39(3-4), pp. 281-290, 1978.
104. M. Mehrjoo, N. Khaji, H. Moharrami and A. Bahreininejad, Damage detection of truss bridge joints using Artificial Neural Networks, *Expert Systems with Applications*, 35, pp. 1122–1131, 2008.

105. F.J. Agosto, D. Serrano, B. Shafiq and A. Cecchini, Neural network based nondestructive evaluation of sandwich composites, *Composites: Part B*, 39, pp. 217–225, 2008.
106. N. Saravanan, V.N.S. Kumar Siddabattuni and K.I. Ramachandran, Fault diagnosis of spur bevel gear box using artificial neural network (ANN), and proximal support vector machine (PSVM), *Applied Soft Computing*, 10, pp. 344–360, 2010.
107. A.J. Oberholster and P.S. Heyns, On-line fan blade damage detection using neural networks, *Mechanical Systems and Signal Processing*, 20, pp. 78–93, 2006.
108. J.D. Wu and J.J. Chan, Faulted gear identification of a rotating machinery based on wavelet transform and artificial neural network, *Expert Systems with Applications*, 36, pp. 8862–8875, 2009.
109. J.D. Wu and C.H. Liu, Investigation of engine fault diagnosis using discrete wavelet transform and neural network, *Expert Systems with Applications*, 35, pp. 1200–1213, 2008.
110. Meruane and W. Heylen, An hybrid real genetic algorithm to detect structural damage using modal properties, *Mechanical Systems and Signal Processing*, 25, pp. 1559–1573, 2011.
111. M. Nobahari and S.M. Seyedpoor, Structural damage detection using an efficient correlation-based index and a modified genetic algorithm, *Mathematical and Computer Modelling*, 53, pp. 1798–1809, 2011.
112. B. Li, P. I. Zhang, H. Tian, S.S. Mi, D.S. Liu and G.G. Ren, A new feature extraction and selection scheme for hybrid fault diagnosis of gearbox, *Expert Systems with Applications*, 38, pp. 10000–10009, 2011.
113. S. B. Fernando, B. R. Marta and P. F. Carlos, Damage detection with genetic algorithms taking into account a crack contact model, *Engineering Fracture Mechanics*, 78, pp. 695–712, 2011.

114. H. Han, B. Gu, T. Wang and Z.R. Li, Important sensors for chiller fault detection and diagnosis (FDD) from the perspective of feature selection and machine learning, *International Journal of refrigeration*, 34 , pp.586-599,2011.
115. S.Hussain, H. A. Gabbar, A novel method for real time gear fault detection based on pulse shape analysis, *Mechanical Systems and Signal Processing*, 25, pp.1287–1298, 2011.
116. S.K. Singh and R. Tiwari, Identification of a multi-crack in a shaft system using transverse frequency response functions, *Mechanism and Machine Theory*, 45, pp.1813–1827, 2010.
117. Y. Lei, M.J. Zuo, Z. He and Y.Zi, A multidimensional hybrid intelligent method for gear fault diagnosis, *Expert Systems with Applications*, 37, pp.1419–1430, 2010.
118. S. Sette, L. Boullart-Lieva and V. Langenhove, Optimizing a production process by a neural network/genetic algorithm approach, *Engineering Applications of Artificial Intelligence*, 9, pp. 681-689,1996.
119. J. Xiang , Y. Zhong, X. Chen and H. Zhengjia, Crack detection in a shaft by combination of wavelet- based elements and genetic algorithm, *International journal of solids and structures*, 45, pp.4782-4795,2008.
120. Y.He, D. Guo and F.Chu, Using genetic algorithms and finite element methods to detect shaft crack for rotor-bearing system, *Mathematics and Computers in Simulation*, 57 pp. 95–108, 2001.
121. L. Zhang, L. B. Jack and A. K. Nandi, Fault detection using genetic programming, *Mechanical Systems and Signal Processing*, 19, pp. 271–289, 2005.
122. Y.Zhang and R.B.Randall, Rolling element bearing fault diagnosis based on the combination of genetic algorithms and fast kurtogram, *Mechanical Systems and Signal Processing*, 23, pp.1509–1517, 2009.

123. M.T.V.Baghmisheh, M. Peimani , M. H. Sadeghi and M. M. Ettefagh, Crack detection in beam-like structures using genetic algorithms, *Applied Soft Computing*, 8 , pp. 1150–1160, 2008.
124. R. Perera, A. Ruiz and Carlos Manzano, Performance assessment of multi criteria damage identification genetic algorithms, *Computers and Structures*, 87, pp. 120–127, 2009.
125. M.I. Friswell, J.E.T. Penny and S.D. Garvey, A combined genetic and Eigen sensitivity algorithm for the location of damage in structures, *Computers and Structures*, 69, pp. 547-556, 1998.
126. D. Goldberg, Genetic Algorithms, *Addison Wesley*, 1988.
127. J.-S.R. Jang, C.T. Sun and E. Mizutani, Neuro-Fuzzy and Soft Computing, A Computational Approach to Learning and Machine Intelligence, *Prentice-Hall*, New Jersey, 1997.
128. J.S.R. Jang, ANFIS: Adaptive-network-based fuzzy inference system, *IEEE Transactions on Systems, Man and Cybernetics*, 23 (3), pp.665-684 1993.
129. G. Derringer and R. Suich , Simultaneous optimization of several response variables, *Journal of Quality Technology*, 12, pp.214-219, 1980.
130. C.B.Cheng, C.J. Cheng and E.S. Lee, Neuro-fuzzy and Genetic Algorithm in multi response optimization, *Computers and Mathematics with applications*, 44, pp.1503-1514, 2002.
131. G.Buyukozkan and Orhan Feyzioglu, A new approach based on soft computing to accelerate the selection of new product ideas, *Computers in Industry*, 54 , pp.151–167,2004.
132. S. Hengjie, C.Miao, Z. Shen , W. Roel, M.D.Hondt and C.Francky, A probabilistic fuzzy approach to modeling nonlinear systems, *Neuro computing* ,74, pp.1008–1025,2011.

133. C. Vairappan, H.Tamura, S. Gao and Z.Tang, Batch type local search-based adaptive neuro-fuzzy inference system(ANFIS) with self-feed backs for time-series prediction, *Neuro-computing*, 72 ,pp. 1870–1877,2009.
134. M.R. Gholamian, S.M.T. Fatemi Ghomi and M. Ghazanfari, A hybrid intelligent system for multi objective decision making problems, *Computers & Industrial Engineering*, 51, pp. 26–43, 2006.
- 135.K. Ellithy, A. Al-Naamany, A hybrid neuro-fuzzy static var compensator stabilizer for power system damping improvement in the presence of load parGoogleUpdate.ex□nty, *Electric Power Systems Research* ,56 , pp.211–223,2000.
136. A. F. Guneri, T. Ertay and A. Yucel, An approach based on ANFIS input selection and modeling for supplier selection problem, *Expert Systems with Applications*, 38, pp.14907–14917, 2011.
137. S. Nagarajan , J. Shanmugam and T.R. Rangaswamy, MANFIS Observer Based Sensor Fault Detection and Identification in Interacting Level Process with NN Based Threshold Generator, *International Journal of Soft Computing Year*, 3(5) , pp. 344-354,2008.
138. S. Jassar, Z. Liao and L. Zhao, Adaptive neuro-fuzzy based inferential sensor model for estimating the average air temperature in space heating systems, *Building and Environment*, 44(8), pp. 1609-1616, 2009.
139. G.D. Asensi , J.Hinojosa, R.Ruiz and J.A.D.Diaz-Madrid , Accurate and reusable macro modeling technique using a fuzzy-logic approach, Circuits and Systems, ISCAS 2008, *IEEE International Symposium*, pp. 508-511, 2008.
140. J.Zhang, W.Dai, M.Fan, H.Chung, Z.Wei and D.Bi , An Investigation into the Use of Delay Coordinate Embedding Technique with MIMO ANFIS for Nonlinear Prediction of Chaotic Signals Book: Lecture notes on computer science, Springer Berlin, 3614, pp.677-688,2008.

141. N. Nguyen and H. Lee, Bearing fault diagnosis using adaptive network based fuzzy inference system, *International Symposium on Electrical & Electronics Engineering*, pp. 280-285, 2007.
142. Y. Lei, Z. He, Y. Zi and Q. Hu, Fault diagnosis of rotating machinery based on multiple ANFIS combination with Gas, *Mechanical Systems and Signal Processing*, 21(5), pp. 2280-2294, 2007.
143. Y. Lei, Z. He and Y. Zi, A new approach to intelligent fault diagnosis of rotating machinery, *Expert Systems with Applications*, 35(4), pp.1593-1600, 2008.
144. K. Salahshoor, M. S. Khoshro and M. Kordestani, Fault detection and diagnosis of an industrial steam turbine using a distributed configuration of adaptive neuro-fuzzy inference systems, *Simulation Modeling Practice and Theory*, 19, pp.1280–1293, 2011.
145. M. Sadeghian and A. Fatehi, Identification, prediction and detection of the process fault in a cement rotary kiln by locally linear neuro-fuzzy technique, *Journal of Process Control*, 21, pp.302–308, 2011.
146. R. Eslamloueyan, Designing a hierarchical neural network based on fuzzy clustering for fault diagnosis of the Tennessee–Eastman process, *Applied Soft Computing*, 11, pp.1407–1415, 2011.
147. L. L. Simon and K. Hungerbuhler, Industrial batch dryer data mining using intelligent pattern classifiers: Neural network, neuro-fuzzy and Takagi–Sugeno fuzzy models, *Chemical Engineering Journal*, 157, pp.568–578, 2010.
148. A. Quteishat and C. P.Lim, A modified fuzzy min–max neural network with rule extraction and its application to fault detection and classification, *Applied Soft Computing*, 8, pp. 985–995, 2008.
149. I. B. Topcu, C. Karakurt and M. Sarıdemir, Predicting the strength development of cements produced with different pozzolans by neural network and fuzzy logic, *Materials and Design*, 29, pp. 1986–1991, 2008.

150. V. T. Tran, B.S. Yang , M.S. Oh and A.C. C. Tan, Fault diagnosis of induction motor based on decision trees and adaptive neuro-fuzzy inference, *Expert Systems with Applications*, 36, pp. 1840–1849, 2009.
151. X. Fang, H. Luo and J. Tang, Structural damage detection using neural network with learning rate improvement, *Computers and Structures*, 83, pp. 2150–2161, 2005.
152. P. Beena and R.Ganguli, Structural damage detection using fuzzy cognitive maps and Hebbian learning, *Applied Soft Computing*, 11, pp. 1014–1020, 2011.
153. H.C. Kuo, and H.K. Chang, A new symbiotic evolution-based fuzzy-neural approach to fault diagnosis of marine propulsion systems, *Engineering Applications of Artificial Intelligence*, 17, pp. 919–930, 2004.
154. Z. Ye , A. Sadeghian and B. Wu, Mechanical fault diagnostics for induction motor with variable speed drives using Adaptive Neuro-fuzzy Inference System, *Electric Power Systems Research*, 76, pp. 742–752, 2006.
155. R. J. Kuo, Intelligent Diagnosis for Turbine Blade Faults Using Artificial Neural Networks and Fuzzy Logic, *Engineering Application in AI*, 8(1), pp. 25-34, 1995.
156. E. Zio and G. Gola, A neuro-fuzzy technique for fault diagnosis and its application to rotating machinery, *Reliability Engineering and System Safety*, 94, pp.78–88, 2009.
157. W. Q. Wang, M. F. Golnaraghi and F. Ismail, Prognosis of machine health condition using neuro-fuzzy systems, *Mechanical Systems and Signal Processing*, 18, pp.813–831, 2004.
158. L. Zhang, G. Xiong, H. Liu, H. Zou and W. Guo, Bearing fault diagnosis using multi-scale entropy and adaptive neuro-fuzzy inference, *Expert Systems with Applications*, 37, pp.6077–6085, 2010.

159. Q. Wu, Hybrid fuzzy support vector classifier machine and modified genetic algorithm for automatic car assembly fault diagnosis, *Expert Systems with Applications*, 38, pp.1457–1463, 2011.
160. I. Pan, S. Das and A. Gupta, Tuning of an optimal fuzzy PID model with stochastic algorithms for networked control systems with random time delay, *ISA Transactions*, 50, pp.28–36, 2011.
161. P. M. Pawar and R. Ganguli, Genetic fuzzy system for online structural health monitoring of composite helicopter rotor blades, *Mechanical Systems and Signal Processing*, 21, pp. 2212–2236, 2007.
162. S.Yuan and F.Chu, Fault diagnosis based on support vector machines with parameter optimization by artificial immunization algorithm, *Mechanical Systems and Signal Processing*, 21, pp. 1318–1330, 2007.
163. P. Thrift, Fuzzy logic synthesis with genetic algorithms, *Proceedings of the Fourth International Conference on Genetic Algorithms*, San Diego, USA, pp. 509–513, 1991.
164. A. Hajnayeb, A. Ghasemloonia, S.E. Khadem and M.H. Moradi, Application and comparison of an ANN-based feature selection method and the genetic algorithm in gearbox fault diagnosis, *Expert Systems with Applications*, 38, 10205–10209, 2011.
165. C.S.Chen and J.S. Chen, Rotor faults diagnosis system based on GA-based individual neural networks, *Expert Systems with Applications*, 38(9), pp.10822-10830, 2011.
166. H. Firpi and G. Vachtsevanos, Genetically programmed-based artificial features extraction applied to fault detection, *Engineering Applications of Artificial Intelligence*, 21, pp.558–568, 2008.
167. B. Samanta, Gear fault detection using artificial neural networks and support vector machines with genetic algorithms, *Mechanical Systems and Signal Processing*, 18, pp.625–644, 2004.

168. L. B. Jack and A. K. Nandi, fault detection using support vector Machines and artificial neural networks, Augmented by genetic algorithms, *Mechanical Systems and Signal Processing*, 16, pp.373–390, 2002.
169. D. Z. Li and W.Wang, An enhanced GA technique for system training and prognostics, *Advances in Engineering Software*, 42(7), pp.452-462, 2011.
170. S.J. Zheng, Z.Q. Li and H.T. Wang, A genetic fuzzy radial basis function neural network for structural health monitoring of composite laminated beams, *Expert Systems with Applications*, 38(9),pp.11837-11842,2011.
171. K.M. Saridakis, A.C. Chasalevris, C.A. PapadoPoulos and A.J. Dentsoras , Applying neural networks, genetic algorithms and fuzzy logic for the identification of cracks in shafts by using coupled response measurements, *Computer and Structures*, 86, pp.1318-1338,2008.
172. T. Kolodziejczyk, R. Toscano, S. Fouvry, and G. Morales-Espejel, Artificial intelligence as efficient technique for ball bearing fretting wear damage prediction, *Wear*, 268 , pp.309–315, 2010.
173. J. H. Gordis and Y. W. Kwon, Frequency domain structural synthesis for quasi-static crack propagation: Global–local analysis, *Computers and Structures*, 89, pp.762–771, 2011.
174. N. Bachschmid, P.Pennacchi and E.Tanzi, A sensitivity analysis of vibrations in cracked turbo-generator units versus crack position and depth, *Mechanical Systems and Signal Processing* ,24 ,pp.844–859,2010.
175. B.H. Jun, Fault detection using dynamic time warping (DTW) algorithm and discriminant analysis for swine waste water treatment, *Journal of Hazardous Materials* , 185, pp.262–268, 2011.
176. C.T. Yiakopoulos, K.C. Gryllias and I.A. Antoniadis, Rolling element bearing fault detection in industrial environments based on a K-means clustering approach, *Expert Systems with Applications*, 38, 2888–2911, 2011.

177. J. Cusido, L. Romeral, J.A. Ortega, A. Garcia and J.R. Riba, Wavelet and PDD as fault detection techniques, *Electric Power Systems Research* 80, pp.915–924, 2010.
178. M. Cao and P. Qiao, Novel Laplacian scheme and multi resolution modal curvatures for structural damage identification, *Mechanical Systems and Signal Processing* , 23, pp.1223–1242, 2009.
179. E. Fagerholt, C. Dørum, T. Børvik, H.I. Laukli and O.S. Hopperstad, Experimental and numerical investigation of fracture in a cast aluminum alloy, *International Journal of Solids and Structures* ,47(24), pp.3352–3365, 2010.
180. C. Karaagac, H. Ozturk and M. Sabuncu, Free vibration and lateral buckling of a cantilever slender beam with an edge crack: Experimental and numerical studies, *Journal of Sound and Vibration*, 326, pp.235–250, 2009.
181. G. Rus and R. Gallego, Hyper singular shape sensitivity boundary integral equation for crack identification under harmonic elastodynamic excitation, *Computer Methods Appl. Mech. Engg.* , 196, pp.2596–2618, 2007.
182. C. Kyriacazoglou, B.H.L. Page, and F. J. Guild, Vibration damping for crack detection in composite laminates, *Composites Part A: Applied Science and Manufacturing*, 35, pp.945-953, 2004.
183. Z. K. Peng, Z.Q. Lang and S.A. Billings, Crack detection using non linear output frequency response functions (NOFRFS), *Journal of sound and vibration*, 301, pp-777-788,2007.
184. M. I. Friswell, Damage identification using inverse methods, *Philosophical transactions of the royal society A: physical and engineering sciences*, 365, pp.393-410, 2007.
185. D.Y. Zehng and S.C. Fan, Vibration and stability of cracked hollow sectional beam, *Journal of sound and vibration*, 267, pp.933-954, 2003.
186. J. H. Leontios, E. Douka and A. Trochidis, Crack detection in beams using Kurtosis , *Computers and structures*, 83, pp.909-919,2005.

187. N.L. Bayissa, N. Haritos and S. Thelandersson, Vibration based structural damage identification using wavelet transform, *Mechanical systems and signal processing*, 22, pp.1194-1215, 2008.
188. M. Dilella and A. Morassi, Structural health monitoring of rods based on natural frequency and anti-resonant frequency measurements, *Structural health monitoring*, pp. 149-173, 2009.
189. H. Kim, A. Tan, J. Mathew and B. Choi, Bearing fault prognosis based on health state probability estimation, *Expert Systems with Applications*, 39 (5), pp. 5200–5213, 2012
190. A. Jafari, A. K. Ilkhchi, Y. Sharghi and K. Ghanavati, Fracture density estimation from petrophysical log data using the adaptive neuro-fuzzy inference system, *Journal of Geophysics and Engineering*, 9 (1), pp.105-114, 2012.
191. K. Bacha, S. Souahlia and M. Gossa, Power transformer fault diagnosis based on dissolved gas analysis by support vector machine, *Electric Power Systems Research*, 83 (1), pp.73–79, 2012.
192. S. K. Mandal, F. T. S. Chan and M.K. Tiwari, Leak detection of pipeline: An integrated approach of rough set theory and artificial bee colony trained SVM, *Expert Systems with Applications*, 39 (3), pp. 3071–3080, 2012.
193. D.Srinivasarao, K. M. Rao and G.V.Raju, crack identification on a beam by vibration measurement and wavelet analysis, *International Journal of Engineering Science and Technology*, 2, pp.907-912, 2010.
194. S.T. Quek, Q. Wang, L. Zhang and K.K. Ang, Sensitivity analysis of crack detection in beams by wavelet technique, *International Journal of Mechanical Sciences*, 43, pp. 2899-2910, 2001.
195. Q. Wang and X. Deng, Damage detection with spatial wavelets, *International Journal of Solids and Structures*, 36, pp. 3443-3468, 1999.
196. S. Loutridis, E. Douka and A. Trochidis, Crack identification in double-cracked beams using wavelet analysis, *Journal of Sound and Vibration*, 277, pp. 1025–1039, 2004.

197. A. Gentile and A. Messina, on the continuous wavelet transforms applied to discrete vibrational data for detecting open cracks in damaged beams, *International Journal of Solids and Structures*, 40, pp. 295–315, 2003.
198. J. K. Pieper, Optimal control of a flexible manipulator and model order reduction, *Optimal Control Applications and Methods*, 19, pp. 331–343, 1998.
199. M. Torres-Torriti, Scan-to-map matching using the Hausdorff distance for robust mobile robot localization, *IEEE International Conference on Robotics and Automation ICRA 2008*, pp. 455-460 2008.
200. B.K. Rout, R.K. Mittal, Tolerance Design of Manipulator Parameters Using Design of Experiment Approach , *Structural Multidisciplinary Optimization*, 34 pp 445-462, 2007.
201. A.K. Samantaray, S.S. Dasgupta, R. Bhattacharyya, Bond Graph Modeling of an Internally Damped Non-ideal Flexible Spinning Shaft, *Trans. ASME J. Dyn. Sys., Meas., Control*, 132(6), pp.61502-61511, 2010.
202. B. K. Panigrahi and V. R. Pandi, A Comparative Study of Evolutionary Computing Methods for Parameter Estimation of Power Quality Signals, *International Journal of Applied Evolutionary Computation*, 1, pp. 28 – 59,2010.
203. E. Z. Casanova, S. D. Quijada, J. G. García-Bermejo, J. R. Peran Gonzalez, Micromodel based system for 2D localization, *Mechatronics* , 15, pp. 1109-1126, 2005.
204. M. S. Packianather, S.S. Dimov, C. A. Griffiths, B. Sha, Investigation of micro-injection moulding: factors affecting the replication quality, *Journal of Materials Processing Technology*, 183, pp. 284-296, 2007.
205. T. Takagi and M. Sugeno, Fuzzy identification of systems and its application to modelling and control, *IEEE Trans. on Systems, Man, Cybernetics*, 15(1), pp.116-132, 1985.
206. S. Haykin, Neural Networks, A comprehensive foundation. *Pearson Education*, 2006.
207. W. McCulloch and W. Pitts, A logical calculus of the ideas immanent in nervous activity, *Bulletin of Mathematical Biophysics*, 5, pp. 115-133, 1943.
208. F. Rosenblatt, the perceptron: A probabilistic model for information storage and organization in the brain, *Psychological Review*, 65, pp.386-408, 1958.

PUBLISHED PAPERS:

1. D. R. K. Parhi and Dash Amiya Kumar, Analysis of methodologies applied for diagnosis of fault in vibrating structures, *Int. J. Vehicle Noise and Vibration*, Vol. 5, No. 4, 271-286, 2009.
2. D.R.K. Parhi, Amiya Kumar Dash, Faults detection by finite element analysis of a multi cracked beam using vibration signatures, *Int. J. Vehicle Noise and Vibration*, Vol. 6, No. 1, 40-54, 2010.
3. Amiya Kumar Dash, Dayal.R. Parhi, Development of an inverse methodology for crack diagnosis using AI technique, *International Journal of Computational Materials Science and Surface Engineering (IJCMSSE)*, 4(2), 143-167, 2011.
4. Dayal.R.Parhi, Amiya K. Dash, Application of neural network and finite element for condition monitoring of structures, *Proceedings of the Institution of Mechanical Engineers, Part C: Journal of Mechanical Engineering Science*, 225, pp. 1329-1339, 2011.
5. D.R.K.Parhi, Amiya Kumar Dash, H.C. Das Formulation of a GA based methodology for multiple crack detection in a beam structure, *Australian Journal of structural engineering*, 12 (2), pp. 59-71, 2011.
6. Amiya Kumar Dash, D.R.K.Parhi, A vibration based inverse hybrid intelligent method for structural health monitoring, *International Journal of Mechanical and Materials Engineering*, 6(2), pp. 212-230, 2011.
7. Amiya Kumar Dash, Dayal R.Parhi, Development of a crack diagnostic application using MANFIS technique, *International Journal of acoustics and vibration (IJAV)*, In Press.
8. Das H. C., Dash A. K., Parhi D. R., Experimental Validation of Numerical and Fuzzy Analysis of a Faulty Structure, 5th International Conference on System of Systems Engineering (SoSE), 2010, Loughborough, U.K., 22-24 June, pp.1-6.

PAPERS COMMUNICATED TO INTERNATIONAL JOURNALS:

1. A.K. Dash, D.R. Parhi, "Analysis of an intelligent hybrid system for fault diagnosis in cracked structure" *Arabian Journal for Science and Engineering (Springer)*. **(Accepted)**
2. D.R. Parhi, A.K. Dash, "Analyzing the GA, NN and FL for development of a hybrid vibration system for condition monitoring of cracked structure" *Proceedings of the Institution of Mechanical Engineers, Part E: Journal of Process Mechanical Engineering*.

Analysis of methodologies applied for diagnosis of fault in vibrating structures

D.R.K. Parhi*

Department of Mechanical Engineering,
N.I.T. Rourkela-769008, Orissa, India
E-mail: dayalparhi@yahoo.com

*Corresponding author

Dash Amiya Kumar

Department of Mechanical Engineering,
ITER, Khandagiri, Bhubaneswar-30, Orissa, India
E-mail: amiyadash@yahoo.com

Abstract: This paper presents a comprehensive review of methodologies and technologies in the domain of dynamic vibration of cracked structures. At first, the developments of work till date in the area of dynamic vibration of various structures are discussed. In the second phase, different methodologies are described with regard to the analysis of faulty structures. The methodologies mainly consist of energy methods, finite element methods, fuzzy inference techniques, neural networks, neuro-fuzzy adaptive techniques and genetic algorithms used for identifying the intensity and location of cracks. It has been found that, apart from conventional methods, artificial intelligence methods can be applied efficiently and smartly to detect faults in various dynamic systems.

Keywords: fuzzy; finite element; vibration; crack; genetic algorithm; GA.

Reference to this paper should be made as follows: Parhi, D.R.K. and Kumar, D.A. (2009) 'Analysis of methodologies applied for diagnosis of fault in vibrating structures', *Int. J. Vehicle Noise and Vibration*, Vol. 5, No. 4, pp.271–286.

Biographical notes: Dayal R. Parhi received his first PhD in Mobile Robotics from Cardiff School of Engineering, UK, and his second PhD in Vibration Analysis of Cracked Structures from Sambalpur University, Orissa, India. He has 16 years of research and teaching experience in his fields. Presently, he is engaged in mobile robot navigation research, and he is a Faculty member in the Department of Mechanical Engineering, National Institute of Technology Rourkela-08, Orissa, India.

Dash Amiya Kumar is currently an Assistant Professor in the Institute of Technical Education and Research, Bhubaneswar. His ongoing research is in the areas of application of artificial intelligence techniques in the domain of dynamically vibrating structures. He received his undergraduate degree in Mechanical Engineering from Sambalpur University and Postgraduate degree in Machine Design from the National Institute of Technology at Rourkela.

Faults detection by finite element analysis of a multi cracked beam using vibration signatures

D.R.K. Parhi*

Department of Mechanical Engineering,
NIT Rourkela-769008, Orissa, India
Fax: +91 661 2462999
E-mail: dayalparhi@yahoo.com
*Corresponding author

Amiya Kumar Dash

Department of Mechanical Engineering,
ITER, Khandagiri, Bhubaneswar-30, Orissa, India
E-mail: amiyadash@yahoo.com

Abstract: In this paper, analysis for fault identification in a cracked beam has been carried out. Theoretical, finite element and experimental analyses for identification of the crack depths and their positions in a beam containing multiple transverse cracks are carried out. It has been established that a crack in a beam has an important effect on its dynamic behaviour. The strain energy density function is used to evaluate the additional flexibility produced due to the presence of crack. Based on the flexibility, a new stiffness matrix is deduced and subsequently that is used to calculate the natural frequencies and mode shapes of the cracked beam. The analysis of the crack structure is done using theoretical, finite element and experimental analysis. The results from finite element method and experimental method are compared with the results from the numerical analysis for validation. The results are found to be in good agreement.

Keywords: finite element method; FEM; crack; natural frequencies; fault; vibration.

Reference to this paper should be made as follows: Parhi, D.R.K. and Dash, A.K. (2010) 'Faults detection by finite element analysis of a multi cracked beam using vibration signatures', *Int. J. Vehicle Noise and Vibration*, Vol. 6, No. 1, pp.40–54.

Biographical notes: Dayal R. Parhi received his first PhD in Mobile Robotics from Cardiff School of Engineering, UK and second PhD in Vibration Analysis of Cracked Structures from Sambalpur University, Orissa, India. He has 17 years of research and teaching experience in his fields. Presently, he is engaged in mobile robot navigation research, and a Faculty member in the Department of Mechanical Engineering, National Institute of Technology Rourkela-08, Orissa, India.

Amiya Kumar Dash is currently an Assistant Professor in Institute of Technical Education and Research, Bhubaneswar. His ongoing research is in the areas of application of artificial intelligence techniques in the domain of dynamically vibrating structures. He received his undergraduate in Mechanical Engineering from Sambalpur University and received his Postgraduate in Machine Design from National Institute of Technology at Rourkela.

Development of an inverse methodology for crack diagnosis using AI technique

Amiya Kumar Dash*

Department of Mechanical Engineering,
Institute of Technical Education and Research,
Khandagiri, Bhubaneswar – 751030, Orissa, India
E-mail: amiyadash@yahoo.com

*Corresponding author

Dayal R.K. Parhi

Department of Mechanical Engineering,
National Institute of Technology,
Rourkela – 769008, Orissa, India
Fax: +91-661-2462999
E-mail: dayalparhi@yahoo.com

Abstract: The influence of cracks on the dynamic behaviour of a cracked cantilever beam with rectangular cross section is discussed in this work. Analytical and experimental investigations are carried out to find the relation between the change in natural frequencies and mode shapes for the cracked and un-cracked beam. Finite element analysis is being performed on the cracked structure to measure the vibration signatures, which is subsequently used in the design of smart system based on fuzzy logic for prediction of crack depths and locations following inverse problem approach. The fuzzy system is developed with relative natural frequencies and mode shapes as input parameters based on the triangular membership functions to calculate the deviation in the vibration parameters for the cracked dynamic structure. Results from experimental analysis are very close to the results predicted by the theoretical, finite element and fuzzy analysis.

Keywords: vibration; computational; multiple cracks; fuzzy; mode shape; natural frequency.

Reference to this paper should be made as follows: A.K. Dash and Parhi, D.R.K. (2011) 'Development of an inverse methodology for crack diagnosis using AI technique', *Int. J. Computational Materials Science and Surface Engineering*, Vol. 4, No. 2, pp.143–167.

Biographical notes: Amiya Kumar Dash is currently an Assistant Professor at the Institute of Technical Education and Research, Bhubaneswar. His ongoing research is in the areas of application of artificial intelligence techniques in the domain of dynamically vibrating structures. He received his undergraduate degree in Mechanical Engineering from Sambalpur University and received his postgraduate degree in Machine Design from National Institute of Technology at Rourkela.

Application of neural network and finite element for condition monitoring of structures - Windows Internet Explorer

http://pic.sagepub.com/content/225/6/1329.abstract

File Edit View Favorites Tools Help

Application of neural net... Sign In

Institution: NATIONAL INST OF TECHNOLOGY ROURKELA Sign In My Tools Contact Us HELP

SAGE journals Search all journals Advanced Search Search History Browse Journals

JOURNAL OF MECHANICAL ENGINEERING SCIENCE

Home OnlineFirst All Issues Subscribe RSS Email Alerts

Search this journal Advanced Journal Search

Application of neural network and finite element for condition monitoring of structures

D R Parhi^{1*}
A K Dash²

¹Department of Mechanical Engineering, National Institute of Technology, Rourkela, Orissa, India
²Department of Mechanical Engineering, Institute of Technical Education and Research, Bhubaneswar, Orissa, India

* Department of Mechanical Engineering, National Institute of Technology, C/14 NIT Campus Rourkela 769008, Orissa, India. email: dayalparhi@yahoo.com

Abstract

This article analyses the dynamic behaviour of a beam structure containing multiple transverse cracks using neural network controller. The first three natural frequencies and mode shapes have been calculated using theoretical, finite-element, and experimental analysis for the cracked and un-cracked beam. Comparisons of the results among theoretical, finite-element, and experimental analysis have also been presented. The calculated vibration signatures were used to train the feed forward multi

« Previous | Next Article »
Table of Contents

This Article
doi: 10.1177/0954406210395883
Proceedings of the Institution of Mechanical Engineers, Part C: Journal of Mechanical Engineering Science
June 2011 vol. 225 no. 6 1329-1339

» Abstract Free
Full Text (PDF)
References

Services

- » Email this article to a colleague
- » Alert me when this article is cited
- » Alert me if a correction is posted
- » Similar articles in this journal
- » Download to citation manager
- » Request Permissions
- » Request Reprints

Citing Articles

- » Citing articles via Google Scholar

Google Scholar

- » Articles by Parhi, D. R.

Current Issue
» April 2012, 226 (4)

Alert me to new issues of Proceedings of the Institution of Mechanical Engineers, Part C: Journal of Mechanical Engineering Science

Submit a Manuscript
Free Sample Copy
Email Alerts
RSS feed
More about this journal

start Amiya thesis word_thesis AMIYA 2... Application of neural ... 10:55 AM

Informit - Australian Journal of Structural Engineering - Formulation of a genetic algorithm ba - Windows Internet Explorer

http://search.informit.com.au/documentSummary;dn=829162515948125;res=IENG

File Edit View Favorites Tools Help

Favorites Genetic Algorithm Descriptio... Suggested Sites Upgrade Your Browser

Informit - Australian Jour... Informit - Pay-Per-View

Help | Login
Welcome: Guest User

Search Titles Databases

Publication Type Subjects Publishers

All Journals Conferences Reports

Databases in use: Engineering Collection [Change databases](#)

[Manage Search History](#) | [Manage Alerts](#)

[Back to Table of Contents](#) Citation [Save](#) | [Print](#) | [Email](#) Text size A | A | A

Australian Journal of Structural Engineering
Volume 12 Issue 2 (2012)

Formulation of a genetic algorithm based methodology for multiple crack detection in a beam structure

Parhi, DR¹; Dash, AK²; Das, HC³

Abstract: In the current analysis, the vibration characteristics of a cracked cantilever beam having different crack locations and depths have been studied. Numerical and finite element methods have been used to extract the diagnostic indices (natural frequencies, mode shapes) from the beam structure. An intelligent genetic algorithm based controller has been designed to automate the fault identification process. Single point crossover and mutation procedure have been followed to find out the optimal solution from the search space. The outcome from the developed controller shows that the system could not only detect the cracks but also predict their locations and severities.

[Full Text PDF \(Buy Now - AU\\$33.00\) \(608kb\)](#)

To cite this article: Parhi, DR; Dash, AK and Das, HC. Formulation of a genetic algorithm based methodology for multiple crack detection in a beam structure [online]. *Australian Journal of Structural Engineering*, Vol. 12, No. 2, 2012: 127-139. Availability: <<http://search.informit.com.au/documentSummary;dn=829162515948125;res=IENG>> ISSN: 1328-7982. [cited 27 Apr 12].

Personal Author Parhi, DR; Dash, AK; Das, HC

Search Indexes Thesauri

Search Query:

in Any field

AND

in Any field

[Add more terms](#)

☐ Also Search Full Text of Articles

[Clear search](#) | [Search hints](#) [Search](#)

Limit To:

☐ Full Text Records Only

☐ Date Range: 1970 to 2012

Legend

☒ Peer Reviewed

☒ Full content available

☒ Citation only

start published paper of A... word_thesis AMIYA fi... Untitled - Notepad Adobe Acrobat Profe... Informit - Australian J... 11:55 AM

A VIBRATION BASED INVERSE HYBRID INTELLIGENT METHOD FOR STRUCTURAL HEALTH MONITORING

A.K. Dash¹ and D.R. Parhi²

¹Department of Mechanical Engineering, I.T.E.R., S 'O' A University, Bhubaneswar

²Department of Mechanical Engineering, N.I.T Rourkela
E-mail: amiyadash@yahoo.com

Received 25 January 2011, Accepted 13 March 2011

ABSTRACT

In this paper, a novel identification algorithm (hybrid intelligent system) using inverse analysis of the vibration response of a cracked cantilever beam has been proposed. The crack identification algorithm utilizes the vibration signatures of the cracked beam derived from finite element and theoretical analysis. The hybrid controller is designed to predict the crack locations and their severities by integrating the capabilities of fuzzy logic and neural network technique. The measured modal parameters along with the outputs from the fuzzy controller are the inputs to the neural segment of the hybrid system, where as final relative crack depths and final relative crack locations are the output parameters. The derived vibration parameters are used to establish series of fuzzy rules and training patterns for the fuzzy and neural controller. Finally, the reliability of the proposed crack identification algorithm is established by comparing the results obtained from the experimental analysis.

Key words: Vibration; Multiple cracks; Natural frequency; Mode shape; Fuzzy neural controller

1. INTRODUCTION

The presence of a crack in a structural member introduces a local flexibility that affects its dynamic response. Moreover, the crack will open and close in time depending on the loading conditions and vibration amplitude. The changes in dynamic characteristics can be measured and lead to an identification of the structural changes, which eventually might lead to the detection of a structural flaw. So engineers and researchers are working towards development of methodology for detection of fault in damaged structures using the changes in vibration response. An energy based method for damage identification (Mazanoglu et al., 2009) in non-uniform Euler – Bernoulli beams having open cracks using Rayleigh – Ritz approximation method has been proposed. Method has been presented to identify crack in a beam (Lee, 2009) by modeling the cracks as rotational springs. Newton-Rapson method has been adapted by him to identify the locations and sizes of the crack in a beam. A damage assessment technique has been presented (Faverjon & Sinou 2009) for detection of size of the open crack in beams. They have used constitutive

relation error updating method for identification of crack location and size of the beam. The stress intensity factor and local flexibility matrix for cracked pipes have been calculated (He et al., 2009) by dividing the cracked pipe into series of these annuli. They have described that the local flexibility matrix for cracked pipes have been calculated experimentally without calculating the Stress intensity factor. The influence of two transverse open cracks on the anti resonances of a double cracked cantilever beam (Douka et al., 2009) both analytically and experimentally have been presented. The results of experiments performed by them on Plexiglas beams for crack location and severity are in good agreement with theoretical predictions. Three different linear theories: Euler – Bernoulli, Timoshenko and Two dimensional elasticity (Labuschagne et al., 2009) for crack detection of cantilever beams have been presented. A clonal selection programming (CSP)-based fault detection system has been developed (Gan et al., 2009) to perform induction machine fault detection and analysis. The proposed CSP-based machine fault diagnostic system has been intensively tested with unbalanced electrical faults and mechanical faults operating at different rotating speeds. A fuzzy finite element approach has been proposed (Akpan et al., 2001) for modeling smart structures with imprecise parameters.

Theories for strain energy density function with the help of stress intensity factor (Tada et al., 1973) at the crack section have been proposed to calculate the local flexibility matrix. A mobile robot navigation control system has been designed (Parhi, 2005) using fuzzy logic. Fuzzy rules embedded in the controller of a mobile robot enable it to avoid obstacles in a cluttered environment that includes other mobile robots. The use of neural network has been presented (Haykin, 1999) as a data processing tool for various applications. A neural network technique has been developed (Zubaydi et al., 2002) for identifying the damage occurrence in the side shell of a ship's structure. The input to the network is the autocorrelation function of the vibration response of the structure. The response is obtained using a finite element model of the structure. An optimized gear fault identification system (Rafiee et al., 2009) has been developed using genetic algorithm

INTERNATIONAL JOURNAL OF ACOUSTICS AND VIBRATION (IJAV)
PUBLISHED BY THE INTERNATIONAL INSTITUTE OF ACOUSTICS AND VIBRATION (IIAV)

Malcolm J. Crocker
Editor-in-Chief
Dept. of Mechanical Engineering, 202 Ross Hall
Auburn University, AL 36849-5341, USA

Tel: (334) 844-3310
Fax: (334) 844-3306
E-mail: mcrocker@eng.auburn.edu

EDITOR-IN-CHIEF
Malcolm J. Crocker
Auburn
USA

MANAGING EDITOR
Marek Pawelczyk
Gliwice
POLAND

ASSOCIATE EDITORS
Dariusz Bismor
Gliwice
POLAND

Nickolay Ivanov
St. Petersburg
RUSSIA

Zhuang Li
Lake Charles
USA

EDITORIAL BOARD
Jorge P. Arenas
Valdivia
CHILE

Jonathan D. Blotter
Provo
USA
Leonid Gelman
Cranfield
UNITED KINGDOM
Samir Gerges
Florianopolis
BRAZIL
Victor T. Grinchenko
Kiev
UKRAINE
Colin H. Hansen
Adelaide
AUSTRALIA
Hanno Heller
Braunschweig
GERMANY
Hugh Hunt
Cambridge
ENGLAND
Finn Jacobsen
Lyngby
DENMARK
Dan Marghitu
Auburn
USA
M. L. Munjal
Bangalore
INDIA
David E. Newland
Cambridge
ENGLAND
Kazuhide Ohta
Fukuoka
JAPAN
Goran Pavic
Villeurbanne
FRANCE
Subhash Sinha
Auburn
USA

February 1, 2012

Dear Drs. Dash and Parhi,

Thank you for submitting your paper "Development of a Vibration Based Crack Diagnostic Application Using MANFIS Technique" for possible publication in the *International Journal of Acoustics and Vibration*. We have surveyed your revisions, and we are pleased to say that your paper has now been officially accepted for publication in the journal.

Please prepare your manuscript in accordance with the suggested revisions and the guidelines in the author's instructions (available at <http://www.iiav.org/ijav/index.php?va=viewpage&vaid=121> and attached to this email). Then, please upload the revised version of your paper in both PDF and Word document (or LaTeX) form to the *IJAV* website as Paper 525 source file. Also, please upload a head-and-shoulders black-and-white photograph and brief 100–200 word biography for each of the authors, separate files for each figure, and the completed copyright form by no later than **March 1, 2012**. Please respond to this letter and confirm your intent to upload these necessary files by emailing my assistant Melissa Flowers (vibrate@auburn.edu).

Thank you again for your submission to the *IJAV*.

Sincerely,



Malcolm J. Crocker, Editor-in-Chief

Experimental validation of numerical and fuzzy analysis of a faulty structure

H. C. Das

Deptt. of Mechanical Engg.
I.T.E.R., Bhubaneswar, India
Harishdas1965@gmail.com

Amiya Kumar Dash

Deptt. of Mechanical Engg.
ITER, Bhubaneswar, India
amiyadash@yahoo.com

Dayal R. Parhi

Deptt. of Mechanical Engg.
N.I.T. Rourkela
dayal.parhi@yahoo.com

D.N.Thatoi

Deptt. of Mechanical Engg.
ITER, Bhubaneswar, India

Abstract— In the current analysis numerical and fuzzy methods are adopted for detection of damage in a cracked beam structure containing transverse cracks. Based on the flexibility produced due to the crack a new stiffness matrix is deduced and subsequently that is used to calculate the natural frequencies and mode shapes of the cracked beam using numerical method. The fuzzy inference system is designed by setting up various fuzzy rules with the modal parameters as input data obtained from theoretical analysis. The output from the fuzzy system is relative crack depth and relative crack location. The results of the numerical and fuzzy analysis are being validated with the result from experimental analysis. The results are found to be in good agreement.

Keywords— fuzzy; crack; natural frequencies; fault

1 Introduction

Generally presence of crack in a beam structure is the main reason for failure of the component. Structural failure is initiated when the material is stressed to its strength limit, thus causing fracture or excessive deformations. When this limit is reached, damage to the material has been done, and its load-bearing capacity is reduced permanently, significantly and quickly. Therefore intensive research has been going on amongst the scientists and engineers to find an effective methodology to predict the location and intensity of damage beforehand.

Baeza et al. [1] have analyzed a beam with a breathing crack under harmonic excitation and concluded that increase in crack parameters increases the vibration erratically. Capozucca et al. [2] has analyzed the dynamic response of a carbon fiber reinforced polymer (CFRP) rod in damaged and undamaged condition and presented the change in vibration parameters. The results of the theoretical analysis are validated with experimental results. Radzieński et al. [3] have presented experimental verification and comparison of damage detection methods such as assurance criterion (MAC), strain energy (SE), and Wavelets Transform (WT). He has developed data preprocessing algorithms for increasing damage assessment effectiveness. A finite element model has been simulated to identify cracks in a beam using the vibration signatures by Lee [4]. He has modeled the crack as massless rotational spring and used Newton-Raphson method for fault detection. Ariaci et al. [5] presented an analytical method for determining the dynamic response of Euler-Bernoulli beams with breathing cracks under a point moving mass using the discrete element technique (DET) and the finite element method (FEM) considering the effects of Coriolis and centrifugal forces.

The results are validated against those reported in the literature and also compared with results from the finite element method. Yu et al. [6] have analyzed the vibration characteristics of a cracked structural member using two-dimensional finite element analysis and suitable expression for stress intensity factor. The results of the analytical methods are in good agreement with experimental results. Morbidini et al. [7] in this paper proposes a methodology to study the detectability of fatigue cracks in metals using thermo sonics using finite-element thermal models. The results obtained from the method are validated by performing experiments on mild steel beams. Zheng et al. [8] have presented a method based on finite element method for detection of crack in faulty structural member. The result obtained from the proposed method is validated using experimental analysis. Tada et al. [9] have provided the basis for computation of compliance matrix for damage detection following fracture mechanics theory. Shekhar et al. [10] have derived a method for crack detection in a cracked shaft using finite element analysis using correct expression for strain energy release rate function. He has used an experimental set-up for validating the results obtained from the proposed method. Khoshnoud et al. [11] have proposed a novel vibration modeling method based on fuzzy sets. In this method, fuzzy rules are set using the vibration modal parameters. The proposed methodology use fuzzy representations of mode shape forms (MSFs), mixed artificial intelligence and experimental validation, together with human interface/intelligence for assessment of crack in a structure.

In this paper method has been developed for prediction of crack severity and its location in a cracked beam structure. The structure has been analyzed using theoretical and fuzzy techniques. Comparative study has been carried out between theoretical, fuzzy technique and experimental analysis. A good agreement between the results has been observed.

2 Theoretical analysis

2.1 Local flexibility of a cracked beam under bending and axial loading.

The presence of a transverse surface crack of depth ' a_1 ' on beam of width ' B ' and height ' W ' introduces a local flexibility, which can be defined in matrix form, the dimension of which depends on the degrees of freedom. Here a 2x2 matrix is considered. A cantilever beam is subjected to axial force (P_1) and bending moment (P_2), shown in figure 1 which gives coupling with the longitudinal and transverse motion.

AJSE: Your manuscript entitled Analysis of an intelligent hybrid system for fault diagnosis in cracked structure

Monday, 11 June, 2012 12:19 PM

From:

"Bassam El Ali" <belali@kfupm.edu.sa>

[Add sender to Contacts](#)

To:

"amiya dash" <amiyadash@yahoo.com>

Ref.: Ms. No. AJSE-D-11-00672R3

Analysis of an intelligent hybrid system for fault diagnosis in cracked structure

The Arabian Journal for Science and Engineering (AJSE)

Dear Dr. dash,

It is my pleasure, on behalf of the Editorial Board, to inform you that your paper AJSE-D-11-00672R3 entitled "Analysis of an intelligent hybrid system for fault diagnosis in cracked structure" has been accepted for publication in AJSE.

You will receive proofs of your article for proofreading once it is scheduled for publication.

Thank you for submitting your work to AJSE.

Sincerely yours,

Dr. Bassam El Ali
Managing Editor, AJSE

APPENDIX:

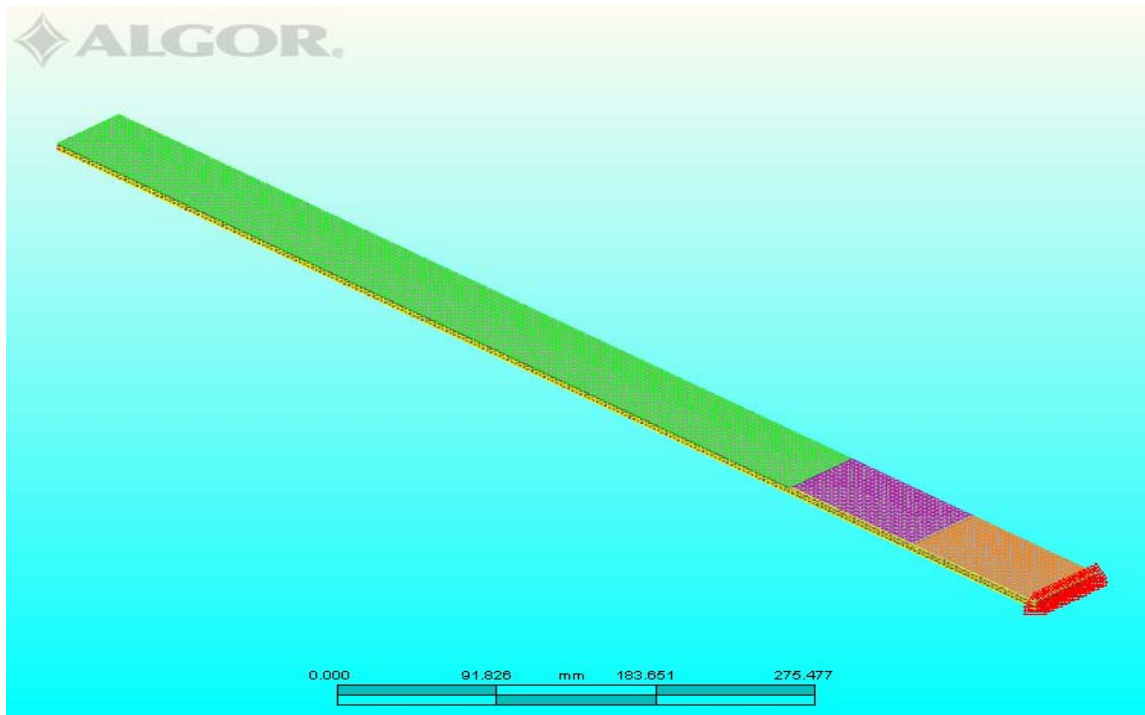


Fig. A1 FEA model of the cantilever beam model

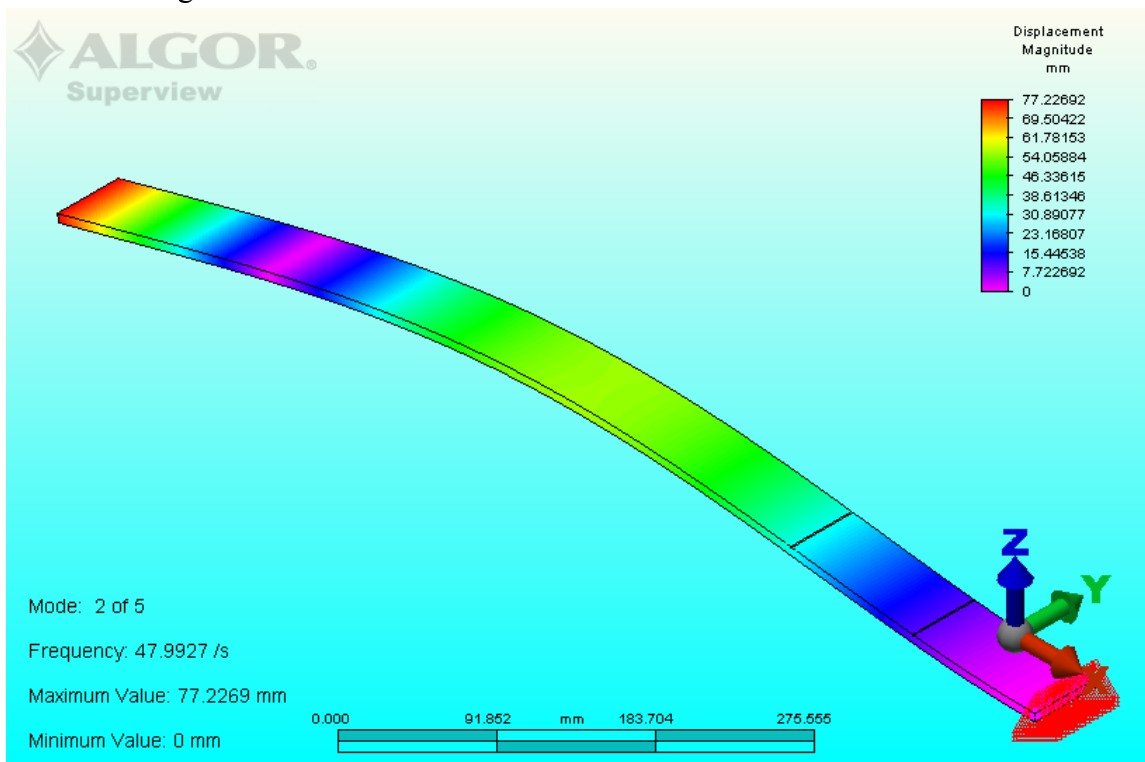


Fig. A2 ALGOR generated 2nd mode vibration of the cantilever beam model

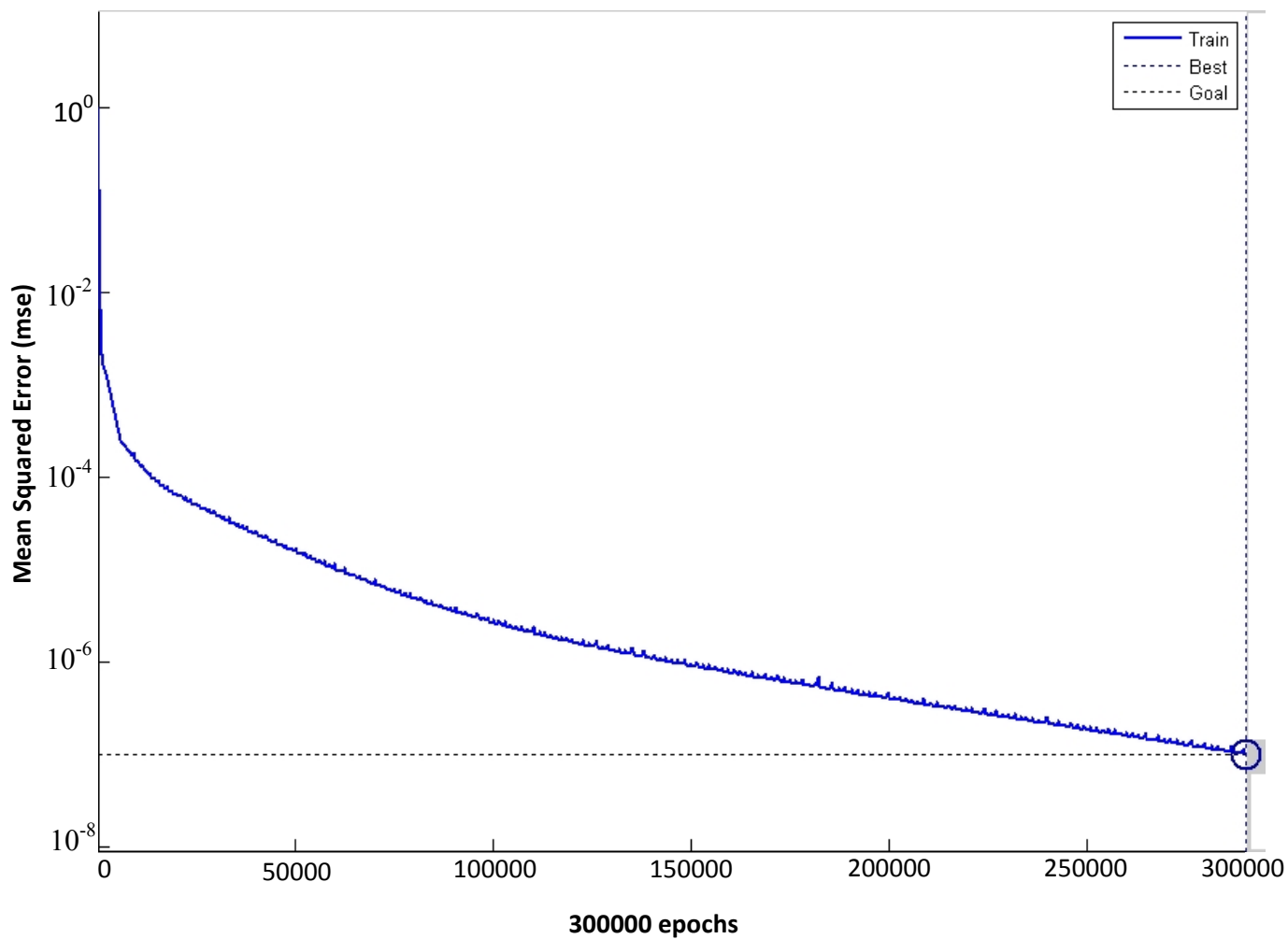


Fig. A3 plot of graph for epochs vs mean squared error from NN

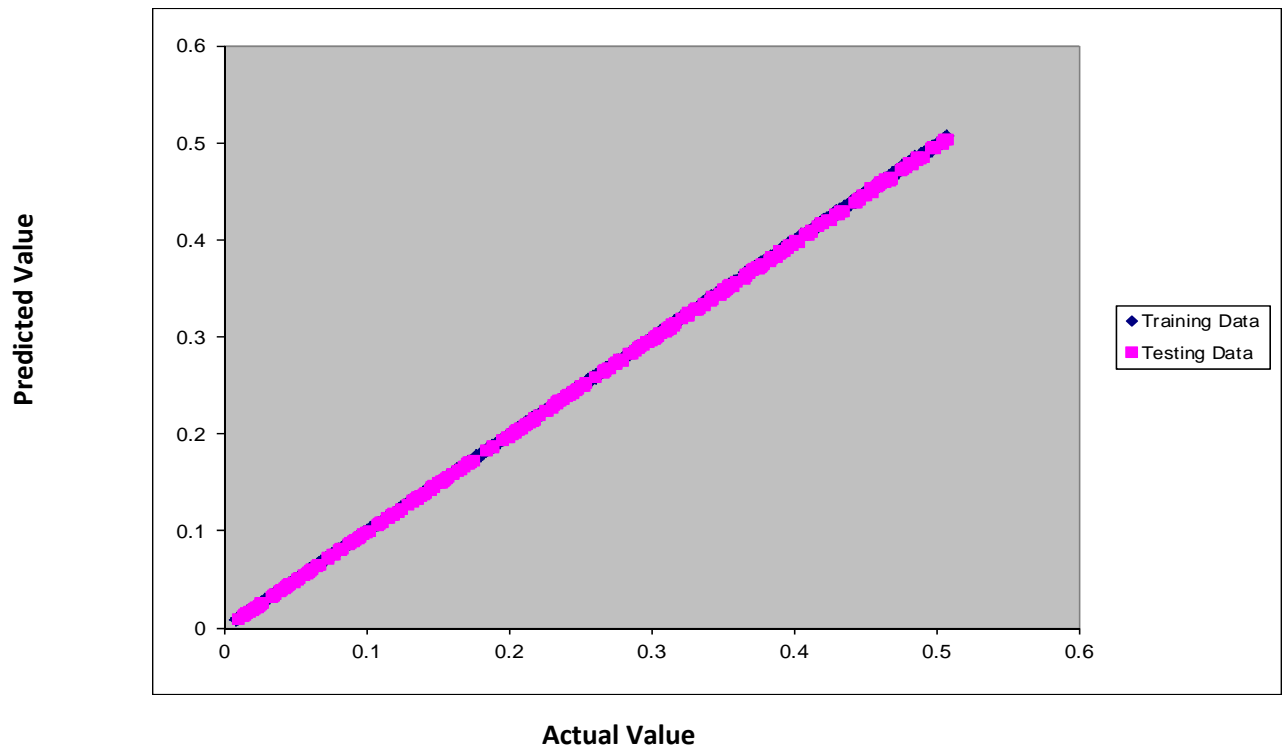


Fig. A4 Plot of graph for actual value vs predicted value

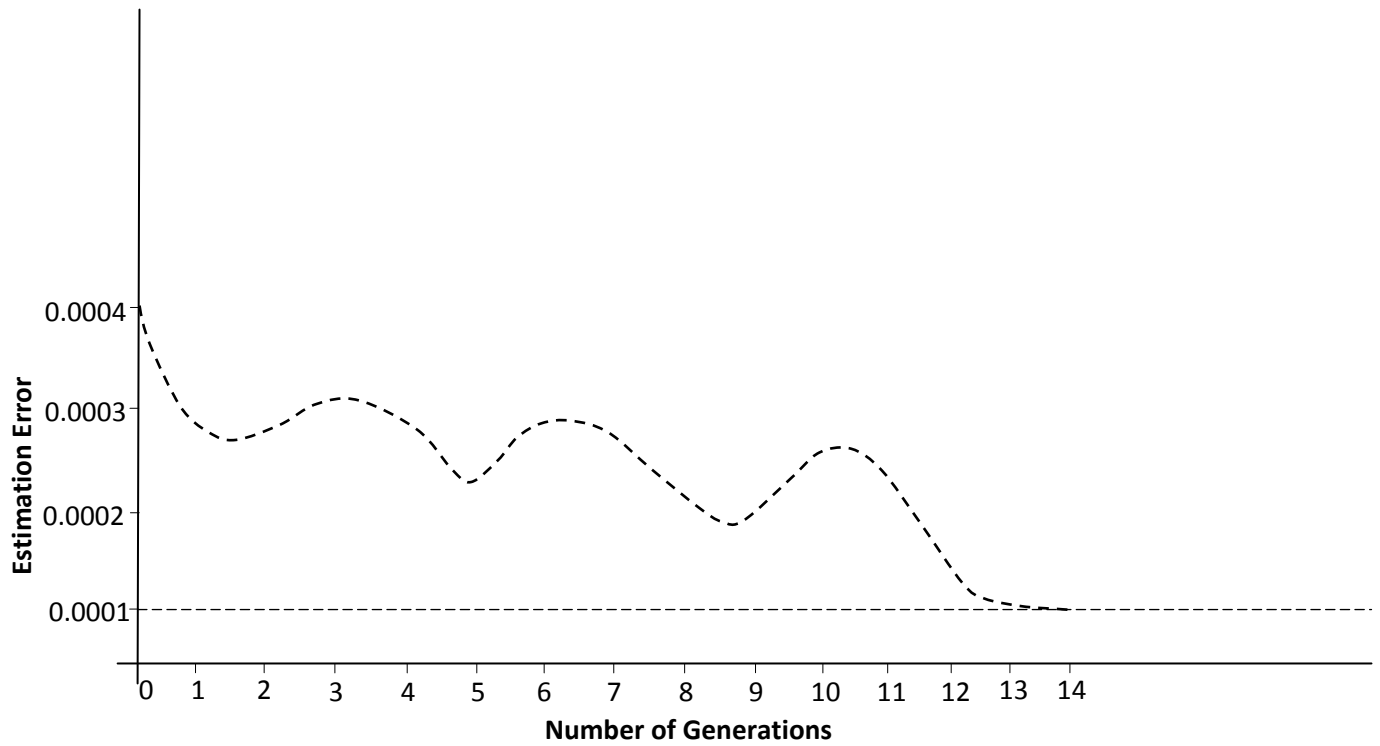


Fig. A5 Plot of graph for Estimation Error vs Number of Generations